

**Modelling and benchmarking of potentially
bioactive molecules from plants- design and
implementation of two strategies**

A thesis submitted for the degree of

Doctor of Philosophy

Institute for Sustainable Industries & Liveable Cities
College of Engineering & Science
Victoria University

by

Kavitha Menon

March 2020



Abstract

Natural products and derivatives thereof have contributed significantly to drug discovery and development and have also been used in traditional medicine for the treatment of various disease states. Sometimes, the use of such traditional medicines may be based upon many hundreds, if not thousands, of years of human experience. An advantage of drugs derived from natural products compared to synthetic drugs is their availability and the likelihood of reduced side effects. Drugs and drug leads derived from natural products may also be less time consuming and expensive to develop and may be more accessible to developing countries. An exciting advance in this area is the application of computational chemistry to potentially bioactive molecules that can be identified in such natural products. Thus, the structural and physicochemical properties of such molecules can be reconciled with current theories on the molecular aspects of a given disease and/or be used to improve upon such theories or to develop new ones.

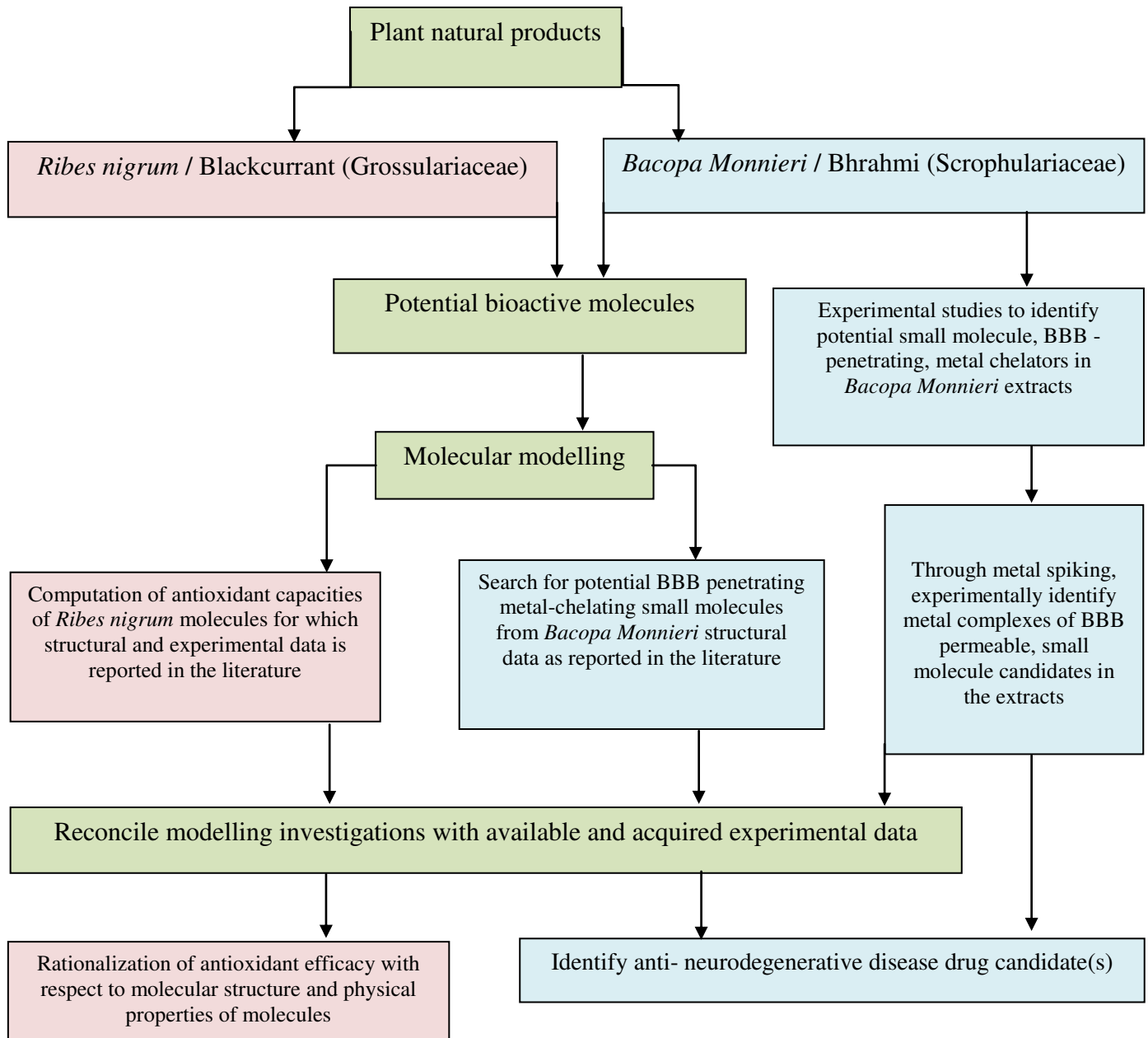
Computed properties may also be benchmarked to experimental data for isolated molecules of interest that can lead to improved molecular design. In this context, two different strategies have been devised and implemented for the identification and development of potentially bioactive compounds from medicinal plant materials whereby reliable molecular structures and experimental data, that have been previously reported in the peer reviewed scientific literature, have been reconciled with carefully designed computational chemistry calculations and/or further experimentation - with a view to (I) developing improved antioxidants as potential anti-inflammatory drugs and (II) to identify small molecule potential metal chelators that may pass through the blood brain barrier and potentially ameliorate neurodegenerative diseases such as Alzheimer's or Parkinson's disease. Thus two bioactive products derived from medicinal plants, namely *Ribes nigrum* (Blackcurrant leaves) and *Bacopa Monnieri* (Brahmi tea), that are traditionally employed to treat rheumatic disease and neurodegenerative symptoms, respectively, have been chosen for investigation under these strategies. These plant materials have been extensively investigated in the scientific literature in terms of the identification of the structures of their potentially bioactive molecules and also with respect to experimental and biological investigations. For the former material, the

purported anti-inflammatory effects of the component poly phenolic molecules, in terms of their reported experimental radical scavenging propensities, have been reconciled with their computed antioxidant capacities. These have also been related to a range of computed qualitative and quantitative structural and physicochemical properties. This is with a view to optimizing their antioxidant potential and possibly designing anti-inflammatory drug candidates. For the latter material, a screening of the reported molecular structures of potentially bioactive components has identified two smaller molecular fragments, namely the isomers jujubogenin and pseudojujubogenin, that may also be present in the plant extract and that are deemed capable of passing through the blood brain barrier and complexing transition elements within the brain, specifically copper and/or zinc, that are associated with stabilizing the amyloid plaque of Alzheimer's disease, or iron, that may over-load the substantial nigra in Parkinson's disease. In this thesis, the metal complexes of these two molecules have been modelled utilizing semi-empirical quantum chemistry and density functional calculations and the characteristics of the copper, zinc and iron complexes have been described. These studies clearly show that the diaquo, square planar copper complex of jujubogenin is the preferred structure, revealing that jujubogenin is an excellent bidentate ligand for this particular transition metal. The corresponding zinc complex was also shown to be feasible, but less likely to form; whereas the iron complex was shown not to be accommodated at all. To complement these studies, the Brahmi tea material was extracted with a range of solvents, and fractions were systematically subjected to ESI-MS. Scrutiny of the resultant spectra revealed the presence of the protonated jujubogenin moiety in one of the ethyl acetate fractions. Subsequent spiking of this fraction with copper, zinc and iron revealed the presence in the spectra of the diaquo copper complex of jujubogenin, exactly as predicted from the computer modelling. Notably, no zinc or iron complexes could be detected and competition experiments only revealed the presence of the copper complex - also consistent with the computer modelling. Subsequent MS/MS experiments on the copper complex yielded the free ligand.

In summary, for possible anti-inflammatory agents, these investigations show that the computed homolytic bond dissociation energies of the component poly phenolics, by themselves, are not sufficient to explain enhanced antioxidant activity and suggest that

other properties such as molecular conformation, steric effects and, in particular, the magnitude and direction of the dipole moment also have important roles to play. In relation to possible drug leads for the treatment of neurological conditions, the discovery of the extraordinary copper specificity of the jujubogenin molecule, both computationally and experimentally, makes this molecule a candidate for a BBB penetrating chelating agent that could be active towards the amelioration of Alzheimer's disease and possibly other conditions. This is an exciting discovery and warrants the isolation of jujubogenin and its derivatives in for further testing. Thus, the design and implementation of the key strategies devised and described within this thesis and their respective application to two selected traditional medicines relating to specific disease states, is demonstrably useful in the rational design of drug candidates and suggest new avenues for future research.

Conceptual Framework



Declaration

"I Kavitha Menon declare that the PhD thesis entitled '**Modelling and benchmarking of potentially bioactive molecules from plants - design and implementation of two strategies**' is no more than 100,000 words in length including quotes and exclusive of tables, figures, appendices, bibliography, references and footnotes. This thesis contains no material that has been submitted previously, in whole or in part, for the award of any other academic degree or diploma. Except where otherwise indicated, this thesis is my own work".



Signature

Date 13/03/2020

Kavitha Menon

March 2020

Journal publications and conference presentations relevant to this thesis.

Draft Publications

1. Menon, K., Smallridge A. and Orbell, J.D. (in preparation), 'Two strategies for the discovery and development of drug leads from medicinal plants', - to be submitted to *Phytochemistry* as a 'Viewpoint' article.

2. Menon, K., Smallridge A. and Orbell, J.D. (in preparation), 'Molecular modelling studies of antioxidant lignoid molecules from the leaves of *Ribes nigrum*', - to be submitted to the *Journal of Natural Products* as a full paper.

3. Menon, K., Smallridge A. and Orbell, J.D. (in preparation), 'The identification of a potential anti-Alzheimer's Disease molecule in an Ayurvedic traditional 'brain tonic' medicine', - to be submitted to *Nature* as a Letter.

Awards and conference platform presentations

'Young researcher forum award' for the presentation: The search for anti-neurodegenerative drug leads from an Indian traditional herbal medicinal that is regarded as a 'brain tonic', 5th International Conference and Exhibition on Pharmacognosy, Phytochemistry and Natural Products, 2017, July 24-25, Melbourne, Australia.

*I wish to dedicate this thesis to
my loving family*

Acknowledgements

I am obliged to many people who directly and/or indirectly supported me during my research studies. I would like to thank Victoria University for giving me this opportunity and supporting this research.

Firstly, I would like to express my sincere gratitude to **Professor John Orbell**, and thank him for his patience, persistence and priceless contributions to my research as my Principal Supervisor. I wish to thank him whole-heartedly for his timely advice, constant motivation and frequent work discussions.

I am also particularly grateful to my Associate Supervisor, **Professor Andrew Smallridge**, for his insightful feedback and contributions to my research project.

I would like to thank Joe Pelle and Daniel Collins for their help with analytical instrumentation and equipment. I would also like to acknowledge and thank Drs Domenico Caridi, Sunaja Devi, Anitha Varghese and Paul Joseph for their help. Also, thanks to Stacey Lloyd, Min Nyugen, Chathuri Priyadasa, Mary Marshall and Nishantha Illangantilaka for their assistance.

Thanks to my friends Drs Swathy Garg Goel, Sudha Teenu, Shyla George, Jorphin Joseph and Suresh Kumar, Anoop Ali, Soumya, Sruthy, Easwari, Lekshmi, Aparna and Devu who encouraged me in my research journey.

None of my achievements would have been possible without the support and dedication of my family. Many thanks to my mother (Indira), my father (Narayanankutty Menon), my son (Deven Menon) and my daughter (Devi Menon) for their support and encouragement. Last, but never the least, thanks to my husband Hary Menon, who has always been there as a source of inspiration to me.

Table of Contents

Abstract	2
Conceptual Framework.....	5
Declaration	6
Journal publications and conference presentations relevant to this thesis.....	7
Draft Publications.....	7
Awards and conference platform presentations.....	7
Acknowledgements	9
List of Tables	16
List of Figures.....	18
CHAPTER 1.....	28
General introduction and background	28
1.1 Traditional medicines and natural products	28
1.2 Natural products as drugs.....	29
1.3 Antioxidants from natural products	29
1.4 Advantages of natural products as medicines	30

1.5 Neurological disorders	31
1.6 Oxidative stress	31
1.7 Metal ions and neurodegenerative diseases	32
1.8 Correlation between the presence of metal ions and beta amyloid or tau protein accumulation in the brain	33
1.9 Blood-Brain Barrier (BBB) permeability of molecule(s)/ drug(s)	33
1.10 Overview of <i>in vitro</i> experimental methods for antioxidant activity assays	34
1.10.1 <i>In vitro</i> experimental methods	34
1.10.1.1 Metal chelating activity method	34
1.10.1.2 Beta carotene bleaching method/ beta carotene linoleic acid method /conjugated diene assay	35
1.10.1.3 Cupric ion reducing antioxidant capacity method (CUPRAC)	35
1.10.1.4 N, N-dimethyl-p-phenylenediamine dihydrochloride (DMPD) method	35
1.10.1.5 Thiobarbituric acid method	35
1.10.1.6 Ferric thiocyanate (FTC) method	36
1.10.1.7 Oxygen radical absorbance capacity (ORAC) method	36
1.10.1.8 Phospho molybdenum complex method	36
1.10.1.9 HORAC (hydroxyl radical averting capacity) method	36
1.10.1.10 Reducing power (RP) method	37

1.10.1.11 Trolox equivalent antioxidant capacity (TEAC) method	37
1.10.1.12 Hydrogen peroxide scavenging assay	37
1.10.1.13 Superoxide radical scavenging activity assay	38
1.10.1.14 DPPH (1, 1-diphenyl-2- picryl hydrazyl) free radical scavenging assay	39
1.11 Computational methods and analysis for antioxidant molecules	40
1.12 Research aims	41
PART A	43
CHAPTER 2	44
A computational study of potential antioxidants from the leaves of <i>Ribes nigrum</i> (“blackcurrant”)	44
2.1 Research Strategy	44
2.2 Preamble	45
2.3 The antioxidant and anti-inflammatory characteristics of <i>Ribes nigrum</i>	45
2.4 Reported structures and experimental antioxidant data for <i>Ribes nigrum</i> lignoids	47
2.5 Density Functional Theory (DFT)	51
2.6 Establishing equilibrium geometries	51
2.7 (Homolytic) bond dissociation energies (BDEs) and “secondary” BDEs	52
2.8 Single point energy calculations	53

2.9 Dipole moment calculations	53
2.10 Polar surface area (PSA)	54
2.11 Log₁₀P	54
2.12 Intra molecular hydrogen bonding (IMHB)	55
2.13 Computing the relative O-H bond dissociation energies of the polyphenolics	60
2.14 Computation of relevant physical properties (qualitative and quantitative)	62
2.15 Result and discussion	65
<i>1. Why are the Molecules of Group 2, namely molecules 2, 3, 6, 9 and 10, Table 2.3, only active towards superoxide and not towards DPPH?</i>	65
<i>2.Molecules of Group 3, namely Molecules 4 and 13, Table 2.4, are active towards both superoxide and DPPH. Why?</i>	73
2.16 Comparison of Molecules	76
2.16.1 Molecules 1-6 and Molecule 15	76
2. 16.2 Set 1 (Molecules 1-6 and 15)	76
2.16.3 Set 2 (Molecules 7, 8 and 9)	78
2.16.4 Set 3 (Molecules 10, 13 and 14)	79
2.16.5 Molecules 7 and 8 inactive towards both.	79
2.17 Effect of intra molecular hydrogen bonding on dipole moment	79
2.18 Effect of ionization potential over methoxy substituent	82

2.19 Conclusions	84
References	86
PART B	90
CHAPTER 3	91
A strategy for the identification of a potential drug candidate from a traditional medicine	91
3.1 Preamble	91
3.2 Traditional Ayurvedic medicine – Brahmi (<i>Bacopa monnieri</i>)	94
3.3 Drug leads for the treatment and prevention of Alzheimer’s disease (AD)	95
3.4 Prior research studies of <i>Bacopa monnieri</i> (BM)	96
3.5 Role of metal ions in Alzheimer’s disease (AD)	97
3.5.1 Cu in biological systems	98
3.5.2 Zn in biological systems	98
3.5.3 Fe in biological systems	99
3.6 Metal chelators as potential drugs	99
3.7 Structures of some saponins and bacosides of BM from chemical analysis	100
3.8 Jujubogenin as a drug candidate	101
3.8.1 The isomers Jujubogenin and Pseudojujubogenin	101

3.9 Computational analysis of potential Cu²⁺ and Zn²⁺ complexes of Jujubogenin and Psuedojujubogenin, as bidentate ligands	103
3.9.1 Preamble	103
3.9.2 Computational method	104
3.9.3 MW, Log₁₀P and BBB penetration	106
3.9.4 Intra molecular hydrogen bonding (IMHB)	106
3.9.5 Polar surface area (PSA)	107
3.10 Computed structures of JJ, PJJ and their Cu²⁺ and Zn²⁺ complexes	108
3.10.1 The refined JJ and PJJ structures	108
3.10.2 The refined Cu²⁺ and Zn²⁺ stuctures of JJ and PJJ	110
3.10.3 Discussion of the Cu and Zn complexation with JJ and PJJ	114
3.10.4 Strain energy during molecular modelling	114
3.11 Experimental methods for BM extraction	116
3.11.1 Materials and reagents	116
3.11.2 Instrumentation	116
3.11.3 BM extract preparation	116
3.11.3.1 Different solvents	116
3.11.3.2 Ethyl acetate extraction	116

3.11.4 Phytochemical screening of different plant extracts	117
3.11.4.1 Test for triterpenoids	117
3.11.4.2 Test for flavonoids	117
3.11.4.3 Test for saponins	117
3.11.4.4 Test for steroids	117
3.11.4.5 Test for tannins	118
3.11.5 Column chromatography	119
3.11.6 Preparation of metal solutions and spiking experiments	119
3.11.6.1 Spiking experiment with copper	119
3.11.6.2 Spiking experiment with Zinc and Iron	119
3.11.7 ESI-MS and MS/MS experiments	119
3.12 Results and discussion	120
3.12.1 ESI-MS studies of <i>Bacopa monnieri</i> extracts	120
3.12.2 Chelating potential of JJ/PJJ	123
3.12.2.1 Spiking with Cu²⁺, Zn²⁺ and Fe³⁺	123
3.12.2.2 ESI-MS and MS/MS of potential metal complexes	124
3.12.2.3 Triple quad experiment with copper complex	124
3.12.2.4 Preference of Cu complexation over Zn or Fe	124

3.13 Conclusions and recommendation for future research	127
References.....	128
Appendices.....	141

List of Tables

Table 2.1 Experimental antioxidant data (superoxide anion and DPPH radical scavenging activities) of reported, isolated compounds from the leaves of <i>Ribes nigrum</i> (Sasaki et al. 2013b). Note that >50 μ M is inactive.....	53
Table 2.2 Computed properties of molecules that are inactive towards both superoxide and DPPH, Group 1 – Colour Code Orange.....	60
Table 2.3 Computed properties of molecules that are active towards superoxide but not towards DPPH, Group 2 - Colour Code Blue.....	60
Table 2.4 Computed properties of molecules that are active towards both superoxide and DPPH, Group 3 – Colour Code Green.....	61
Table 2.5 Relevant computed properties for all molecules included in this study.....	64
Table 2.6 Experimental and computational data of <i>Ribes nigrum</i> lignoid molecules....	65
Table 2.7 Minimum computed BDE values compared to experimental superoxide and DPPH radical scavenging values, where activity is towards superoxide only.	66
Table 2.8 Computed values of lignoid molecules with the values of dipole moment of parent and radical species and the number of intramolecular hydrogen bonding.	84
Table 3.1 Intramolecular hydrogen bonding characteristics in JJ and PJJ, compared to CQ.....	110
Table 3.2 Computed values of Log ₁₀ P, PSA, and IMHB of Jujubogenin, Pseudojujubogenin, and its Cu ²⁺ and Zn ²⁺ complexes.	113

Table 3.3 Coordination sphere bond lengths and bond angles for the refined structure of the Cu ²⁺ and Zn ²⁺ diaquo complexes of JJ and PJJ; (w) = water.	114
Table 3.4 Strain energies of Cu ²⁺ and Zn ²⁺ complexes of Jujubogenin and Pseudojujubogenin during molecular modelling.	116
Table 3. 5 Experimental analysis of phytochemicals in the extracts of methanol, octanol, ethyl acetate and water (+ = presence and - = absence of phytochemicals).	119

List of Figures

Figure 1.1 Schematic representation of the classification of antioxidant molecules (Carocho & Ferreira 2013).	32
Figure 1.2 Schematic representation of diseases caused by oxidative stress (Förstermann 2008; Lin & Beal 2006).....	34
Figure 1.3 Schematic representation of DPPH free radical scavenging activity (Ji, Tang & Zhang 2005).	41
Figure 1.4 Schematic representation of H-transfer mechanism/free radical neutralization reaction.	42
Figure 2.1 <i>Ribes nigrum</i> (“blackcurrant”)	47
Figure 2.2 Set 1 - reported molecular structures (Sasaki et al. 2013a) of the phenolic compounds 1 to 6 and 15 from the leaves of <i>Ribes nigrum</i> . Note that the original numbering scheme for these molecules has been retained for ease of reference to Sasaki et al. 2013.	49
Figure 2.3 Set 2 - reported molecular structures (Sasaki et al. 2013a) of the phenolic compounds 7 to 9 from the leaves of <i>Ribes nigrum</i> . Note that the original numbering scheme for these molecules has been retained for ease of reference to Sasaki et al. 2013.	50
Figure 2.4 Set 3 - reported molecular structures (Sasaki et al. 2013a) of the phenolic compounds 10, 13 and 14 from the leaves of <i>Ribes nigrum</i> . Note that the original	

numbering scheme for these molecules has been retained for ease of reference to Sasaki et al. 2013.	51
Figure 2.5 Isomeric structures of Butylated hydroxy anisole (BHA).....	51
Figure 2.6 Modelled structures of <i>Ribes nigrum</i> Molecules (1-4), Set 1.	57
Figure 2.7 Modelled structures of <i>Ribes nigrum</i> Molecules (5, 6, and 15), Set 1 continued.	58
Figure 2.8 Modelled structures of <i>Ribes nigrum</i> Molecules (7-9), Set 2.	58
Figure 2.9 Modelled structures of <i>Ribes nigrum</i> Molecules (10, 13, and 14), Set 3.....	59
Figure 2.10 Modelled structure of Vitamin E, control for computational analysis.....	59
Figure 2.11 Modelled structure of BHA, control for experimental data.	59
Figure 2.12 Chemical structures and the calculated bond dissociation energy values (BDEs in kcal/mol) of compounds 1-9 and compound 15. The “primary” BDEs are indicated in black type and the “secondary” BDEs of these molecules are indicated in green type (activated) or red type (deactivated).	62
Figure 2.13 Chemical structures and the calculated bond dissociation energy values (BDEs in kcal/mol) of compounds 10, 13, and compound 14. The “primary” BDEs are indicated in black type and the “secondary” BDEs of these molecules are indicated in green type (activated) or red type (deactivated).	63
Figure 2.14 Chemical structures and the calculated bond dissociation energy values (BDEs in kcal/mol) for compounds 1 and 2. Since these are mono-phenolics the values are necessarily primary BDEs.	63

Figure 2.15 Representation of electrostatic energy maps of Molecule 9 with (a) superoxide and (b) DPPH.....	68
Figure 2.16 Representation of electrostatic potential maps of the Molecule 2 with (a) superoxide and (b) DPPH. In this diagram, the spin potential of the DPPH is also shown.....	69
Figure 2.17 Representation of electrostatic energy map of Molecule 3 with (a) superoxide anion and (b) DPPH. IN this diagram, the spin potential of the DPPH is also shown to high light the accessibility of this region to the antioxidant region of Molecule 3.....	71
Figure 2.18 Representation of electrostatic energy maps of Molecule 6 with (a) Superoxide and (b) DPPH.	72
Figure 2.19 Representation of electrostatic energy maps of Molecule 10 with (a) superoxide and (b) DPPH.....	73
Figure 2.20 Representation of electrostatic energy maps of Molecule 4 with (a) superoxide and (b) DPPH.....	75
Figure 2.21 Representation of electrostatic energy maps of Molecule 13 with (a) superoxide and (b) DPPH. Not that the spin potential is also indicated in the DPPH molecule to high light its accessibility to the active OH moiety.....	76
Figure 2.22 Representation of electrostatic energy map of Molecule 15 with (a) superoxide and (b) DPPH.....	78
Figure 2.23 Representation of Molecule 2 with Intra Molecular Hydrogen Bonding. ...	81
Figure 2.24 Representation of Molecule 4 with Intra Molecular Hydrogen Bonding. ...	81

Figure 2.25 Representation of Molecule 9 with Intra Molecular Hydrogen Bonding. ..	81
Figure 2.26 Representation of Molecule 13 with Intra Molecular Hydrogen Bonding. 82	
Figure 2.27 Representation of Molecule 15 with Intra Molecular Hydrogen Bonding. 82	
Figure 2. 28 Representation of electrostatic energy map of Molecule 7.....	83
Figure 2. 29 Representation of electrostatic energy map of Molecule 8.....	83
Figure 3.1 <i>Bacopa monnieri</i> (Brahmi)	96
Figure 3.2 Schematic representation of A β mediated free radical generation and the peptide when it binds in the presents of catalytic amounts of Cu ²⁺ / Fe ³⁺ /Zn ²⁺ ions. .	99
Figure 3.3 Structures of some Bacosaponins and Bacosides of BM.	102
Figure 3.4 The molecular structures of the isomers (1) Jujubogenin and (2) Pseudojujubogenin.....	103
Figure 3.5 The molecular structure of Lanosterol.	103
Figure 3. 6 Schematic representations of (a) Jujubogenin; (b) Pseudojujubogenin; (c) Cu ²⁺ - Jujubogenin complex; (d) Cu ²⁺ -Pseudojujubogenin complex; (e) Zn ²⁺ - Jujubogenin complex and (f) Zn ²⁺ -Pseudojujubogenin complex. Also shown are the atom numbering schemes(Ramasamy et al. 2015), the IMHBs and favoured bidentate metal co-ordination sites (note that the metals are also assumed to be coordinated to two water molecules but these have been omitted for clarity). The relevant bond lengths and computed energies of the IMHB are given in Table 3.1.	105
Figure 3.7 Representations of energy level schemes for (a) square planar coordination splitting pattern and (b) tetrahedral coordination splitting pattern.	106

Figure 3.8 Schematic representation of IMHB across the bidentate coordination site in CQ.....	108
Figure 3.9 Jujubogenin with intramolecular hydrogen bonding (dotted line). Red indicates oxygen, white hydrogen and grey carbon. Note that a potential bidentate metal coordination site can be identified as involving the two oxygen atoms of the IMHB.	109
Figure 3.10 Pseudojujubogenin with intramolecular hydrogen bonding (dotted line).Red indicates oxygen, white hydrogen and grey carbon. Note that a potential bidentate metal coordination site can be identified as involving the two oxygen atoms of the IMHB.	109
Figure 3.11 Cu ²⁺ - JJ square planar complex, showing the bond angles of the square planar coordination sphere, Table 3.2. Red indicates oxygen, white hydrogen and grey carbon.	111
Figure 3.12 Cu ²⁺ - PJJ square planar complex, showing the bond angles of the square planar coordination sphere. Red indicates oxygen, white hydrogen and grey carbon.	112
Figure 3.13 Zn ²⁺ - JJ tetrahedral complex showing the bond angles of the tetrahedral coordination sphere. Red indicates oxygen, white hydrogen and grey carbon.	112
Figure 3.14 Zn ²⁺ - PJJ tetrahedral complex showing the bond angles of the tetrahedral coordination sphere. Red indicates oxygen, white hydrogen and grey carbon.	113
Figure 3.15 Schematic representation of Cu ²⁺ octahedral complexes in equilibrium with square planar complexes and Zn ²⁺ octahedral complexes in equilibrium with tetrahedral complexes.	115
Figure 3.16 The ESI-MS spectra of [C ₃₀ H ₄₈ O ₄] ⁺ in positive ion mode m/z 473; loss of H ₂ O from [C ₃₀ H ₄₈ O ₄] ⁺ in positive ion mode m/z 455. No attempt has been made to assign the other peaks in this spectrum.	122

Figure 3.17(a) MS/MS of m/z 473, polarity: positive, Collision Energy (CE) –25 V; (b, d) MS/MS of m/z 473, polarity: positive, CE-35 V; (c) MS/MS of m/z 473, polarity: positive, CE-30 V; (e) MS/MS of m/z 473, polarity: positive, CE-40 V..... 124

Figure 3.18 ESI-MS spectra of $[C_{30}H_{48}O_4Cu(H_2O)_2]^+$ (positive ion mode), compared to the theoretical isotopic profile of $[C_{30}H_{48}O_4]Cu(H_2O)_2^+$ 125

Figure 3.19 Triple quad mass spectra of +571 ion, $[C_{30}H_{48}O_4 Cu(H_2O)_2]^+$ fractionate as +473 m/z of jujubogenin $[C_{30}H_{48}O_4]^+CE(25V)$ 126

Figure 3.20 ESI-MS spectra of competition experiment with Cu, Fe and Zn in positive ion mode; Insets (a) theoretical isotopic profile of $[C_{30}H_{48}O_4Cu(H_2O)_2]^+$; (b) theoretical isotopic profile of $[C_{30}H_{48}O_4Zn(H_2O)_2]^+$; (c) theoretical isotopic profile of $[C_{30}H_{48}O_4Fe(H_2O)_2]^{2+}$. Note that only the copper complex is present. A similar experiment with Zn and Fe failed to detect either. 127

List of Abbreviations and symbols

-	Negative
+	Positive
<	Less
>	Greater
±	Plus or minus
AD	Alzheimer's disease
A β	Beta amyloid
BM	<i>Bacopa Monnieri</i>
BDEs	Bond dissociation energies
BDE _M	Bond dissociation energy of molecule
BDE _{BM}	Bond dissociation energy of benchmark molecule
BHA	Butylated hydroxyl anisole
Cu	Copper
DFT	Density functional theory
DPPH	1, 1-diphenyl-2-picrylhydrazyl
EC ₅₀	50% of the amount of extract needed to inhibit free radicals at a specified time
EDTA	Ethylene di amine tetra acetic acid
FeCl ₂	Ferrous chloride
H ₂ O ₂	Hydrogen peroxide
JJ	Jujubogenin

PJJ	Pseudojubilogenin
PSA	Polar surface areas
IPs	Ionization potentials
<i>In vivo</i>	Experiment performed in live specimen
<i>In vitro</i>	Laboratory experiment performed outside the specimen biological context
IAPI	Intrinsic antioxidant potential index
Zn	Zinc
NPs	Natural products
OS	Oxidative stress
ROS	Reactive oxygen species
CE	Collision energy
TMs	Traditional medicines

List of SI units

% w/v	Percentage weight per volume
% w/w	Percentage weight per weight
%	Percentage
°C	Degrees centigrade
ml	Micro litre
µm	Micrometre
µM	Micro molar
g/dL	Gram per decilitre
g/L	Gram per litre
g	Gram
kg	Kilogram
V	Volume
d	Distance
m	Mass
n	Amount of substance
t	Time
T	Temperature
Q	Electric charge
<i>I</i>	Luminous intensity
I	Electric current
m	Meter
L	Liter
mol	Mole

s	Second
K	Kelvin
D	Density
E	Energy
A	Area
hr	Hour
L/L	Litre per litre
M	Molar
mg/g	Milligram per gram
mg/kg	Milligram per kilogram
mg/ml	Milligram per millilitre
mg	Milligram
min	Minute
ml/kg	Milligram per kilogram
ml	Millilitre
mM	Mill molar
mol/L	Molar per litre
N	Normality
nm	Nanometre

CHAPTER 1

General introduction and background

1.1 Traditional medicines and natural products

Traditional medicines (TMs) derived from natural products has been given fruitful contributions in modern medicine (Yuan et al. 2016). One of the main advantage of TMs are the available data of known clinical experiences and biological activities. While developing synthetic drug(s) from or based on natural products, it will be useful to know the known chemical structure of the target molecule. The TMs have been practiced in some areas of the world are traditional Chinese medicine, traditional Indian medicine (Ayurveda), traditional Korean medicine¹, and Unani² etc. Though, the scientifically researched natural products/ plant materials are fewer and should be explored more, will be valuable for modern medicine. Based on TMs, numerous modern medicines/drugs were reported for anticancer, anti-neurodegenerative, anti-migraine, anti-allergic, antibacterial, anti-diabetic, antiulcer, anti-inflammatory etc., (Joo 2014; Newman, Cragg & Snader 2003). In addition, natural product based TMs may contain huge amount of phytochemicals as its constituents (Chitwood 2002; Ehrman, Barlow & Hylands 2007). These phytochemical constituents (e.g. glycosides, triterpenoids, flavonoids, saponins, alkaloids etc.) either together or alone contributes the desired pharmacological effects.

¹ Traditional Korean medicine includes herbal medicine, acupuncture, moxibustion, cupping therapy and “physical therapies” such as hot pack applications, massage, chiropractic manipulation and infrared irradiation.

² Unani medicine is a system of alternative medicine that originated in ancient Greece but is now practiced primarily in India. Involving the use of herbal remedies, dietary practices, and alternative therapies, Unani medicine addresses the prevention and treatment of disease.

1.2 Natural products as drugs

Natural products have significant role in developing and discovering new drugs in modern medicine. Most of the biologically active natural products are found to be effective and desirable for treating many human diseases (Clark 1996; Shu 1998). Thus, natural products and/or naturally derived drug(s) lead an evolutionary transition in the development of synthetic drug(s) in modern medicine. For example, the first pharmacologically active drug derived from natural product was morphine from opium (Ellison & Lewis 1984; Jonsson et al. 1988; Joo 2014; Säwe et al. 1981) and furthermore, several clinically proven anticancer drugs are either natural products or its derivatives (Gordaliza 2007). The emerging need for developing new synthetic drug(s) for many human diseases lead to do research in natural products.

1.3 Antioxidants from natural products

The antioxidants are classified mainly as three categories (Carocho & Ferreira 2013). The classification of antioxidants are depicted in Figure 1.1. Various medicinal plants exhibits natural antioxidant characteristics. The antioxidants are widely distributed in certain foods such as vegetables, fruits, mushrooms etc. The antioxidants in human body can scavenge free radicals and reduce oxidative stress (Sen & Chakraborty 2011). Oxidative stress will be produced by the lack of cellular antioxidants and so natural antioxidants/antioxidant therapeutics have an emerging need in current research (Uttara et al. 2009). More than a few naturally derived antioxidants may contain polyphenolic molecules, which can acts as free radical chain breakers, free radical scavengers, reducing agents, and metal ion chelators and thus exhibits therapeutic benefits (El Gharras 2009). For example, naturally derived phytochemicals are widely used for the treatment for Alzheimer's (Lim, GP et al. 2001), Parkinson's (Newman, Cragg & Snader 2003) and other neurodegenerative diseases (Chowdhuri et al. 2002). It was reported that biologically active molecules and phytochemicals of few natural products may delay Alzheimer's Disease (AD) onset or inhibit beta amyloid aggregation in the brain (Newman, Cragg & Snader 2003). Most of the synthetic drugs in the market for AD and other neurodegenerative diseases are anti-oxidative, anti-inflammatory, in nature but have side effects (Orhan, Orhan & Sener 2006).

In general, Part A of this thesis was a search for polyphenolic antioxidants and part B for potential, bioactive metal chelating molecules from natural products.

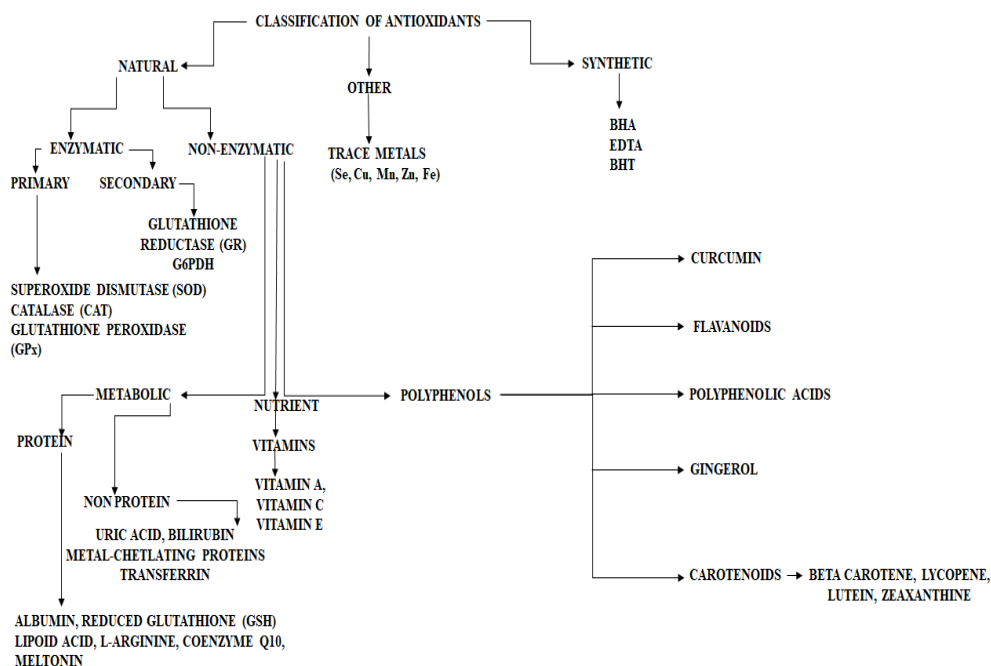


Figure 1.1 Schematic representation of the classification of antioxidant molecules (Carocho & Ferreira 2013).

1.4 Advantages of natural products as medicines

Natural products and their derivatives contributed significantly in drug discovery and development today. Natural products have been used since prehistoric times for the treatment of various diseases. Furthermore, drugs or drug leads derived from natural products are less time consuming and may be more accessible to developing countries. Numerous naturally derived drugs have no side effects or mild level side effects when compared with that of synthetic drugs (Karimi, Majlesi & Rafieian-Kopaei 2015). The structure-based drug designing (known chemical structure of medicinal plants) and molecular modelling (of desired molecules) diminishes experimental efforts with less time and minimum outlay. Experimentally, trial and error methods were found to be the most effective method for the development and discovery of a new molecule/ drug lead(s). The advantage of natural products over synthetic drugs is to abolish the toxic side effects which are usually persuaded by synthetic drug molecules. Many naturally

derived traditional medicines, whose efficacy has been tested in clinical experiments, had proven therapeutic benefit at different levels on multiple targets and pathways.

1.5 Neurological disorders

Any disorder of a human body associated with nervous system, comes under the category of neurological disorder. The nervous system in human brain is a very complex communication network, in which the neurons can frequently send and accept messages. Impairment of one these neurons may cause brain dysfunction and thus results neurological disorders (Pfaender & Grabrucker 2014). Naturally derived phytochemicals have proven ability to eradicate few neurological disorders (Newman, Cragg & Snader 2003; Ng, Or & Ip 2015). The neurological diseases like Alzheimer's and Parkinson's were considered to be the repercussions of damaged neurons inside the brain (Huang et al. 1999; Pfaender & Grabrucker 2014). Some of the reasons proposed for neurodegeneration are 1) oxidative stress (Lim, GP et al. 2001; Lin & Beal 2006) 2) accumulation of certain metals such as Cu^{2+} , Fe^{2+} , Zn^{2+} in the brain (Atwood et al. 1998; Atwood et al. 2000; Barnham & Bush 2008; Pedersen, Østergaard, et al. 2011) and 3) the beta amyloid and or tau protein accumulation in the brain (Goedert 1993; Martin et al. 2013; Shankar et al. 2008; Zhou et al. 2007) etc. Currently there are limited number of effective treatment for these kind of neurological disorders. It was reported that some potential, bioactive, natural products/derivatives of medicinal plant extracts are effective against neurodegenerative diseases (Ng, Or & Ip 2015).

1.6 Oxidative stress

Oxidative stress is considered as one of the major reasons for most of the diseases including cancer (Valko et al. 2006; Willcox, Ash & Catignani 2004), cardiovascular diseases/atherosclerosis (Stephens et al. 1996; Street et al. 1994), (Hodis et al. 1995; Steinberg 1991) and several neurodegenerative disorders like Alzheimer's and Parkinson's disease (Desagher, Glowinski & Premont 1996). In human body during cellular respiration, free radicals are generating continuously as a by-product (Lushchak 2014; Pham-Huy, He & Pham-Huy 2008). These free radicals are highly reactive and less stable but can participate in high diversity of reactions (Lushchak 2014). Majority of these free radicals are generated from oxygen atoms by the reduction of molecular

oxygen through one and four electron transfer mechanism (Lushchak 2014). These highly reactive, less stable $O_2^{\cdot-}$, H_2O_2 and HO^{\cdot} are collectively known as reactive oxygen species (ROS) (Lushchak 2014). Iron or copper ions acts as a catalyst during the generation or production of $O_2^{\cdot-}$, H_2O_2 (Halliwell 1992). At reasonable levels (ROS) are beneficial to human health, whereas the disparity of the amount of (ROS) and the amount of antioxidants lead to oxidative stress (Pham-Huy & He). This oxidative stress produces stress in the tissues and cells by damaging DNA, proteins and unsaturated fatty acids and thus lead to a numerous pathological conditions including cancer (Valko et al. 2006), neurodegenerative disorders (Pham-Huy & He).

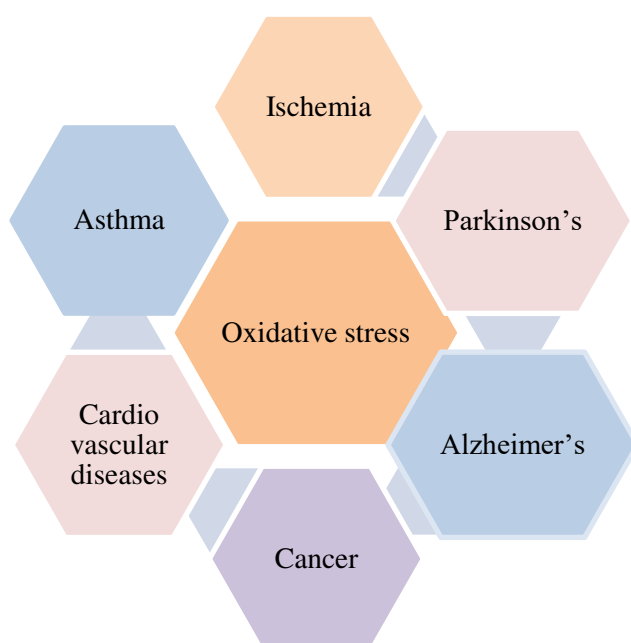


Figure 1.2 Schematic representation of diseases caused by oxidative stress (Förstermann 2008; Lin & Beal 2006).

1.7 Metal ions and neurodegenerative diseases

Numerous neurodegenerative diseases are associated with the poorly regulated metal ions in the human body and the central nervous system (Atwood et al. 1998; Barnham & Bush 2008; Benedet & Shibamoto 2008; Dexter et al. 1989). Many divalent metal ions were found to be capable enough to bind with proteins *in vivo* (Pfaender & Grabrucker 2014). The imbalance of these divalent metal ions may affect the brain homeostasis. For example, it was reported that the presence of elevated amount of total iron content in the substantial nigra of the Parkinson's disease patient's brain (Dexter et

al. 1989). The disparity of (paucity or excess) one of the biometal can change the equilibrium of the other metals *in vivo* (Pfaender & Grabrucker 2014). In addition, recent studies indicate that the presence of elevated levels of Cu and Zn in the hair, nail and serum samples of other neurological disordered patients (Faber et al. 2009; Pfaender & Grabrucker 2014).

1.8 Correlation between the presence of metal ions and beta amyloid or tau protein accumulation in the brain

Alzheimer's disease (AD) is a degenerative and fatal brain disease, in which cell to cell connections in the brain are lost (Hardy & Selkoe 2002). It has been reported that beta amyloid (A β) protein accumulation or A β plaques and neurofibrillary tangles in the brain are responsible for this disease (Shankar et al. 2008). Since A β and tau protein accumulation enhances the neuronal toxicity in the brain, it is significant to inhibit these protein assembly. Cu (II) has a significant effect in the accumulation of A β and tau protein as Cu (II) is capable enough to alter the conformation of the peptide associated with it (Kowalik-Jankowska et al. 2002; Zhou et al. 2007). Furthermore, it has been reported that the Cu/Zn metal chelators can selectively separate A β protein from the post-mortem brain tissues sample of the AD patients and transgenic mice brains (Gouras & Beal 2001; Kowalik-Jankowska et al. 2002). It was reported that A β protein can bind with copper and zinc (Cherny et al. 2001; Gouras & Beal 2001) and also, Cu/Zn chelators solubilize A β from post-mortem brain samples of AD patients. One of the reported metal chelator clioquinol (CQ), is found to be effective in liberating A β from post-mortem brain samples of AD patients (Gouras & Beal 2001).

1.9 Blood-Brain Barrier (BBB) permeability of molecule(s)/ drug(s)

The blood-brain barrier (BBB), is a stationary and inflexible wall among the central nervous system and the periphery (Oldendorf 1974). One of the key aspects for the treatment of neurological disorders, is to know the ability of a molecule(s) /drug(s) that can pass through the BBB. Lipophilic molecules may be able to diffuse through the cell membrane and thus can cross the BBB (Lohmann, Hüwel & Galla 2002). The major obstacle in neurodegenerative drug discovery is to determine whether the drug/molecule

can cross the BBB and to attack the target site. Therefore, BBB permeability have vital role in maintaining brain homeostasis. The permeability of a drug/molecule through this complex physiological barrier can be interpretable by molecular modelling studies (Caron, Vallaro & Ermondi 2018). Many techniques or computing methods has been used extensively in molecular modelling for interpreting the BBB permeability, including $\text{Log}_{10}P$, polar surface area, linear regression techniques, and ionization potential. This research work was done by using quantum chemical methods (Semi-empirical and Density Functional Theory) to compute the equilibrium geometries of the molecules of interest and calculated a range of relative physicochemical parameters and structural features that could contribute to their experimentally observed relative antioxidant activities and/or to interpret the BBB permeability.

1.10 Overview of *in vitro* experimental methods for antioxidant activity assays

Antioxidants, especially Vitamin E, have a vital role in the human body as it provide protection against lipid per oxidation. Antioxidants derived from natural products also offer a potential ‘defence mechanism’ for the human body. Depending on their chemical structures and physicochemical properties, different antioxidants (e.g. from food, synthetic, natural products) show varying antioxidant potency. There are a number of established *in vitro* and *in vivo* assays for antioxidant efficacy. These are outlined below:

1.10.1 *In vitro* experimental methods

1.10.1.1 Metal chelating activity method

Colorimetric reaction of the radical with ferrozine - Fe^{2+} complex, estimates decrease in red colour of the complex with the chelation as the metal ion coordinated with the phenolic antioxidants (Soler-Rivas, Espín & Wichers 2000). The metal chelating capacity of the ferrous ion can be calculated as follows

$$\% = [(A_0 - A_1) / A_0] \times 100$$

Where A_0 is the absorbance of the standard solution (all reagents without polyphenols) and A_1 is the absorbance of all reagents with polyphenols /standard (Soler-Rivas, Espín & Wichers 2000).

1.10.1.2 Beta carotene bleaching method/ beta carotene linoleic acid method /conjugated diene assay

Colorimetric method estimating the rate of beta carotene bleaching and measured the absorbance at 470 nm using spectrophotometer. The reagents used for beta carotene oxidation reactions are beta carotene, chloroform, linoleic acid and emulsifier mixture (Kabouche et al. 2007).

1.10.1.3 Cupric ion reducing antioxidant capacity method (CUPRAC)

Colorimetric assay used for the estimation of total antioxidant potencies of polyphenols, vitamin C, vitamin E etc. This includes the oxidation of polyphenolics which then converted to corresponding quinones by copper complex and measured absorption at 450 nm (Apak et al. 2008). Antioxidant potencies of antioxidants slightly varies with various assays - for example, CUPRAC methods gives greater antioxidant activity for catechin, quercetin, gallic acid etc. Furthermore, this assay is based on electron transfer mechanism and the polyphenols oxidized rapidly with copper complex (Apak et al. 2008).

1.10.1.4 N, N-dimethyl-p-phenylenediamine dihydrochloride (DMPD) method

In this colorimetric method, the radical cations generated by the reagents are responsible for the reaction and colour. Antioxidant activity in food and similar matrices can be measured, absorbance at 505 nm (Fogliano et al. 1999). The percentage of radical cation (uninhibited) can be evaluated by

$$\% = [(1-A_1)/A_0] \times 100$$

Where A_0 is the absorbance of radical cation (uninhibited) and A_1 is the absorbance measured after 10 min, of all the reagents with antioxidants.

1.10.1.5 Thiobarbituric acid method

Reagents used for this colorimetric method are trichloroacetic acid and thiobarbituric acid. The reaction mixture (reagents and antioxidant sample) placed in water bath for 10 minutes, centrifuged and measured the absorbance at 552 nm (Ottolenghi 1959).

1.10.1.6 Ferric thiocyanate (FTC) method

Colorimetric method measured absorbance at 500 nm based on the preparation of stable emulsion by vigorously shaking the reagents (ethanol, linoleic acid, phosphate buffer, and distilled water) with antioxidant sample. Antioxidant potency can be evaluated by calculating the percentage of inhibition with respect to the control (Alam, Bristi & Rafiqzaman 2013; Kikuzaki, Usuguchi & Nakatani 1991).

1.10.1.7 Oxygen radical absorbance capacity (ORAC) method

This is one of the widely used method for the estimation of total antioxidant capacity of the sample and also used for product development. This simple test tube analysis method developed in two different ways, lipophilic ORAC assay and hydrophilic ORAC assay. For the determination of lipophilic antioxidants in plasma and other biological samples, lipophilic ORAC assay is used. The reagent used for this assay is 2, 2-azobis-2-amidopropanedihydrochloride (AAPH). Decrease in fluorescence is measured with the scavenging of free radicals (Prior et al. 2003).

1.10.1.8 Phospho molybdenum complex method

Spectrophotometric method used for the quantitative determination of total antioxidant potency of a sample via formation of phospho molybdenum complex. The reagents (sulphuric acid, sodium phosphate, and ammonium molybdate) mixed with the analyte and the absorbance can be measured at 695 nm against blank (Prieto, Pineda & Aguilar 1999).

1.10.1.9 HORAC (hydroxyl radical averting capacity) method

Colorimetric assay involves the formation of metal-chelating cobalt complex with the antioxidants. The reagents used for the cobalt complex formation are hydrogen peroxide in distilled water, $\text{CoF}_2 \cdot 4\text{H}_2\text{O}$, and picolinic by using regression equation (Ou et al. 2002).

1.10.1.10 Reducing power (RP) method

Colorimetric method measured the capacity of antioxidant with reducing power of the reaction mixture. The antioxidant potency increases with the formation of ferric-ferrous blue complex. The reagents used for this assay are potassium ferricyanide, ferric chloride and trichloroacetic acid and measured the absorbance at 700 nm. The intensity of absorbance increases with antioxidant capacity (Jayaprakasha, Singh & Sakariah 2001) acid. Metal-chelation/ protecting capacity against the formation of hydroxyl radical evaluated.

1.10.1.11 Trolox equivalent antioxidant capacity (TEAC) method

Diode-array spectrophotometer used to measure the decrease in colour with antioxidant potency, measures the absorbance at 750 nm. In this reaction reduction occurs to the antioxidants with ABTS [2, 2-azino-bis (3-ethylbenzthiazoline-6-sulfonic acid)] and decolorize it(Seeram et al. 2006).

1.10.1.12 Hydrogen peroxide scavenging assay

Hydrogen peroxide is a weak oxidizing agent, oxidizes the essential thiol group (-SH) and deactivated certain enzymes. Hydrogen peroxide has the capacity to penetrate the cell membrane, reacts with Fe^{2+} , Cu^{2+} etc. and produces toxic hydroxyl radicals. Therefore, to control the amount of hydrogen peroxide in biological membrane is essential. Hydrogen peroxide can accept proton or electron and reduced to water. In this assay iron chelators donates electron or proton to hydrogen peroxide, which then reduced to water. Hydrogen peroxide prepared in phosphate buffer mixed with the sample and measured the absorbance at 230 nm (Ruch, Cheng & Klaunig 1989). The percentage of hydrogen peroxide scavenging capacity can be evaluated as follows

$$\% = [(A_0 - A_1) / A_0] \times 100$$

Where A_0 is the absorbance of the standard solution (all reagents without polyphenols) and A_1 is the absorbance of all reagents with polyphenols /standard

The following two methods are relevant to this thesis.

1.10.1.13 Superoxide radical scavenging activity assay

Superoxide (O_2^-), hydrogen peroxide (H_2O_2) and the hydroxyl radical (OH^\cdot) are referred to as reactive oxygen species (ROS) and are considered responsible for many age-related diseases (Chun, Kim & Lee 2003). During cellular respiration, superoxide radicals are generated inside the human body as a by-product and are considered toxic in higher concentrations (Chun, Kim & Lee 2003). Elevated concentrations of superoxide (*in vivo*) damages DNA and deactivates enzymes (Fridovich 1978) that can lead to neurodegenerative disease, cancer etc. (Finkel & Holbrook 2000; Govindappa et al. 2013). Superoxide chemistry also has a vital role in lipid per oxidation reactions (Husain, Cillard & Cillard 1987). Thus, *in vitro* analysis of antioxidant activity and the mechanism of action of superoxide radical (scavenging) by antioxidants is of great importance. For example, superoxide radical inhibition with polyphenolic antioxidants/ flavonoids are reported to occur either by single electron transfer or hydrogen atom transfer mechanisms (Zhishen, Mengcheng & Jianming 1999).

Superoxide radical scavenging activity can be performed by the nitro blue tetrazolium dye reduction method (NBT) with the absorbance measured at 560 nm (Govindappa et al. 2013). The reagents used are nitro blue tetrazolium solution, EDTA, riboflavin and phosphate buffer (Govindappa et al. 2013). Reduction of O_2^- occurs during the scavenging reaction by a single electron transfer mechanism.

The experimental data accessed in this thesis (Sasaki et al. 2013b) was based on experimental antioxidant activity assays of isolated *Ribes nigrum* lignoid molecules. The assay used by these workers for superoxide anion scavenging activity was riboflavin-light-NBT system. The reagent was prepared by mixing phosphate buffer (0.5 mL), riboflavin (0.3 mL), phenazine methosulphate (0.25 mL) and 0.1 mL of nitro blue tetrazolium (NBT). The reaction mixture was incubated for 20 minutes and measured the absorbance at 560 nm. The standard solution used for the analysis was ascorbic acid. The antioxidant potential calculated by determining the percentage of superoxide radical scavenged.

$$\text{Percentage of superoxide radical scavenged} = [(1 - A_s)/A_c] \times 100$$

Where A_c is the absorbance of the control solution and A_s is the absorbance of the sample.

1.10.1.14 DPPH (1, 1-diphenyl-2-picryl hydrazyl) free radical scavenging assay

In 1958, Blois developed a method for the evaluation of total antioxidant potential of certain antioxidant molecules. This method is popular for free radical scavenging assays, as it is simple, fast, reliable and stable. During the reaction, the antioxidant molecules either donate an electron or proton (H^+) to DPPH free radical.

The DPPH usually prepared in methanol solvent forms violet colour and it turns colourless after the reaction. DPPH is a stable free radical and is considered as the suitable method to measure the free radical scavenging activity. The radical scavenging potency estimated using this method by measuring the discoloration of the solution after the reaction and measures the absorbance at 517 nm (Molyneux 2004).

The experimental data accessed in this thesis (Sasaki et al. 2013b) was based on experimental antioxidant activity by DPPH assay of isolated *Ribes nigrum* lignoid molecules. The assay used by these workers for DPPH antioxidant activity (Saeed, Khan & Shabbir 2012) was based on the method by preparing the stock solution of DPPH. Dissolved 24 mg DPPH in 100 mL methanol and kept at 20°C as a stock solution. It was then diluted with methanol so as to accomplish the absorbance at 517 nm using spectrophotometer. The diluted solution (3 mL) mixed with 100 μ l of the sample solution (isolated *Ribes nigrum* lignoid) at different concentrations. The incubated reaction mixture then placed at room temperature for 15 minutes and measured the absorbance at 517 nm. The control (standard) solution also prepared by employing the same method without sample solution. The scavenging activity can be determined by calculating the percentage of DPPH radical scavenged.

$$\text{DPPH radical scavenged (\%)} = [(A_c - A_s) / A_c] \times 100$$

Where A_c is the absorbance of the control solution and A_s is the absorbance of the sample.

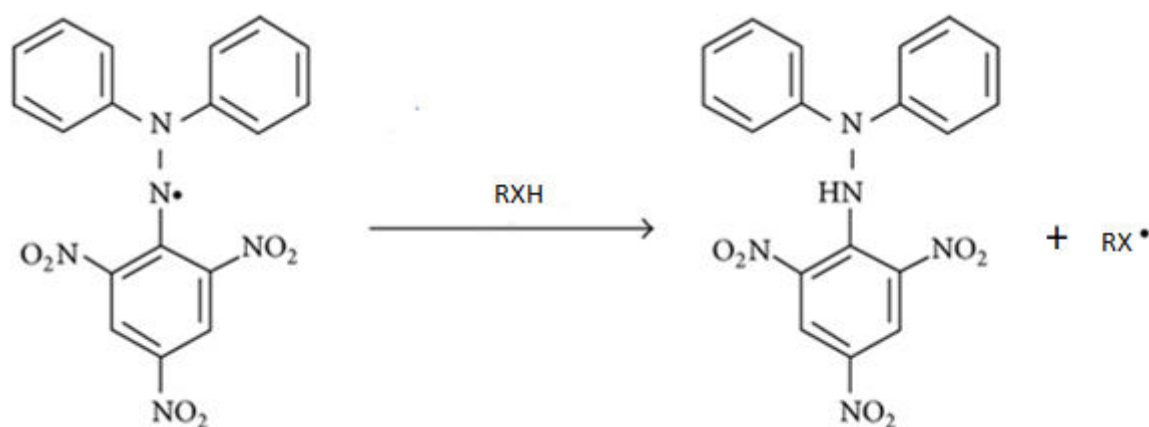


Figure 1.3 Schematic representation of DPPH free radical scavenging activity (Ji, Tang & Zhang 2005).

1.11 Computational methods and analysis for antioxidant molecules

Computational analysis has a vital role in determining antioxidant properties as well as in the drug designing of a polyphenolic bioactive compound. In this research work computational analysis was accomplished with the modelled values of vitamin E as a benchmark.

It was found that, the BDE of some hydroxyl groups attached to the aromatic ring could strongly influence or activate the antioxidant potency of other O-H groups present in the compound. In addition to that, steric hindrance/conformations, geometry and intra molecular hydrogen bonding strongly influences the BDE of each hydroxyl groups present in the compound. Free radical scavenging activity is allied with BDE of these bioactive molecules as the free radical scavenging occurs either by the donation of H-atom or electron transfer (Sadasivam & Kumaresan 2011). It was reported that the H-atom transfer occurred from phenolic antioxidants and that assists reactive free radical termination in living organisms (Klein & Lukeš 2006).

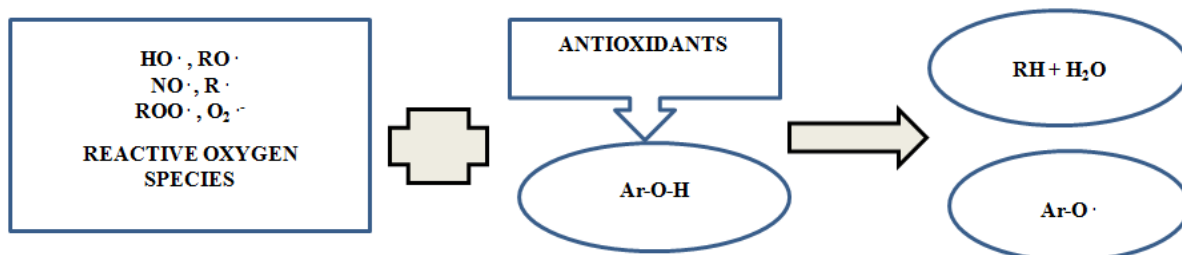


Figure 1.4 Schematic representation of H-transfer mechanism/free radical neutralization reaction.

1.12 Research aims

The leaves of *Ribes nigrum* contains a number of structurally related phenolic compounds that exhibit a range of antioxidant and anti-inflammatory characteristics. One of the aims of this research is to utilize quantum chemical methods (Semi-empirical and Density Functional Theory) to compute the equilibrium geometries of the reported thirteen such potentially bioactive compounds and their bond dissociation energies (BDEs) of the phenolic groups, the dipole moments, polar surface areas (PSA), Log_{10}P values and ionization potentials (IPs). Furthermore, to calculate a range of relative physicochemical parameters, their equilibrium structures, the extent of intra molecular hydrogen bonding and the structural features that could contribute to their experimentally observed relative antioxidant activities. These molecules were chosen since previous investigations by other researchers have reported their experimental antioxidant activities and this data can be reconciled with the computationally derived parameters and structures. The BDE, by itself, is not sufficient to explain enhanced antioxidant activity and so suggest to explore the molecular conformations, steric effects and, in particular, the magnitude and direction of the dipole moments etc. Apart from the overall shape and geometry of the individual molecules, such parameters include the relative O-H homolytic bond dissociation energies (BDE) (Woldu & Mai 2012), the magnitude and direction of their dipole moments (Goto et al. 2001; Jayaprakasam, Padmanabhan & Nair), their relative ionization potentials (IP) (Wijtmans et al. 2003) and the presence and influence of intra molecular hydrogen bonding. Other parameters that have been calculated and discussed that could relate to

antioxidant activity include “secondary” O-H BDEs³, as well as the spin potential energy distribution, frontier molecular orbitals, polar surface areas (PSAs) and Log₁₀P values.

Metal ions like Cu, Zn and Fe are enriched in A β deposits in AD (Atwood et al. 1998; Atwood et al. 2000; Barnham & Bush 2008; Lovell et al. 1998), that may be dissolve by selective metal chelators *in vitro* (Gouras & Beal 2001). It has been reported that chelation of Cu²⁺ and Zn²⁺ ions *in vivo* may prevent A β deposition (Hardy & Selkoe 2002). Based on the hypothesis the metal chelating molecules that can pass through the BBB and strip metals such as Cu²⁺ and Zn²⁺ from amyloid plaque could be a potential drug(s) for the treatment of AD (Atwood et al. 2000; Bush, Pettingell, Paradis, et al. 1994; Bush, Pettingell, Multhaup, et al. 1994). Chemical constituents, from certain plant-extracts can act as metal chelators and may diminish the aggregation of A β , by dissolving A β deposits in brain. This research work aims to investigate the understanding of A β toxicity in AD and to know about the metal ion chelation of a bioactive, memory enhancing drug candidate at molecular level and thus how it could scavenge the aggregation of A β from the brain, to cure AD. Though the exact mechanism of action of BM is unknown till date, this research works highlights the hypothesis that, one of the identified, de-glycosylated and bioactive small molecules can pass through the blood brain barrier (BBB) and chelate with the free metal ions (Cu²⁺, Zn²⁺, and Fe²⁺) and thus inhibits A β production *in vivo*. Thus, the hypothesis of this research study is to find the potential metal chelators are capable enough to attract metal ions which were bound with A β . Hence, selectively scavenge the excess intracellular Cu²⁺, Zn²⁺ and Fe³⁺ ions to a soluble nontoxic product, which could pass through blood brain barrier (BBB), or enhance A β clearance from the brain.

³ The lowest value O-H BDE is usually associated with the highest antioxidant activity. “Secondary” O-H BDEs are the BDEs of the remaining O-H groups in a polyphenolic after the lowest value O-H has lost its hydrogen atom. This gives an indication as to whether the remaining O-H groups are subsequently activated or deactivated with respect to antioxidant activity.

PART A

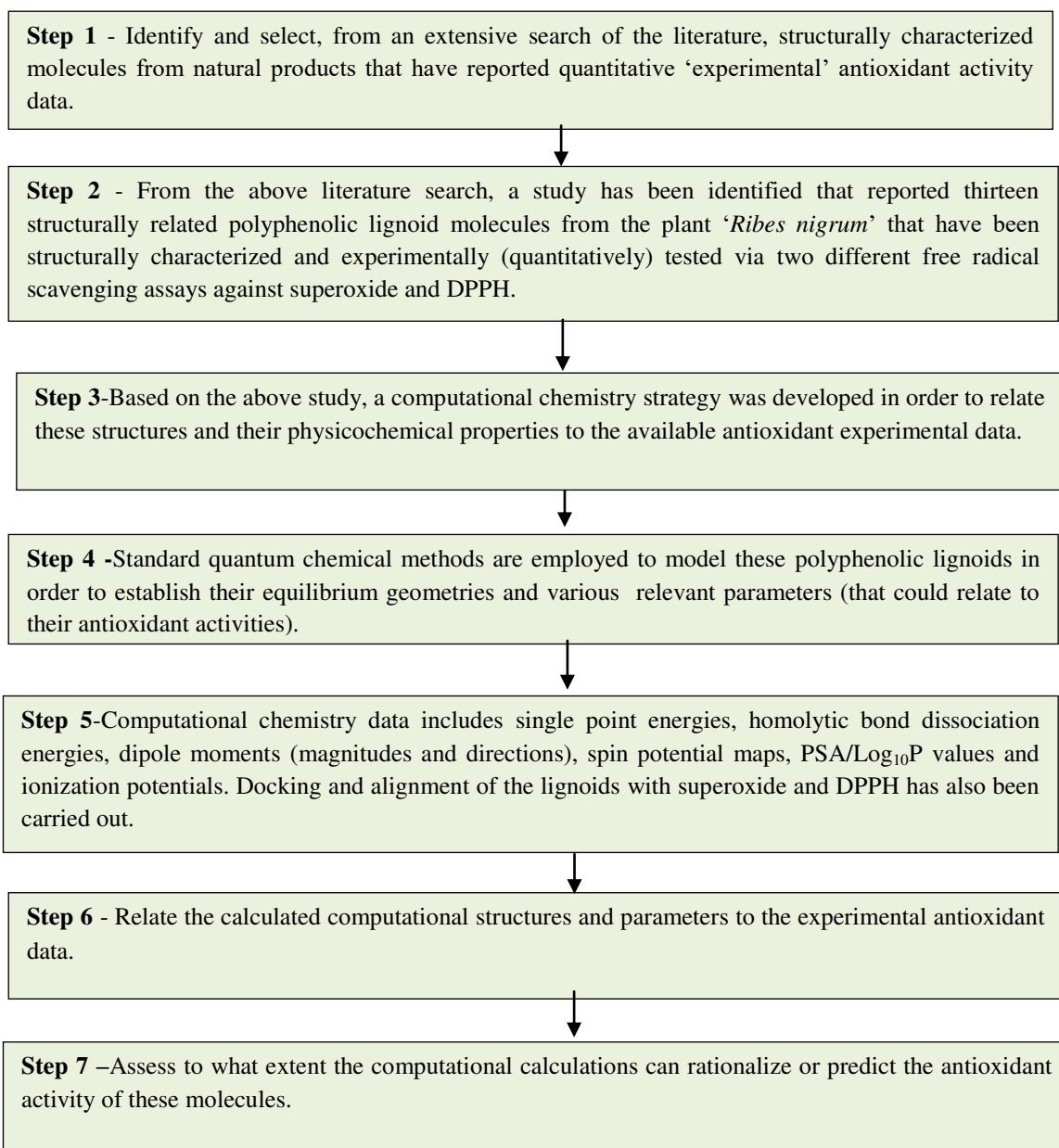
CHAPTER 2

A computational study of potential antioxidants from the leaves of *Ribes nigrum* (“blackcurrant”)

2.1 Research Strategy

A research strategy was devised in order to apply computational chemistry methods to the rationalization of the antioxidant activities of some natural product molecules by benchmarking computed results to available structural and experimental data. The overall strategy is described in Scheme 1.

Scheme 1



2.2 Preamble

Bioactive small molecules from natural products have an enduring and vital role in drug discovery, primarily due to the likelihood of reduced side effects compared to synthetic drugs (Harvey 2008). Thus the discovery of antioxidant lignoids (El Diwani, El Rafie & Hawash 2009; Granato, Katayama & Castro 2010) from leaves of the *Ribes nigrum* plant, colloquially referred to as “blackcurrant”, has led to the identification and isolation of thirteen polyphenolic lignoid molecules, that have been structurally characterized and experimentally tested by these researchers for their scavenging activity against the superoxide anion and the DPPH free radical (Sasaki et al. 2013b). These molecules and their associated structural and experimental data have been selected by the author of this thesis to form the basis of a computational chemistry enquiry that is aimed at identifying the structural and physico-chemical characteristics that, either individually or in concert, contribute to their relative antioxidant potencies. In this regard, computational methods have been applied to these molecules in order to evaluate their relative structural characteristics, including the importance of steric effects, the relevance of the structural alignment of the reactants (lignoids and radical species), their relative O-H homolytic bond dissociation energies (intrinsic antioxidant capacity) and their dipole moment magnitudes and directions. Such computed parameters have been benchmarked against the available experimental data for both individual molecules and for various groups of structurally related molecules within the set.

2.3 The antioxidant and anti-inflammatory characteristics of *Ribes nigrum*

Ribes nigrum (“blackcurrant”), is a small shrub belonging to the family Grossulariaceae (Schultheis & Donoghue 2004; Tabart et al. 2012) Figure.2.1. The leaves of *Ribes nigrum* contains a number of structurally related phenolic compounds that exhibit a range of antioxidant and anti-inflammatory characteristics.



Figure 2.1 *Ribes nigrum* (“blackcurrant”)

The fruits of *Ribes nigrum* have been used for the treatment of cardiovascular disorders (Slimestad & Solheim 2002; Tabart et al. 2012) and the leaves are reputed to be useful for the treatment of rheumatic disease (Garbacki et al. 2004; Sasaki et al. 2013a; Tabart et al. 2012). In this regard, it is widely proposed that antioxidant, bioactive compounds of such natural products may act as radical scavengers that diminish oxidative stress (Sanz et al. 1994). It was reported that the polyphenolic extracts of blackcurrant leaves and fruits have beneficial effects by protecting the cell membrane against oxidation (Moyer et al. 2002). Furthermore, *Ribes nigrum* lignoids in the fruits of blackberries have high amounts of phenolic compounds (Benvenuti et al. 2004; Häkkinen et al. 1999). Notably, although the antioxidant and anti-inflammatory (Garbacki et al. 2004; Tabart et al. 2012) properties of the constituents of *Ribes nigrum* have been extensively studied (Sasaki et al. 2013a), molecular modelling and ‘theoretical’ investigations of these molecules is currently lacking. Such studies are desirable since the antioxidant potency of bioactive compounds *in vitro* and *in vivo*

depend on their physicochemical and structural properties. In this case, the identification and characterization of the active molecules in the leaves of *Ribes nigrum* and the experimental characterization of their experimental antioxidant properties by Sasaki et al. provides a potent platform for subsequent computational analysis. Thus, most of the potentially active compounds isolated from the leaves of *Ribes nigrum* are polyphenolics that show a range of free radical scavenging activities in relation to the superoxide anion and 2, 2-diphenyl-1-picrylhydrazyl (DPPH). Notably, a number of these isolates show no activity at all regardless of their being phenolic and despite their close structural similarity to other active components. Such differences could provide insights into the molecular features and properties that enable antioxidant potency.

2.4 Reported structures and experimental antioxidant data for *Ribes nigrum* lignoids

The molecular structures that have been characterized by Sasaki et al. have been divided into three structural sets shown in Figures 2.2, 2.3 and 2.4, respectively. The molecules are all phenolics, either tri-, di- or mono-phenolic. The seven di-phenolic structures represented in Figure 2.2 are closely related, but with subtle differences. Similarly for the three tri-phenolic structures in Figure 2.3. The three structures in Figure 2.4 represent mono- and quatero-phenolics and are structurally more diverse. The experimental radical scavenging data for these molecules is tabulated in Table 2.1 in terms of EC₅₀ values. EC₅₀ or the half maximal effective concentration of a drug, antibody or toxicant is used to measure the potency of a drug(s) at a definite exposure time. Usually, the EC₅₀ evaluation process starts at the early stage of the drug discovery process as a means for determining the suitability and performance of a drug(s). The experimental evaluation of antioxidant potency of a drug(s) can be determined using a range of different methods (Jiang & Kopp-Schneider 2014). Such methods may involve the measurement of a maximal response concentration or half of a maximum response concentration (i.e. EC₅₀) (Jiang & Kopp-Schneider 2014; Sebaugh 2011). It was reported that the lower the EC₅₀ value, the lower the concentration of the drug that is required for a 50% of maximum response (Alexander et al. 1999). Thus, the lower the EC₅₀ value, the higher the antioxidant potency. Experimentally, the EC₅₀ values are

measured from a concentration-effect curve for the drug (Jiang & Kopp-Schneider 2014).

Notably, in spite of the close structural similarities between the Molecules⁴ **1** to **6** and Molecules **7** to **9** in Figures 2.2 and 2.3, respectively, the experimental scavenging abilities towards superoxide and DPPH are very different. For example, for Molecules **1** to **6** in Figure 2.2⁵, **1** and **5** show no activity towards *either* superoxide *or* DPPH. Molecule **4** is the only molecule that shows activity towards both superoxide *and* DPPH. Molecules **2**, **3** and **6** show activity towards superoxide, albeit to different extents, but show no activity towards DPPH.

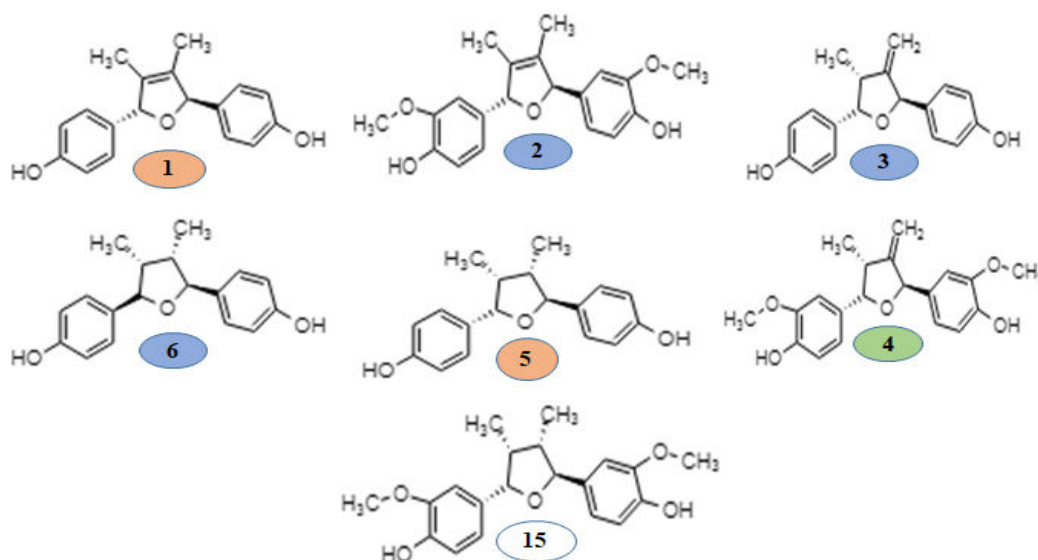


Figure 2.2 Set 1 - reported molecular structures (Sasaki et al. 2013a) of the phenolic compounds 1 to 6 and 15 from the leaves of *Ribes nigrum*. Note that the original numbering scheme for these molecules has been retained for ease of reference to Sasaki et al. 2013.

For Molecules **7** to **9** in Figure 2.3, Molecule **9** shows activity towards superoxide but not towards DPPH. However, Molecules **7** and **8** show no activity towards superoxide *or* DPPH.

⁴ The chemical names of all the molecules is provided in appendix

⁵ There is no reported experimental data for Molecule 15.

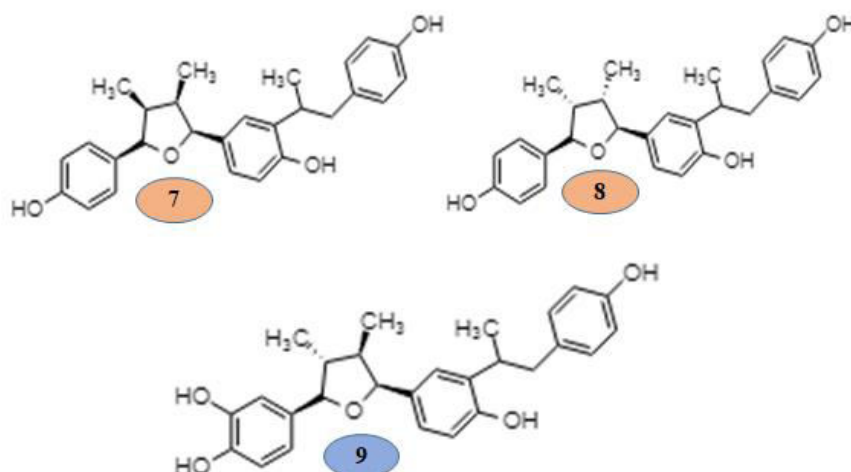


Figure 2.3 Set 2 - reported molecular structures (Sasaki et al. 2013a) of the phenolic compounds 7 to 9 from the leaves of *Ribes nigrum*. Note that the original numbering scheme for these molecules has been retained for ease of reference to Sasaki et al. 2013.

For Molecules **10**, **13** and **14** in Figure 2.4, Molecule **13** is the only one that shows activity towards DPPH whereas Molecules **10** and **13**, but not Molecule **14**, show activity towards superoxide. Overall, in terms of relative radical scavenging ability, the order is: $9 > 4 > 3 > 6 > 10 > 13 > 2$ for superoxide and $13 > 4$ for DPPH. This provides an opportunity to investigate the origin(s) of the extent of antioxidant activity from molecule to molecule.

The reported antioxidant activities of the 70% ethanol extract, Table 2.1, where there is significant activity towards both superoxide and DPPH, is also of interest since it could provide an indicator of synergistic antioxidant effects. In the 70% extract, it is assumed that all of the molecules under study are present simultaneously.

Similarly, the reported antioxidant activity of BHA (that is used as a positive control in the experiments) towards both superoxide and DPPH is also of interest given that the structure, Figure 2.5, and properties of BHA may be well characterized by our computational methods.

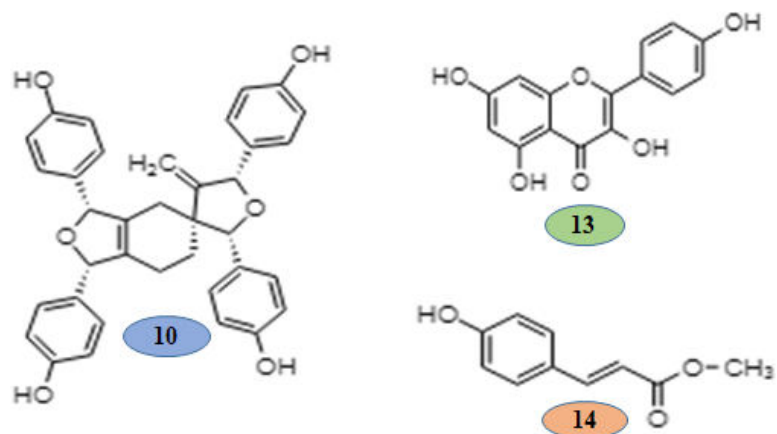


Figure 2.4 Set 3 - reported molecular structures (Sasaki et al. 2013a) of the phenolic compounds 10, 13 and 14 from the leaves of *Ribes nigrum*. Note that the original numbering scheme for these molecules has been retained for ease of reference to Sasaki et al. 2013.

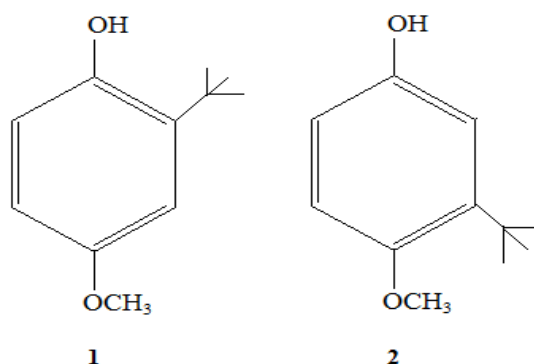


Figure 2.5 Isomeric structures of Butylated hydroxy anisole (BHA).

This thesis work is based on the experimentally determined antioxidant potencies of *Ribes nigrum* lignoid molecules via superoxide and DPPH free radical scavenging assays (Sasaki et al. 2013b). These values are given in Table 2.1.

Selected, reported bioactive polyphenolic *Ribes nigrum* lignoids were modelled using semi-empirical quantum chemical calculations and density functional theory (DFT) utilizing Spartan '06 and '16 software (Tugcu et al. 2012). Thus, single point energy calculations were carried out for parent and radical species using the B3LYP/6-31G*/PM3 method. This enabled different equilibrium geometries to be examined and compared and also allowed relative formation energies and homolytic bond dissociation energies to be calculated and compared. The equilibrium geometries (structures) of all

of the investigated molecules, as determined by PM3 semi empirical quantum chemical calculations are depicted in Figures 2.6 to 2.11. Also see Figures 2.2 to 2.5, *vide supra*. These have been grouped into different structural categories, as discussed previously.

2.5 Density Functional Theory (DFT)

Electronic structure calculations of a large variety of systems, especially condensed-matter systems, have been carried out based on density functional theory (DFT)(Parr 1980). Experimentally, the electron density of a molecule can be measured by X-ray diffraction methods(Koch, Holthausen & Holthausen 2001). Computational chemistry applications of DFT was in progress by the late 1960's using the 'scattered-wave' concept (Illas et al. 2000; Kohn, Becke & Parr 1996).More accurate, reliable computational strategies were developed for density functional computational chemistry by the 1980s(Kohn, Becke & Parr 1996). DFT explains the total electronic energy in terms of the interaction of electrons with positively charged nuclei (Columbic interaction of electrons), inter electronic interactions (Hann, Leach & Harper 2001) and the kinetic energy of electrons. B3LYP is one of the most effective hybrid density functional methods that has been used extensively in quantum chemical calculations, especially in transition metal chemistry, although it is limited in accounting for long range electron correlations (Koch, Holthausen & Holthausen 2001).

DFT is now an established method for measuring a range of physicochemical parameters, including homolytic bond dissociation energies. Sufficient benchmarking of such calculations to experimental data have validated DFT as a highly effective research tool, hence its application in this research.

2.6 Establishing equilibrium geometries

The equilibrium geometry of a molecule is considered to be the starting point for calculating the energy of that particular molecule and for the calculation of other thermodynamic parameters (Schlegel 1982). It provides the most energetically favourable conformation (structure) of a molecule (Schlegel 1982);(Peng et al. 1996). The structure may be predictive of the properties of the molecule, although other factors also contribute. In this research work, we have established the equilibrium geometries of the parent and radical molecules of *Ribes nigrum* lignoids and used these as starting

points for subsequent relative energy calculations and for calculation of various physico-chemical parameters.

Table 2.1 Experimental antioxidant data (superoxide anion and DPPH radical scavenging activities) of reported, isolated compounds from the leaves of *Ribes nigrum*(Sasaki et al. 2013b). Note that >50 μM is inactive.

Compound(s)	Superoxide EC ₅₀ in μM *in $\mu\text{g/mL}$	DPPH EC ₅₀ in μM *in $\mu\text{g/mL}$
70% EtOH extract	1.84*	34.07*
1	NA	NA
2	6.09	NA
3	2.05	NA
4	1.24	32.33
5	NA	NA
6	3.05	NA
7	NA	NA
8	NA	NA
9	1.12	NA
10	3.26	NA
13	4.85	31.52
14	NA	NA
Butylated hydroxy anisole (isomer mixture) – positive control.	17.02	26.71

2.7 (Homolytic) bond dissociation energies (BDEs) and “secondary” BDEs

The homolytic bond dissociation energy (BDE) of a molecule is the minimum energy required to cleave a molecular bond so as to form new fragments of the corresponding radical species. In this thesis, attention is directed at the homolytic O-H BDE of the phenolic -O-H moiety to generate a “parent” radical, $-\text{O}^{\bullet}$, and a hydrogen atom, H^{\bullet} , the

latter being considered to be a radical scavenger. The magnitude of the BDE is highly dependent upon the molecular environment of the –O-H moiety and is related to a molecule's anti-oxidant efficacy. In polyphenolic compounds the –O-H BDEs are therefore not expected to be the same and it is likely that one moiety is the primary antioxidant site. However, it is worth asking the question as to whether or not the loss of this hydrogen atom activates or deactivates the antioxidant potential of the remaining –O-H moieties. This can be determined using computational methods and has been investigated in this thesis.

The O-H homolytic BDE for R–O-H can be computed as follows (Giacomelli et al. 2004) :

$$\mathbf{BDE = E (R-OH) - [E (H\cdot) + E (RO\cdot)]}$$

Where **E (R-OH)** is the (formation) energy calculated for the parent molecule, **E (H \cdot)** is the energy calculated for the hydrogen free radical and **E (RO \cdot)** is the energy calculated for the parent radical molecule. Such energies (absolute or relative) are usually computed using DFT and are considered to be highly reliable (Giacomelli et al. 2004).

2.8 Single point energy calculations

A single point energy calculation in computational chemistry (Pedersen, Ostergaard, et al.) is the total formation energy of a system (at an established equilibrium geometry), with nuclei and electrons represented by the sum of all of the energies of nuclei-nuclei interaction, nuclei-electron interaction, electron-electron interaction, nuclear kinetic energy and electronic kinetic energy (Chuang, Corchado & Truhlar 1999).

2.9 Dipole moment calculations

The dipole moment of a molecule is considered as a measure of its charge density or polarity (Jayaprakasam, Padmanabhan & Nair 2010). The dipole moment can be defined in terms of charge density i.e., two separated charges of opposite sign form an electric dipole in a molecule (Grimme et al. 2007; Sadasivam & Kumaresan 2011). Dipole moment is a vector quantity as the vectors determine the position of the two charges in space (Sadasivam & Kumaresan 2011).

A molecule with an increased level of intramolecular hydrogen bonding may decrease the DM by hydrogen-bonded ring closure (Goto et al. 2001). Thus intra molecular hydrogen-bonding may influence hydrophobicity via a change in the DM (Goto et al. 2001; Terada, Muraoka & Fujita 1974). It should be noted here that the presence of intra-molecular hydrogen bonding has also been found in this thesis to affect the calculated BDEs. This has been described in more detail in section 2.12.

In this thesis, both the presence of intra molecular hydrogen bonding and the magnitude *and* direction of the DM are considered to be highly relevant in the overall rationalization of antioxidant efficacy. Therefore, these have all been characterized computationally, especially in relation to the interaction of the lignoid molecules with the DPPH and superoxide anion radicals. Electrostatic potential energy maps and spin potential distributions have also been computed and assessed in this regard.

2.10 Polar surface area (PSA)

Polar surface area (PSA) is the total surface area that is allied to polar atoms. Calculation of the PSA has an important role in drug design as it gives an indication of the molecule's bioavailability. Furthermore, it was reported that, increased PSA values of a drug candidate/molecule decreases its BBB permeability (Ertl, Rohde & Selzer 2000).

2.11 Log₁₀P

The lipophilicity of a molecule indicates the affinity of a drug(s) towards a lipophilic environment and is represented by the water/octanol partition coefficient P. This is measured by evaluating the ratio of the concentration of a solute in octanol and its concentration in water, at equilibrium. Log₁₀P has a vital role in determining the efficacy of a drug(s) and its optimization. For example, depending on the structural properties of a drug(s) the preferred BBB permeable range for Log P is in between 1 and 5.5 (Caron, Vallaro & Ermondi 2018).

2.12 Intra molecular hydrogen bonding (IMHB)

Intra molecular hydrogen bonding involves the non covalent bonding between a hydrogen bond donor (HBD) (O-H, N-H etc.) and an adjacent electronegative hydrogen bond acceptor atom (HBA) with both HBD and HBA belonging to the same molecule (Caron, Kihlberg & Ermondi 2019). It is relevant in the biological activity of molecules and in drug design as it can influence the absorptivity, solubility and potency of drug(s) (Caron, Kihlberg & Ermondi 2019; Caron, Vallaro & Ermondi 2018). For example, IMHB can be crucial in drug design as it may lead to “polarity masking” and thus influences membrane permeability, solubility/bioavailability and a molecule’s antioxidant potency (Caron, Kihlberg & Ermondi 2019), especially when the IMHB involves phenolic moieties, as in this thesis. More specifically, IMHB may impact the Log_{10}P value, whereby this parameter is effectively lowered by polarity masking (Caron, Vallaro & Ermondi 2018). This may result in an enhancement of Blood Brain Barrier (BBB) passage. The work presented here comprises three different categories of compounds designated with respect to their molecular weight, structural similarity and size. These categories are represented in Figures 2.6 – 2.9 where compounds 2, 4, 15, 9 and 13 are capable of exhibiting IMHB giving rise to the possibility of polarity masking and of a variance in O-H BDEs depending upon where these IMHBs are “engaged” or “disengaged”.

From Tables 2.2 - 2.4 it may be seen that all compounds with IMHB are active towards superoxide, with two such compounds active towards *both* superoxide and DPPH. Notably, all compounds that are inactive towards superoxide and DPPH lack intramolecular hydrogen bonding. This will be discussed later in Section 2.8.2.

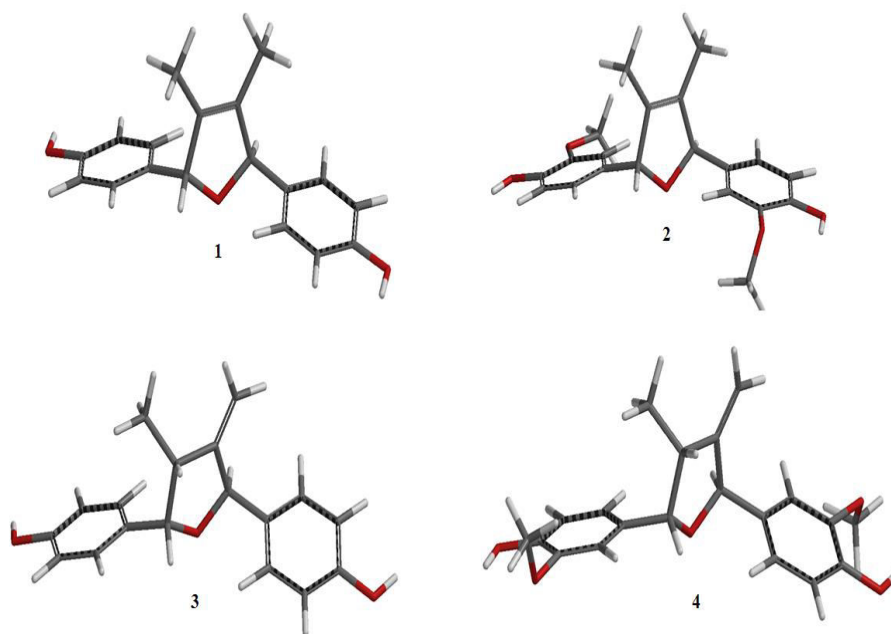


Figure 2.6 Modelled structures of *Ribes nigrum* Molecules (1-4), Set 1.

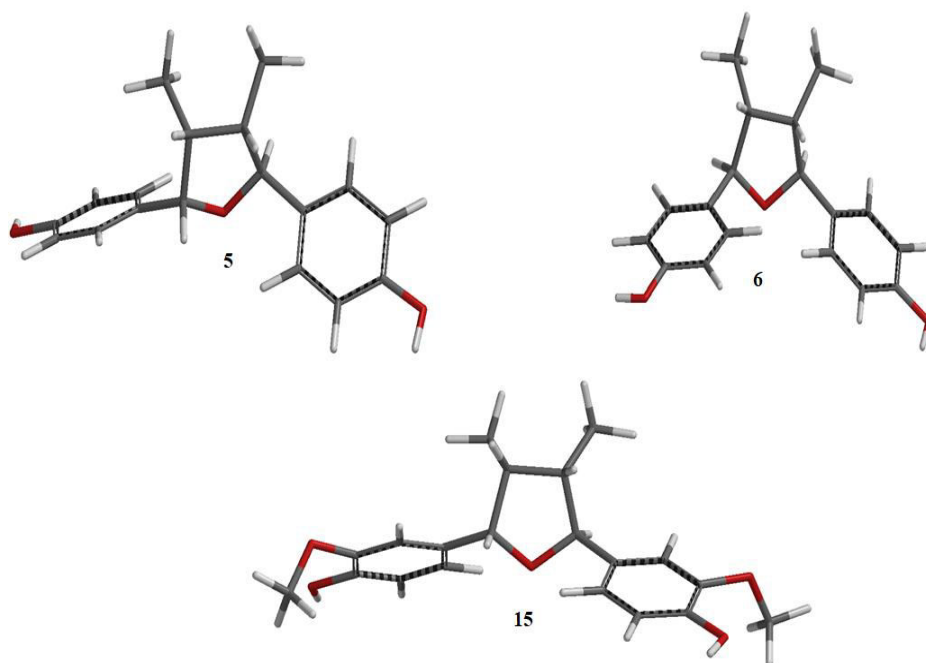


Figure 2.7 Modelled structures of *Ribes nigrum* Molecules (5, 6, and 15), Set 1 continued.

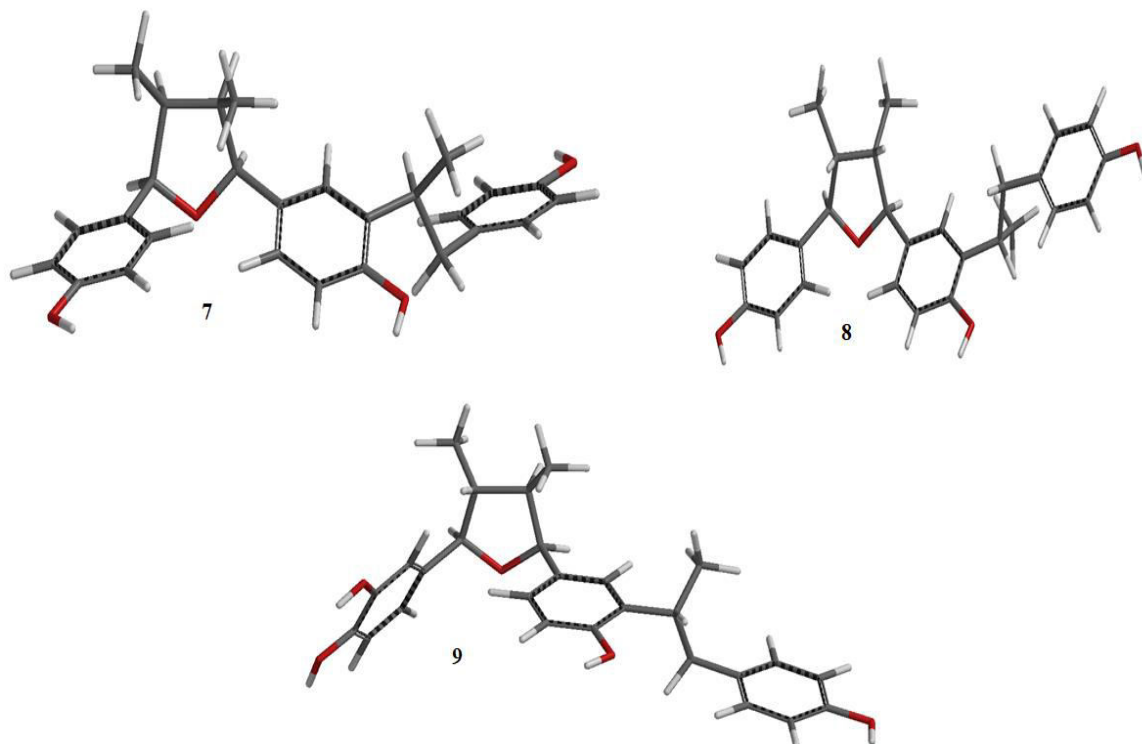


Figure 2.8 Modelled structures of *Ribes nigrum* Molecules (7-9), Set 2.

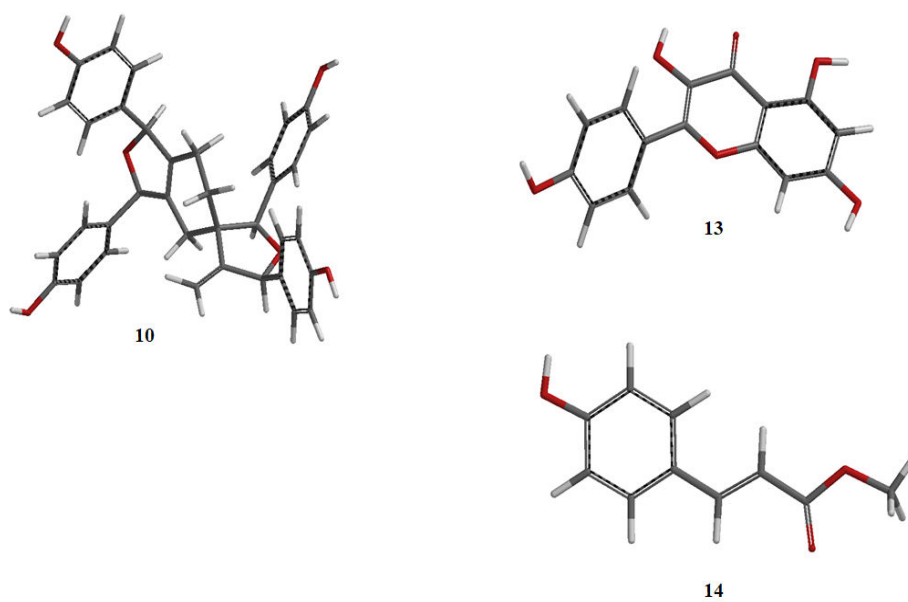


Figure 2.9 Modelled structures of *Ribes nigrum* Molecules (10, 13, and 14), Set 3.

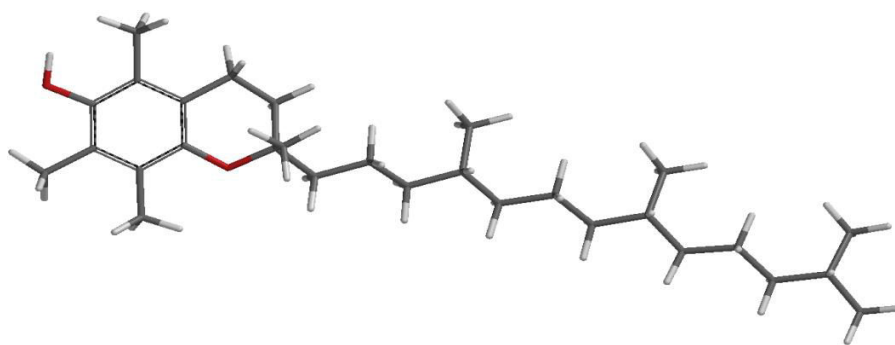


Figure 2.10 Modelled structure of Vitamin E, control for computational analysis.



Figure 2.11 Modelled structure of BHA, control for experimental data.

Based on the available quantitative experimental data, Table 2.1, for the superoxide and DPPH scavenging activity of twelve of the molecules that are depicted in Figures 2.2 to 2.4, these molecules may be divided into three broad “scavenging behaviour” groups:

These groups have been colour coded in Figures 2.2 to 2.4, where the molecules are categorized into their sets based on their broad structural similarities. Given that all of these molecules are phenolic and have structural similarities, this research has attempted to rationalize the broad property characteristic of Groups 1 to 3 by a detailed consideration of various properties and structural features derived from computational chemistry calculations. Such properties are summarized in Tables 2.2 to 2.4.

Group 1: Molecules that are inactive towards both superoxide and DPPH. These are molecules **1, 5, 7, 8** and **14** -Table 2.2. Colour Code: Orange

Group 2: Molecules that are active towards superoxide but not towards DPPH. These are molecules **2, 3, 6, 9** and **10** Table 2.3. Colour Code: Blue

Group 3: Molecules that are active towards both superoxide and DPPH. These are molecules **4** and **13** Table 2.4. Colour Code: Green

Table 2.2 Computed properties of molecules that are inactive towards both superoxide and DPPH, Group 1 – Colour Code Orange.

Molecules inactive towards SO and DPPH	BDEs (kcal/mol)	PSA (Å)	DM (Debye)	IP	Log ₁₀ P	HBD	HBA	IMHB
1	85.5	46.3	1.72	168.4	3.36	2	3	0
5	84.4	45.7	0.85	163.8	3.85	2	3	0
7	79.5	63.4	1.71	156.7	6.30	3	4	0
8	82.6	64.6	3.05	158.2	6.30	3	4	0
14	83.8	40.4	3.6	173.5	1.98	1	2	0

Table 2.3 Computed properties of molecules that are active towards superoxide but not towards DPPH, Group 2 - Colour Code Blue.

Molecules active towards SO and not towards DPPH	BDEs (kcal/mol)	PSA (Å)	DM (Debye)	IP	Log ₁₀ P	HBD	HBA	IMHB
2	79.8	59.5	1.98	157.2	3.11	2	5	1
3	84.4	45.8	2.65	163.9	3.49	2	3	0
6	85.8	46.2	2.25	166.5	3.85	2	3	0
9	72.1	83.8	3.6	155.2	5.91	4	5	1
10	83.6	92.5	4.19	163.1	5.98	4	6	0

Table 2.4 Computed properties of molecules that are active towards both superoxide and DPPH, Group 3 – Colour Code Green.

Molecules active towards both SO and DPPH	BDEs (kcal/mol)	PSA (Å)	DM (Debye)	IP	Log₁₀P	HBD	HBA	IMHB
4	80.9	60.1	1.93	154.2	3.24	2	5	2
13	81.6	95.9	3.45	153.8	0.32	4	6	1

2.13 Computing the relative O-H bond dissociation energies of the polyphenolics

Figures 2.12 to 2.14 show the computed homolytic bond dissociation energies (BDEs) for the molecules under investigation. Both “primary” and “secondary” BDEs have been computed for these molecules. A primary BDEs represents an individual BDE for a specific phenolic O-H moiety. For polyphenolics, where the O-H moieties may well have different molecular environments. These values are likely to be different and only one of the O-H moieties (that with the lowest value) is likely to be involved in significant radical scavenging. That is, it will react more rapidly with the target radical – this being under kinetic control. However, when this moiety loses its H radical, the question arises as to what effect this will subsequently have on the O-H BDEs of the remaining O-H moieties. Will they be “activated” (have their BDEs lowered) or “deactivated” (have their BDEs increased). For this reason, the remaining O-H BDE values of the parent radical species under consideration have also been calculated – these are termed the “secondary” BDEs.

It is worth commenting further on how the BDEs are represented by referring to several examples in Figure 2.12. For example, Molecule **9** is a tetra-phenolic. Each O-H moiety can be seen to have a different BDE ranging from 72.1 to 84.8 kcal/mol. It is reasonably assumed that any radical scavenging activity will occur primarily via the O-H site with the lowest BDE of 72.1 kcal/mol. The red and green numbers are the calculated secondary BDEs for the parent radical of the 72.1 kcal/mol site. It may be noted that one such site is subsequently slightly activated, and two sites are subsequently deactivated (fairly strongly).

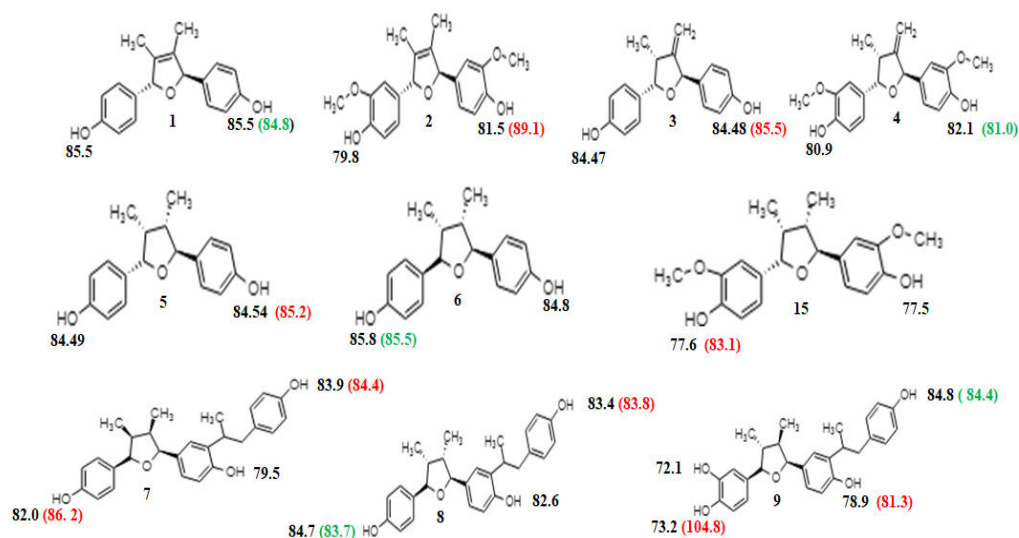


Figure 2.12 Chemical structures and the calculated bond dissociation energy values (BDEs in kcal/mol) of compounds 1-9 and compound 15. The “primary” BDEs are indicated in black type and the “secondary” BDEs of these molecules are indicated in green type (activated) or red type (deactivated).

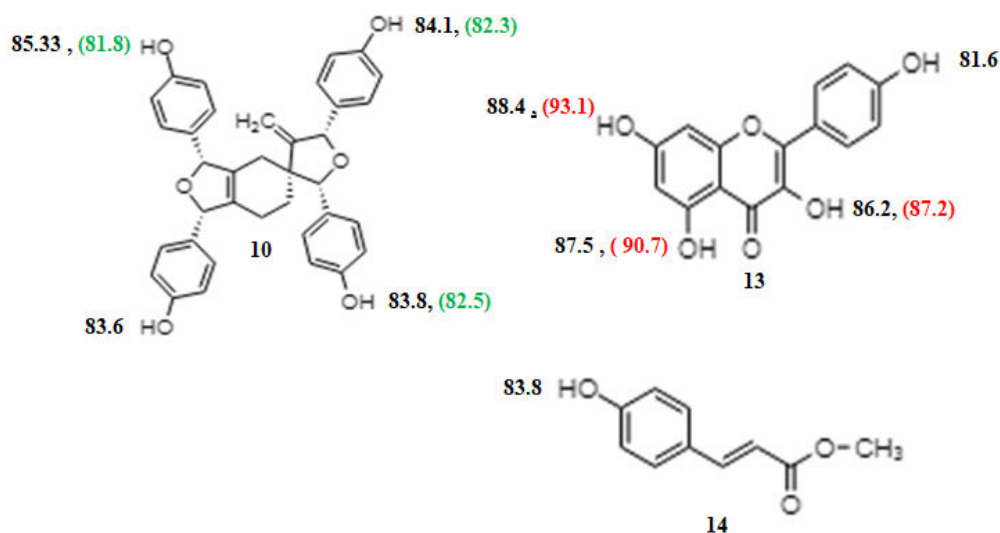


Figure 2.13 Chemical structures and the calculated bond dissociation energy values (BDEs in kcal/mol) of compounds 10, 13, and compound 14. The “primary” BDEs are indicated in black type and the “secondary” BDEs of these molecules are indicated in green type (activated) or red type (deactivated).

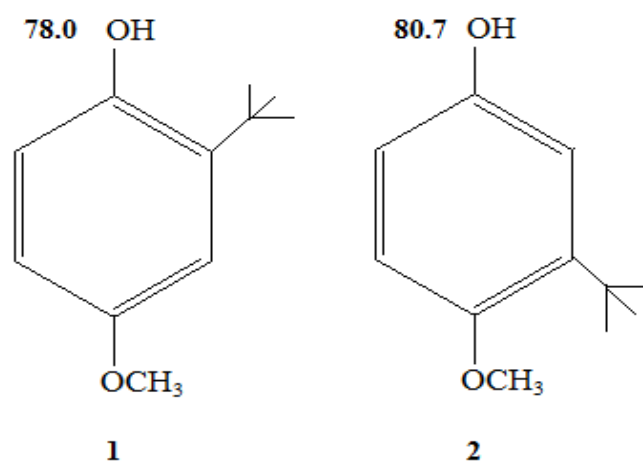


Figure 2.14 Chemical structures and the calculated bond dissociation energy values (BDEs in kcal/mol) for compounds 1 and 2. Since these are mono-phenolics the values are necessarily primary BDEs.

2.14 Computation of relevant physical properties (qualitative and quantitative)

For the molecules under study, their experimentally determined antioxidant properties have been examined in the light of their various computed structural and physical properties. These are summarized in Table 2.5 and Table 2.6.

Table 2.5 Relevant computed properties for all molecules included in this study.

Molecules	Molecular weight	Lowest BDE (kcal/mol)	Polar Surface Area (Å)	Number of Hydrogen Bond Donors (HBD)	Number of Hydrogen Bond Acceptors (HBA)	Number of intra-molecular hydrogen bond (IMHB)	Log₁₀P
1	282.33	85.5	46.3	2	3	0	3.36
2	342.39	79.8	59.5	2	5	1	3.11
3	282.33	84.4	45.8	2	3	0	3.49
4	342.39	80.9	60.1	2	5	2	3.24
5	284.35	84.4	45.7	2	3	0	3.85
6	284.35	84.8	46.2	2	3	0	3.85
7	418.53	79.5	63.4	3	4	0	6.30
8	418.53	82.6	64.6	3	4	0	6.30
9	434.53	72.1	83.8	4	5	1	5.91
10	560.64	83.6	92.5	4	6	0	5.98
13	286.23	81.6	95.9	4	6	1	0.32
14	178.18	83.8	40.4	1	2	0	1.98
15	344.40	77.5	60.1	2	5	2	3.60
BHA-1	180.24	80.8	23.64	1	2	0	3.20
BHA-2	180.24	78.0	23.64	1	2	0	3.22
Vitamin E	429.70	75.3	18.74	0	2	0	9.98

Table 2.6 Experimental and computational data of *Ribes nigrum* lignoid molecules.

Molecules	EC ₅₀ ^a Superoxide anion	EC ₅₀ ^a DPPH	IP	DM (Debye) PARENT	DM (Debye) RADICAL	PSA (Å) PARENT	PSA (Å) RADICAL	BDE (kcal/ mol)	IAPI
1	NA	NA	168.4	1.72	6.23	46.3	42.2	85.5	135.3
2	6.09	NA	157.2	1.98	2.47	59.5	53.8	79.8	61.1
3	2.05	NA	163.9	2.65	5.31	45.8	41.2	84.4	121.8
4	1.24	32.33	154.2	1.93	2.54	60.1	52.8	80.9	74.8
5	NA	NA	163.8	0.85	4.99	45.7	41.1	84.4	122.0
6	3.05	NA	166.5	2.25	6.24	46.2	41.2	84.8	127.5
7	NA	NA	156.7	1.71	4.37	63.4	82.3	79.5	56.8
8	NA	NA	158.2	3.05	3.75	64.6	59.7	82.6	96.7
9	1.12	NA	155.2	3.6	5.71	83.8	77.7	72.1	-41.2
10	3.26	NA	163.1	4.19	5.91	92.5	88.3	83.6	110.5
13	4.85	31.52	153.8	3.45	6.21	95.9	89.8	81.6	83.8
14	NA	NA	173.5	3.55	2.84	40.4	35.9	83.8	112.9
15			156.6	1.50	2.91	60.1	52.8	77.5	29.2
BHA-1	17.02	26.71		2.47	5.23	23.8	19.1	80.8	72.6
BHA-2	17.02	26.71		2.34	4.37	23.8	20.1	78.0	36.1
Vitamin E			147.9	2.62	5.32	22.3	19.3	75.3	

2.15 Result and discussion

1. Why are the Molecules of Group 2, namely molecules 2, 3, 6, 9 and 10, Table 2.3, only active towards superoxide and not towards DPPH?

Molecules belonging to Group 2 (that are active towards superoxide but not towards DPPH) are the Molecules **2**, **3**, **6**, **9** and **10**, Table 2.3 - Colour Coded Blue. Experimentally, these molecules show activity *only* towards superoxide, but to different extents, in the order $2 < 10 < 6 < 3 < 9$ and no activity at all towards DPPH. Molecules in this Group exhibit their lowest BDEs in the order $9 (72.1 \text{ kcal/mol}) < 2 (79.8 \text{ kcal/mol}) < 10 (83.6 \text{ kcal/mol}) < 3 (84.4 \text{ kcal/mol}) < 6 (84.8 \text{ kcal/mol})$. The fact that these orders do not correspond with the experimental orders, Table 2.7, indicates that the BDE values *alone* are not sufficient to explain the antioxidant activities.

Table 2.7 Minimum computed BDE values compared to experimental superoxide and DPPH radical scavenging values, where activity is towards superoxide only.

Group 2 Molecules	Minimum computed BDE (kcal/mol)	Experimental superoxide scavenging (EC ₅₀ in μM)	Experimental DPPH scavenging – not observed. Comments on reason(s) for inactivity.
2	79.8	6.09	Steric hindrance
3	84.4	2.05	Threshold exceeded
6	84.8	3.05	Threshold exceeded
9	72.1	1.12	Steric hindrance.
10	83.6	3.26	Steric hindrance and threshold exceeded

However, it is worth noting that the molecule that has the lowest BDE, i.e. Molecule **9**, also has the highest superoxide scavenging activity. Here, the BDE of 72.1 kcal/mol is remarkably low (with reference to the Vitamin E computed benchmark value of 75.3 kcal/mol), Table 2.6. Figure 2.15 (a) depicts the (space filling) electrostatic potential energy maps of Molecule **9** and superoxide and our modelling has explored how these molecules might approach one another (this figure is a “snapshot” of many possible approaches that have been examined). During the manual docking process, the influence of the relative directions of the dipole moments have also been considered. Thus, the O-

H moiety with the lowest BDE of 72.1 kcal/mol is in an electrostatically favoured part of the molecule with respect to an approach by the superoxide anion and is also sterically accessible with respect to all of our tested docking trajectories. Hence its scavenging propensity towards superoxide is to be expected. Given the low DBE of this molecule, it is perhaps surprising that there is no activity at all toward the DPPH.

Figure 2.15 (b) depicts the electrostatic energy maps of Molecule **9** and DPPH, representing a “snapshot” of how these molecules might approach one another. What becomes clear from these experiments is that the steric bulk of the DPPH significantly hinders its approach to the antioxidant region of Molecule **9**. It is also worth noting that Molecule **9** is not flat - and this accentuates the bulk of this molecules as well. Therefore, we attribute the inactivity towards DPPH to steric factors between these two molecules that are manifestly sufficient to inhibit productive intermolecular interactions, in spite of the low BDE.

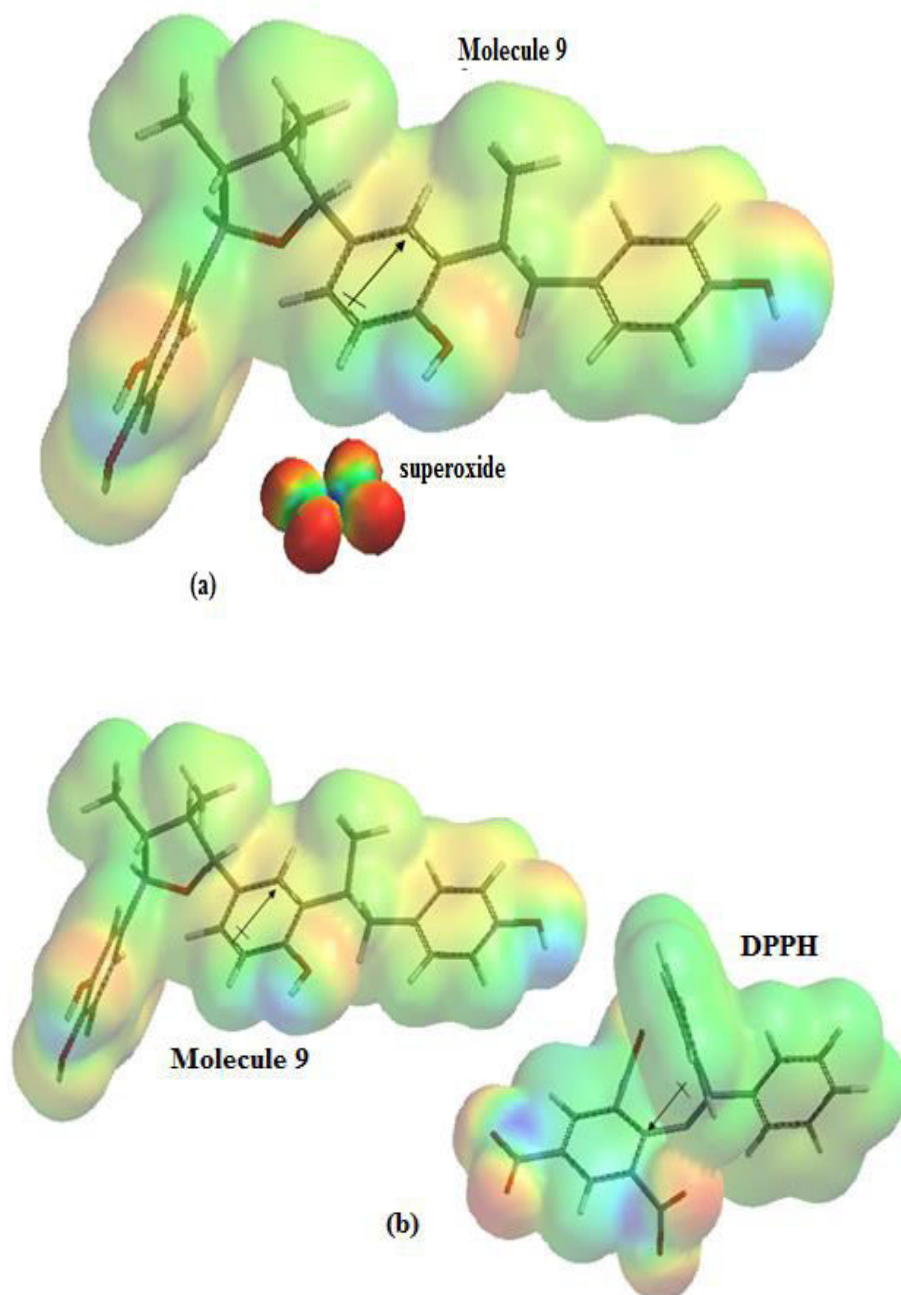


Figure 2.15 Representation of electrostatic energy maps of Molecule **9** with (a) superoxide and (b) DPPH.

If we next turn our attention to the least active molecule towards superoxide that is also inactive towards DPPH, namely Molecule **2**, this has a minimum BDE of 79.8 kcal/mol and, based on our other data, this value is considered unlikely to be above the threshold for activity for either superoxide or DPPH.

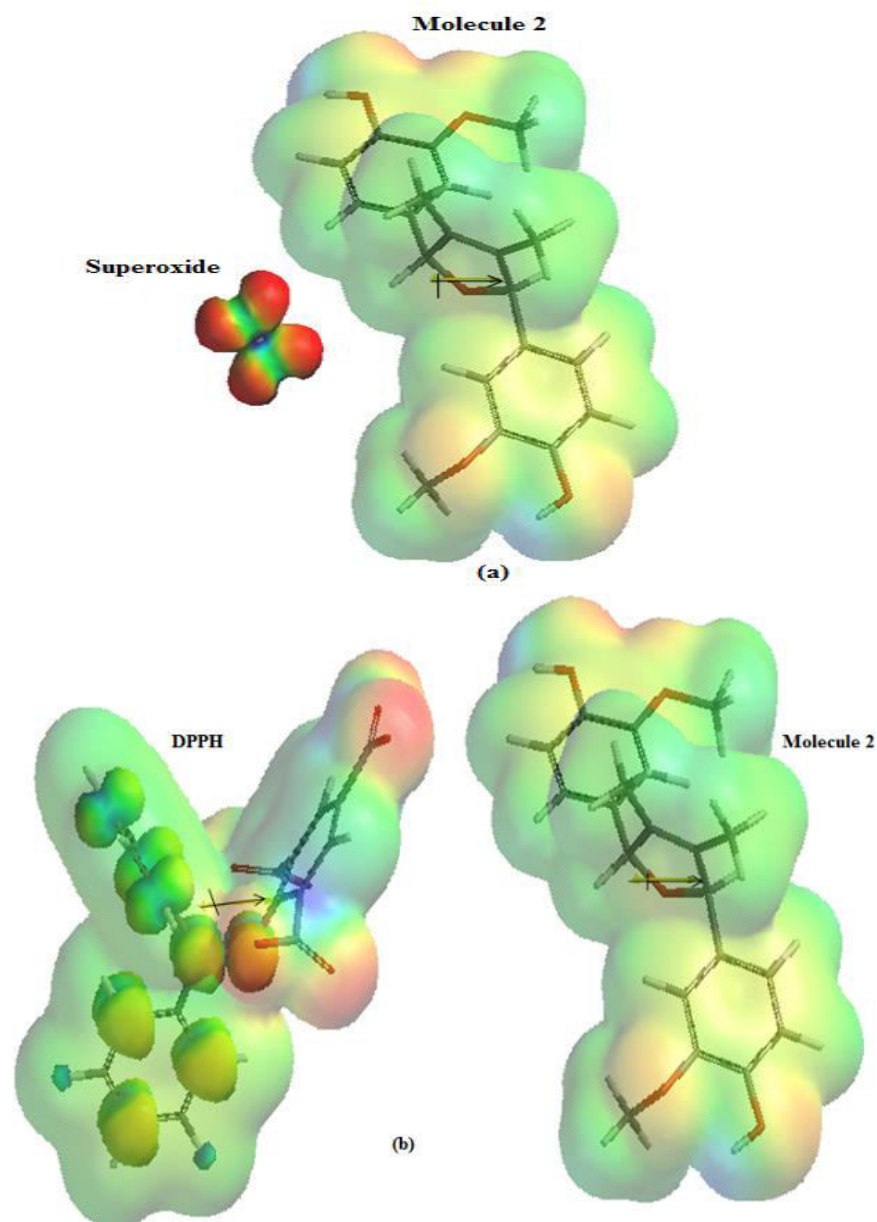


Figure 2.16 Representation of electrostatic potential maps of the Molecule 2 with (a) superoxide and (b) DPPH. In this diagram, the spin potential of the DPPH is also shown.

Figure 2.16 (a) depicts the electrostatic potential energy maps of Molecule 2 and superoxide and represents a “snapshot” of how these molecules might approach one another. Note that the dipole vector is perpendicular to the plane of the molecule and this would tend to direct the superoxide anion towards the centre of the molecule rather

than towards the antioxidant regions at the ends. This, together with some steric influence of the methoxy groups, may well have some inhibitory effect on the reaction, hence making this molecule less potent towards superoxide, as observed.

Figure 2.16 (b) depicts the electrostatic potential energy maps of Molecule **2** and DPPH approaching one another. It is noteworthy that both of these molecules are comparable in size and both have steric bulk (Molecule **2** via the methoxy moieties). Our docking experiments suggest that the resulting steric hindrance could be sufficient to prevent a productive interaction between these two molecules.

The minimum BDE for Molecule **3** that is moderately active towards superoxide but inactive towards DPPH is 84.4 kcal/mol. Figure 2.17 (a) depicts the electrostatic energy maps of Molecule **3** and superoxide and represents a snapshot of their possible approach. Here, it may be seen that both the active O-H's of Molecule **3** are accessible to superoxide and this approach is electrostatically favoured and not sterically restricted - and thus, as expected, it shows activity towards superoxide.

Figure 2.17 (b) represents the electrostatic and spin potential maps of DPPH with Molecule **3** and considers the approach of both the molecules aligned with their dipole moments. From these studies it can be shown that DPPH clearly has access to the OH moiety and suggests that the 84.4 kcal/mol is above the threshold for the DPPH and that this is the limiting factor.

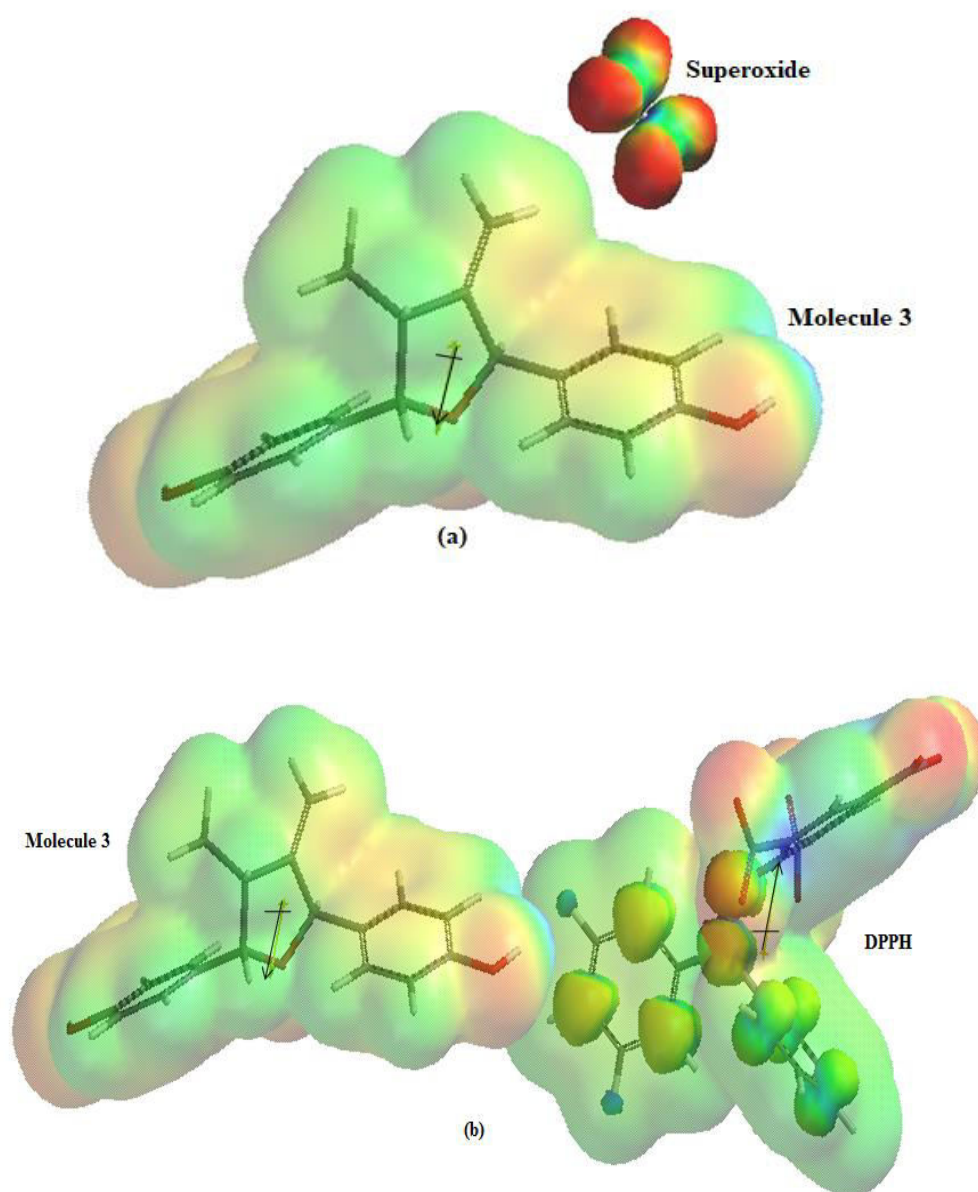


Figure 2.17 Representation of electrostatic energy map of Molecule **3** with (a) superoxide anion and (b) DPPH. In this diagram, the spin potential of the DPPH is also shown to high light the accessibility of this region to the antioxidant region of Molecule **3**.

Figure 2.18 (a) depicts the electrostatic energy maps of Molecule **6** and superoxide and represents a snapshot of their one of the possible approach trajectories. Both the active O-H's of Molecule **6** (two equivalent minima BDEs of 84.8 kcal/mol) are accessible to superoxide, and this approach is also electrostatically favoured and not sterically

restricted. Since this molecule shows activity towards superoxide, this indicates that this BDE value is below the threshold for superoxide activity.

Figure 2.18 (b) represents a snapshot of electrostatic energy maps of Molecule **6** and DPPH and considers how these molecules might approach one another. Although both the O-H's are accessible to DPPH, both electrostatically and sterically, Molecule **6** shows inactivity towards DPPH. Therefore, this is attributed to a threshold effect and suggests that 84.8 kcal/mol is above the threshold for DPPH. Thus DPPH has a higher BDE threshold than superoxide suggesting that the BDE threshold is actually species dependent.

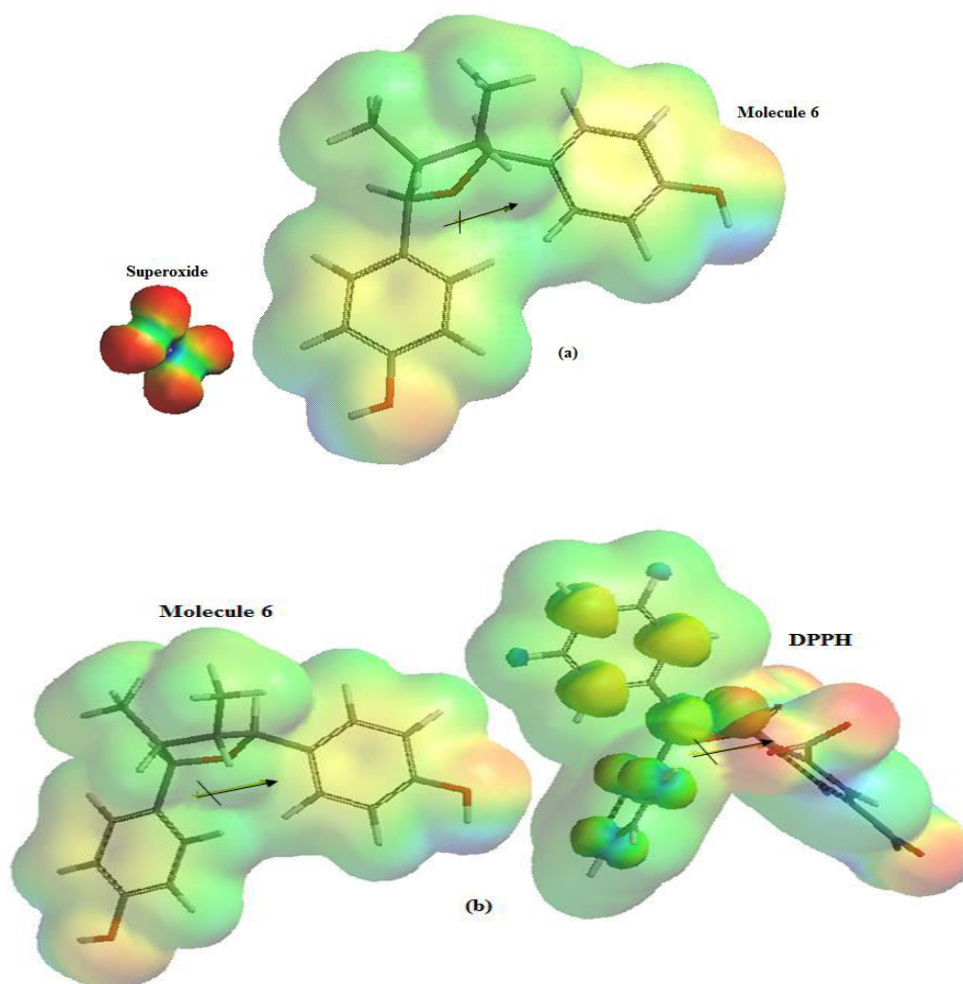


Figure 2.18 Representation of electrostatic energy maps of Molecule **6** with (a) Superoxide and (b) DPPH.

Figure 2.19 (a) depicts the electrostatic energy maps of Molecule **10** and superoxide and considers how these molecules might approach one another. All four O-H moieties of Molecule **10** are easily accessible to superoxide and all approaches are electrostatically favoured and not sterically restricted. The minimum BDE of 83.6 kcal/mol is below the threshold for superoxide and it is therefore not surprising that this molecule show activity towards this radical species. It should also be noted from Figure 2.13 that the remaining three OH moieties are all activated upon the loss of an H atom from the minimum BDE moiety and these secondary BDEs are all below the superoxide threshold.

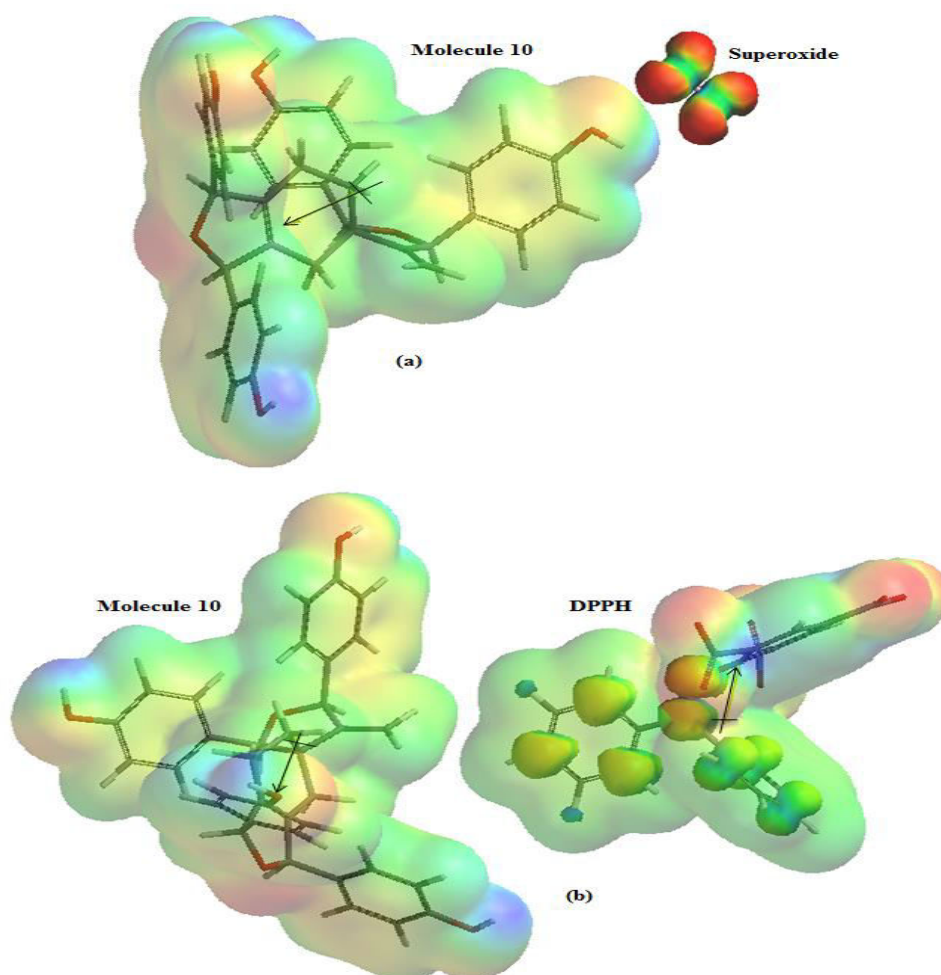


Figure 2.19 Representation of electrostatic energy maps of Molecule **10** with (a) superoxide and (b) DPPH.

Figure 2.19 (b) depicts the electrostatic energy maps of Molecule **10** and DPPH and considers how these molecules might approach one another. All four O-H moieties of Molecule **10** are not accessible to DPPH as it is neither electrostatically nor sterically favoured. The BDE of 83.6 kcal/mol is above the threshold for DPPH and it is therefore not surprising that this molecule is inactive towards this radical species.

2. Molecules of Group 3, namely Molecules 4 and 13, Table 2.4, are active towards both superoxide and DPPH. Why?

Molecules belonging to Group 3 (that are active towards both superoxide and DPPH) are the Molecules **4** and **13**, Table 2.4 - Colour Coded Green. Experimentally, these molecules show activity towards both superoxide and DPPH. Figure 2.20 (a) depicts the electrostatic potential energy maps for Molecule **4** and superoxide considers how these molecules might approach one another. Figure 2.20 (b) depicts the electrostatic potential energy maps for Molecule **4** and DPPH and represents a snapshot of their possible interaction. The minimum BDE of Molecule **4** is 80.9 kcal/mol and this is below threshold value for both superoxide and DPPH. For both species, the electrostatics and the steric requirements are favourable for interaction. It is worth noting that for the previously discussed Molecule **2**, that is structurally very similar to Molecules **4**, Figure, 2.12, the electrostatic and steric factors are not considered favourable, the latter being influenced by the bulkier saturated carbon substituent. This is a testimony to the subtlety of steric effects.

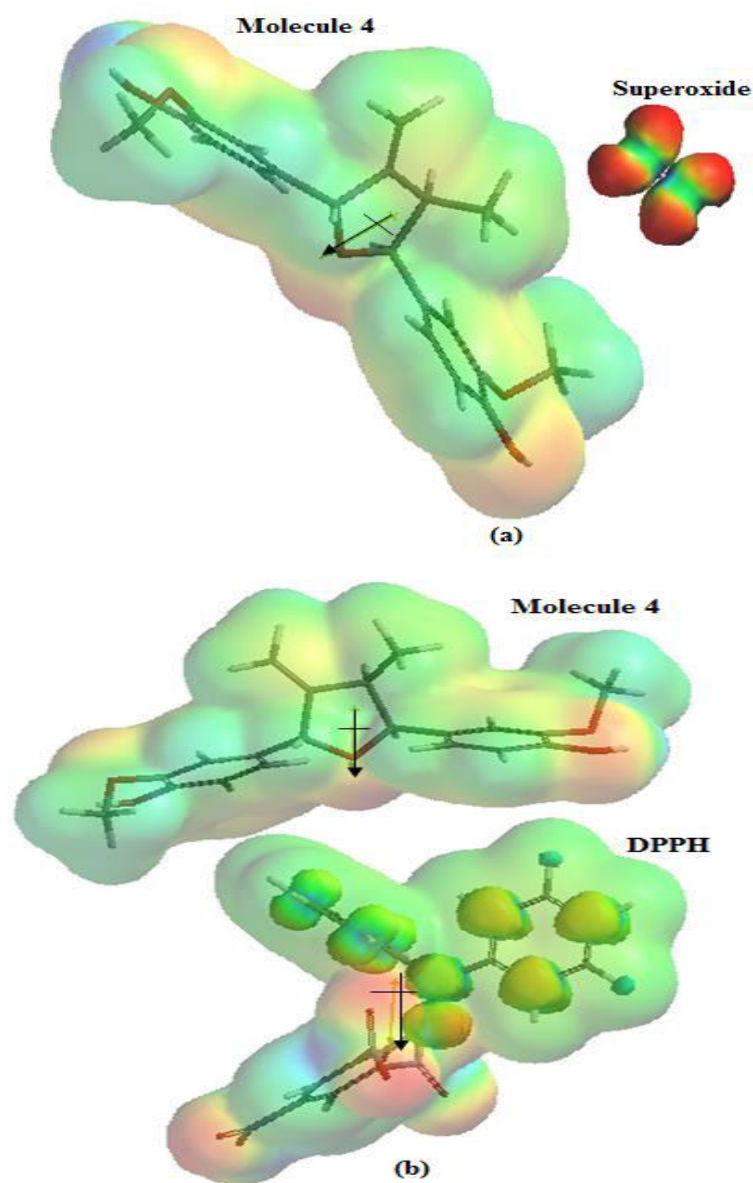


Figure 2.20 Representation of electrostatic energy maps of Molecule 4 with (a) superoxide and (b) DPPH.

Figure 2.21 (a) and (b) depict the electrostatic potential energy maps for Molecule 13 and superoxide and DPPH and represent snapshots of their possible interactions. All the O-H moieties are easily accessible for both superoxide and DPPH, both

electrostatically and sterically. The minimum BDE of 81.6 kcal/mol is below the threshold value for both species.

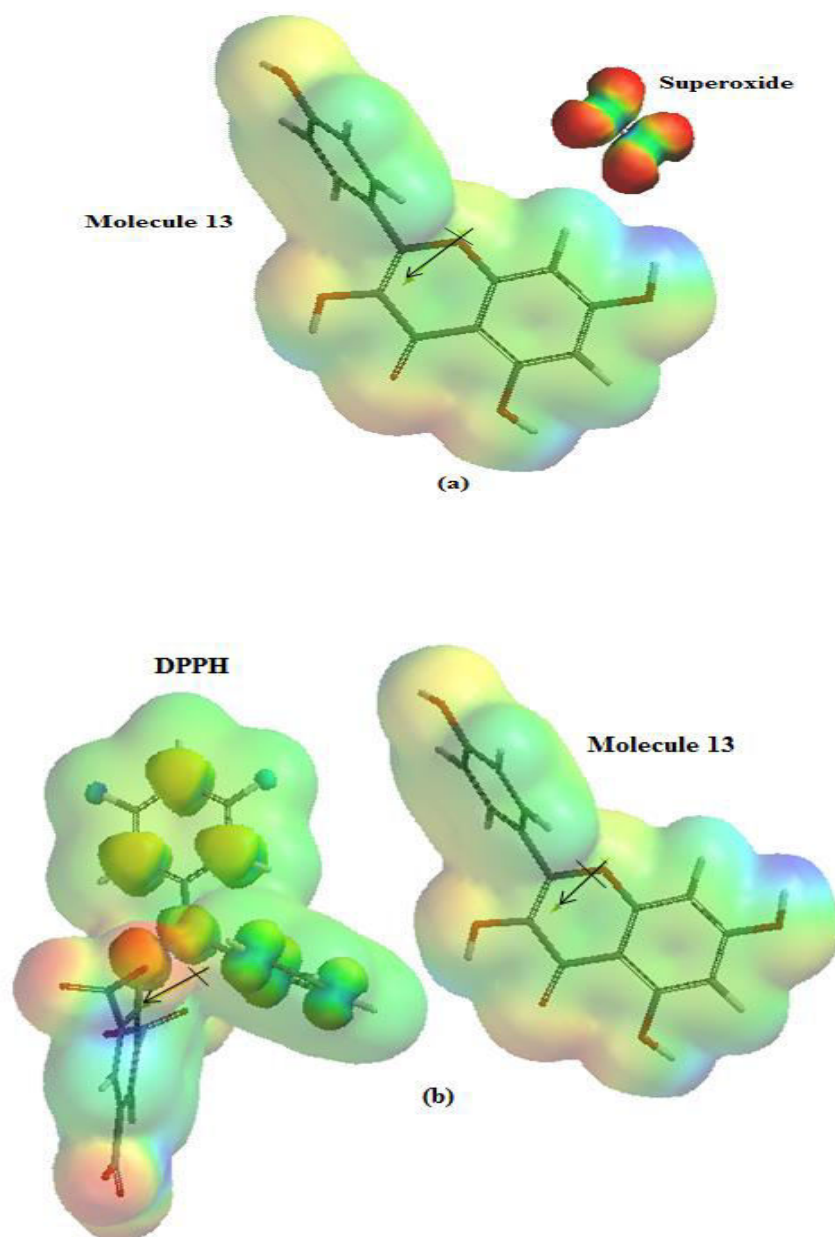


Figure 2.21 Representation of electrostatic energy maps of Molecule **13** with (a) superoxide and (b) DPPH. Not that the spin potential is also indicated in the DPPH molecule to highlight its accessibility to the active OH moiety.

2.16 Comparison of Molecules

2.16.1 Molecules 1-6 and Molecule 15

For Molecule **15** there is no experimental data available although it is structurally similar to Molecules **1** to **6** (Set 1, Figure 2.22). Based on the previous analysis of Molecules **1** to **6**, it is possible to predict the behaviour of Molecule **15** towards superoxide and DPPH. Molecules **1-6** and **15** are structurally similar but shows different antioxidant potency. Their antioxidant potency increasing order is $2 < 6 < 3 < 4$ and Molecules **1** and **5** neither show superoxide anion scavenging nor DPPH activity. Molecule **4** shows both EC_{50}^a and DPPH activity, the presence of methoxy groups at 3 and 3' positions and the presence of carbon-carbon double bond is the reason for its unique character from rest of the Molecules. Due to the presence of methoxy moieties in Molecules **2**, **4** and **15** the O-H homolytic bond cleavage occurs easily. The methoxy moieties are interconnected by intra molecular hydrogen bonding and thus **2**, **4** and **15** show least BDEs (79.8, 80.9, and 77.5 Kcal/mol) respectively.

Furthermore, in Molecule **4**, one of the methyl group was replaced by =CH₂ group, decreased its steric hindrance, and thus improved its accessibility towards DPPH. The high DM and low BDE also lead Molecule **4** more attractive towards superoxide anion. The electron dense unpaired spin of DPPH is away from the active hydroxyl moiety of Molecules **2** emphasize the experimental results of DPPH activity. Whereas in Molecules **4** and **15** the unpaired spin of DPPH is overlapping the active hydroxyl moiety, compliments the experimental results.

Some research questions based on the experimental data relating to the superoxide anion and DPPH free radical scavenging assays are as follows.

2.16.2 Set 1 (Molecules 1-6 and 15)

Set 1 (Molecules **1**, **2**, **3**, **4**, **5**, **6** and **15**). Molecules **2**, **4** and **15** have IMHB with relatively low BDEs. Molecules **1**, **3**, **5** and **6** lack IMHB and have relatively high BDEs.

1. Only Molecules **1** and **5** from **Set 1** are inactive towards both the superoxide anion and DPPH, why?

2. Molecule **4** is the only one from **Set 1** that shows activity towards both the superoxide anion and DPPH why?

3. Molecules **2, 3** and **6** from **Set 1** show activity towards superoxide only - but to different extents $3 > 6 > 2$, why?

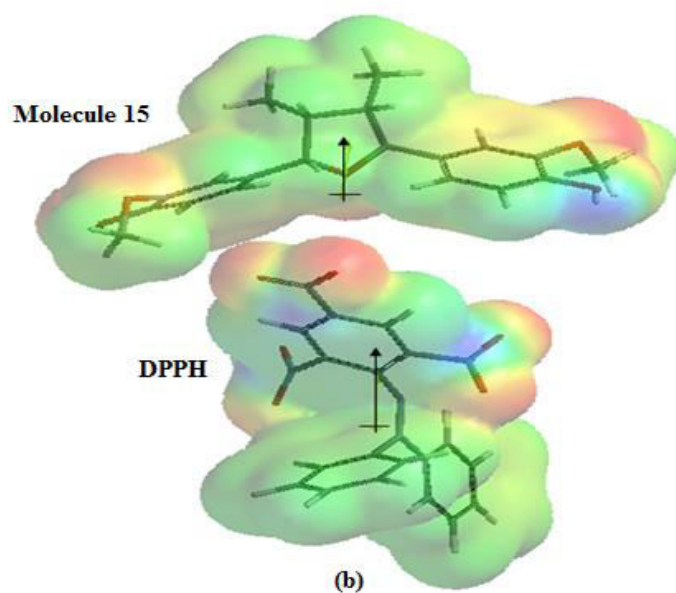
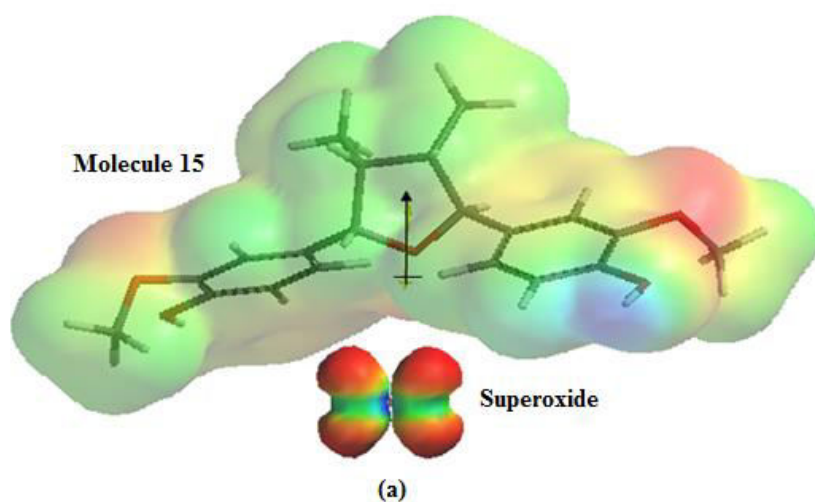


Figure 2.22 Representation of electrostatic energy map of Molecule **15** with (a) superoxide and (b) DPPH.

Set 1, that are grouped together based on structural similarities, contains Molecules **1-6** and **15**. The primary observation was about the inactivity of Molecules **1** and **5** towards both superoxide and DPPH. There are few observed structural differences for these Molecules. Whereas, the BDEs for these molecules are quite high (85.5 kcal/mol for Molecule **1** and 84.4 kcal/mol for Molecule **5**) and poor structural accessibility for superoxide and DPPH free radical. Furthermore, bottom side of Molecule **1** the negatively charged superoxide facing repulsion and through the top side of the molecule superoxide was unable to approach because of steric hindrance by the two methyl groups. In addition, the lower DM of Molecule **1** reduces the polarity and thus decreased the attraction of superoxide towards Molecule **1**.

Molecules **1** and **5** exhibits relatively low DMs, indicating less polarity, together with relatively high BDEs. In addition, there is poor structural accessibility to the O-H moieties for both superoxide and DPPH free radicals, Figure 2.12. All these factors can be considered as being consistent with the observed inactivity.

2.16.3 Set 2 (Molecules 7, 8 and 9)

Set 2 (Molecules **7, 8** and **9**). Molecules **7** and **8** lack IMHB and Molecule **9** has IMHB. Molecule **9** is active towards superoxide but not to DPPH: High activity of Molecule **9** towards superoxide anion show high antioxidant potential towards superoxide anion Table 2.1 and have no activity towards DPPH. Figure 2.15 depicts the dipole vectors of the Molecule **9** with superoxide and DPPH. The lowest BDEs of Molecules **7** and **8** are (79.5, 82.6 kcal/mol) respectively and for Molecule **9** (72.1kcal/mol) indicates that the BDEs are below threshold. However, only Molecule **9** show activity towards superoxide. This could be because of its structural accessibility (the active hydroxyl moiety at position 3 of Molecule **9**) whereas, for Molecules **7** and **8** the active O-H moiety is situated at the mid of the molecule, which prohibited its accessibility for superoxide and DPPH due to steric effect. Furthermore, Molecule **9** show relatively low IP than Molecules **7** and **8**, Table 2.1 which also emphasize the better antioxidant potency of Molecule **9**, as the IP is inversely proportional to antioxidant activity (K. Sadasivam et.al 2011).

2.16.4 Set 3 (Molecules 10, 13 and 14)

All the molecules in **Set 3** are neither structurally similar nor comparable molecular weight. Though, Molecules **10** and **14** lack IMHB, Molecule **10** show activity towards superoxide but not towards DPPH; whereas Molecule **14** is inactive towards both superoxide and DPPH. Molecule **13** exhibits IMHB and show activity towards both superoxide and DPPH. The presence of IMHB in Molecule **13** lowers its polarity by masking which is a qualitative physical property for representing the antioxidant activity of molecules with polar atoms.

2.16.5 Molecules 7 and 8 inactive towards both.

Molecules **7** and **8** are inactive towards both superoxide and DPPH. One of the observed differences of these molecules **7** and **8** from Molecule **9** is the “cage” like orientation of the aromatic rings. This orientation of these molecules **7** and **8**, (unlike Molecule **9**) restricts the accessibility for DPPH and superoxide. Furthermore, the BDEs of these molecules **7** and **8** are relatively higher than Molecule **9**. The active O-H (O-H with lowest BDE) is situated at the mid of these molecules which are not easily accessible due to steric effect. The electrostatic energy maps of both molecules **7** and **8**, Figures 2.28 and 2.29 show similar orientations of the aromatic rings forming a ‘cage like’ structure.

2.17 Effect of intra molecular hydrogen bonding on dipole moment

As an index of polarity, DM could predict the physicochemical properties of drug(s) molecules. On scrutinize the effect of IMHB, it was observed that the DM decreased in molecules **2**, **4**, **9**, **13** and **15** which possesses IMHB; computed IMHB values and dipole moment of parent and radical species of lignoid molecules are given in Table 2.8. The decrease in DM is due to the fact that, the hydrogen- bonded ring closure diminished the polarity and increased the lipophilicity/hydrophobicity (Goto et al. 2001).

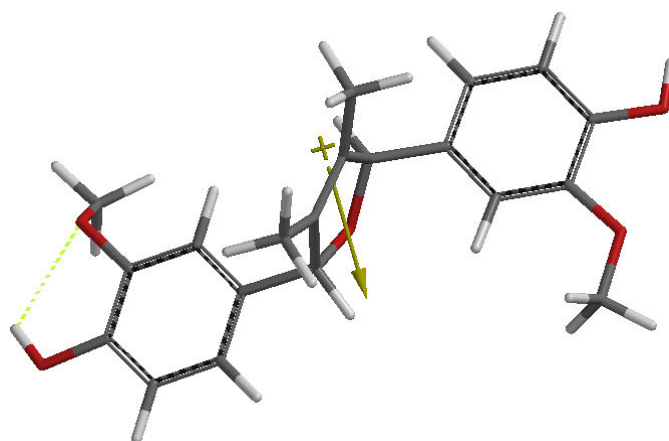


Figure 2.23 Representation of Molecule 2 with Intra Molecular Hydrogen Bonding.

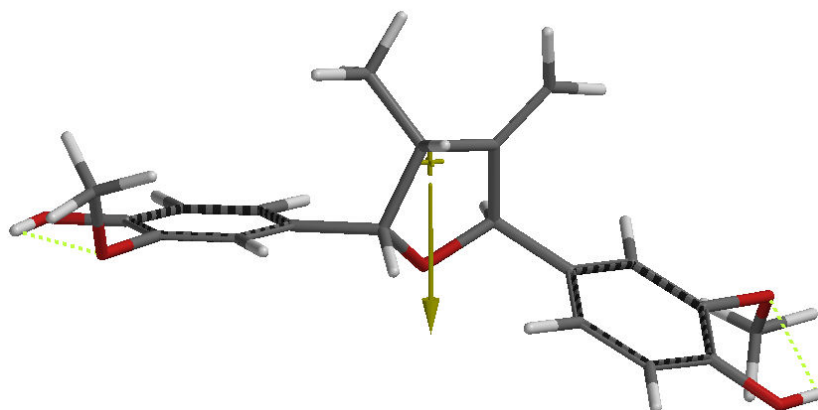


Figure 2.24 Representation of Molecule 4 with Intra Molecular Hydrogen Bonding.

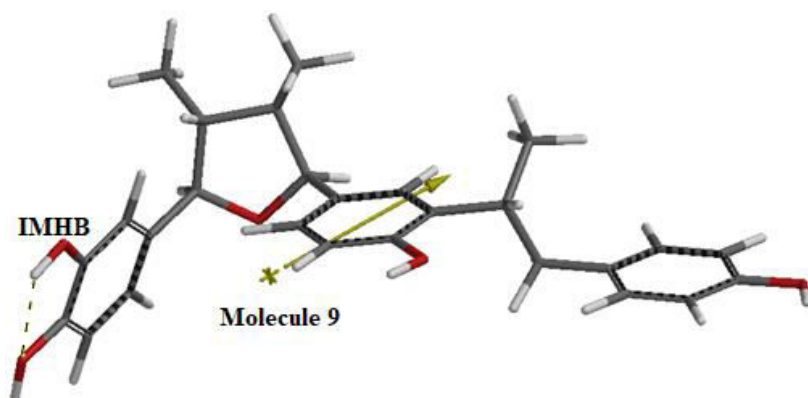


Figure 2.25 Representation of Molecule 9 with Intra Molecular Hydrogen Bonding.

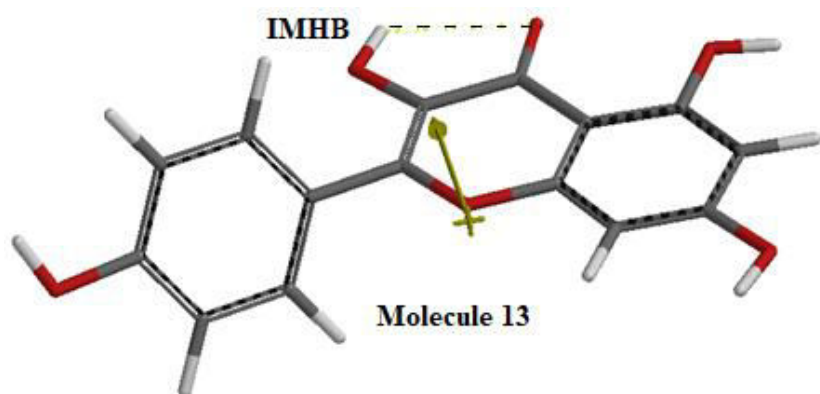


Figure 2.26 Representation of Molecule 13 with Intra Molecular Hydrogen Bonding.

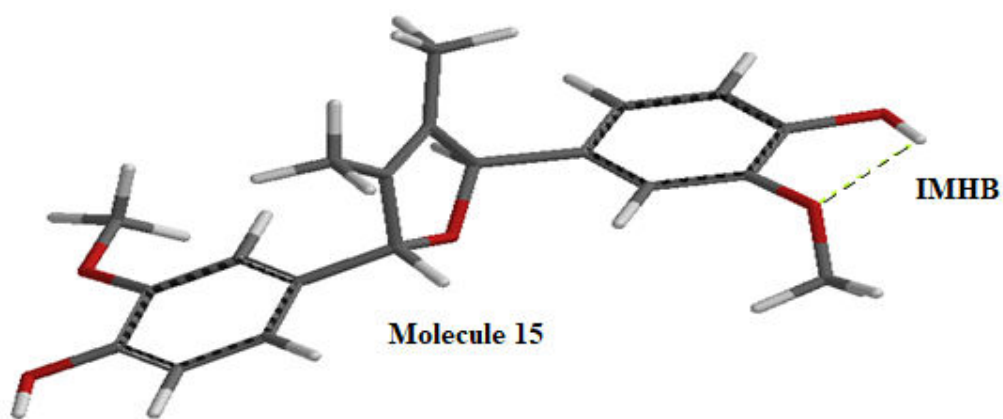


Figure 2.27 Representation of Molecule 15 with Intra Molecular Hydrogen Bonding.

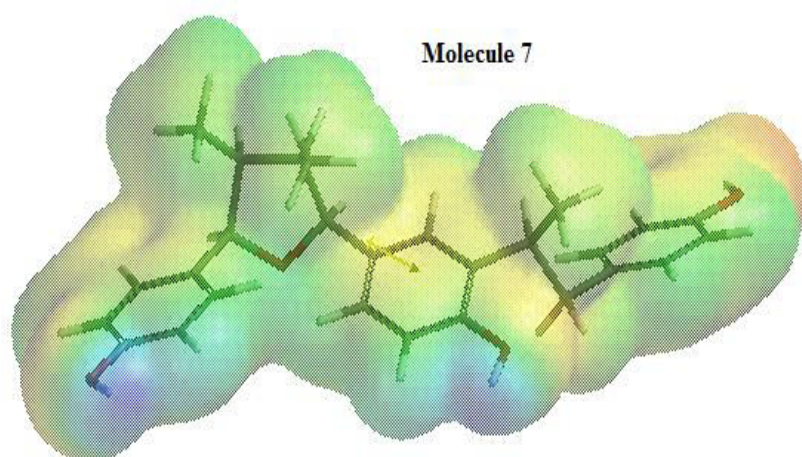


Figure 2. 28 Representation of electrostatic energy map of Molecule 7

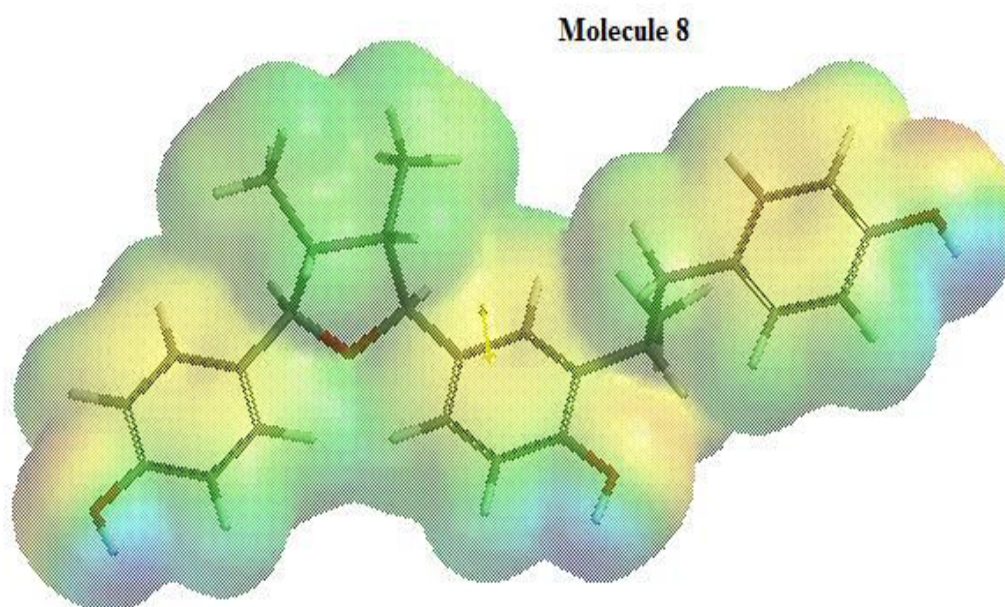


Figure 2. 29 Representation of electrostatic energy map of Molecule 8

2.18 Effect of ionization potential over methoxy substituent

The methoxy group attached compounds are 2, 4, and 15. The Molecules 1 and 2 are structurally differ by the presence of methoxy moieties at 3 and 3' positions of the aromatic ring. On comparison of both molecules, Molecule 2 shows activity as a superoxide anion scavenger as the electron withdrawing -methoxy groups at positions 3 and 3' favours intra molecular hydrogen bonding and superoxide anion. For example,

the conformational analysis of both compounds designates that the BDE of the former is quite high (85.5 kcal/mol) and the other is (79.8 kcal/mol). This difference in BDE is due to the presence of intra molecular hydrogen bonding that deteriorate the bonding. In addition, Molecule 2 shows least IP than Molecule 1. The greater the degree of dissociation, the more H⁺ ions will be produced in turn, the extent of dissociation depends on the IP of the corresponding molecule.

Table 2.8 Computed values of lignoid molecules with the values of dipole moment of parent and radical species and the number of intra molecular hydrogen bonding.

Molecules	Number of intra-molecular hydrogen bond (IMHB)	DM (Debye) PARENT	DM (Debye) RADICAL
1	0	1.72	6.23
2	1	1.98	2.47
3	0	2.65	5.31
4	2	1.93	2.54
5	0	0.85	4.99
6	0	2.25	6.24
7	0	1.71	4.37
8	0	3.05	3.75
9	1	3.6	5.71
10	0	4.19	5.91
13	1	3.45	6.21
14	0	3.55	2.84
15	2	1.50	2.91
BHA-1	0	2.47	5.23
BHA-2	0	2.34	4.37
Vitamin E		2.62	5.32

2.19 Conclusions

For molecules that are inactive towards both superoxide and DPPH (**Group 1**), the computed BDEs are relatively high (in the low to mid 80's of kcal/mol) for Molecules **1, 5, 8** and **14**; the exception is Molecule **7** that has a BDE of 79.5 kcal/mol. For the former group of molecules, it is concluded that the inactivity is due to both the BDE threshold being exceeded for both radicals and to steric hindrance that may be observed upon the (docking) approach of both of the radicals to the 'antioxidant region' of the poly phenolic. For the latter molecule, i.e. Molecule **7**, it is concluded that the inactivity is due to both steric hindrance and opposing dipole moments with respect to accessing the antioxidant region.

For molecules that are active towards superoxide but not towards DPPH (**Group 2**), three of the molecules, Molecules **3, 6** and **10**, have BDEs in the mid 80's (of kcal/mol) and two, Molecules **2** and **9**, have BDEs in the high and low 70's. In particular, one of these latter molecules, Molecule **9**, has a computed BDE value that is considered to be very low, at 72.1 kcal/mol (c.f. benchmarked to BDE of Vitamin E; 75.3 kcal/mol, under the same method). For Molecules **3, 6** and **10**, it is concluded that the BDE thresholds are exceeded for activity towards DPPH since the antioxidant part of these molecules are considered to be fully accessible, according to the modelling and docking experiments and given that adverse dipole-dipole interactions were not found to be a contributing factor. This suggests that the BDE threshold for DPPH is different from that of superoxide, all else being equal. This is, perhaps, not surprising. For Molecules **2** and **9**, steric hindrance with respect to DPPH is found to be explicitly present for both of the molecules and especially for Molecule **9** that has the very low BDE - that would otherwise be expected to be highly active. This emphasises the importance of steric hindrance.

For the molecules that are active towards both superoxide and DPPH (**Group 3**), namely Molecules **4** and **13**, the computed BDEs are in the low 80's. The values of the BDEs are thus considered to be below the threshold for activity for both superoxide and DPPH and an examination of the molecular structures and their docking with the free radicals, show no steric hindrance with respect to their approach to the antioxidant

regions. It is also found that the dipoles are compatible for a favourable reaction orientation.

The above outcomes show that although it is difficult to rationalize the observed experimental antioxidant activities based on the lowest BDE energies alone, this can be achieved to some extent when the structural characteristics of the molecules are considered in the light of steric hindrance and dipole - dipole compatibility. This clearly demonstrates that all such factors need to be taken into account in rationalizing the observed antioxidant activity and/or in the design of more effective antioxidant molecules. If such molecules are being designed as drugs, then other computed parameters, such as $\text{Log}_{10}P$, should also be taken into account for considerations such as bioavailability. Computational Chemistry is a powerful tool for this approach. A particularly important realization is that the rationalization of the antioxidant activity is both qualitative *and* quantitative, with qualitative components (such as structure, steric effects, dipole direction and charge distribution) being just as important as quantitative parameters such as the BDE. For this reason, we have not approached this problem with multiple linear regression analysis in mind.

References

Alexander, B, Browse, D, Reading, S & Benjamin, I 1999, 'A simple and accurate mathematical method for calculation of the EC50', *Journal of pharmacological and toxicological methods*, vol. 41, no. 2-3, pp. 55-8.

Benvenuti, S, Pellati, F, Melegari, Ma & Bertelli, D 2004, 'Polyphenols, anthocyanins, ascorbic acid, and radical scavenging activity of Rubus, Ribes, and Aronia', *Journal of Food Science*, vol. 69, no. 3, pp. 164-9.

Caron, G, Kihlberg, J & Ermondi, G 2019, 'Intramolecular hydrogen bonding: An opportunity for improved design in medicinal chemistry', *Medicinal research reviews*.

Caron, G, Vallaro, M & Ermondi, G 2018, 'Log P as a tool in intramolecular hydrogen bond considerations', *Drug Discovery Today: Technologies*, vol. 27, pp. 65-70.

Chuang, Y-Y, Corchado, JC & Truhlar, DG 1999, 'Mapped interpolation scheme for single-point energy corrections in reaction rate calculations and a critical evaluation of dual-level reaction path dynamics methods', *The Journal of Physical Chemistry A*, vol. 103, no. 8, pp. 1140-9.

El Diwani, G, El Rafie, S & Hawash, S 2009, 'Antioxidant activity of extracts obtained from residues of nodes leaves stem and root of Egyptian *Jatropha curcas*', *African Journal of Pharmacy and Pharmacology*, vol. 3, no. 11, pp. 521-30.

Ertl, P, Rohde, B & Selzer, P 2000, 'Fast calculation of molecular polar surface area as a sum of fragment-based contributions and its application to the prediction of drug transport properties', *Journal of medicinal chemistry*, vol. 43, no. 20, pp. 3714-7.

Galano, A & Alvarez-Idaboy, JR 2013, 'A computational methodology for accurate predictions of rate constants in solution: Application to the assessment of primary antioxidant activity', *Journal of Computational Chemistry*, vol. 34, no. 28, pp. 2430-45.

Garbacki, N, Tits, M, Angenot, L & Damas, J 2004, 'Inhibitory effects of proanthocyanidins from *Ribes nigrum* leaves on carrageenin acute inflammatory reactions induced in rats', *BMC pharmacology*, vol. 4, no. 1, p. 25.

Giacomelli, C, Miranda, FdS, Gonçalves, NS & Spinelli, A 2004, 'Antioxidant activity of phenolic and related compounds: a density functional theory study on the O–H bond dissociation enthalpy', *Redox Report*, vol. 9, no. 5, pp. 263-9.

Goto, S, Kogure, K, Abe, K, Kimata, Y, Kitahama, K, Yamashita, E & Terada, H 2001, 'Efficient radical trapping at the surface and inside the phospholipid membrane is responsible for highly potent antiperoxidative activity of the carotenoid astaxanthin', *Biochimica et Biophysica Acta*, vol. 1512, no. 2, pp. 251-8.

Granato, D, Katayama, F & Castro, I 2010, 'Assessing the association between phenolic compounds and the antioxidant activity of Brazilian red wines using chemometrics', *LWT-Food Science and Technology*, vol. 43, no. 10, pp. 1542-9.

Grimme, S, Antony, J, Schwabe, T & Mück-Lichtenfeld, C 2007, 'Density functional theory with dispersion corrections for supramolecular structures, aggregates, and complexes of (bio) organic molecules', *Organic & Biomolecular Chemistry*, vol. 5, no. 5, pp. 741-58.

Häkkinen, S, Heinonen, M, Kärenlampi, S, Mykkänen, H, Ruuskanen, J & Törrönen, R 1999, 'Screening of selected flavonoids and phenolic acids in 19 berries', *Food Research International*, vol. 32, no. 5, pp. 345-53.

Hann, MM, Leach, AR & Harper, G 2001, 'Molecular complexity and its impact on the probability of finding leads for drug discovery', *Journal of chemical information and computer sciences*, vol. 41, no. 3, pp. 856-64.

Harvey, AL 2008, 'Natural products in drug discovery', *Drug discovery today*, vol. 13, no. 19-20, pp. 894-901.

Illas, F, Moreira, IP, De Graaf, C & Barone, V 2000, 'Magnetic coupling in biradicals, binuclear complexes and wide-gap insulators: a survey of ab initio wave function and density functional theory approaches', *Theoretical Chemistry Accounts*, vol. 104, no. 3-4, pp. 265-72.

Jayaprakasam, B, Padmanabhan, K & Nair, MG 2010, 'Withanamides in *Withania somnifera* fruit protect PC-12 cells from β -amyloid responsible for Alzheimer's disease', *Phytotherapy Research*, vol. 24, no. 6, pp. 859-63.

Jiang, X & Kopp-Schneider, A 2014, 'Summarizing EC50 estimates from multiple dose-response experiments: A comparison of a meta-analysis strategy to a mixed-effects model approach', *Biometrical Journal*, vol. 56, no. 3, pp. 493-512.

Koch, W, Holthausen, MC & Holthausen, MC 2001, *A chemist's guide to density functional theory*, vol. 2, Wiley Online Library.

Kohn, W, Becke, AD & Parr, RG 1996, 'Density functional theory of electronic structure', *The Journal of Physical Chemistry*, vol. 100, no. 31, pp. 12974-80.

Moyer, RA, Hummer, KE, Finn, CE, Frei, B & Wrolstad, RE 2002, 'Anthocyanins, phenolics, and antioxidant capacity in diverse small fruits: Vaccinium, Rubus, and Ribes', *Journal of Agricultural and Food Chemistry*, vol. 50, no. 3, pp. 519-25.

Musialik, M & Litwinienko, G 2005, 'Scavenging of dpph• radicals by vitamin E is accelerated by its partial ionization: the role of sequential proton loss electron transfer', *Organic Letters*, vol. 7, no. 22, pp. 4951-4.

Parr, RG 1980, *Density functional theory of atoms and molecules*, Horizons of Quantum Chemistry, Springer.

Pedersen, JT, Ostergaard, J, Rozlosnik, N, Gammelgaard, B & Heegaard, NH 2011, 'Cu (II) mediates kinetically distinct, non-amyloidogenic aggregation of amyloid- β peptides', *Journal of Biological Chemistry*, vol. 286, pp. 26952-63.

Peng, C, Ayala, PY, Schlegel, HB & Frisch, MJ 1996, 'Using redundant internal coordinates to optimize equilibrium geometries and transition states', *Journal of Computational Chemistry*, vol. 17, no. 1, pp. 49-56.

Sadasivam, K & Kumaresan, R 2011, 'A comparative DFT study on the antioxidant activity of apigenin and scutellarein flavonoid compounds', *Molecular Physics*, vol. 109, no. 6, pp. 839-52.

Sanz, M, Ferrandiz, M, Cejudo, M, Terencio, MC, Gil, B, Bustos, G, Ubeda, A, Gunasegaran, R & Alcaraz, M 1994, 'Influence of a series of natural flavonoids on free radical generating systems and oxidative stress', *Xenobiotica*, vol. 24, no. 7, pp. 689-99.

Sasaki, T, Li, W, Zaike, S, Asada, Y, Li, Q, Ma, F, Zhang, Q & Koike, K 2013a, 'Antioxidant lignoids from leaves of *Ribes nigrum*', *Phytochemistry*, vol. 95, pp. 333-40.

Schlegel, HB 1982, 'Optimization of equilibrium geometries and transition structures', *Journal of Computational Chemistry*, vol. 3, no. 2, pp. 214-8.

Schultheis, LM & Donoghue, MJ 2004, 'Molecular phylogeny and biogeography of *Ribes* (Grossulariaceae), with an emphasis on gooseberries (subg. *Grossularia*)', *Systematic Botany*, vol. 29, no. 1, pp. 77-96.

Sebaugh, J 2011, 'Guidelines for accurate EC50/IC50 estimation', *Pharmaceutical statistics*, vol. 10, no. 2, pp. 128-34.

Slimestad, R & Solheim, H 2002, 'Anthocyanins from black currants (*Ribes nigrum* L.)', *Journal of Agricultural and Food Chemistry*, vol. 50, no. 11, pp. 3228-31.

Tabart, J, Franck, T, Kevers, C, Pincemail, J, Serteyn, D, Defraigne, J-O & Dommes, J 2012, 'Antioxidant and Anti-inflammatory Activities of *Ribes nigrum* extracts', *Food Chemistry*, vol. 131, no. 4, pp. 1116-22.

Terada, H, Muraoka, S & Fujita, T 1974, 'Structure activity relations. 7. Structure-activity relations of fenamic acids', *Journal of medicinal chemistry*, vol. 17, no. 3, pp. 330-4.

Tugcu, G, Saçan, MT, Vracko, M, Novic, M & Minovski, N 2012, 'QSTR modelling of the acute toxicity of pharmaceuticals to fish', *SAR and QSAR in Environmental Research*, vol. 23, no. 3-4, pp. 297-310.

PART B

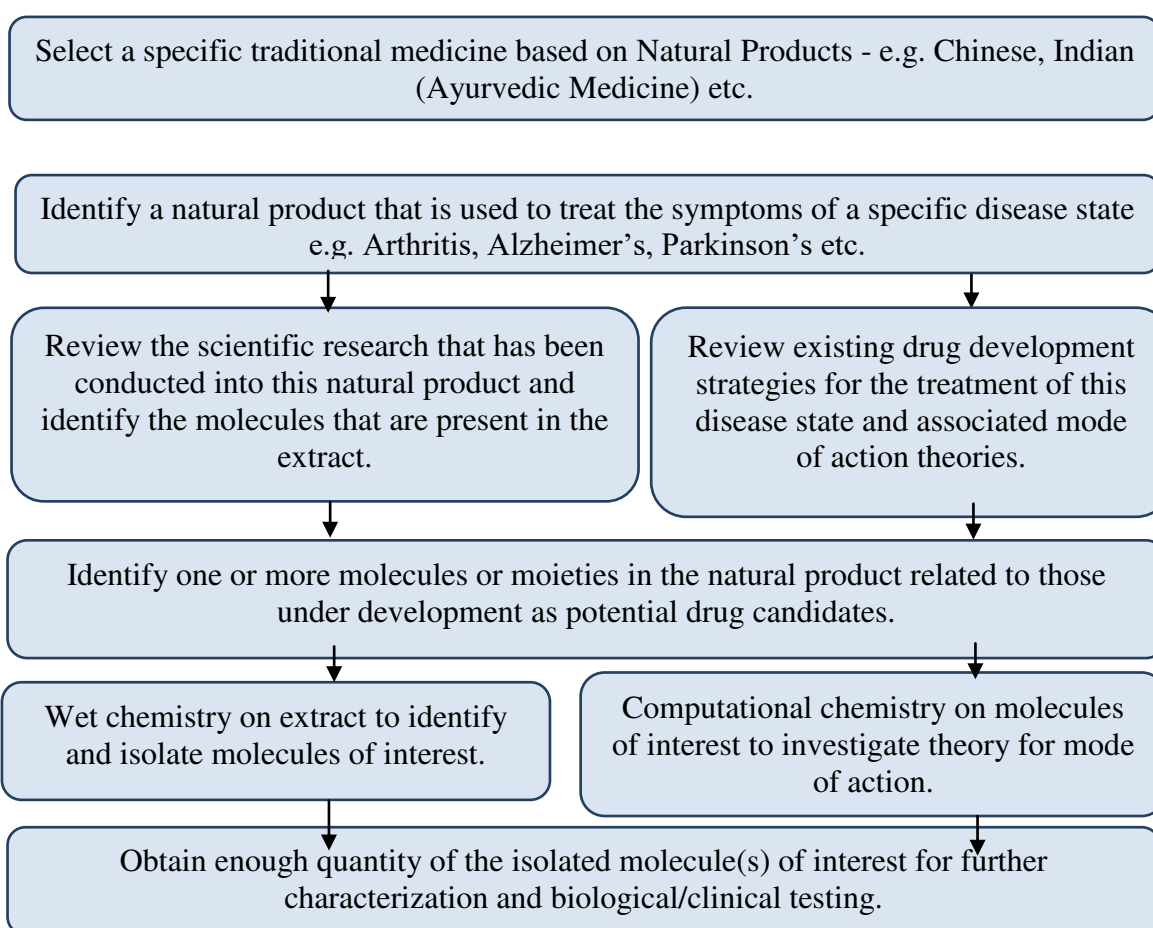
CHAPTER 3

A strategy for the identification of a potential drug candidate from a traditional medicine

3.1 Preamble

The general objective of this research is to select a well-known traditional medicine derived from a natural product, for which some information on its chemical composition is known within the scientific literature and for which a specific recalcitrant medical condition is identified as a target for such a medicine. Existing conventional scientific approaches to the design of potential drug candidates towards the aforementioned condition are employed to identify molecular species in the extract that represent naturally occurring potential drug candidates. Simultaneous computational chemistry experiments are then carried out that support (or otherwise) the existing theory (or theories) for the purported mode of action of the nominated molecular species. It is anticipated that this approach is applicable to a wide range of natural products and disease states. This general strategy is depicted in **Scheme 1**.

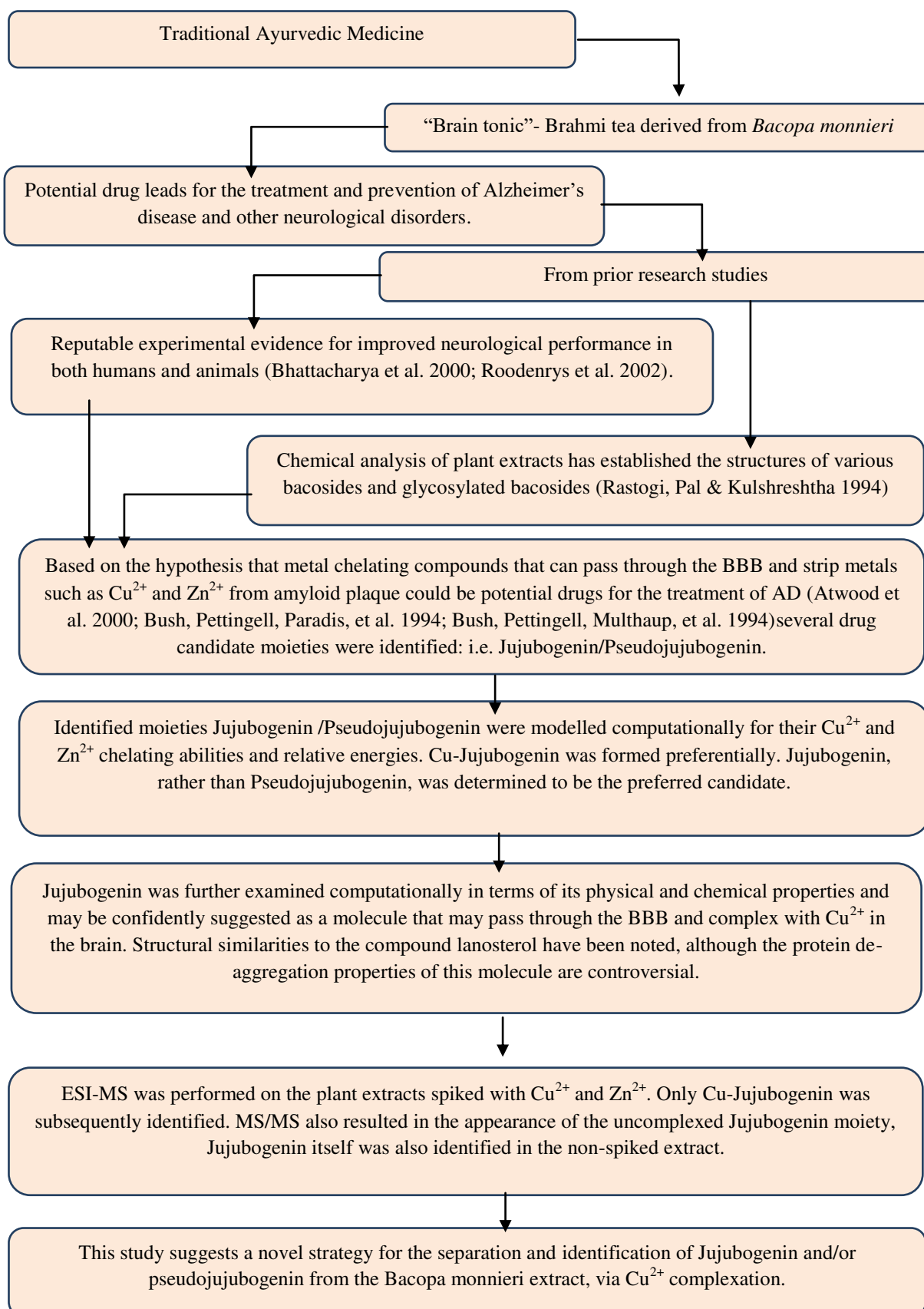
Scheme1- General Strategy



For this thesis, the natural product chosen is derived from traditional Indian (Ayurvedic) medicine. The medicine is in the form of a drink that is referred to as “Brahmi tea” which is derived from the plant *Bacopa monnieri* (BM). This traditional medicine is considered to be a “brain tonic” and is used to treat persons who are suffering from the symptoms of various neurological conditions, particularly Alzheimer’s disease (AD). Considerable conventional scientific research has been conducted into Brahmi tea with respect to its molecular composition as well as animal studies relating to its memory enhancing properties (Bihaqi et al. 2009; Jyoti & Sharma 2006; Thomas et al. 2013; Vollala, V, Upadhya & Nayak 2011; Vollala, VR, Upadhya & Nayak 2010). In this context, one established approach to finding a drug to treat Alzheimer’s disease is based on identifying a small molecule that will pass through the blood brain barrier and chelate with various transition metals such as Cu^{2+} , Zn^{2+} , and Fe^{3+} . These metals are known to bind to and consolidate the associated amyloid plaque in the brain of AD victims. The theory is (Atwood et al. 2000; Barnham & Bush 2008; Bin et al. 2013; Bush, Pettingell, Paradis, et al. 1994; Bush, Pettingell, Multhaup, et al. 1994; Hung, Bush & Cherny 2010; Kim, Nevitt & Thiele 2008; Rao et al. 2012; Tōugu et al. 2009; Willcox, Ash & Catignani 2004) that reducing the levels of these metals and stripping them away from the plaque will cause it either not to aggregate and/or to disaggregate and/or disperse with a concomitant reduction in disease symptoms and progression. Thus, from an examination of the known molecular composition of Brahmi tea, a small molecule candidate that is capable of passing through the blood barrier and forming complexes with various transition metals has been identified in this thesis as a deglycosylated moiety of a previously identified (glycosylated) Bacoside or Bacosaponins (Deepak et al. 2005; Majumdar et al. 2013; Murthy et al. 2006; Russo & Borrelli 2005), Figure 3.3. More specifically, this molecule is identified as Jujubogenin (together with its isomer Pseudojujubogenin). The molecular structures of these two molecules are shown in Figure 3.4. Consequently, using ESI-MS we have been able to identify both the Jujubogenin and/or Pseudojujubogenin molecules in the Brahmi tea extract as well as the copper complex of Jujubogenin (in a Cu-spiked tea extract). Computational chemistry investigations have confirmed the feasibility and structure of the copper complex and have allowed us to distinguish between the isomers. The computational studies also explain why the Cu complex is formed preferentially to the

Zn complex. Therefore, Jujubogenin, Figure 3.4, has been identified as a possible drug lead for the treatment of AD. Notably, to date, the total synthesis of this molecule has not yet been reported. A schematic of this specific strategy is given in **Scheme 2**.

Scheme 2 – Specific strategy



3.2 Traditional Ayurvedic medicine – Brahmi (*Bacopa monnieri*)

Bacopa monnieri(BM), an Ayurvedic medicinal herb (known as Brahmi), is from the family Scrophulariaceae and is reputed for its memory enhancing ability and improvement of brain function (Majumdar et al. 2013; Mathew & Subramanian 2014; Ramasamy et al. 2015; Roodenrys et al. 2002; Saini, Singh & Sandhir 2012; Stough et al. 2001; Tripathi et al. 1996; Uabundit et al. 2010; Vollala, V, Upadhy & Nayak 2011; Vollala, VR, Upadhy & Nayak 2010). In Ayurveda, Brahmi is primarily known as a “brain tonic” for lifting mood, clarity and memory. Indeed, Brahmi has been used in Ayurveda for thousands of years as a memory enhancer, sedative, anti-inflammatory, antipyretic, analgesic, and for treating stress-related mood swings (Mathew & Subramanian 2014; Murthy et al. 2006; Ramasamy et al. 2015; Russo & Borrelli 2005; Saini, Singh & Sandhir 2012; Stough et al. 2001; Thomas et al. 2013). It is also used for the treatment of Parkinson’s disease and epilepsy (Mathew & Subramanian 2014; Tripathi et al. 1996). It has been proposed that BM can be used as an adjuvant for neurodegenerative disorders involving oxidative stress (Shinomol, Mythri & Bharath 2012).

The major chemical components found in Brahmi are referred to as “saponins” (Bhandari et al. 2009; Deepak et al. 2005; Ganzera et al. 2004; Kalachaveedu et al. 2016; Murthy et al. 2006; Rastogi, Pal & Kulshreshtha 1994). Saponins (that are glycosides) are compounds found in plants which form a lather with water (hence the name) and upon hydrolysis yield sugar moieties (e.g. glucose, galactose etc.) and an aglycone moiety. The aglycone moiety may be a flavonoid, triterpene or another natural product. It was reported that, in Brahmi, the major chemical constituents of the saponins, namely; bacosides A1- A3, bacopasaponins A – G and bacopasides I-VIII, are responsible for memory enhancing activity both in humans and animals (Devendra et al. 2018). Specifically, in Brahmi, the aglycone moiety is the steroid molecule Jujubogenin or its isomer Pseudojujubogenin, Figures 3.3 and 3.4.

The detailed chemical composition of Brahmi has been investigated (Zehl et al. 2007) and the observed memory-enhancing effects of BM are proposed to be due to the presence of saponin glycosides (Kumar, Navneet et al. 2016). Depending on the positions of the side chains attached to the aglycones, saponin glycosides in BM may

exist as the steroids jujubogenin and psuedojujubogenin glycosides, Figure 3.4. In fact, there are more than 30 saponin glycosides that have been reported which differ only in the glycosides that are attached to the aglycone (Dowell, Davidson & Ghosh 2015).



Figure 3.1 *Bacopa monnieri* (Brahmi)

3.3 Drug leads for the treatment and prevention of Alzheimer's disease (AD).

Alzheimer's is a degenerative and a fatal brain disease, in which cell to cell connections in the brain are lost. Most of the drugs on the market for AD are purely symptomatic, with little or no effect on the disease progression. For example, at present the commonly used, approved drugs on the market for AD are galantamine, rivastigmine and donepezil (plant derived alkaloids) are purely symptomatic (Mathew & Subramanian 2014).

The difficulty of certain potential drugs to cross the BBB has constrained their efficacy as anti-Alzheimer's drugs. Beta Amyloid ($A\beta$) protein accumulation in the brain is considered to be the primary reason for this disease. Thus prevention of $A\beta$ accumulation is considered essential for an effective therapeutic intervention for AD. Prior research has found that Cu^{2+} , Zn^{2+} and Fe^{3+} are enriched in $A\beta$ deposits in AD patients (Bartzokis et al. 1994) and that such deposits may be dissolved *in vitro* by

selective metal chelators. For example, clioquinol (CQ) was found to be an effective metal chelator, (Hardy & Selkoe 2002; Kumar, N & Knopman 2005) in releasing A β from the post-mortem brain specimens of AD patients (Gouras & Beal 2001). Chemical constituents, from certain plant-extracts can act as naturally occurring metal chelators and may act to diminish the aggregation of A β by dissolving A β deposits in brain – provided they can cross the BBB. Current treatments for AD only delay the onset of AD or dismissing symptom rather than targeting the root cause.

Several studies demonstrate that BM improves cognitive function, and enhances memory in humans and animals (Jyoti & Sharma 2006; Roodenrys et al. 2002; Stough et al. 2001; Vollala, V, Upadhyaya & Nayak 2011; Vollala, VR, Upadhyaya & Nayak 2010). These research studies indicate that BM could contain an effective drug lead(s) which could inhibit the production of A β and thus enhance the memory *in vivo*. Such a molecule(s) would be valuable for the understanding of A β toxicity in AD and it would be useful to know about the metal ion chelating properties of a bioactive, memory enhancing drug candidate at the molecular level and thus how it could affect the aggregation of A β in the brain, potentially to treat or even cure AD.

3.4 Prior research studies of *Bacopa monnieri* (BM)

Prior research studies of the effect of BM extracts have shown that there is reputable experimental evidence for improved neurological performance in both humans and animals (Jyoti & Sharma 2006; Roodenrys et al. 2002; Stough et al. 2001; Vollala, V, Upadhyaya & Nayak 2011; Vollala, VR, Upadhyaya & Nayak 2010). Thus the neuro-protective potential of BM extract in rats with colchicines-induced dementia has been demonstrated (Calabrese et al. 2008; Saini, Singh & Sandhir 2012; Uabundit et al. 2010). Bhattacharya et.al in 2000 studied the antioxidant effects of Brahmi in the hippocampus and other work supported the human memory enhancing ability of BM extract (Roodenrys et al. 2002). Natural products have been previously been used for the treatment of AD. For example, alkaloids such as galantamine and rivastigmine (a synthetic derivative of physostigmine) were approved by the FDA for the treatment of AD (Ng, Or & Ip 2015). It has been reported that the extracts of BM improve cognitive effects in animals (Uabundit et al. 2010; Vollala, V, Upadhyaya & Nayak 2011; Vollala, VR, Upadhyaya & Nayak 2010). Furthermore, the anti-stress effects of BM plant material

has been reported in a study of adult male Sprague Dawley rats by directing oral doses of 20-40 mg/kg (Chowdhuri et al. 2002). In addition, Singh et al. in 1998 studied the “nerve tonic activity” of BM extract in rats and found that bacosides A and B were effective (Singh et al. 1988).

Seetha Ramasamy et al. in 2015 reported that the aglycones (Jujubogenin and Pseudojujubogenin) and their derivatives (ebelin lactone and bacogenin A1) exhibited good BBB diffusion (Ramasamy et al. 2015). Furthermore, it was reported that the aglycones (Jujubogenin and Pseudojujubogenin) exhibited good CNS drug properties with elevated lipophilicity and good BBB penetration compared to their parent bacosides (Ramasamy et al. 2015).

Nevertheless, the mechanism of action of potential small molecules that may be responsible for memory enhancement has not been studied to date. Within this thesis we are proposing that we have identified a small molecule candidate in BM extract, namely Jujubogenin, that can pass through the blood brain barrier (BBB) and that can demonstrably chelate Cu^{2+} , Zn^{2+} , or Fe^{3+}) and thus potentially inhibits or reverse $\text{A}\beta$ production *in vivo*.

3.5 Role of metal ions in Alzheimer’s disease (AD)

Though metals like Cu, Fe and Zn are essential elements in cell metabolism, increased levels of these metals have been found in the brains of patients who were suffering neurodegenerative diseases (Cuajungco et al. 2000; Mounsey & Teismann 2012). Evidence from prior research specifies, the unusual elevation of Cu^{2+} (Cuajungco et al. 2000) and Zn^{2+} (Bush, Pettingell, Multhaup, et al. 1994) leads to major $\text{A}\beta$ toxicity *in vivo*. Furthermore, these metals play a key role in the demise of neurons resulted by oxidative stress (OS). Alzheimer’s disease (AD) is a degenerative and fatal brain disease, in which cell to cell connections in the brain are lost. It has been reported that Beta amyloid ($\text{A}\beta$) protein accumulation or $\text{A}\beta$ plaques and neurofibrillary tangles in the brain are responsible for this disease (Shankar et al. 2008). Prevention/elimination of $\text{A}\beta$ accumulation is considered to be an essential method for effective treatment of (AD). Metal ions like Cu^{2+} , Zn^{2+} and Fe^{3+} were enriched in such $\text{A}\beta$ deposits (Cuajungco et al. 2000) of AD patients. In the absence of sufficient antioxidants, these

metal ions acts as a catalyst for the production and aggregation of A β protein. In addition, the reduction of Cu²⁺, Zn²⁺ and Fe³⁺, will leads to the production of toxic reactive oxygen species (ROS) that is accountable for the pathogenesis of Alzheimer's disease (Huang et al. 1999) or the interaction of these redox, active metal ions are responsible for oxidative stress in AD (Cuajungco et al. 2000), Figure 3.2. The role of Cu (Yoshiike et al.) against AD was studied and revealed that (Yoshiike et al.) Cu - curcumin complexes were effective than curcumin in scavenging free radicals (Shen, Zhang & Ji 2005) and thus inhibiting A β accumulation (Chandra et al. 1998; Lim, GP et al. 2001). Furthermore, a theoretical study on (Yoshiike et al.) Cu - curcumin complexes reported the metal chelating ability of Cu ion by redox mechanism and thus explained its ROS scavenging activity with DFT (Shen, Zhang & Ji 2005).

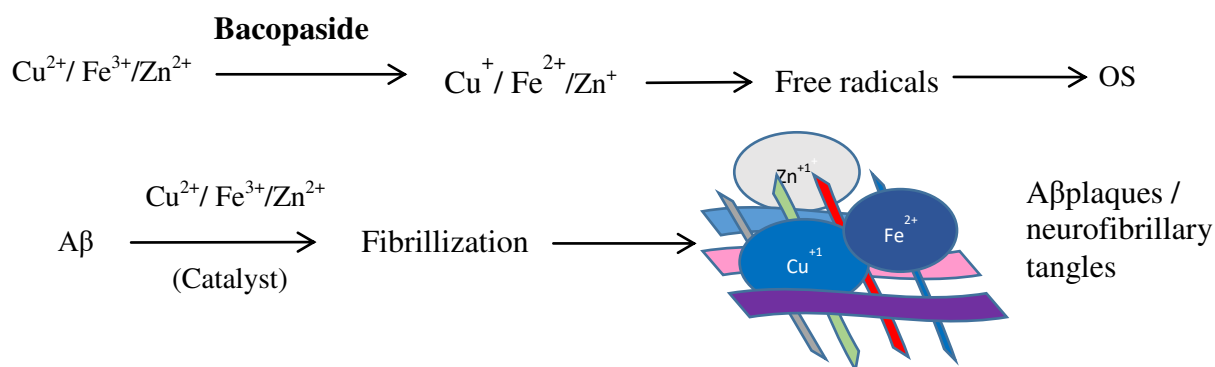


Figure 3.3 Schematic representation of A β mediated free radical generation and the peptide when it binds in the presents of catalytic amounts of Cu²⁺/ Fe³⁺/Zn²⁺ ions.

3.5.1 Cu in biological systems

Studying the role of copper in biological systems is of great importance as it is an essential element for most living systems and it acts as a catalytic cofactor in many biological pathways (Da Silva & Williams 2001). Cu plays a crucial role in oxygen transport and cellular metabolism and a deficiency (or excess) of this metal can lead to neurodegenerative disorders (Kim, Nevitt & Thiele 2008).

3.5.2 Zn in biological systems

Zinc is the second ample transition metal in the human body and it is an essential element for living organisms (Lim, NC, Freake & Brückner 2005). Zinc act as a

structural cofactor in metalloproteinase. Interestingly, the concentration of zinc is large in nerve tissues and the disorder of this metal is one of the reason for several neurological diseases like Parkinson's disease, Alzheimer's disease and epilepsy.

3.5.3 Fe in biological systems

Iron is an essential element for living systems. It has a vital role in biological systems and acts as a catalyst for the formation of reactive hydroxyl radical from hydrogen peroxide (Fenton reaction). Thus, subsequently favours chain reaction of lipid peroxidation (Benedet & Shibamoto 2008). Traces of this metal in biological systems, are high enough to catalyse free radical reactions (Chevion 1988).

3.6 Metal chelators as potential drugs

Previous research indicates that aggregates of A β that bind various metal ions can be "dissolved" by treatment with selective metal chelators that can be delivered to the brain. For example, clioquinol is a good Cu²⁺ and Zn²⁺ chelator that may be shown to reduce A β deposition *in vivo* (Cherny et al. 1999; Gouras & Beal 2001; Hardy & Selkoe 2002). Such potential metal chelators are required to pass through the BBB and to effectively compete for the metal ions that are bound, or which may bind, to A β in the brain. Thus, they may selectively scavenge Cu²⁺, Zn²⁺ and Fe³⁺ ions in the brain to form water soluble nontoxic products that can then be eliminated from the body. In this regards, clinical trials of A β encumbered APP transgenic mice with clioquinol was found to lower A β deposition *in vivo* and this was attributed to the fact that clioquinol may pass through the BBB and is a good chelator of Cu²⁺, Zn²⁺ (Gouras & Beal 2001; Hardy & Selkoe 2002).

As part of the specific strategy, the author of this thesis have searched for such potential metal chelators in BM extract which have the ability to pass through the BBB. Such molecules need to be below a certain size and displays an appropriate log₁₀P value. The memory enhancing ability of BM that has been studied extensively in animal models, suggests that it contains one or more active molecules with the capability of passing through the BBB and this suggests that BM extract could contain one or more promising drug candidates for the treatment of AD. Indeed, using fluorescence imaging,

it has been shown that BM extract can prevent A β aggregation in the brain and to dissociate pre-formed fibrils *in vitro* (Mathew & Subramanian 2012).

The main de-glycosylated constituents of BM are the Jujubogenin and Psuedojujubogenin molecules (Zehl et al. 2007). We have assessed their ability to complex copper, zinc or iron using molecular modelling. One de-glycosylated moiety in particular was found to be a potential candidate that was able considered capable of passing through the BBB and to strongly complex Cu²⁺, Zn²⁺ and Fe³⁺. Interestingly, this molecule is a steroid that also closely resembles a molecule that has recently been found to dissolve protein aggregates that are associated with cataracts (Zhao et al. 2015) and this could represent an alternative or synergistic mechanism for anti-plaque activity, Figure 3.5. These computational studies have been complemented by experimental studies whereby evidence of Cu²⁺, Zn²⁺ or Fe³⁺ chelation has been sought via chemical analyses of BM extracts. In this regard the Cu²⁺ complex of Jujubogenin has been definitively identified via ESI-MS and MS/MS in BM extract. Thus we have established that Jujubogenin is an excellent candidate for passing through the BB barrier and complexing with copper in the brain.

Several pathological effects of BM extract were reported such as memory enhancing, anti-lipid per oxidative (Tripathi et al. 1996), revitalization of sensory organs (Garai et al. 1996) antioxidant (Bhattacharya et al. 2000), superoxide inhibition, analgesic etc. whereas its potential role as a metal chelator has not been reported to date. Our work is novel in this regard.

3.7 Structures of some saponins and bacosides of BM from chemical analysis

Chemical analysis of BM extracts has established the presence of various Bacosides and Bacosaponins, Figure 3.3. Bacosides are dammarane type triterpenoid saponnins (Bhandari et al. 2009; Rastogi, Pal & Kulshreshtha 1994). The main constituents of these are the glycosylated moieties of Jujubogenin (Bacoside A, Bacopasaponin C, Bacopaside I and Bacopaside V) and Psuedojujubogenin (Bacosaponin B and Bacopaside N2).

One de-glycosylated moiety of these structures in particular (Jujubogenin) was found to be a potential drug candidate that is capable of passing through the BBB. The metal chelation capability of this potential drug candidate was studied in this thesis, both computationally and experimentally.

3.8 Jujubogenin as a drug candidate

This research works highlights, one of the identified, de-glycosylated and potentially bioactive small molecule(s) can pass through the blood brain barrier (BBB) and chelate with the free metal ions (Cu^{2+} , Zn^{2+} , and Fe^{3+}) *in vivo*. Thus, Jujubogenin may be confidently suggested as a molecule that may pass through the BBB and complex with Cu^{2+} in the brain. Structural similarities to the compound Lanosterol have also been noted.

3.8.1 The isomers Jujubogenin and Pseudojujubogenin

Figure 3.4 shows the molecular structures of the naturally occurring steroids Jujubogenin (1) and its isomer Pseudojujubogenin (2), both of which could be present in the BM extract as a result of the deglycosylation of the constituent Bacosides or Bacosaponins, Figure 3.3. It should be noted that (1) and/or (2) might be independently present in the BM extract in the deglycosylated form, although this has not yet been reported in the literature⁶.

⁶Note that the ESI/MS studies reported in this thesis have identified the presence of one or both of these isomers in the BM extract. However, it is not possible to determine from this data whether only one or both are present, since they both have the same signal. However, the computational chemistry studies reported herein have established that the detected copper complex is likely to be with Jujubogenin only, from a consideration of the likely kinetics of reaction.

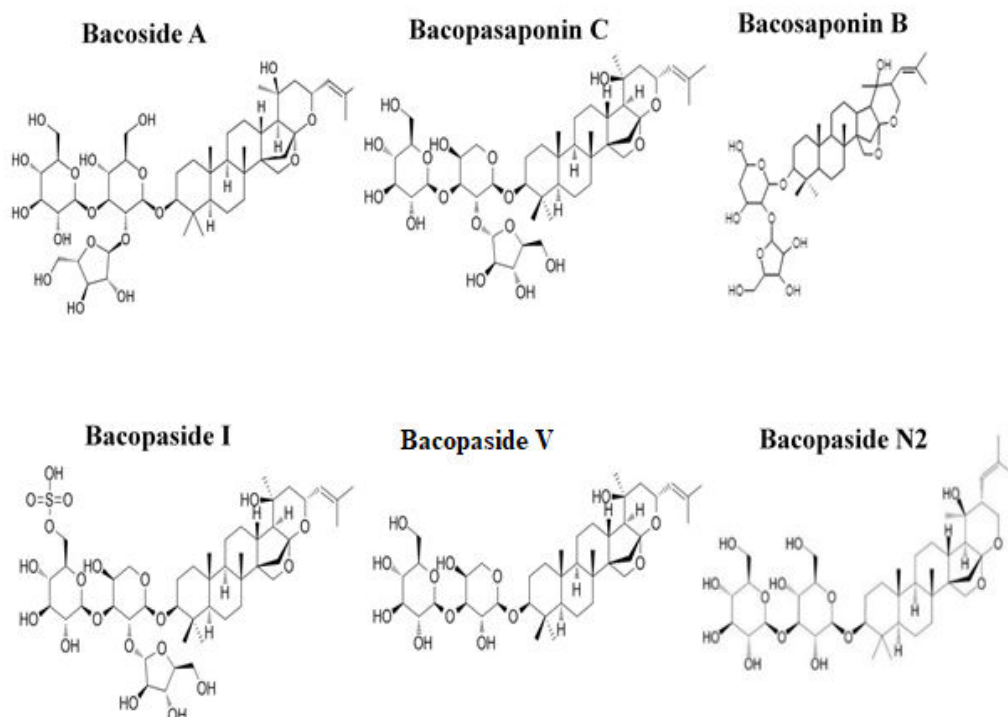


Figure 3.3 Structures of some Bacosaponins and Bacosides of BM.

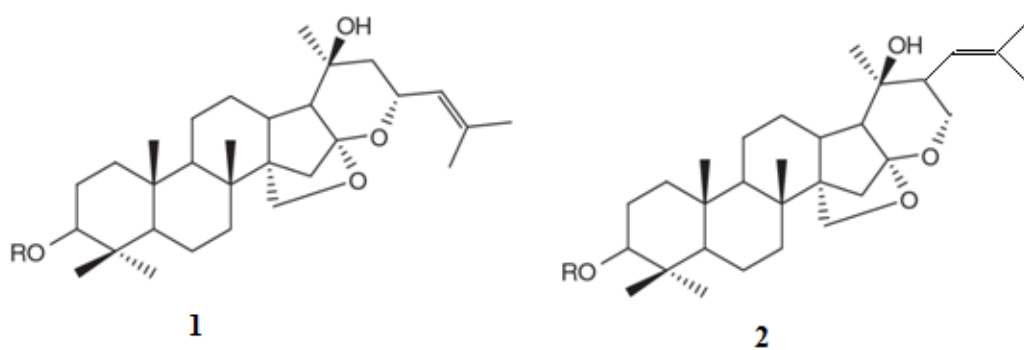


Figure 3.4 The molecular structures of the isomers (1) Jujubogenin and (2) Pseudojujubogenin.

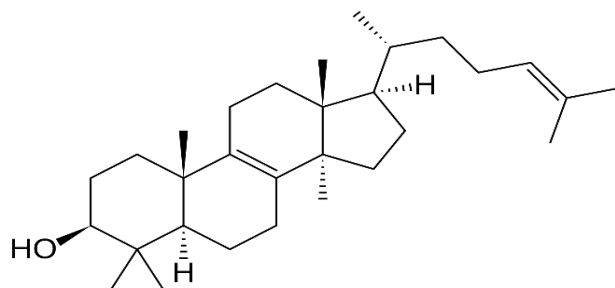


Figure 3.5 The molecular structure of Lanosterol.

3.9 Computational analysis of potential Cu^{2+} and Zn^{2+} complexes of Jujubogenin and Psuedojujubogenin, as bidentate ligands

3.9.1 Preamble

Based on the hypothesis that metal chelating compounds, that can pass through the BBB and sequester metals such as Cu^{2+} and Zn^{2+} from amyloid plaque⁷, could be potential drugs for the treatment of AD (Atwood et al. 2000; Bush, Pettingell, Paradis, et al. 1994; Bush, Pettingell, Multhaup, et al. 1994), two de-glycosylated moieties (aglycones) from the bacoside molecules identified in BM extract (Nuengchamnong, Sookying & Ingkaninan 2016; Ramasamy et al. 2015) have been postulated in this thesis as small molecule candidates for passage through the BBB *and* as potential bidentate coordinators of Cu^{2+} or Zn^{2+} . These candidate molecules are Jujubogenin (JJ) and its isomer Psuedojujubogenin (PJJ), the structures of which are shown in Figure 3.4 and, in more detail, in Figure 3.5. These molecules were subsequently modelled (utilizing semi-empirical quantum chemical and density functional computations) in order to establish their equilibrium geometries and with respect to their potential coordinating abilities towards Cu^{2+} and Zn^{2+} . Various other characteristics of these molecules and their complexes were computed including relevant bond lengths and angles, relative energies and various other properties such as Log_{10}P , PSA, electrostatic potential energies, dipole moments and intramolecular hydrogen bonding.

⁷ Fe^{3+} was also considered since this has also been implicated in a number of neurological conditions. This will be discussed later.

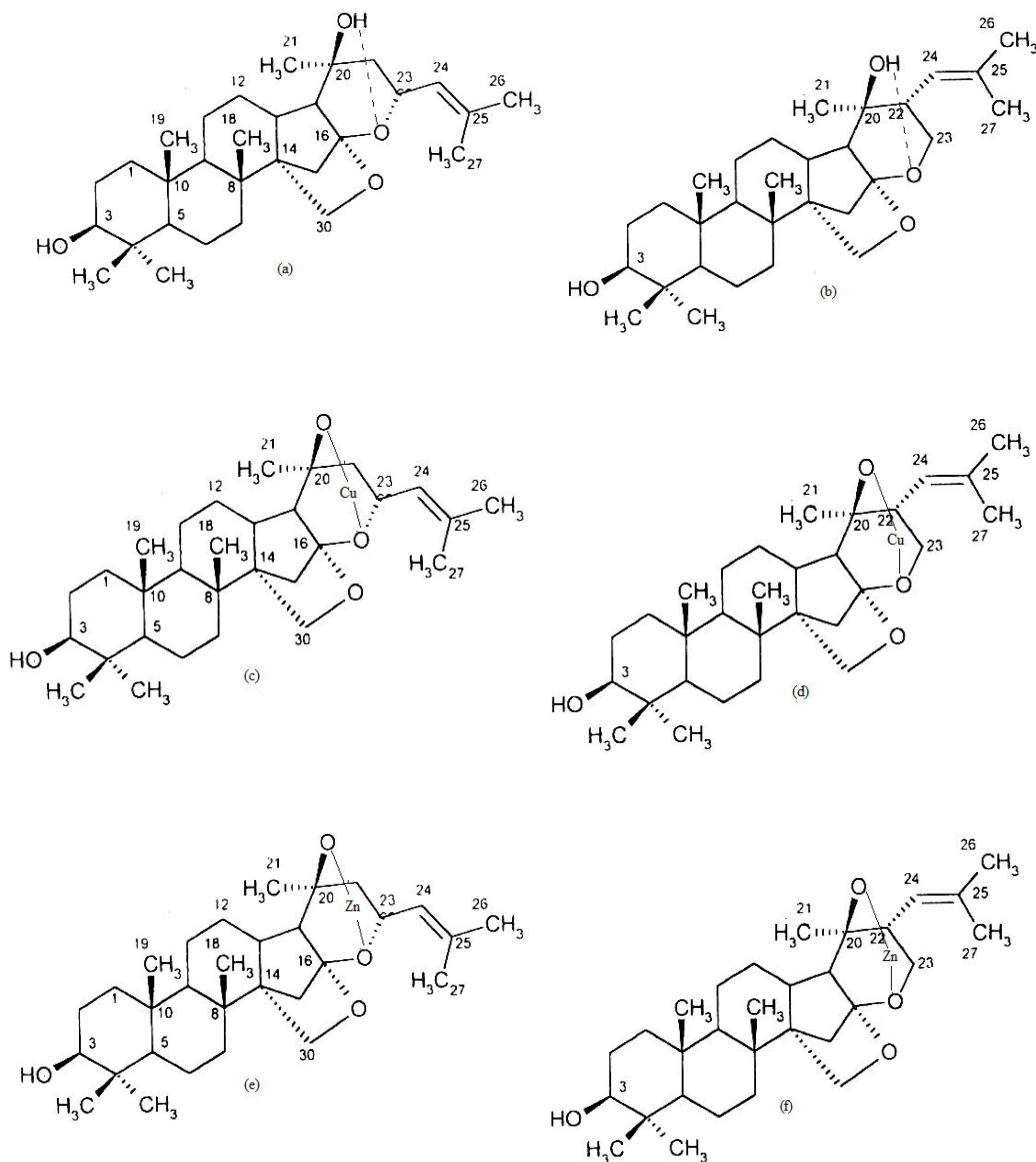


Figure 3.6 Schematic representations of (a) Jujubogenin; (b) Pseudojujubogenin; (c) Cu^{2+} - Jujubogenin complex; (d) Cu^{2+} -Pseudojujubogenin complex; (e) Zn^{2+} -Jujubogenin complex and (f) Zn^{2+} -Pseudojujubogenin complex. Also shown are the atom numbering schemes (Ramasamy et al. 2015), the IMHBs and favoured bidentate metal co-ordination sites (note that the metals are also assumed to be coordinated to two water molecules but these have been omitted for clarity). The relevant bond lengths and computed energies of the IMHB are given in Table 3.1.

3.9.2 Computational method

JJ and PJJ and their Cu^{2+} and Zn^{2+} complexes were modelled using semi-empirical quantum chemical calculations (PM3) and density functional theory (DFT), ((Tugcu et al. 2012) utilizing Spartan '06 and '16 software (wave function, Inc. 18401 Von

Karman Avenue, suite 370, Irvine, CA 92612 USA). The JJ and PJJ ligands themselves refined successfully according to the B3LYP/6-31G*/PM3 method (equilibrium geometry) with acceptable bond lengths and angles and also revealed a significant intramolecular hydrogen bond that is present in both JJ and PJJ, Table 3.1. Feasible bidentate structures for both Cu^{2+} and Zn^{2+} , involving bidentate co-ordination via the O atoms, as indicated in Figure 3.6 (c, d, e, and f), were built and also refined according to the B3LYP/6-31G*/PM3 method (equilibrium geometry). It was found that the favourable coordination geometries were four (square planar) and four (tetrahedral) for Cu^{2+} and Zn^{2+} , respectively. The bond lengths and angles associated with the Cu and Zn coordination geometries are given in Table 3.2, and are consistent with the values reported in the literature from X-ray analyses (Sletten & Fløgstad 1976; Sletten & Thorstensen 1974). Higher coordination geometries could not be accommodated in the modelling due to steric interactions and such refinements were not successful. It is noted that both square planar Cu^{2+} (d^9) is a doublet, and tetrahedral Zn^{2+} (d^{10}) is a singlet, for *both* high spin and low spin - a fortunate coincidence that removes the necessity of a close examination of the crystal field(s) and/or excessive computations. The relevant splitting patterns are shown in Figure 3.7, (An introduction to transition-metal chemistry ligand- field theory, Leslie. E. Orgel).

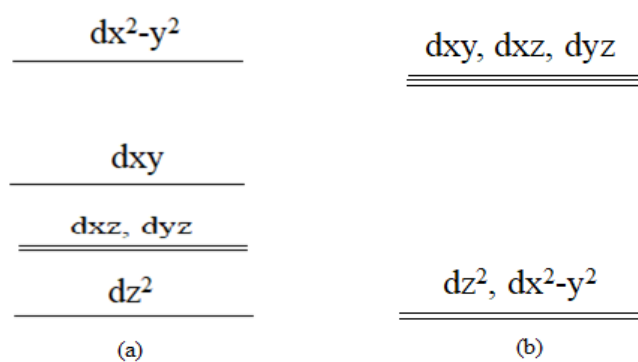


Figure 3.7 Representations of energy level schemes for (a) square planar coordination splitting pattern and (b) tetrahedral coordination splitting pattern.

Our attempts to form Fe^{3+} complexes with a variety of coordination geometries were unsuccessful and it is assumed that these ligands cannot accommodate this metal.

3.9.3 MW, Log₁₀P and BBB penetration

For BBB penetration there is a restriction on the size of the molecule in terms of its MW. This is considered to be less than approximately 500 Da (Caron, Vallaro & Ermondi 2018). The lipophilicity of a molecule indicates the affinity of a drug(s) towards a lipophilic environment and is represented by the water/octanol partition coefficient P. This is measured experimentally by evaluating the ratio of the concentration of a solute in octanol and its concentration in water, at equilibrium. This value may also be determined computationally, as has been done in this thesis. Log₁₀P has a vital role in determining the efficacy of a drug(s) and its optimization. Depending on the structural properties of a drug, the preferred range for Log₁₀P for effective BBB permeability is from 1 to 6 (Caron, Vallaro & Ermondi 2018). The computed Log₁₀P values for the JJ and PJJ molecules are given in Table 3.2 and these values indicate that JJ and PJJ are acceptable candidates for molecules that can permeate the BBB.

3.9.4 Intra molecular hydrogen bonding (IMHB)

Intra molecular hydrogen bonding involves the non covalent bonding between a hydrogen bond donor (HBD) (O-H, N-H etc.) and an adjacent electronegative hydrogen bond acceptor atom (HBA) with both HBD and HBA belonging to the same molecule (Caron, Kihlberg & Ermondi 2019). It is relevant in the biological activity of molecules and in drug design as it can influence the absorptivity, solubility and potency of drug(s) (Caron, Kihlberg & Ermondi 2019; Caron, Vallaro & Ermondi 2018). The IMHBs in JJ and PJJ are depicted in Figures 3.9 and 3.10 and span the postulated bi-dentate binding sites. The computed bond lengths and angles for the IMHBs in JJ and PJJ and their computed bond strengths are given in Table 3.1. These values indicate that they are quite strong (Caron, Kihlberg & Ermondi 2019), with the IMHB of PJJ being considerably stronger than that of JJ. For example, IMHB can be crucial in drug design as it may lead to “polarity masking” (Caron, Vallaro & Ermondi 2018) and thus influence membrane permeability, solubility/bioavailability and, when relevant, a molecule’s antioxidant potency (Caron, Kihlberg & Ermondi 2019). This is especially significant when the IMHB involves phenolic moieties, as in Part A of thesis. More specifically, IMHB may directly impact the Log₁₀P value, whereby this parameter may be effectively lowered by polarity masking (Caron, Vallaro & Ermondi 2018). This may result in an

enhancement of blood brain barrier (BBB) passage. The presence of a strong IMHB across the bidentate binding site in JJ and PJJ would not only be likely to enhance its BBB penetrating capability due to polarity masking, but could also mitigate against the excessive coordination of metals prior to the ligand crossing the BBB. This would be expected to be more pronounced for PJJ where this IMHB is considerably stronger. On this regard, the $\text{Log}_{10}P$ value for PJJ is actually lower than that for JJ. It may well be that the presence of an IMHB across a metal coordination site might help to optimize the passage of a free ligand through the BBB by providing some level of metal coordination mitigation prior to passage. In this regard, it is interesting to note that an IMHB across the bidentate coordination site also exists for CQ and related molecules, Figure.3.8, that are prime candidates for therapeutics of this kind.

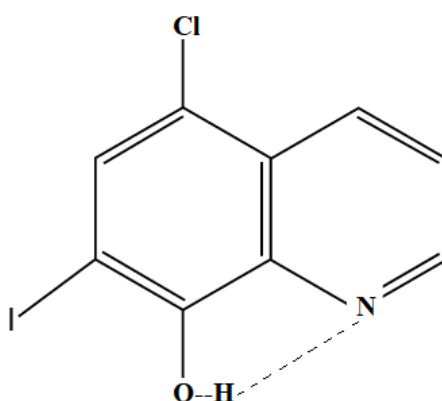


Figure 3.8 Schematic representation of IMHB across the bidentate coordination site in CQ.

3.9.5 Polar surface area (PSA)

Polar surface area (PSA) is the total surface area that is allied to polar atoms. Calculation of the PSA has an important role in drug design as it gives an indication of the molecule's bioavailability. Furthermore, it was reported that, increased PSA values of a drug candidate/molecule decreases its BBB permeability (Ertl, Rohde & Selzer 2000).

Computed values of PSA of Jujubogenin, pseudojujubogenin, and its Cu^{2+} and Zn^{2+} complexes are shown in Table.3.2. Indicates that it is favourable for feasible BBB permeability.

3.10 Computed structures of JJ, PJJ and their Cu^{2+} and Zn^{2+} complexes

3.10.1 The refined JJ and PJJ structures

The refined structures for the JJ and PJJ molecules are shown in Figures 3.9 and 3.10. All bond lengths and angles within these molecules are as expected. Note that there is a strong intra molecular hydrogen bond across the potential coordination site, as indicated by the dotted line. The distances, angles and energies associated with these IMHBs are given in Table 3.1. The potential role of this IMHB will be discussed later (also re HQ/CQ). From an examination of the JJ and PJJ structures shown in Figures 3.9 and 3.10, a potential bidentate metal coordination site was identified for both molecules. Namely, the two oxygen atoms that are involved in the aforementioned IMHB.

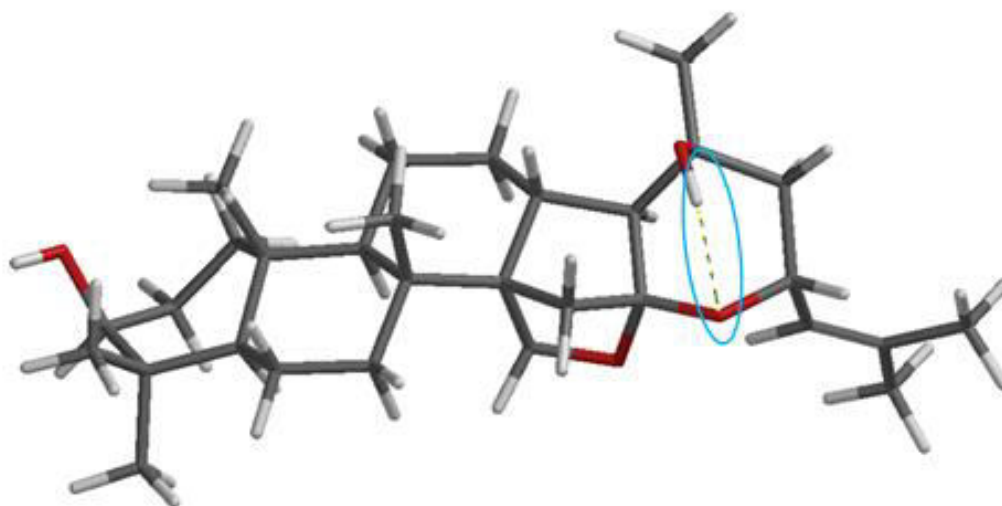


Figure 3.9 Jujubogenin with intramolecular hydrogen bonding (dotted line). Red indicates oxygen, white hydrogen and grey carbon. Note that a potential bidentate metal coordination site can be identified as involving the two oxygen atoms of the IMHB.

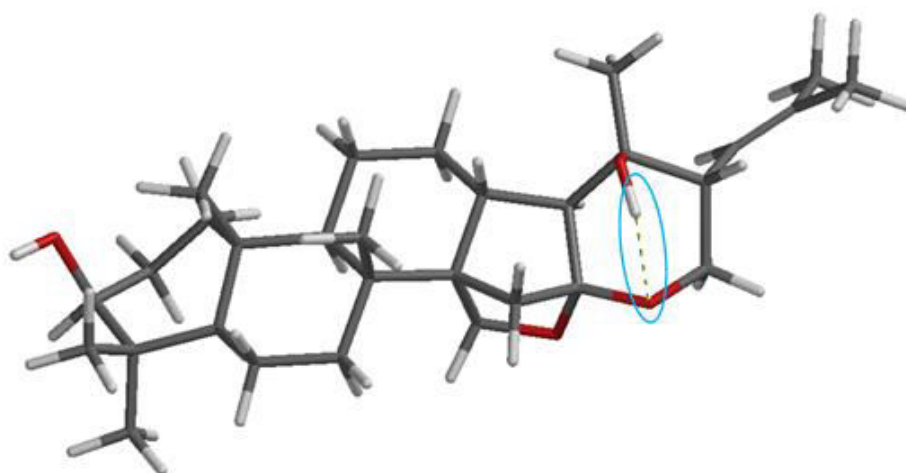


Figure 3.10 Pseudojujubogenin with intra molecular hydrogen bonding (dotted line). Red indicates oxygen, white hydrogen and grey carbon. Note that a potential bidentate metal coordination site can be identified as involving the two oxygen atoms of the IMHB.

Table 3.1 Intra molecular hydrogen bonding characteristics in JJ and PJJ, compared to CQ.

Bond lengths	JJ	PJJ	CQ	References (typical ranges for IMHB)
O(O) - - - - O(N)	2.892 Å	2.858 Å	2.654 Å	-
O-H - - - - O	2.207 Å	2.164 Å	2.037 Å	2.30 – 2.35 Å (Caron, Kihlberg & Ermondi 2019)
Bond angles	JJ	PJJ		
O – H - - - - O	126.48°	127.09°	118.68°	70 - 180° (Caron, Kihlberg & Ermondi 2019)
H – bond energy ⁸ kcal/mol	2.903	3.346	6.712	

⁸ For JJ and PJJ the intramolecular hydrogen bond energies were calculated, via the DFT method B3LYP/6.31G*, by subtracting the energy of the respective JJ and PJJ molecules with H-bonds engaged from the energy of the respective JJ and PJJ molecules with disengaged H-bonds.

3.10.2 The refined Cu^{2+} and Zn^{2+} structures of JJ and PJJ

The refined structures for the diaquo, bidentate, Cu^{2+} complexes of the JJ and PJJ molecules are shown in Figures 3.11 and 3.12, along with the coordination sphere bond angles, these and the corresponding coordination sphere bond lengths are given in Table 3.2. The refined structures for the Zn^{2+} complexes of JJ and PJJ molecules are shown in Figures 3.13 and 3.14 along with the coordination sphere bond angles, these and the corresponding coordination sphere bond lengths are given in Table 3.2.

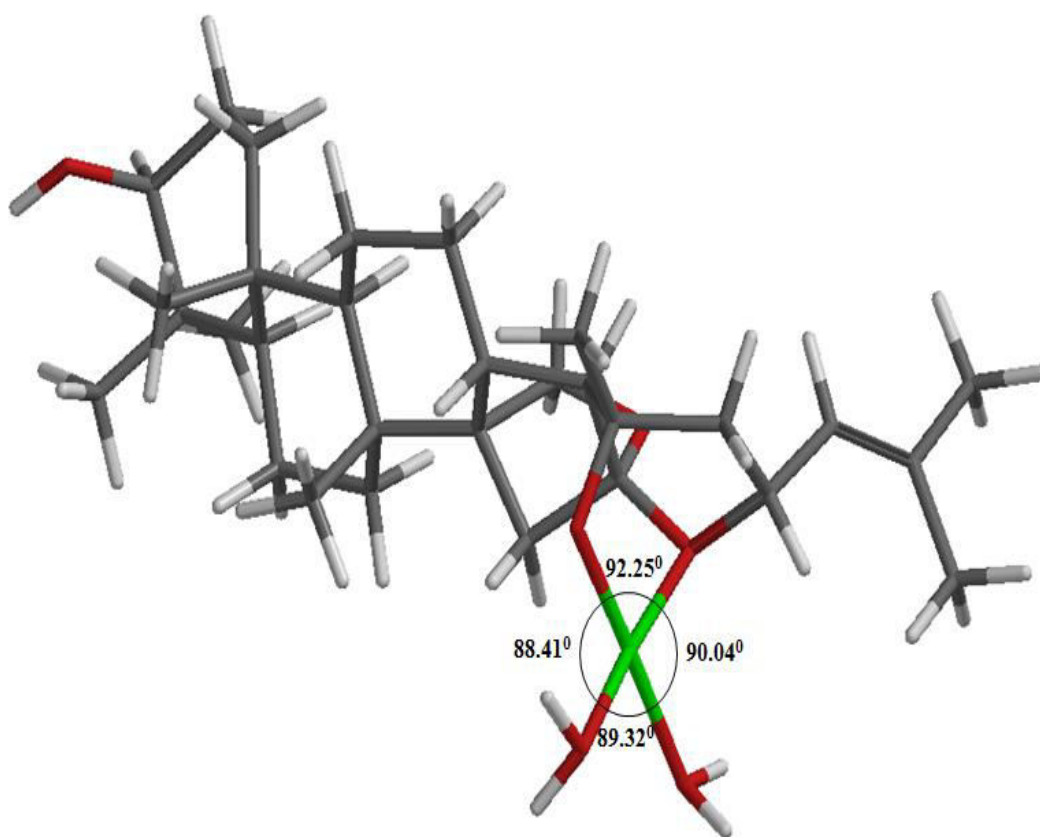


Figure 3.11 Cu^{2+} - JJ square planar complex, showing the bond angles of the square planar coordination sphere, Table 3.2. Red indicates oxygen, white hydrogen and grey carbon.

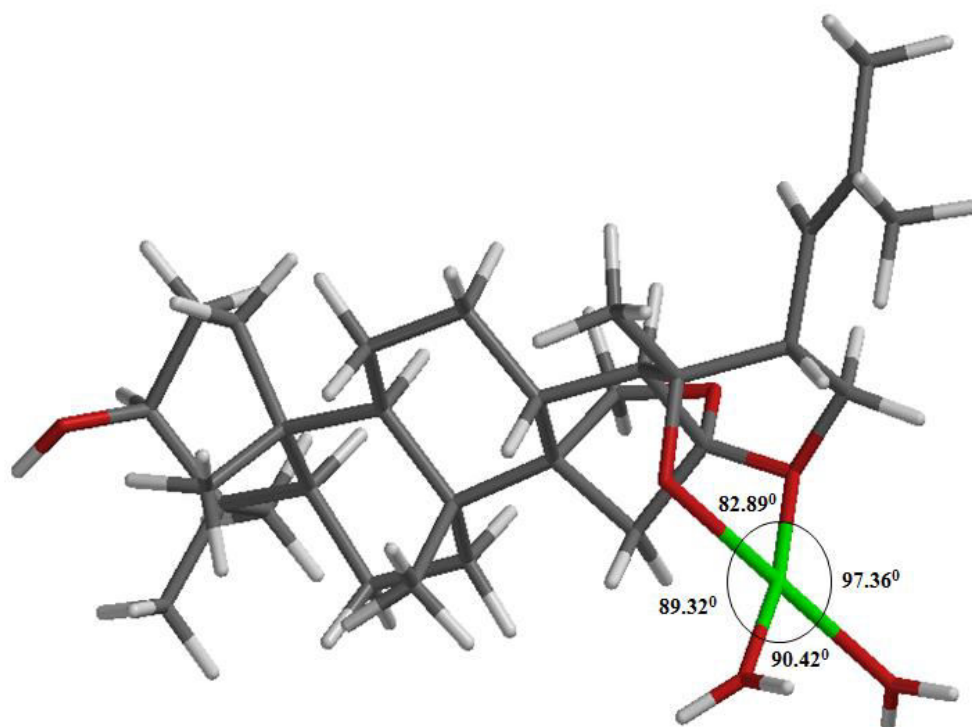


Figure 3.12 Cu^{2+} - PJJ square planar complex, showing the bond angles of the square planar coordination sphere. Red indicates oxygen, white hydrogen and grey carbon.

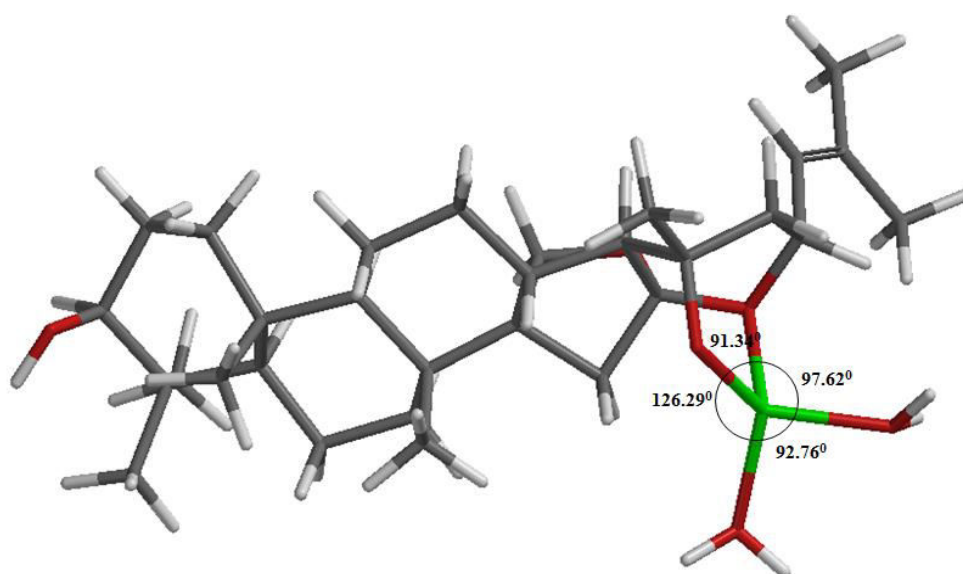


Figure 3.13 Zn^{2+} - JJ tetrahedral complex showing the bond angles of the tetrahedral coordination sphere. Red indicates oxygen, white hydrogen and grey carbon.

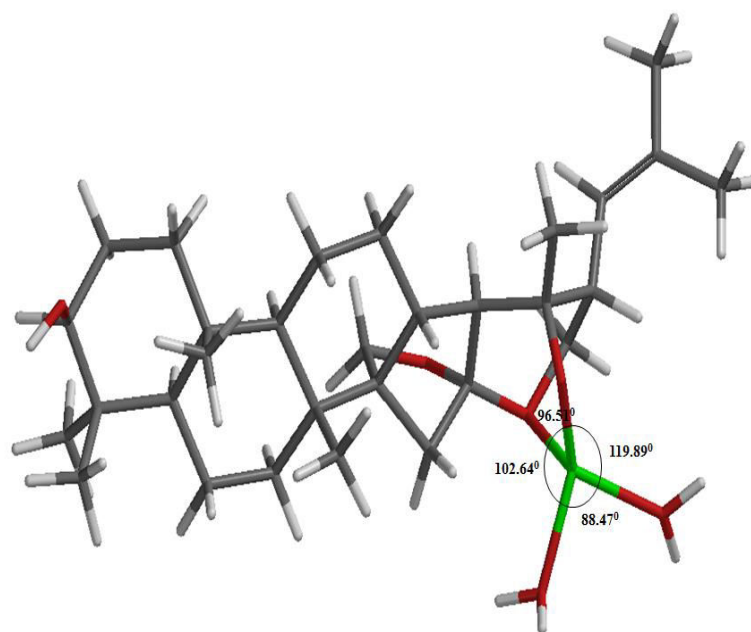


Figure 3.14 Zn^{2+} - PJJ tetrahedral complex showing the bond angles of the tetrahedral coordination sphere. Red indicates oxygen, white hydrogen and grey carbon.

Table 3.2 Computed values of Log_{10}P , PSA, and IMHB of Jujubogenin, Pseudojujubogenin, and its Cu^{2+} and Zn^{2+} complexes.

Compounds	Log_{10}P	MW	PSA (\AA^2)	IMHB
JJ	5.65	472	47.04	1
PJJ	5.53	472	48.14	1
Cu^{2+} - JJ	NA	571	97.35	0
Cu^{2+} - PJJ	NA	571	103.78	0
Zn^{2+} - JJ	NA	572	104.77	0
Zn^{2+} - PJJ	NA	572	106.66	0

Table 3.3 Coordination sphere bond lengths and bond angles for the refined structure of the Cu²⁺ and Zn²⁺ diaquo complexes of JJ and PJJ; (w) = water.

Complexes	M – O bond lengths (Å)	O – M – O bond angles (°)	Literature M – O bond lengths (Å)	Literature O – M – O bond angles(°)	References
Cu²⁺ - JJ Square planar geometry	1.817	92.25	2.001	90.63	(Sletten & Fløgstad 1976; Sletten & Thorstensen 1974)
	2.025	88.41	2.551	87.74	
	1.978 (w)	89.32	2.355	83.25	
	1.992 (w)	90.04	1.995 (w)	96.69	
		269.04 (Cross-over angle)			
Cu²⁺ - PJJ Square planar geometry	1.984	82.89			(Sletten & Fløgstad 1976; Sletten & Thorstensen 1974)
	1.814	89.32			
	1.998 (w)	90.42			
	2.022 (w)	97.36			
Zn²⁺ – JJ Tetrahedral geometry	1.823	91.34	1.953	95.00	(Dudev & Lim 2000; Linder, Baker & Rodgers 2018)
	2.041 (w)	126.29	1.982	125.00	
	2.039 (w)	92.76	2.020 (w)	92.00	
	2.072	97.62	2.049 (w)	96.69	
Zn²⁺ - PJJ Tetrahedral geometry	1.821	96.51	1.960		(Dudev & Lim 2000; Linder, Baker & Rodgers 2018)
	2.051	102.64	1.993		
	2.057 (w)	88.47	2.035		
	2.048 (w)	119.89	2.100		

3.10.3 Discussion of the Cu and Zn complexation with JJ and PJJ

Both Cu^{2+} and Zn^{2+} ions exhibit octahedral geometry in solution and can access a number of lower coordination geometries, (Dudev & Lim 2000; Sletten & Fløgstad 1976; Sletten & Thorstensen 1974). Thus Cu^{2+} octahedral complexes will be in equilibrium with square planar complexes and Zn^{2+} octahedral complexes will be in equilibrium with tetrahedral complexes in solution, Figure 3.15.

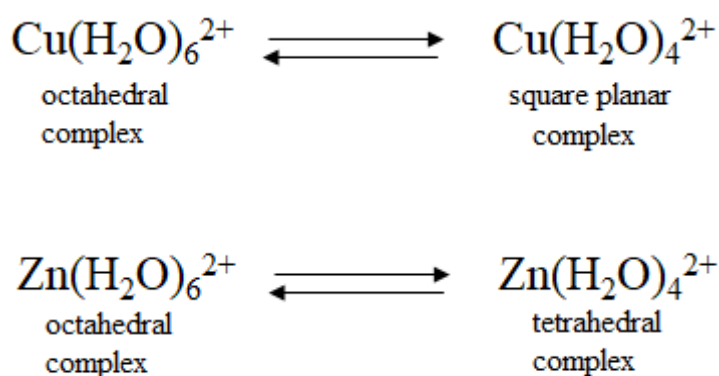


Figure 3.15 Schematic representation of Cu^{2+} octahedral complexes in equilibrium with square planar complexes and Zn^{2+} octahedral complexes in equilibrium with tetrahedral complexes.

Due to the lability of the axial positions in octahedral Cu^{2+} (the Jahn-Teller Effect) (Comba & Zimmer 1994), it is not unreasonable to assume that the hexa-aquo complex can access lower coordination geometries, such as tetra-aquo square planar, with less energy expenditure than octahedral Zn^{2+} .

3.10.4 Strain energy during molecular modelling

Cu^{2+} and Zn^{2+} forms nice complexes with JJ/PJJ that were much more thermodynamically stable than the isolated ligand. Furthermore, it is very apparent that Cu prefers square planar and Zn prefers tetrahedral geometry. Coordination sphere bond lengths and bond angles for the refined structure of the Cu^{2+} and Zn^{2+} diaquo complexes of JJ and PJJ are given in Table 3.3.

Note that Cu^{2+} - JJ is much less strained than the others which suggests that it would be formed faster than any of the other possibilities. The strain energies of Cu^{2+} and Zn^{2+} complexes of Jujubogenin and Pseudojujubogenin during molecular modelling are given in Table 3.4. The strain energy of Cu^{2+} - JJ (1355 kJ/mol) is much less than the strain energy of Zn^{2+} - JJ (1600kJ/mol) indicates that Cu^{2+} - JJ formed preferentially than Zn^{2+} - JJ as the strain energy during molecular modelling is the increase in activation energy involved in the formation of a complex. In addition, Zn^{2+} - JJ bond angle (126.29°) Table 3.3, indicates that it is a distorted tetrahedron than Zn^{2+} - PJJ complex validates the strain energies of Zn^{2+} - JJ and Zn^{2+} - PJJ.

This makes sense since the plane can effectively “slide in” whereas the tetrahedral is potentially more spherical and bulkier. However, also note that the Zn complexes are more thermodynamically stable. However, to conclude, the Cu^{2+} - JJ is formed preferentially since the reaction product is under kinetic control. Thus, “our peak”, when only the Cu is present, is likely to be Cu^{2+} - JJ rather than Cu^{2+} - PJJ, since the Cu^{2+} - JJ is kinetically favoured and is also slightly more thermodynamically stable. If just Zn was present then the Zn^{2+} - PJJ would be favoured kinetically, even though it is less thermodynamically stable. For a mixture of Cu and Zn, the Cu^{2+} - JJ would win out for kinetic reasons.

Table 3.4 Strain energies of Cu^{2+} and Zn^{2+} complexes of Jujubogenin and Pseudojujubogenin during molecular modelling.

Complexes	Strain energy (kJ/mol)	Formation energy (kcal/mol)
Cu^{2+} -JJ	1355	-2049018
Zn^{2+} -JJ	1600	-2136144
Cu^{2+} - PJJ	1472	-2049016
Zn^{2+} - PJJ	1450	-2136130

Having identified a viable ligand system that can complex with Cu and Zn etc. According to our strategy, *vide supra*, we proceeded to search for such species in the BM extract as follows:

3.11 Experimental methods for BM extraction

3.11.1 Materials and reagents

Ethyl acetate, methanol, ethanol, n-butanol, octanol $\text{Cu}(\text{NO}_3)_2 \cdot 3\text{H}_2\text{O}$, $\text{Zn}(\text{NO}_3)_2 \cdot 6\text{H}_2\text{O}$, and $\text{Fe}(\text{NO}_3)_3 \cdot 9\text{H}_2\text{O}$ (were purchased from Sigma Aldrich, Melbourne), Milli-Q water, 0.45 μm disposable membrane filter and syringe filter. All reagents used were analytical grade.

3.11.2 Instrumentation

The instrument used was a Shimadzu LCMS 8045 and the chromatographic experiments were accomplished by using electro spray ionization coupled to mass spectrometer (ESI-MS), which also performs tandem MS, suitable for structural elucidation.

3.11.3 BM extract preparation

3.11.3.1 Different solvents

Systematic extractions were carried out on dried, ground plant material using different solvents including water, methanol, ethanol, n-butanol, ethyl acetate (Meepagala et al. 2013) and octanol and the extract fractions were collected via column chromatography. The collected fractions from each extract were subjected to ESI-MS experiments both in positive and negative ion mode. The fraction from ethyl acetate extraction revealed the presence of Jujubogenin or Pseudojujubogenin after ESI-MS analysis. Peaks consistent with protonated Jujubogenin (or Pseudojujubogenin) and dehydrated Jujubogenin (or dehydrated Pseudojujubogenin) were detected at m/z 473 and m/z 455 respectively, Figure 3.16.

3.11.3.2 Ethyl acetate extraction

Sun-dried plant material of BM (100g), was kept in an oven for 5h at 50 °C and then crushed in a grinder to a fine powder. This was transferred into a conical flask and 500 mL of ethyl acetate was added. The mixture was stirred vigorously for 6h at 45°C. The ethyl acetate extract was filtered (Whatman quantitative filter Paper #1). This process

was repeated 4 to 5 times. The combined extracts were concentrated to dryness at 40°C using a rotary evaporator. A green powder was obtained. This powder (approx. 1 g) was then completely dissolved in 100mL of pure methanol which was used as a stock solution for subsequent column chromatography.

3.11.4 Phytochemical screening of different plant extracts

The following tests were carried out for the phytochemical screening of different plant extracts according to the procedure of (Kumar, A et al. 2009). As with the ethyl acetate extraction, methanol, octanol and water extracts were concentrated to dryness at 40 °C using a rotary evaporator. Thus, obtained powder/crude extract (approx. 1 g) of each was then completely dissolved in 100 mL of pure methanol which was used as a stock solution for phytochemical screening(Kumar, A et al. 2009).

3.11.4.1 Test for triterpenoids

5 mL of each stock solution was added 2 mL of chloroform, 1mL acetic anhydride and 1mL conc. H₂SO₄. A reddish violet colour will indicate the presence of triterpenoids.

3.11.4.2 Test for flavonoids

To 1 mL of each stock solution, a few drops of dilute sodium hydroxide was added. For a positive test an intense yellow coloured solution will be obtained, which then becomes colourless on the addition of a few drops of dilute hydrochloric acid.

3.11.4.3 Test for saponins

1 mL of each stock solution was diluted with 10 mL Milli-Q water and agitated in a graduated cylinder for 10-15 minutes. A foam (usually approx. a 1 cm layer) indicates the presence of saponins.

3.11.4.4 Test for steroids

To 1 mL of the stock solution, 10mL of chloroform was added and then 10mL of conc. H₂SO₄ was added as a film along the inside wall of the test tube. The presence of steroids is indicated by the upper layer of the solution turning red.

3.11.4.5 Test for tannins

To 5 mL of each stock solution, a few drops of 1% w/v lead acetate solution was added. The formation of yellow precipitate indicates the presence of tannins.

3.11.4.6 Test for glycosides

Each stock solution was hydrolysed with hydrochloric acid for 2 hours on a water bath. 1 mL pyridine and 5 drops of sodium nitroprusside were added to the hydrolysate and then to that sodium hydroxide was added. Presence of glycosides is indicated by the appearance of pink coloured solution turning red.

Table 3.5 summarizes the outcomes of the above tests for each of the BM extracts.

Table 3. 5 Experimental analysis of phytochemicals in the extracts of methanol, octanol, ethyl acetate and water (+ = presence and - = absence of phytochemicals)⁹.

Phytochemicals	Methanol	Octanol	Ethyl acetate	Water
Triterpenoids	+	+	+	+
Flavonoids	+	+	+	+
Saponins	+	+	-	+
Steroids	+	+	+	+
Tannins	-	-	-	-
Glycosides	+	-	-	+

Experiments were carried out to detect the phytochemicals present in all the extracts (methanol, octanol, ethyl acetate and water) and observed the presence of triterpenoids, flavonoids and steroids in all the extracts whereas the presence of saponin was not observed in ethyl acetate extract. Tannins were absent in all the extracts. The absence of glycosides in both octanol and ethyl acetate extract indicates the presence of de-glycosylated moieties (jujubogenin/pseudojujubogenin).

⁹The screening of the ethanol and n-butanol extracts could not be carried out due to insufficient remaining stock solution.

3.11.5 Column chromatography

The column used was silica gel 60-120 mesh with acid washed sand and glass wool. 10 mL of the above BM ethyl acetate extract stock solution was subjected to column chromatography using 7:3 ethyl acetate: water as eluent and 24 fractions were collected. Each of these 24 fractions were then subjected to ESI-MS screening and tandem mass experiments¹⁰.

3.11.6 Preparation of metal solutions and spiking experiments

0.01g of $\text{Cu}(\text{NO}_3)_2 \cdot 3\text{H}_2\text{O}$, was dissolved in 10mL of 7:3 methanol-water solution and filtered using a 0.45 μm disposable syringe filter. Similarly, metal solutions were prepared using $\text{Zn}(\text{NO}_3)_2 \cdot 6\text{H}_2\text{O}$, and $\text{Fe}(\text{NO}_3)_3 \cdot 9\text{H}_2\text{O}$. These solutions were used as stock solutions for the spiking experiments.

3.11.6.1 Spiking experiment with copper

To 1 mL of fraction 5, where Jujubogenin and/or Pseudojujubogenin were detected by the ESI-MS experiments, Figure 3.16, 1 mL of the copper stock solution was added with stirring. The resultant solution was filtered and then, again, subjected to ESI-MS experiment. From this experiment, the copper complex of Jujubogenin or Pseudojujubogenin was also detected, Figure 3.18.

3.11.6.2 Spiking experiment with Zinc and Iron

The above copper spiking experiment was repeated for zinc and Iron but no corresponding zinc or Iron complex could be found.

3.11.7 ESI-MS and MS/MS experiments

All fractions were subjected to ESI-MS analysis and this data is included in the Appendix and the pH of each fraction was noted¹¹. For tandem MS, three collision energies (CEs) were trailed namely, 15V, 20V, 30V, 35V and 40V. The instrument was a triple quad offering high accuracy, especially for MS/MS. Both positive and negative-

¹⁰Fraction 5 revealed the compounds of interest.

¹¹The pH of Fraction 5 was 5.1. The pH of all the fractions ranged from 3.4 to 5.5.

ion modes were used for screening and characterization. The solvent used was 7:3 methanol: water for all the experiments.

3.12 Results and discussion

3.12.1 ESI-MS studies of *Bacopa monnieri* extracts

There are a number of research studies reported for the identification of the molecular components of BM (Bhandari et al. 2009). Recently, liquid chromatography/ electrospray ionization/ quadrupole time-of-flight/ mass spectrometry (LC-ESI-QTOF-MS) studies assigned peaks to JJ/PJJ at m/z 473 and dehydrated jujubogenin at m/z 455 (Nuengchamng, Sookying & Ingkaninan 2016). Research studies of BM extract were also carried out using electrospray ionization ion trap ESI-IT and atmospheric pressure-matrix-assisted laser desorption/ionization ion trap (AP-MALDI)-IT analysis. These workers reported a peak at m/z 473 supporting the presence of JJ/PJJ (Nuengchamng, Sookying & Ingkaninan 2016).

The objective of the research reported in this thesis was to systematically extract the saponins and their breakdown products (especially the aglycones) from the dried, ground BM plant material using a range of solvents including water, methanol, ethanol, n-butanol, ethyl acetate and octanol. These extracts were subjected to fractionation via column chromatography. For each solvent, the dried BM extract was dissolved in methanol and subjected to column chromatography, using 7:3 ethyl acetate: water as the eluent and 24 fractions were collected for each extraction. These fractions (6 x 24 = 144) were then subjected to ESI-MS screening both in positive and negative ion mode. A fraction from the ethyl acetate extract revealed a peak at m/z 473 that was assigned to protonated JJ/PJJ, Figure.3.16; and a peak at m/z 455 was assigned to dehydrated JJ/PJJ -consistent with the literature results that are reported above¹². These molecules could not be detected in the other extracts. These results are consistent with the chemical screen tests reported in Table 3.5, *vide supra*.

Subsequent MS/MS on the peak at m/z 473, at different Collision Energies (CEs), confirmed the structural identity of the aglycone isomers, JJ and PJJ, Figure 3.17. Thus

¹²Note that the m/z range searched was restricted to 250 to 550 as only the JJ and PJJ were targeted. Due to time constraints, other entities such as the glycosylated species were not targeted in our search.

fragments of JJ and or PJJ, (m/z 473) ions were identified at m/z 39, m/z 173, m/z 305, m/z 391, m/z 441, at CE-25V; m/z 63, m/z 209, m/z 383, m/z 317, m/z 173, m/z 39, m/z 403 at CE-35V; m/z 39, m/z 131, m/z 213, m/z 265, m/z 309, m/z 400, at CE-30V and m/z 129, m/z 169 at CE-40. There was no fragments at CE-20V for m/z 473.

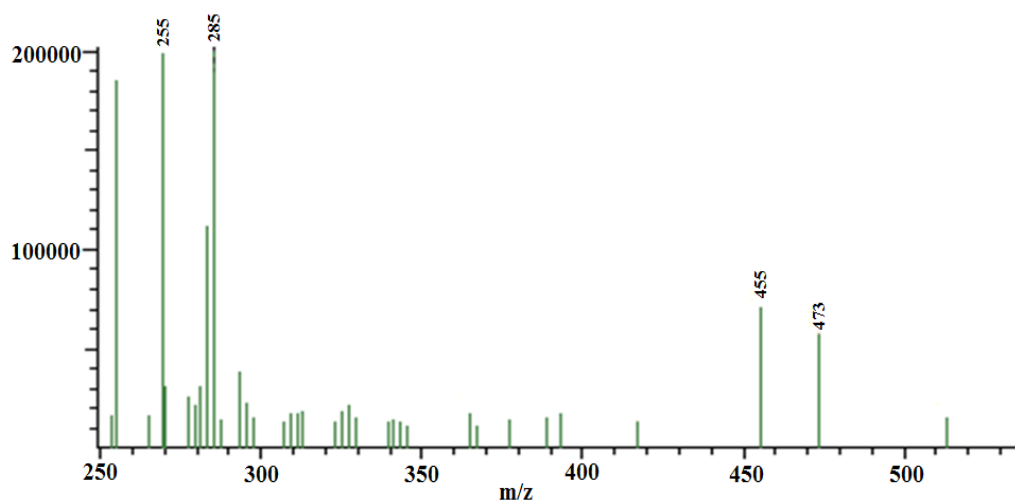
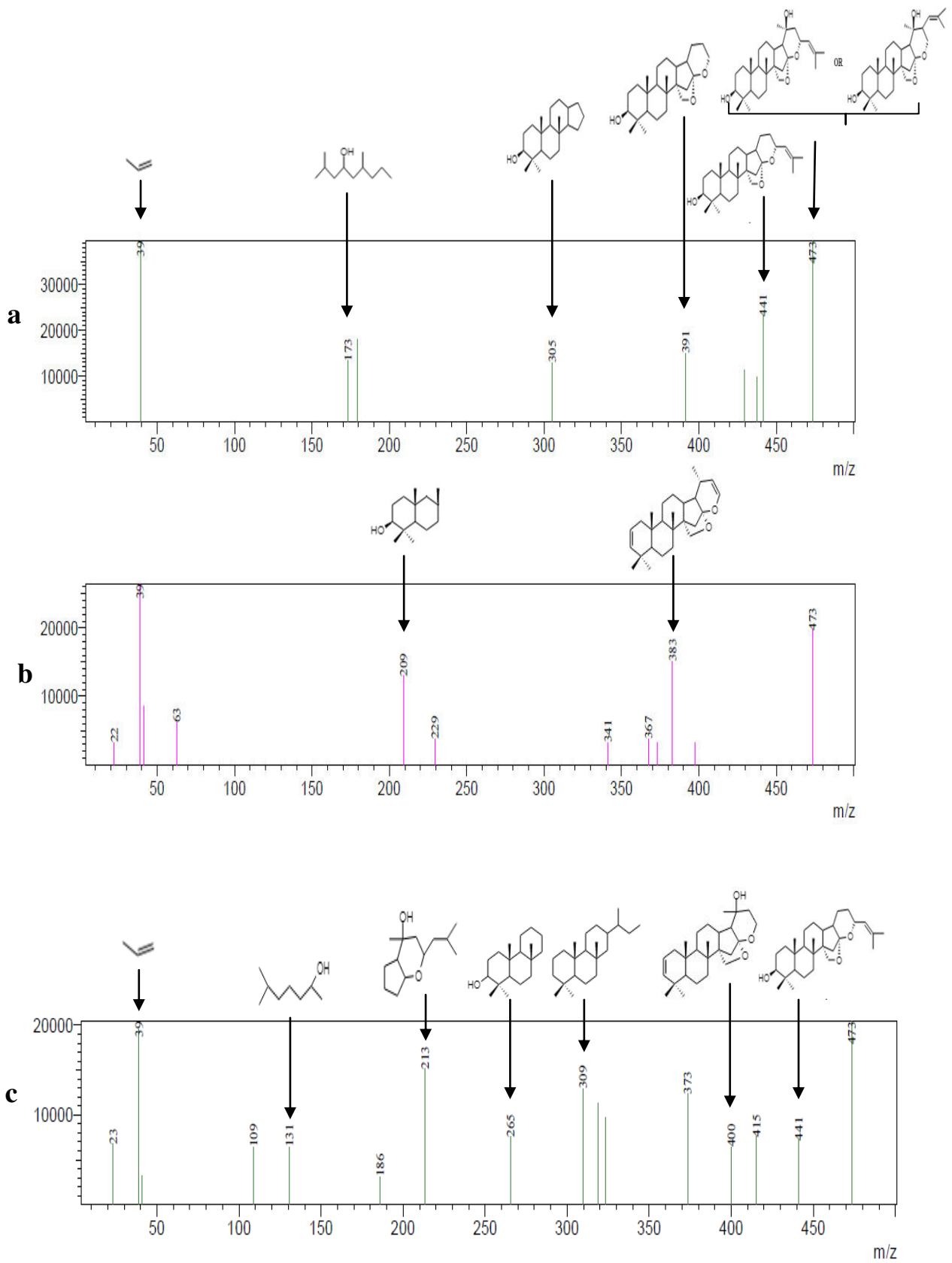


Figure 3.16 The ESI-MS spectra of $[C_{30}H_{48}O_4]^+$ in positive ion mode m/z 473; loss of H_2O from $[C_{30}H_{48}O_4]^+$ in positive ion mode m/z 455. No attempt has been made to assign the other peaks in this spectrum.



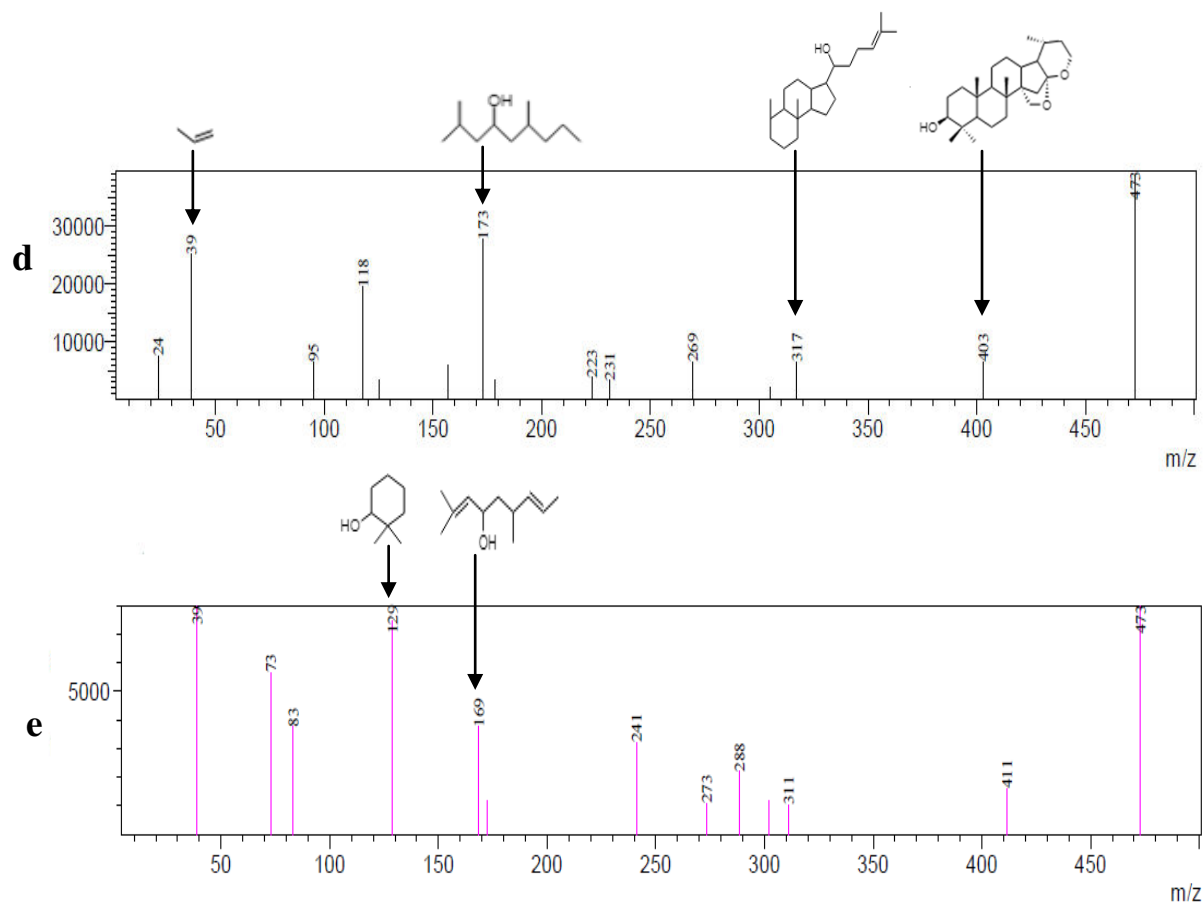


Figure 3.17(a) MS/MS of m/z 473, polarity: positive, Collision Energy (CE) –25 V; (b, d) MS/MS of m/z 473, polarity: positive, CE-35 V; (c) MS/MS of m/z 473, polarity: positive, CE-30 V; (e) MS/MS of m/z 473, polarity: positive, CE-40 V.

3.12.2 Chelating potential of JJ/PJJ

Having identified the presence of JJ and/or PJJ in fraction 5 of the ethyl acetate extract - and having established the potential for these molecules to act as bidentate ligands towards Cu^{2+} , Zn^{2+} and Fe^{3+} ions in our parallel computational chemistry investigations as described above in the computational chemistry Section 3.9, we conducted the following metal spiking experiments followed by ESI/MS in order to identify any such metal complexes in solution.

3.12.2.1 Spiking with Cu^{2+} , Zn^{2+} and Fe^{3+}

Fraction 5 from the ethyl acetate extract contained was concentrated and divided into 3 equal portions. Aliquots of each metal ion solution (in 7:3 methanol: water) was added to each of the extract portions as described previously and each reaction mixture was

filtered using a 0.45 μ M syringe filter and subjected to ESI-MS and MS/MS, in both positive and negative ion mode.

3.12.2.2 ESI-MS and MS/MS of potential metal complexes

We were able to definitively identify the presence of the Cu-JJ (or Cu-PJJ) complex, $[\text{C}_{30}\text{H}_{48}\text{O}_4\text{Cu}(\text{H}_2\text{O})_2]^+$, from the characteristic isotopic profile of copper, Figure 3.18. The corresponding Zn and Fe complexes could not be found. This complex was subsequently successfully modelled using semi-empirical quantum chemical and density functional methods, as described in Section 3.9 above.

3.12.2.3 Triple quad experiment with copper complex

In order to further establish the presence of Cu-JJ/PJJ complex, MS/MS tandem mass spectrometry was used on the Cu-JJ/PJJ peak of 571 and the experiment was carried out at increasing collision energies of 15V, 20V, 25V, 30V, 35V and 40V as the resultant fragments are different in different CEs. The resulting fragmentation gave a peak for the JJ/PJJ free protonated ligand $[\text{C}_{30}\text{H}_{48}\text{O}_4]^+$ at m/z +473, Figure.3.19. This represents further compelling evidence for the formation of the Cu-JJ/PJJ complex $[\text{C}_{30}\text{H}_{48}\text{O}_4\text{Cu}(\text{H}_2\text{O})_2]^+$ in solution.

3.12.2.4 Preference of Cu complexation over Zn or Fe

Our inability to observe any complexation with Zn or Fe indicated an interesting specificity of JJ or PJJ for Cu. In this regard, several competition experiments were carried out, involving Cu/Zn Figure 3.20 and Cu/Fe. In these experiments, we were unable to find any evidence for Zn or Fe chelation. However, both of these complexes are considered feasible based on our computer modelling studies, Section 3.9, and these studies are suggestive of the reasons for the Cu selectivity.

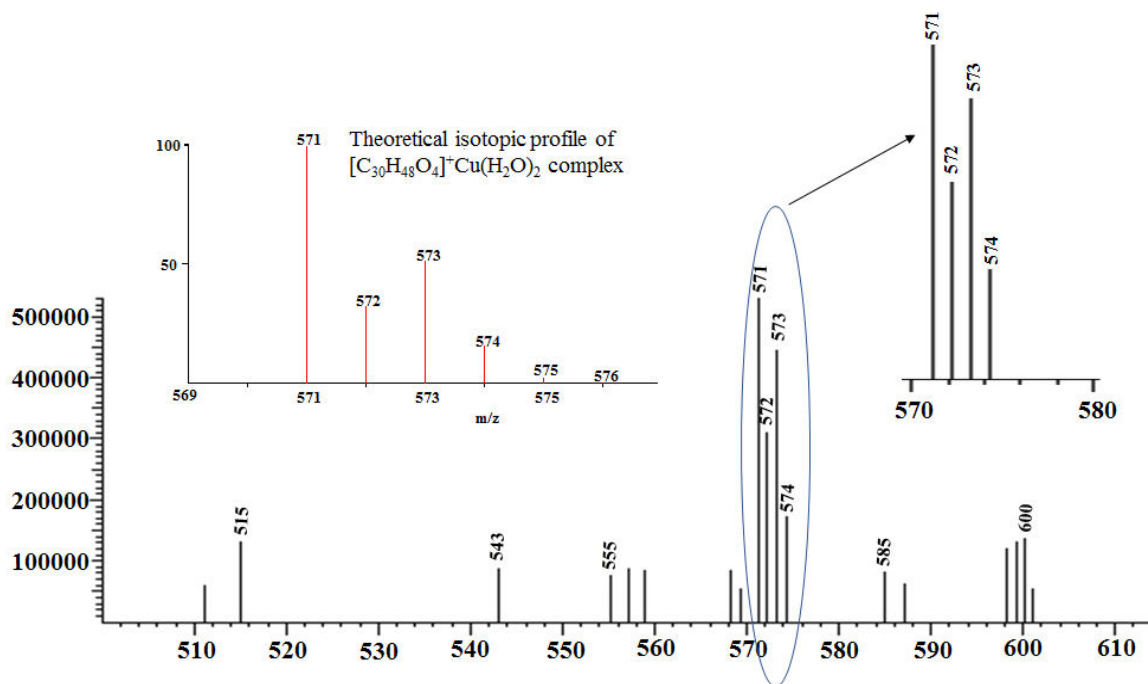


Figure 3.18 ESI-MS spectra of $[\text{C}_{30}\text{H}_{48}\text{O}_4\text{Cu}(\text{H}_2\text{O})_2]^+$ (positive ion mode), compared to the theoretical isotopic profile of $[\text{C}_{30}\text{H}_{48}\text{O}_4]\text{Cu}(\text{H}_2\text{O})_2]^+$.

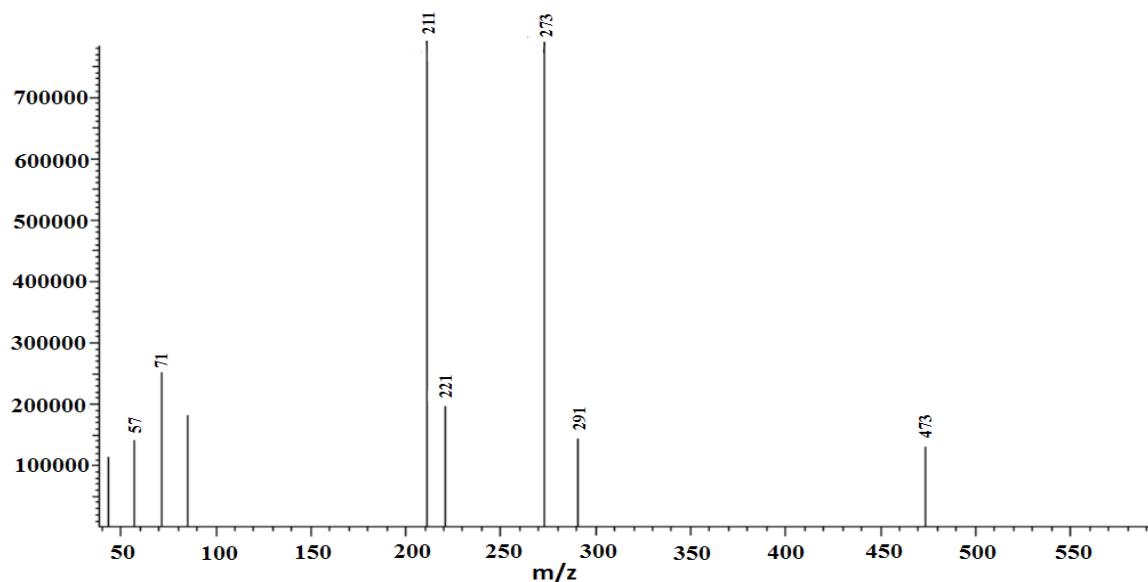


Figure 3.19 Triple quad mass spectra of +571 ion, $[\text{C}_{30}\text{H}_{48}\text{O}_4\text{Cu}(\text{H}_2\text{O})_2]^+$ fractionate as +473 m/z of jujubogenin $[\text{C}_{30}\text{H}_{48}\text{O}_4]^+\text{CE}(25\text{V})$.

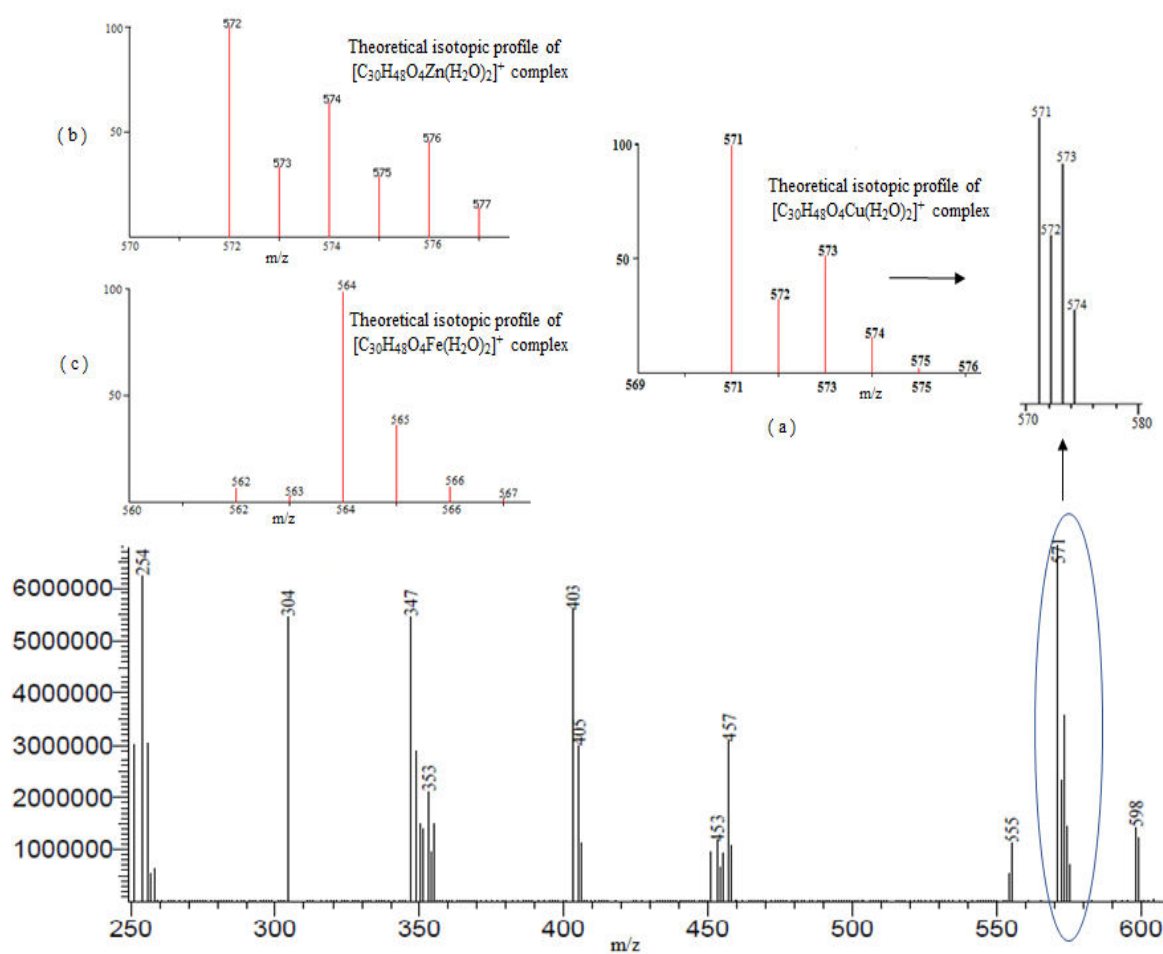


Figure 3.20 ESI-MS spectra of competition experiment with Cu, Fe and Zn in positive ion mode; Insets (a) theoretical isotopic profile of $[C_{30}H_{48}O_4Cu(H_2O)_2]^+$; (b) theoretical isotopic profile of $[C_{30}H_{48}O_4Zn(H_2O)_2]^+$; (c) theoretical isotopic profile of $[C_{30}H_{48}O_4Fe(H_2O)_2]^{2+}$. Note that only the copper complex is present. A similar experiment with Zn and Fe failed to detect either.

3.13 Conclusions and recommendation for future research

The designed strategy was implemented for an Indian (Ayurvedic) traditional medicinal plant (Brahmi) used as a tea for the treatment of neurological disease symptoms. This strategy was found to be highly successful for the identification and characterization of a potential, BBB-penetrating, molecule in the extract of Brahmi tea (a purported “brain tonic”), that is a good candidate for sequestering copper ions in the brain of Alzheimer’s disease victims. Under the employed strategy, the theory employed is the suggestion that removal of metal ions from amyloid plaque in the brain by a BBB-penetrating chelator molecule would constitute an effective treatment for Alzheimer’s disease. It is anticipated that such a natural product candidate would convey numerous advantages over synthetic molecules, such as chloroquine (CQ).

Both computer modelling, systematic extraction and ESI-MS and MS/MS have identified the above candidate molecule to be Jujubogenin. Both the Jujubogenin molecule (protonated) and its bidentate diaquo Cu^{2+} complex have been characterized computationally and experimentally. These studies suggest that the Jujubogenin molecule has a unique specificity for Cu^{2+} and could also be developed as a copper specific reagent - with possible implications for the recovery of copper from waste water.

The isomer Pseudojujubogenin has also been investigated and has very similar properties to Jujubogenin with respect to transition metal coordination. However, Jujubogenin has been shown to coordinate Cu^{2+} preferentially. However, both of these isomers warrant further investigation with respect to their respective binding to a range of transition elements, including Zn^{2+} , Ni^{2+} and Mn^{2+} .

Since Jujubogenin has not been successfully synthesized, our research provides a means for obtaining quantitative amounts, either as the protonated ligand or as the copper complex – possibly by preparative cation exchange chromatography of the extract or by solid phase extraction (SPE). This is a priority area of further research for conducting clinical trials. It is possible that modified or truncated structures derived from Jujubogenin could be proposed and be more readily synthesized- and which retain BBB-penetrating capability and Cu^{2+} specificity. Such possibilities could be readily explored via computational chemistry and is also an exciting area for future research.

References

Alam, MN, Bristi, NJ & Rafiquzzaman, M 2013, 'Review on in vivo and in vitro methods evaluation of antioxidant activity', *Saudi pharmaceutical journal*, vol. 21, no. 2, pp. 143-52.

Alexander, B, Browse, D, Reading, S & Benjamin, I 1999, 'A simple and accurate mathematical method for calculation of the EC50', *Journal of pharmacological and toxicological methods*, vol. 41, no. 2-3, pp. 55-8.

Apak, R, Güçlü, K, Özyürek, M & Celik, SE 2008, 'Mechanism of antioxidant capacity assays and the CUPRAC (cupric ion reducing antioxidant capacity) assay', *Microchimica Acta*, vol. 160, no. 4, pp. 413-9.

Atwood, CS, Moir, RD, Huang, X, Scarpa, RC, Bacarra, NME, Romano, DM, Hartshorn, MA, Tanzi, RE & Bush, AI 1998, 'Dramatic aggregation of Alzheimer A β by Cu (II) is induced by conditions representing physiological acidosis', *Journal of Biological Chemistry*, vol. 273, no. 21, pp. 12817-26.

Atwood, CS, Scarpa, RC, Huang, X, Moir, RD, Jones, WD, Fairlie, DP, Tanzi, RE & Bush, AI 2000, 'Characterization of copper interactions with Alzheimer amyloid β peptides', *Journal of neurochemistry*, vol. 75, no. 3, pp. 1219-33.

Barnham, KJ & Bush, AI 2008, 'Metals in Alzheimer's and Parkinson's diseases', *Current opinion in chemical biology*, vol. 12, no. 2, pp. 222-8.

Bartzokis, G, Sultzer, D, Mintz, J, Holt, LE, Marx, P, Phelan, CK & Marder, SR 1994, 'In vivo evaluation of brain iron in Alzheimer's disease and normal subjects using MRI', *Biological psychiatry*, vol. 35, no. 7, pp. 480-7.

Benedet, J & Shibamoto, T 2008, 'Role of transition metals, Fe (II), Cr (II), Pb (II), and Cd (II) in lipid peroxidation', *Food Chemistry*, vol. 107, no. 1, pp. 165-8.

Benvenuti, S, Pellati, F, Melegari, Ma & Bertelli, D 2004, 'Polyphenols, anthocyanins, ascorbic acid, and radical scavenging activity of Rubus, Ribes, and Aronia', *Journal of Food Science*, vol. 69, no. 3, pp. 164-9.

Bhandari, P, Kumar, N, Singh, B & Kaur, I 2009, 'Dammarane triterpenoid saponins from *Bacopa monnieri*', *Canadian Journal of Chemistry*, vol. 87, no. 9, pp. 1230-4.

Bhattacharya, S, Bhattacharya, A, Kumar, A & Ghosal, S 2000, 'Antioxidant activity of *Bacopa monniera* in rat frontal cortex, striatum and hippocampus', *Phytotherapy Research*, vol. 14, no. 3, pp. 174-9.

Bihaqi, SW, Sharma, M, Singh, AP & Tiwari, M 2009, 'Neuroprotective role of *Convolvulus pluricaulis* on aluminium induced neurotoxicity in rat brain', *Journal of ethnopharmacology*, vol. 124, no. 3, pp. 409-15.

Bin, Y, Li, X, He, Y, Chen, S & Xiang, J 2013, 'Amyloid- β peptide (1–42) aggregation induced by copper ions under acidic conditions', *Acta biochimica et biophysica Sinica*, p. gmt044.111111111111

Bush, AI, Pettingell, W, Paradis, M & Tanzi, RE 1994, 'Modulation of A β adhesiveness and secretase site cleavage by zinc', *Journal of Biological Chemistry*, vol. 269, no. 16, pp. 12152-8.

Bush, AI, Pettingell, WH, Multhaup, G, d Paradis, M, Vonsattel, J-P, Gusella, JF, Beyreuther, K, Masters, CL & Tanzi, RE 1994, 'Rapid induction of Alzheimer A beta amyloid formation by zinc', *Science*, vol. 265, no. 5177, pp. 1464-7.

Calabrese, C, Gregory, WL, Leo, M, Kraemer, D, Bone, K & Oken, B 2008, 'Effects of a standardized *Bacopa monnieri* extract on cognitive performance, anxiety, and depression in the elderly: a randomized, double-blind, placebo-controlled trial', *The journal of alternative and complementary medicine*, vol. 14, no. 6, pp. 707-13.

Carocho, M & Ferreira, IC 2013, 'A review on antioxidants, prooxidants and related controversy: natural and synthetic compounds, screening and analysis methodologies and future perspectives', *Food and chemical toxicology*, vol. 51, pp. 15-25.

Caron, G, Kihlberg, J & Ermondi, G 2019, 'Intramolecular hydrogen bonding: An opportunity for improved design in medicinal chemistry', *Medicinal research reviews*.

Caron, G, Vallaro, M & Ermondi, G 2018, 'Log P as a tool in intramolecular hydrogen bond considerations', *Drug Discovery Today: Technologies*, vol. 27, pp. 65-70.

Chandra, V, Ganguli, M, Pandav, R, Johnston, J, Belle, S & DeKosky, S 1998, 'Prevalence of Alzheimer's disease and other dementias in rural India: the Indo-US study', *Neurology*, vol. 51, no. 4, pp. 1000-8.

Cherny, RA, Atwood, CS, Xilinas, ME, Gray, DN, Jones, WD, McLean, CA, Barnham, KJ, Volitakis, I, Fraser, FW & Kim, Y-S 2001, 'Treatment with a copper-zinc chelator

markedly and rapidly inhibits β -amyloid accumulation in Alzheimer's disease transgenic mice', *Neuron*, vol. 30, no. 3, pp. 665-76.

Cherny, RA, Legg, JT, McLean, CA, Fairlie, DP, Huang, X, Atwood, CS, Beyreuther, K, Tanzi, RE, Masters, CL & Bush, AI 1999, 'Aqueous dissolution of Alzheimer's disease A β amyloid deposits by biometal depletion', *Journal of Biological Chemistry*, vol. 274, no. 33, pp. 23223-8.

Chevion, M 1988, 'A site-specific mechanism for free radical induced biological damage: the essential role of redox-active transition metals', *Free Radical Biology and Medicine*, vol. 5, no. 1, pp. 27-37.

Chitwood, DJ 2002, 'Phytochemical based strategies for nematode control', *Annual review of phytopathology*, vol. 40, no. 1, pp. 221-49.

Chowdhuri, DK, Parmar, D, Kakkar, P, Shukla, R, Seth, P & Srimal, R 2002, 'Antistress effects of bacosides of *Bacopa monnieri*: modulation of Hsp70 expression, superoxide dismutase and cytochrome P450 activity in rat brain', *Phytotherapy Research*, vol. 16, no. 7, pp. 639-45.

Chuang, Y-Y, Corchado, JC & Truhlar, DG 1999, 'Mapped interpolation scheme for single-point energy corrections in reaction rate calculations and a critical evaluation of dual-level reaction path dynamics methods', *The Journal of Physical Chemistry A*, vol. 103, no. 8, pp. 1140-9.

Chun, OK, Kim, D-O & Lee, CY 2003, 'Superoxide radical scavenging activity of the major polyphenols in fresh plums', *Journal of agricultural and food chemistry*, vol. 51, no. 27, pp. 8067-72.

Clark, AM 1996, 'Natural products as a resource for new drugs', *Pharmaceutical research*, vol. 13, no. 8, pp. 1133-41.

Comba, P & Zimmer, M 1994, 'Molecular mechanics and the Jahn-Teller effect', *Inorganic Chemistry*, vol. 33, no. 24, pp. 5368-9.

Cuajungco, MP, Goldstein, LE, Nunomura, A, Smith, MA, Lim, JT, Atwood, CS, Huang, X, Farrag, YW, Perry, G & Bush, AI 2000, 'Evidence that the β -amyloid plaques of Alzheimer's disease represent the redox-silencing and entombment of A β by zinc', *Journal of Biological Chemistry*, vol. 275, no. 26, pp. 19439-42.

Da Silva, JF & Williams, RJP 2001, *The biological chemistry of the elements: the inorganic chemistry of life*, Oxford University Press.

Deepak, M, Sangli, G, Arun, P & Amit, A 2005, 'Quantitative determination of the major saponin mixture bacoside A in *Bacopa monnieri* by HPLC', *Phytochemical Analysis*, vol. 16, no. 1, pp. 24-9.

Desagher, S, Glowinski, J & Premont, J 1996, 'Astrocytes protect neurons from hydrogen peroxide toxicity', *Journal of Neuroscience*, vol. 16, no. 8, pp. 2553-62.

Devendra, PSS, Preeti, B, Santanu, B, Gajanan, D & Rupesh, D 2018, 'Brahmi (*Bacopa monnieri*) as functional food ingredient in food processing industry', *Journal of Pharmacognosy and Phytochemistry*, vol. 7, no. 3, pp. 189-94.

Dexter, D, Wells, F, Lee, A, Agid, F, Agid, Y, Jenner, P & Marsden, C 1989, 'Increased nigral iron content and alterations in other metal ions occurring in brain in Parkinson's disease', *Journal of neurochemistry*, vol. 52, no. 6, pp. 1830-6.

Dowell, A, Davidson, G & Ghosh, D 2015, 'Validation of quantitative HPLC method for bacosides in keenmind', *Evidence-Based Complementary and Alternative Medicine*, vol. 2015.

Dudev, T & Lim, C 2000, 'Tetrahedral vs octahedral zinc complexes with ligands of biological interest: a DFT/CDM study', *Journal of the American Chemical Society*, vol. 122, no. 45, pp. 11146-53.

Ehrman, TM, Barlow, DJ & Hylands, PJ 2007, 'Phytochemical databases of Chinese herbal constituents and bioactive plant compounds with known target specificities', *Journal of chemical information and modeling*, vol. 47, no. 2, pp. 254-63.

El Diwani, G, El Rafie, S & Hawash, S 2009, 'Antioxidant activity of extracts obtained from residues of nodes leaves stem and root of Egyptian *Jatropha curcas*', *African Journal of Pharmacy and Pharmacology*, vol. 3, no. 11, pp. 521-30.

El Gharras, H 2009, 'Polyphenols: food sources, properties and applications—a review', *International journal of food science & technology*, vol. 44, no. 12, pp. 2512-8.

Ellison, N & Lewis, G 1984, 'Plasma concentrations following single doses of morphine sulfate in oral solution and rectal suppository', *Clinical Pharmacy*, vol. 3, no. 6, pp. 614-7.

Ertl, P, Rohde, B & Selzer, P 2000, 'Fast calculation of molecular polar surface area as a sum of fragment-based contributions and its application to the prediction of drug transport properties', *Journal of medicinal chemistry*, vol. 43, no. 20, pp. 3714-7.

Faber, S, Zinn, GM, Kern Li, JC & Skip Kingston, H 2009, 'The plasma zinc/serum copper ratio as a biomarker in children with autism spectrum disorders', *Biomarkers*, vol. 14, no. 3, pp. 171-80.

Finkel, T & Holbrook, NJ 2000, 'Oxidants, oxidative stress and the biology of ageing', *Nature*, vol. 408, no. 6809, pp. 239-47.

Fogliano, V, Verde, V, Randazzo, G & Ritieni, A 1999, 'Method for measuring antioxidant activity and its application to monitoring the antioxidant capacity of wines', *Journal of agricultural and food chemistry*, vol. 47, no. 3, pp. 1035-40.

Förstermann, U 2008, 'Oxidative stress in vascular disease: causes, defense mechanisms and potential therapies', *Nature Reviews Cardiology*, vol. 5, no. 6, p. 338.

Fridovich, I 1978, 'The biology of oxygen radicals', *Science*, vol. 201, no. 4359, pp. 875-80.

Ganzer, M, Gampenrieder, J, Pawar, RS, Khan, IA & Stuppner, H 2004, 'Separation of the major triterpenoid saponins in *Bacopa monnieri* by high-performance liquid chromatography', *Analytica chimica acta*, vol. 516, no. 1, pp. 149-54.

Garai, S, Mahato, SB, Ohtani, K & Yamasaki, K 1996, 'Bacopasaponin DA pseudojujubogenin glycoside from *Bacopa monniera*', *Phytochemistry*, vol. 43, no. 2, pp. 447-9.

Garbacki, N, Tits, M, Angenot, L & Damas, J 2004, 'Inhibitory effects of proanthocyanidins from *Ribes nigrum* leaves on carrageenin acute inflammatory reactions induced in rats', *BMC pharmacology*, vol. 4, no. 1, p. 25.

Giacomelli, C, Miranda, FdS, Gonçalves, NS & Spinelli, A 2004, 'Antioxidant activity of phenolic and related compounds: a density functional theory study on the O–H bond dissociation enthalpy', *Redox Report*, vol. 9, no. 5, pp. 263-9.

Goedert, M 1993, 'Tau protein and the neurofibrillary pathology of Alzheimer's disease', *Trends in neurosciences*, vol. 16, no. 11, pp. 460-5.

Gordaliza, M 2007, 'Natural products as leads to anticancer drugs', *Clinical and Translational Oncology*, vol. 9, no. 12, pp. 767-76.

Goto, S, Kogure, K, Abe, K, Kimata, Y, Kitahama, K, Yamashita, E & Terada, H 2001, 'Efficient radical trapping at the surface and inside the phospholipid membrane is

responsible for highly potent antiperoxidative activity of the carotenoid astaxanthin', *Biochimica et biophysica acta (BBA)-biomembranes*, vol. 1512, no. 2, pp. 251-8.

Gouras, GK & Beal, MF 2001, 'Metal chelator decreases Alzheimer β -amyloid plaques', *Neuron*, vol. 30, no. 3, pp. 641-2.

Govindappa, M, Channabasava, R, Kumar, KS & Pushpalatha, K 2013, 'Antioxidant Activity and Phytochemical Screening of Crude Endophytes Extracts of *Tabebuia argentea* Bur. & K. Sch', *American Journal of Plant Sciences*, vol. 4, no. 08, p. 1641.

Granato, D, Katayama, F & Castro, I 2010, 'Assessing the association between phenolic compounds and the antioxidant activity of Brazilian red wines using chemometrics', *LWT-Food Science and Technology*, vol. 43, no. 10, pp. 1542-9.

Grimme, S, Antony, J, Schwabe, T & Mück-Lichtenfeld, C 2007, 'Density functional theory with dispersion corrections for supramolecular structures, aggregates, and complexes of (bio) organic molecules', *Organic & Biomolecular Chemistry*, vol. 5, no. 5, pp. 741-58.

Häkkinen, S, Heinonen, M, Kärenlampi, S, Mykkänen, H, Ruuskanen, J & Törrönen, R 1999, 'Screening of selected flavonoids and phenolic acids in 19 berries', *Food Research International*, vol. 32, no. 5, pp. 345-53.

Halliwell, B 1992, 'Reactive oxygen species and the central nervous system', *Journal of neurochemistry*, vol. 59, no. 5, pp. 1609-23.

Hann, MM, Leach, AR & Harper, G 2001, 'Molecular complexity and its impact on the probability of finding leads for drug discovery', *Journal of chemical information and computer sciences*, vol. 41, no. 3, pp. 856-64.

Hardy, J & Selkoe, DJ 2002, 'The amyloid hypothesis of Alzheimer's disease: progress and problems on the road to therapeutics', *Science*, vol. 297, no. 5580, pp. 353-6.

Harvey, AL 2008, 'Natural products in drug discovery', *Drug discovery today*, vol. 13, no. 19-20, pp. 894-901.

Hodis, HN, Mack, WJ, LaBree, L, Cashin-Hemphill, L, Sevanian, A, Johnson, R & Azen, SP 1995, 'Serial coronary angiographic evidence that antioxidant vitamin intake reduces progression of coronary artery atherosclerosis', *Jama*, vol. 273, no. 23, pp. 1849-54.

Huang, X, Atwood, CS, Hartshorn, MA, Multhaup, G, Goldstein, LE, Scarpa, RC, Cuajungco, MP, Gray, DN, Lim, J & Moir, RD 1999, 'The A β peptide of Alzheimer's disease directly produces hydrogen peroxide through metal ion reduction', *Biochemistry*, vol. 38, no. 24, pp. 7609-16.

Hung, YH, Bush, AI & Cherny, RA 2010, 'Copper in the brain and Alzheimer's disease', *JBIC Journal of Biological Inorganic Chemistry*, vol. 15, no. 1, pp. 61-76.

Husain, SR, Cillard, J & Cillard, P 1987, 'Hydroxyl radical scavenging activity of flavonoids', *Phytochemistry*, vol. 26, no. 9, pp. 2489-91.

Illas, F, Moreira, IP, De Graaf, C & Barone, V 2000, 'Magnetic coupling in biradicals, binuclear complexes and wide-gap insulators: a survey of ab initio wave function and density functional theory approaches', *Theoretical Chemistry Accounts*, vol. 104, no. 3-4, pp. 265-72.

Jayaprakasam, B, Padmanabhan, K & Nair, MG 2010, 'Withanamides in *Withania somnifera* fruit protect PC-12 cells from β -amyloid responsible for Alzheimer's disease', *Phytotherapy Research*, vol. 24, no. 6, pp. 859-63.

Jayaprakasha, G, Singh, R & Sakariah, K 2001, 'Antioxidant activity of grape seed (*Vitis vinifera*) extracts on peroxidation models *in vitro*', *Food Chemistry*, vol. 73, no. 3, pp. 285-90.

Ji, HF, Tang, GY & Zhang, HY 2005, 'Theoretical elucidation of DPPH radical-scavenging activity difference of antioxidant xanthenes', *QSAR & Combinatorial Science*, vol. 24, no. 7, pp. 826-30.

Jiang, X & Kopp-Schneider, A 2014, 'Summarizing EC50 estimates from multiple dose-response experiments: A comparison of a meta-analysis strategy to a mixed-effects model approach', *Biometrical Journal*, vol. 56, no. 3, pp. 493-512.

Jonsson, T, Christensen, CB, Jordening, H & Frølund, C 1988, 'The bioavailability of rectally administered morphine', *Pharmacology & toxicology*, vol. 62, no. 4, pp. 203-5.

Joo, Y-E 2014, 'Natural product-derived drugs for the treatment of inflammatory bowel diseases', *Intestinal research*, vol. 12, no. 2, p. 103.

Jyoti, A & Sharma, D 2006, 'Neuroprotective role of *Bacopa monniera* extract against aluminium-induced oxidative stress in the hippocampus of rat brain', *Neuro Toxicology*, vol. 27, no. 4, pp. 451-7.

Kabouche, A, Kabouche, Z, Öztürk, M, Kolak, U & Topçu, G 2007, 'Antioxidant abietane diterpenoids from *Salvia barrelieri*', *Food Chemistry*, vol. 102, no. 4, pp. 1281-7.

Kalachaveedu, M, Adapala, D, Punnoose, A & Kuruvilla, S 2016, 'Brahmi saponins inhibit proliferation of Hep G2 cells by blocking cell cycle progression and inducing apoptosis', *Acta Horticulturae*, pp. 173-80.

Karimi, A, Majlesi, M & Rafieian-Kopaei, M 2015, 'Herbal versus synthetic drugs; beliefs and facts', *Journal of nephro pharmacology*, vol. 4, no. 1, p. 27.

Kikuzaki, H, Usuguchi, J & Nakatani, N 1991, 'Constituents of Zingiberaceae. I. Diarylheptanoids from the rhizomes of ginger (*Zingiber officinale* Roscoe)', *Chemical and pharmaceutical bulletin*, vol. 39, no. 1, pp. 120-2.

Kim, B-E, Nevitt, T & Thiele, DJ 2008, 'Mechanisms for copper acquisition, distribution and regulation', *Nature chemical biology*, vol. 4, no. 3, pp. 176-85.

Klein, E & Lukeš, V 2006, 'DFT/B3LYP study of O–H bond dissociation enthalpies of para and meta substituted phenols: Correlation with the phenolic C–O bond length', *Journal of Molecular Structure: THEOCHEM*, vol. 767, no. 1-3, pp. 43-50.

Koch, W, Holthausen, MC & Holthausen, MC 2001, *A chemist's guide to density functional theory*, vol. 2, Wiley Online Library.

Kohn, W, Becke, AD & Parr, RG 1996, 'Density functional theory of electronic structure', *The Journal of Physical Chemistry*, vol. 100, no. 31, pp. 12974-80.

Kowalik-Jankowska, T, Ruta-Dolejsz, M, Wisniewska, K, Lankiewicz, L & Kozłowski, H 2002, 'Possible involvement of copper (II) in Alzheimer disease', *Environmental Health Perspectives*, vol. 110, no. suppl 5, pp. 869-70.

Kumar, A, Ilavarasan, R, Jayachandran, T, Decaraman, M, Aravindhan, P, Padmanabhan, N & Krishnan, M 2009, 'Phytochemicals investigation on a tropical plant, *Syzygium cumini* from Kattuppalayam, Erode district, Tamil Nadu, South India', *Pakistan Journal of Nutrition*, vol. 8, no. 1, pp. 83-5.

Kumar, N, Abichandani, L, Thawani, V, Gharpure, K, Naidu, M & Venkat Ramana, G 2016, 'Efficacy of standardized extract of *Bacopa monnieri* (Bacognize®) on cognitive functions of medical students: a six-week, randomized placebo-controlled trial', *Evidence-Based Complementary and Alternative Medicine*, vol. 2016.

- Kumar, N & Knopman, DS 2005, 'SMON, clioquinol, and copper', *Postgraduate medical journal*, vol. 81, no. 954, pp. 227-.
- Lim, GP, Chu, T, Yang, F, Beech, W, Frautschy, SA & Cole, GM 2001, 'The curry spice curcumin reduces oxidative damage and amyloid pathology in an Alzheimer transgenic mouse', *Journal of Neuroscience*, vol. 21, no. 21, pp. 8370-7.
- Lim, NC, Freake, HC & Brückner, C 2005, 'Illuminating zinc in biological systems', *Chemistry—A European Journal*, vol. 11, no. 1, pp. 38-49.
- Lin, MT & Beal, MF 2006, 'Mitochondrial dysfunction and oxidative stress in neurodegenerative diseases', *Nature*, vol. 443, no. 7113, pp. 787-95.
- Linder, DP, Baker, BE & Rodgers, KR 2018, '[$(\text{H}_2\text{O})\text{Zn}(\text{Imidazole})_n^{2+}$: the vital roles of coordination number and geometry in $\text{Zn}-\text{OH}_2$ acidity and catalytic hydrolysis', *Physical Chemistry Chemical Physics*, vol. 20, no. 38, pp. 24979-91.
- Lohmann, C, Hüwel, S & Galla, H-J 2002, 'Predicting blood-brain barrier permeability of drugs: evaluation of different in vitro assays', *Journal of drug targeting*, vol. 10, no. 4, pp. 263-76.
- Lovell, M, Robertson, J, Teesdale, W, Campbell, J & Markesbery, W 1998, 'Copper, iron and zinc in Alzheimer's disease senile plaques', *Journal of the neurological sciences*, vol. 158, no. 1, pp. 47-52.
- Lushchak, VI 2014, 'Free radicals, reactive oxygen species, oxidative stress and its classification', *Chemico-biological interactions*, vol. 224, pp. 164-75.
- Majumdar, S, Basu, A, Paul, P, Halder, M & Jha, S 2013, 'Bacosides and neuroprotection', *Natural Products: Phytochemistry, Botany and Metabolism of Alkaloids, Phenolics and Terpenes*, pp. 3639-60.
- Martin, L, Latypova, X, Wilson, CM, Magnaudeix, A, Perrin, M-L, Yardin, C & Terro, F 2013, 'Tau protein kinases: involvement in Alzheimer's disease', *Ageing research reviews*, vol. 12, no. 1, pp. 289-309.
- Mathew, M & Subramanian, S 2012, 'Evaluation of the anti-amyloidogenic potential of nootropic herbal extracts in vitro', *International Journal of Pharmaceutical Sciences and Research*, vol. 3, no. 11, p. 4276.

— 2014, 'In vitro screening for anti-cholinesterase and antioxidant activity of methanolic extracts of ayurvedic medicinal plants used for cognitive disorders', *PloS one*, vol. 9, no. 1.

Meepagala, KM, Bernier, UR, Burandt, C & Duke, SO 2013, 'Mosquito repellents based on a natural chromene analogue with longer duration of action than N, N-diethyl-metoluamide (DEET)', *Journal of agricultural and food chemistry*, vol. 61, no. 39, pp. 9293-7.

Molyneux, P 2004, 'The use of the stable free radical diphenylpicrylhydrazyl (DPPH) for estimating antioxidant activity', *Songklanakar J. sci. technol*, vol. 26, no. 2, pp. 211-9.

Mounsey, RB & Teismann, P 2012, 'Chelators in the treatment of iron accumulation in Parkinson's disease', *International journal of cell biology*, vol. 2012.

Moyer, RA, Hummer, KE, Finn, CE, Frei, B & Wrolstad, RE 2002, 'Anthocyanins, phenolics, and antioxidant capacity in diverse small fruits: Vaccinium, Rubus, and Ribes', *Journal of agricultural and food chemistry*, vol. 50, no. 3, pp. 519-25.

Murthy, PBS, Raju, VR, Ramakrisana, T, Chakravarthy, MS, Kumar, KV, Kannababu, S & Subbaraju, GV 2006, 'Estimation of twelve bacopa saponins in Bacopa monnieri extracts and formulations by high-performance liquid chromatography', *Chemical and pharmaceutical bulletin*, vol. 54, no. 6, pp. 907-11.

Newman, DJ, Cragg, GM & Snader, KM 2003, 'Natural products as sources of new drugs over the period 1981– 2002', *Journal of natural products*, vol. 66, no. 7, pp. 1022-37.

Ng, YP, Or, TCT & Ip, NY 2015, 'Plant alkaloids as drug leads for Alzheimer's disease', *Neurochemistry international*, vol. 89, pp. 260-70.

Nuengchamnong, N, Sookying, S & Ingkaninan, K 2016, 'LC-ESI-QTOF-MS based screening and identification of isomeric jujubogenin and pseudojujubogenin aglycones in Bacopa monnieri extract', *Journal of Pharmaceutical and Biomedical Analysis*, vol. 129, pp. 121-34.

Oldendorf, WH 1974, 'Blood-brain barrier permeability to drugs', *Annual review of pharmacology*, vol. 14, no. 1, pp. 239-48.

Orhan, G, Orhan, I & Sener, B 2006, 'Recent developments in natural and synthetic drug research for Alzheimer's disease', *Letters in Drug Design & Discovery*, vol. 3, no. 4, pp. 268-74.

Ottolenghi, A 1959, 'Interaction of ascorbic acid and mitochondrial lipides', *Archives of Biochemistry and Biophysics*, vol. 79, pp. 355-63.

Ou, B, Huang, D, Hampsch-Woodill, M, Flanagan, JA & Deemer, EK 2002, 'Analysis of antioxidant activities of common vegetables employing oxygen radical absorbance capacity (ORAC) and ferric reducing antioxidant power (FRAP) assays: a comparative study', *Journal of agricultural and food chemistry*, vol. 50, no. 11, pp. 3122-8.

Parr, RG 1980, *Density functional theory of atoms and molecules*, Horizons of Quantum Chemistry, Springer.

Pedersen, JT, Ostergaard, J, Rozlosnik, N, Gammelgaard, B & Heegaard, NH 2011, 'Cu (II) mediates kinetically distinct, non-amyloidogenic aggregation of amyloid- β peptides', *Journal of Biological Chemistry*, p. jbc. M111. 220863.

Pedersen, JT, Østergaard, J, Rozlosnik, N, Gammelgaard, B & Heegaard, NH 2011, 'Cu (II) mediates kinetically distinct, non-amyloidogenic aggregation of amyloid- β peptides', *Journal of Biological Chemistry*, vol. 286, no. 30, pp. 26952-63.

Peng, C, Ayala, PY, Schlegel, HB & Frisch, MJ 1996, 'Using redundant internal coordinates to optimize equilibrium geometries and transition states', *Journal of Computational Chemistry*, vol. 17, no. 1, pp. 49-56.

Pfaender, S & Grabrucker, AM 2014, 'Characterization of biometal profiles in neurological disorders', *Metallomics*, vol. 6, no. 5, pp. 960-77.

Pham-Huy, LA & He, H 'Free radicals, antioxidants in disease and health'.

Pham-Huy, LA, He, H & Pham-Huy, C 2008, 'Free radicals, antioxidants in disease and health', *International journal of biomedical science: IJBS*, vol. 4, no. 2, p. 89.

Prieto, P, Pineda, M & Aguilar, M 1999, 'Spectrophotometric quantitation of antioxidant capacity through the formation of a phosphomolybdenum complex: specific application to the determination of vitamin E', *Analytical biochemistry*, vol. 269, no. 2, pp. 337-41.

Prior, RL, Hoang, H, Gu, L, Wu, X, Bacchiocca, M, Howard, L, Hampsch-Woodill, M, Huang, D, Ou, B & Jacob, R 2003, 'Assays for hydrophilic and lipophilic antioxidant

capacity (oxygen radical absorbance capacity (ORACFL)) of plasma and other biological and food samples', *Journal of agricultural and food chemistry*, vol. 51, no. 11, pp. 3273-9.

Ramasamy, S, Chin, SP, Sukumaran, SD, Buckle, MJC, Kiew, LV & Chung, LY 2015, 'In silico and in vitro analysis of bacoside A aglycones and its derivatives as the constituents responsible for the cognitive effects of *Bacopa monnieri*', *PloS one*, vol. 10, no. 5, p. 0126565.

Rao, RV, Descamps, O, John, V & Bredesen, DE 2012, 'Ayurvedic medicinal plants for Alzheimer's disease: a review', *Alzheimers Res Ther*, vol. 4, no. 3, pp. 1-9.

Rastogi, S, Pal, R & Kulshreshtha, DK 1994, 'Bacoside A3 · A triterpenoid saponin from *Bacopa monniera*', *Phytochemistry*, vol. 36, no. 1, pp. 133-7.

Roodenrys, S, Booth, D, Bulzomi, S, Phipps, A, Micallef, C & Smoker, J 2002, 'Chronic effects of Brahmi (*Bacopa monnieri*) on human memory', *Neuropsychopharmacology*, vol. 27, no. 2, pp. 279-81.

Ruch, RJ, Cheng, S-j & Klaunig, JE 1989, 'Prevention of cytotoxicity and inhibition of intercellular communication by antioxidant catechins isolated from Chinese green tea', *Carcinogenesis*, vol. 10, no. 6, pp. 1003-8.

Russo, A & Borrelli, F 2005, 'Bacopa monniera, a reputed nootropic plant: an overview', *Phytomedicine*, vol. 12, no. 4, pp. 305-17.

Sadasivam, K & Kumaresan, R 2011, 'A comparative DFT study on the antioxidant activity of apigenin and scutellarein flavonoid compounds', *Molecular Physics*, vol. 109, no. 6, pp. 839-52.

Saeed, N, Khan, MR & Shabbir, M 2012, 'Antioxidant activity, total phenolic and total flavonoid contents of whole plant extracts *Torilis leptophylla* L', *BMC complementary and alternative medicine*, vol. 12, no. 1, p. 221.

Saini, N, Singh, D & Sandhir, R 2012, 'Neuroprotective effects of *Bacopa monnieri* in experimental model of dementia', *Neurochemical research*, vol. 37, no. 9, pp. 1928-37.

Sanz, M, Ferrandiz, M, Cejudo, M, Terencio, MC, Gil, B, Bustos, G, Ubeda, A, Gunasegaran, R & Alcaraz, M 1994, 'Influence of a series of natural flavonoids on free radical generating systems and oxidative stress', *Xenobiotica*, vol. 24, no. 7, pp. 689-99.

Sasaki, T, Li, W, Zaike, S, Asada, Y, Li, Q, Ma, F, Zhang, Q & Koike, K 2013a, 'Antioxidant lignoids from leaves of *Ribes nigrum*', *Phytochemistry*, vol. 95, pp. 333-40.

— 2013b, 'Antioxidant lignoids from the leaves of *Ribes nigrum*', *Phytochemistry*, vol. 95, pp. 333-40.

Säwe, J, Dahlström, B, Paalzow, L & Rane, A 1981, 'Morphine kinetics in cancer patients', *Clinical Pharmacology & Therapeutics*, vol. 30, no. 5, pp. 629-35.

Schlegel, HB 1982, 'Optimization of equilibrium geometries and transition structures', *Journal of Computational Chemistry*, vol. 3, no. 2, pp. 214-8.

Schultheis, LM & Donoghue, MJ 2004, 'Molecular phylogeny and biogeography of *Ribes* (Grossulariaceae), with an emphasis on gooseberries (subg. *Grossularia*)', *Systematic Botany*, vol. 29, no. 1, pp. 77-96.

Sebaugh, J 2011, 'Guidelines for accurate EC50/IC50 estimation', *Pharmaceutical statistics*, vol. 10, no. 2, pp. 128-34.

Seeram, NP, Henning, SM, Niu, Y, Lee, R, Scheuller, HS & Heber, D 2006, 'Catechin and caffeine content of green tea dietary supplements and correlation with antioxidant capacity', *Journal of agricultural and food chemistry*, vol. 54, no. 5, pp. 1599-603.

Sen, S & Chakraborty, R 2011, 'The role of antioxidants in human health', in *Oxidative stress: diagnostics, prevention, and therapy*, ACS Publications, pp. 1-37.

Shankar, GM, Li, S, Mehta, TH, Garcia-Munoz, A, Shepardson, NE, Smith, I, Brett, FM, Farrell, MA, Rowan, MJ & Lemere, CA 2008, 'Amyloid- β protein dimers isolated directly from Alzheimer's brains impair synaptic plasticity and memory', *Nature medicine*, vol. 14, no. 8, pp. 837-42.

Shen, L, Zhang, H-Y & Ji, H-F 2005, 'A theoretical study on Cu (II)-chelating properties of *curcumin* and its implications for *curcumin* as a multipotent agent to combat Alzheimer's disease', *Journal of Molecular Structure*, vol. 757, no. 1-3, pp. 199-202.

Shinomol, GK, Mythri, RB & Bharath, MS 2012, 'Bacopa monnieri extract offsets rotenone-induced cytotoxicity in dopaminergic cells and oxidative impairments in mice brain', *Cellular and molecular neurobiology*, vol. 32, no. 3, pp. 455-65.

- Shu, Y-Z 1998, 'Recent natural products based drug development: a pharmaceutical industry perspective', *Journal of natural products*, vol. 61, no. 8, pp. 1053-71.
- Singh, H, Rastogi, R, Srimal, R & Dhawan, B 1988, 'Effect of bacosides A and B on avoidance responses in rats', *Phytotherapy Research*, vol. 2, no. 2, pp. 70-5.
- Sletten, E & Fløgstad, N 1976, 'Crystallographic studies on metal–nucleotide base complexes. VII. Di-9-methylguaninetriaquacopper (II) sulphate trihydrate', *Acta Crystallographica Section B: Structural Crystallography and Crystal Chemistry*, vol. 32, no. 2, pp. 461-6.
- Sletten, E & Thorstensen, B 1974, 'Crystallographic studies of metal–nucleotide base complexes. IV. Tetraaquo-(9-methyladenine) copper (II) sulphate monohydrate', *Acta Crystallographica Section B: Structural Crystallography and Crystal Chemistry*, vol. 30, no. 10, pp. 2438-43.
- Slimestad, R & Solheim, H 2002, 'Anthocyanins from black currants (*Ribes nigrum* L.)', *Journal of agricultural and food chemistry*, vol. 50, no. 11, pp. 3228-31.
- Soler-Rivas, C, Espín, JC & Wichers, HJ 2000, 'An easy and fast test to compare total free radical scavenger capacity of foodstuffs', *Phytochemical Analysis: An International Journal of Plant Chemical and Biochemical Techniques*, vol. 11, no. 5, pp. 330-8.
- Steinberg, D 1991, 'Antioxidants and atherosclerosis. A current assessment', *Circulation*, vol. 84, no. 3, pp. 1420-5.
- Stephens, NG, Parsons, A, Brown, M, Schofield, P, Kelly, F, Cheeseman, K & Mitchinson, M 1996, 'Randomised controlled trial of vitamin E in patients with coronary disease: Cambridge Heart Antioxidant Study (CHAOS)', *The Lancet*, vol. 347, no. 9004, pp. 781-6.
- Stough, C, Lloyd, J, Clarke, J, Downey, L, Hutchison, C, Rodgers, T & Nathan, P 2001, 'The chronic effects of an extract of *Bacopa monniera* (Brahmi) on cognitive function in healthy human subjects', *Psychopharmacology*, vol. 156, no. 4, pp. 481-4.
- Street, DA, Comstock, GW, Salkeld, RM, Schüep, W & Klag, MJ 1994, 'Serum antioxidants and myocardial infarction. Are low levels of carotenoids and alpha-tocopherol risk factors for myocardial infarction?', *Circulation*, vol. 90, no. 3, pp. 1154-61.

Tabart, J, Franck, T, Kevers, C, Pincemail, J, Serteyn, D, Defraigne, J-O & Dommes, J 2012, 'Antioxidant and anti-inflammatory activities of Ribes nigrum extracts', *Food Chemistry*, vol. 131, no. 4, pp. 1116-22.

Terada, H, Muraoka, S & Fujita, T 1974, 'Structure activity relations. 7. Structure-activity relations of fenamic acids', *Journal of medicinal chemistry*, vol. 17, no. 3, pp. 330-4.

Thomas, RB, Joy, S, Ajayan, M & Paulose, C 2013, 'Neuroprotective potential of Bacopa monnieri and Bacoside A against dopamine receptor dysfunction in the cerebral cortex of neonatal hypoglycaemic rats', *Cellular and molecular neurobiology*, vol. 33, no. 8, pp. 1065-74.

Tõugu, V, Karafin, A, Zovo, K, Chung, RS, Howells, C, West, AK & Palumaa, P 2009, 'Zn (II)-and Cu (II)-induced non-fibrillar aggregates of amyloid- β (1–42) peptide are transformed to amyloid fibrils, both spontaneously and under the influence of metal chelators', *Journal of neurochemistry*, vol. 110, no. 6, pp. 1784-95.

Tripathi, YB, Chaurasia, S, Tripathi, E, Upadhyay, A & Dubey, G 1996, 'Bacopa monniera Linn. as an antioxidant: mechanism of action', *Indian Journal of Experimental Biology*, vol. 34, no. 6, pp. 523-6.

Tugcu, G, Saçan, MT, Vracko, M, Novic, M & Minovski, N 2012, 'QSTR modelling of the acute toxicity of pharmaceuticals to fish', *SAR and QSAR in Environmental Research*, vol. 23, no. 3-4, pp. 297-310.

Uabundit, N, Wattanathorn, J, Mucimapura, S & Ingkaninan, K 2010, 'Cognitive enhancement and neuroprotective effects of Bacopa monnieri in Alzheimer's disease model', *Journal of ethnopharmacology*, vol. 127, no. 1, pp. 26-31.

Uttara, B, Singh, AV, Zamboni, P & Mahajan, R 2009, 'Oxidative stress and neurodegenerative diseases: a review of upstream and downstream antioxidant therapeutic options', *Current neuropharmacology*, vol. 7, no. 1, pp. 65-74.

Valko, M, Rhodes, C, Moncol, J, Izakovic, M & Mazur, M 2006, 'Free radicals, metals and antioxidants in oxidative stress-induced cancer', *Chemico-biological interactions*, vol. 160, no. 1, pp. 1-40.

Vollala, V, Upadhyaya, S & Nayak, S 2011, 'Learning and memory-enhancing effect of Bacopa monniera in neonatal rats', *Bratislavske lekarske listy*, vol. 112, no. 12, pp. 663-9.

Vollala, VR, Upadhya, S & Nayak, S 2010, 'Effect of *Bacopa monniera* Linn.(brahmi) extract on learning and memory in rats: A behavioral study', *Journal of Veterinary Behavior*, vol. 5, no. 2, pp. 69-74.

Wijtmans, M, Pratt, DA, Valgimigli, L, DiLabio, GA, Pedulli, GF & Porter, NA 2003, '6-Amino-3-Pyridinols: Towards Diffusion-Controlled Chain-Breaking Antioxidants', *Angewandte Chemie International Edition*, vol. 42, no. 36, pp. 4370-3.

Willcox, JK, Ash, SL & Catignani, GL 2004, 'Antioxidants and prevention of chronic disease', *Critical reviews in food science and nutrition*, vol. 44, no. 4, pp. 275-95.

Woldu, AS & Mai, J 2012, 'Computation of the bond dissociation enthalpies and free energies of hydroxylic antioxidants using the ab initio Hartree–Fock method', *Redox Report*, vol. 17, no. 6, pp. 252-74.

Yoshiike, Y, Tanemura, K, Murayama, O, Akagi, T, Murayama, M, Sato, S, Sun, X, Tanaka, N & Takashima, A 2001, 'New insights on how metals disrupt amyloid β -aggregation and their effects on amyloid- β cytotoxicity', *Journal of Biological Chemistry*.

Yuan, H, Ma, Q, Ye, L & Piao, G 2016, 'The traditional medicine and modern medicine from natural products', *Molecules*, vol. 21, no. 5, p. 559.

Zehl, M, Pittenauer, E, Jirovetz, L, Bandhari, P, Singh, B, Kaul, VK, Rizzi, A & Allmaier, G 2007, 'Multistage and tandem mass spectrometry of glycosylated triterpenoid saponins isolated from *Bacopa monnieri* : comparison of the information content provided by different techniques', *Analytical chemistry*, vol. 79, no. 21, pp. 8214-21.

Zhao, L, Chen, X-J, Zhu, J, Xi, Y-B, Yang, X, Hu, L-D, Ouyang, H, Patel, SH, Jin, X & Lin, D 2015, 'Lanosterol reverses protein aggregation in cataracts', *Nature*, vol. 523, no. 7562, pp. 607-11.

Zhishen, J, Mengcheng, T & Jianming, W 1999, 'The determination of flavonoid contents in mulberry and their scavenging effects on superoxide radicals', *Food Chemistry*, vol. 64, no. 4, pp. 555-9.

Zhou, L-X, Du, J-T, Zeng, Z-Y, Wu, W-H, Zhao, Y-F, Kanazawa, K, Ishizuka, Y, Nemoto, T, Nakanishi, H & Li, Y-M 2007, 'Copper (II) modulates in vitro aggregation of a tau peptide', *Peptides*, vol. 28, no. 11, pp. 2229-34.

Appendices

PART A

Molecule **1** - ribesin A - (7R,7'R)-8(8')-ene-4,4'-dihydroxy-7,7'-epoxylignan

Molecule **2** - ribesin B - (7R,7'R)-8(8')-ene-4,4'-dihydroxy-3,3'-dimethoxy-7,7'-epoxylignan

Molecule **3** - ribesin C - (7S,7'S,8R)-8'(9')-ene-4,4'-dihydroxy-7,7'-epoxylignan

Molecule **4** - ribesin D - (7S,7'S,8R)-8'(9')-ene-4,4'-dihydroxy-3,3'-dimethoxy-7,7'-epoxylignan

Molecule **5** - (7S,7'S,8R,8'S)-4,4'-dihydroxy-7,7'-epoxylignan

Molecule **7** - ribesin E - rel-(7R,8S,7'S,8'R)-4,4'-dihydroxy-3'-[1-methyl-2-(4-hydroxyphenyl)]ethyl-7,7'-epoxylignan

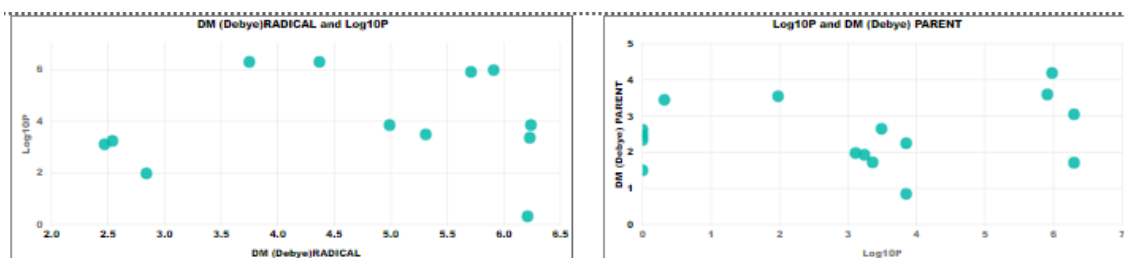
Molecule **8** - ribesin F - rel-(7R,8R,7'S,8'S)-4,4'-dihydroxy-3'-[1-methyl-2-(4-hydroxyphenyl)]ethyl-7,7'-epoxylignan.

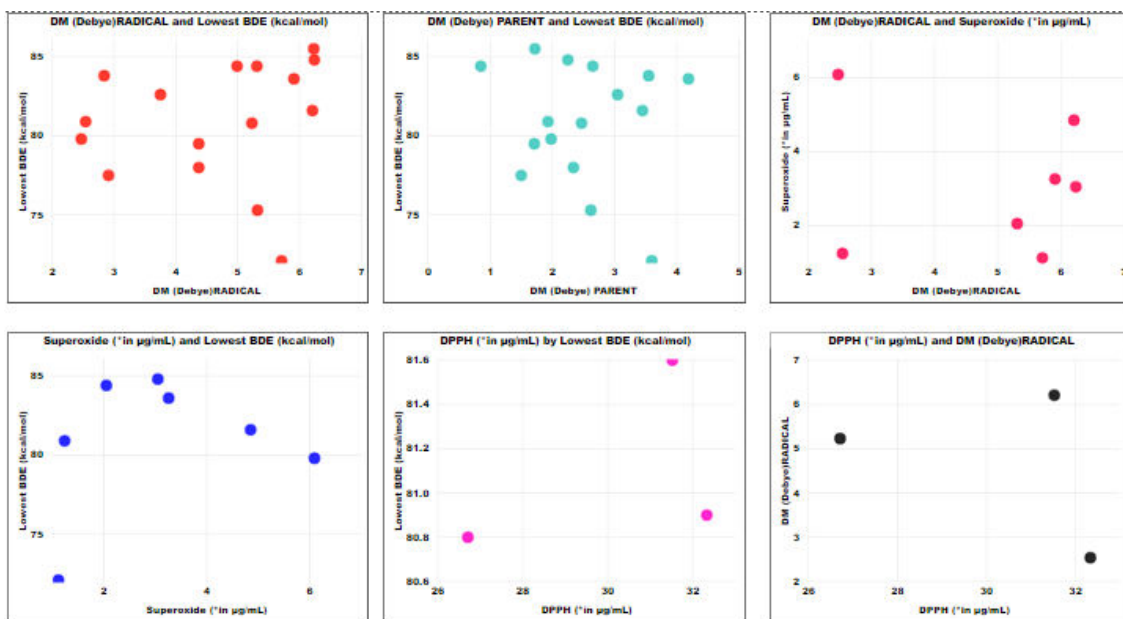
Molecule **9** - ribesin G - rel-(7R,8R,7'S,8'R)-3,4,4'-trihydroxy-3'-[1-methyl-2-(4-hydroxyphenyl)]ethyl-7,7'-epoxylignan.

Molecule **10** - ribesin H - rel-(2R,3S,5S,1'S,3'R)-2,5,1',3'-tetra(4hydroxyphenyl)-4-methylene-4,5,3',4',6',7'-hexahydro-1'H,2Hspiro[furan-3,5'-isobenzofuran]

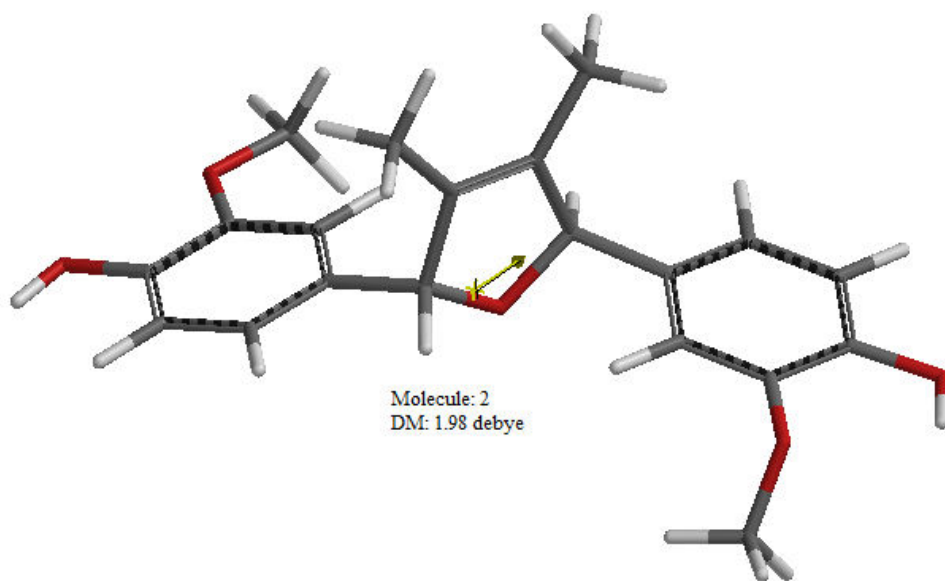
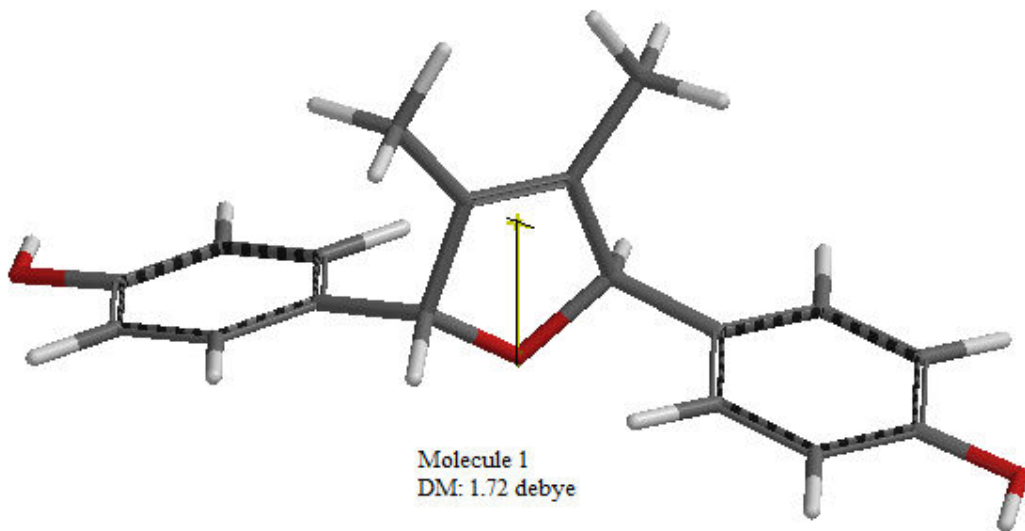
Molecule **15** - (7S,70S,8R,80S)-4,40-dihydroxy-3,30-dimethoxy-7,70-epoxylignan

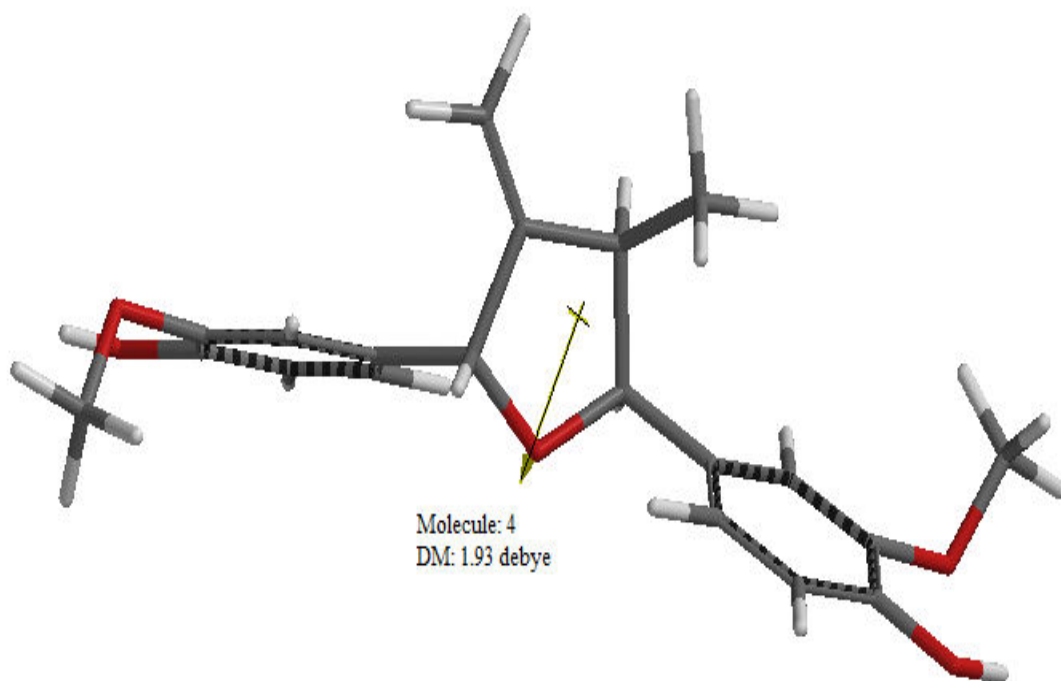
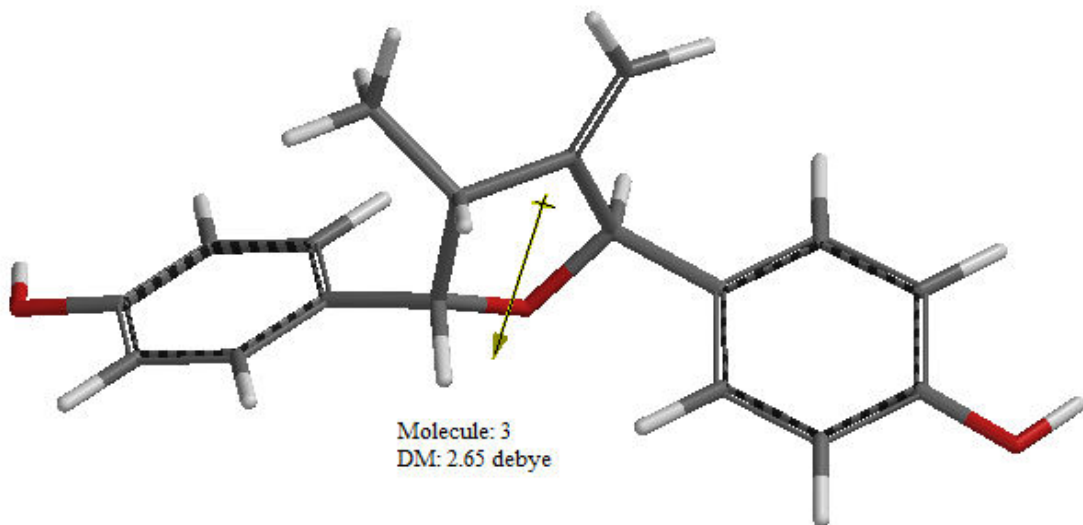
Scatter Plots

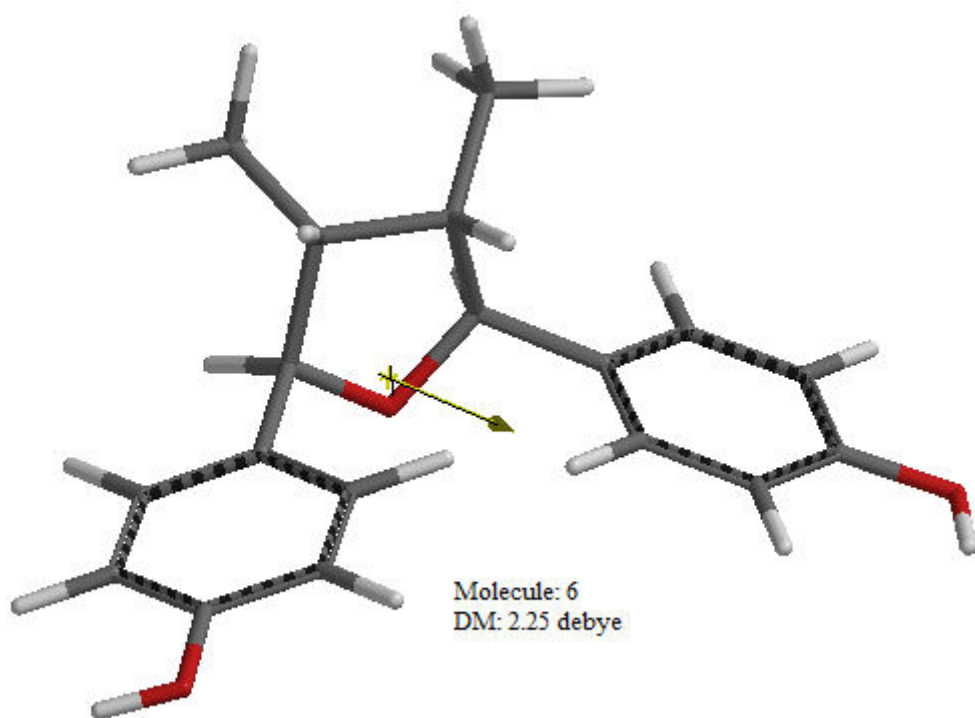
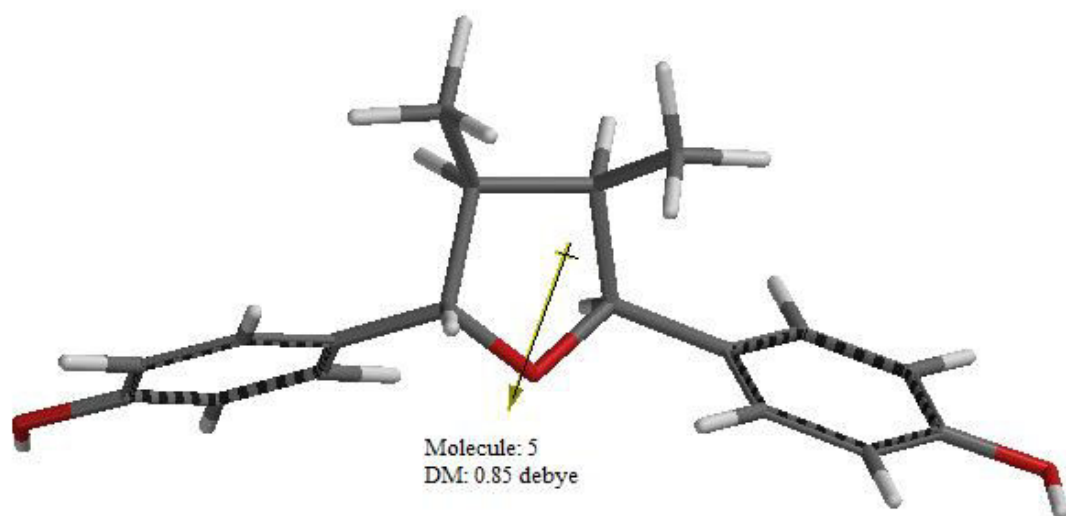


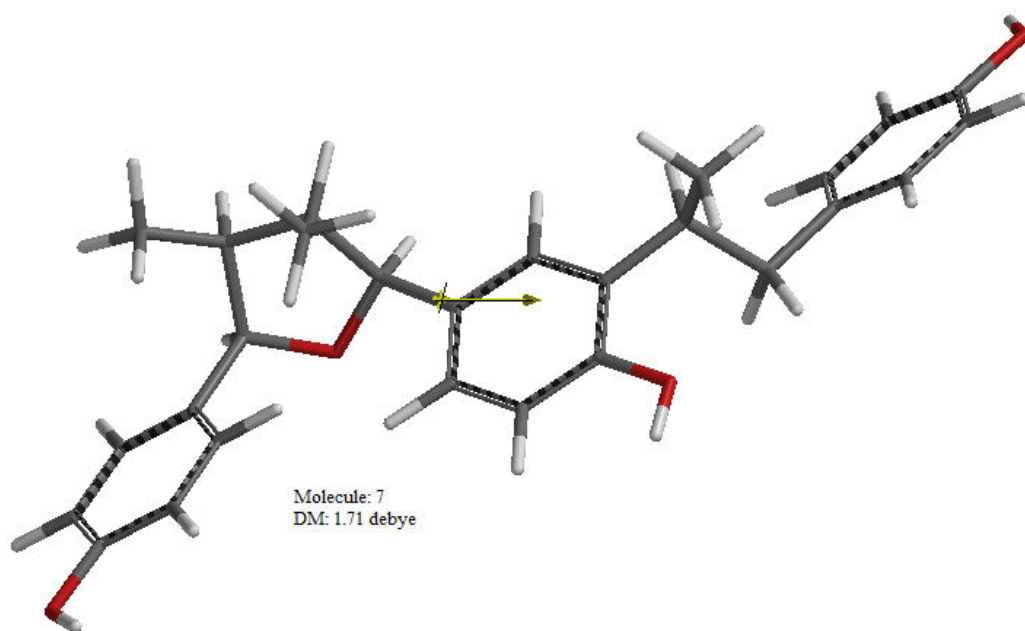


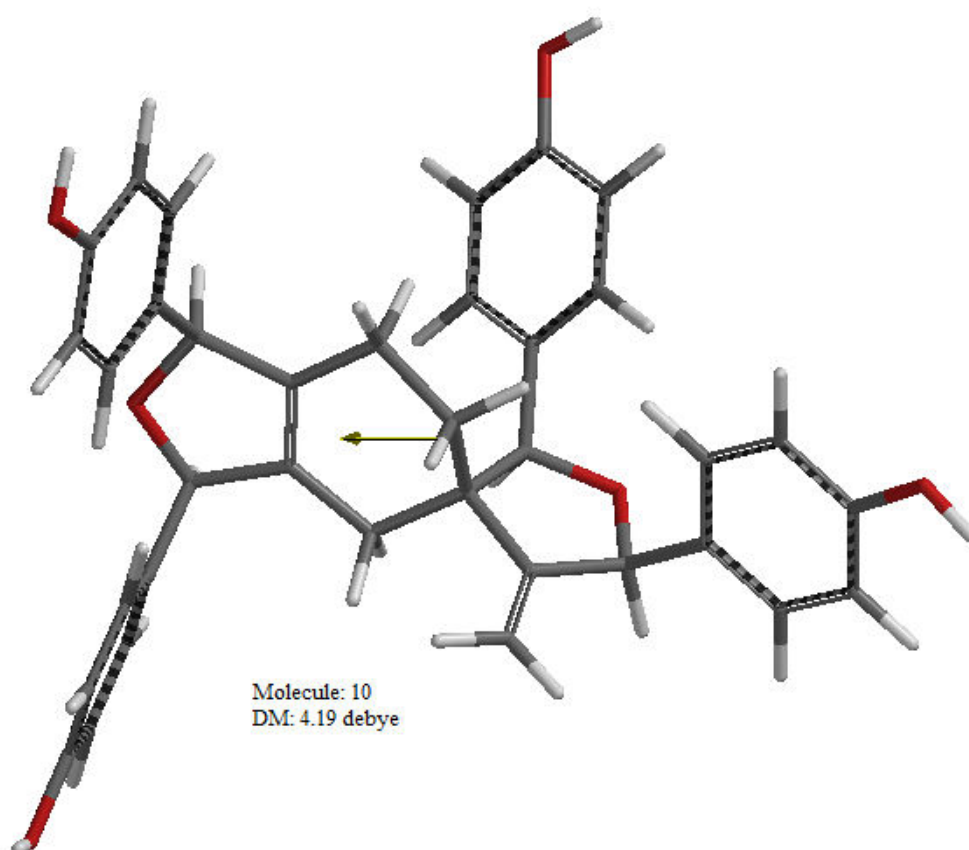
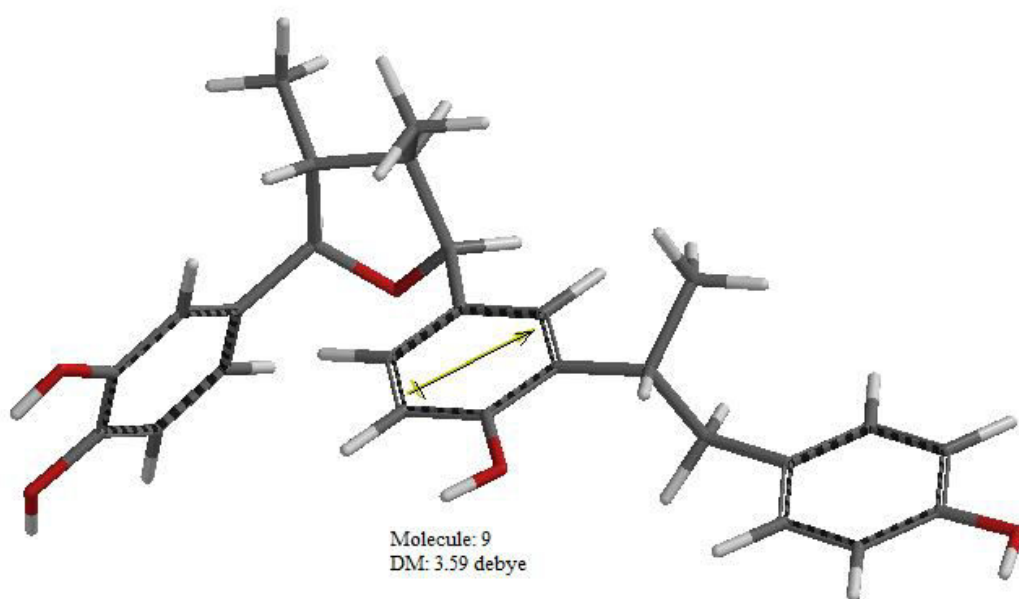
Superoxide scavenging activity is inversely proportional to BDE, the molecules with least BDE show better superoxide scavenging activity. The cluster is observed in the scatter plot of BDE vs. DM indicates the effect of DM influences BDEs.

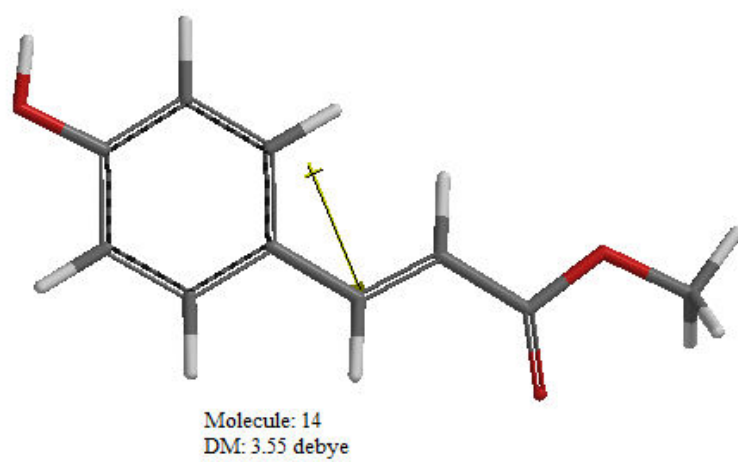
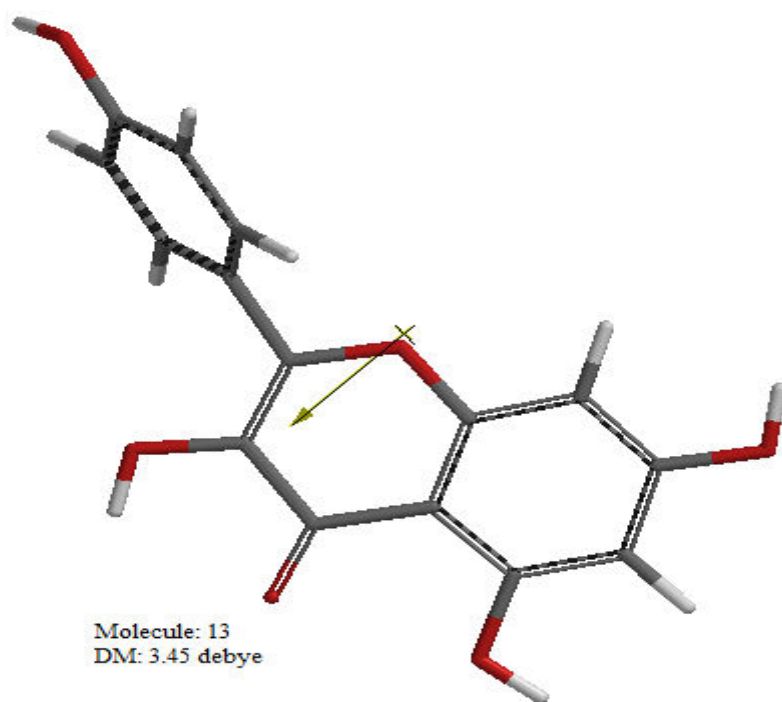


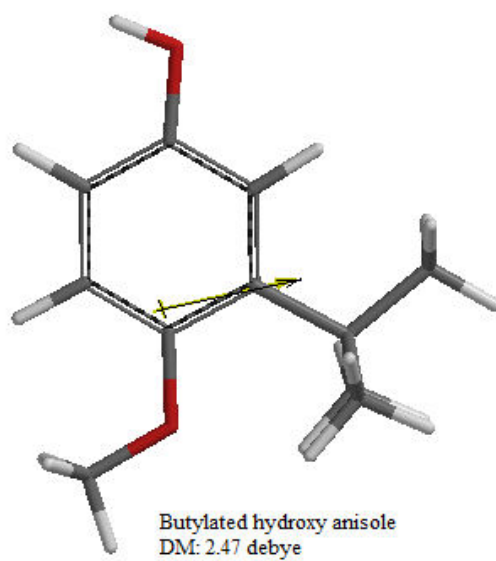
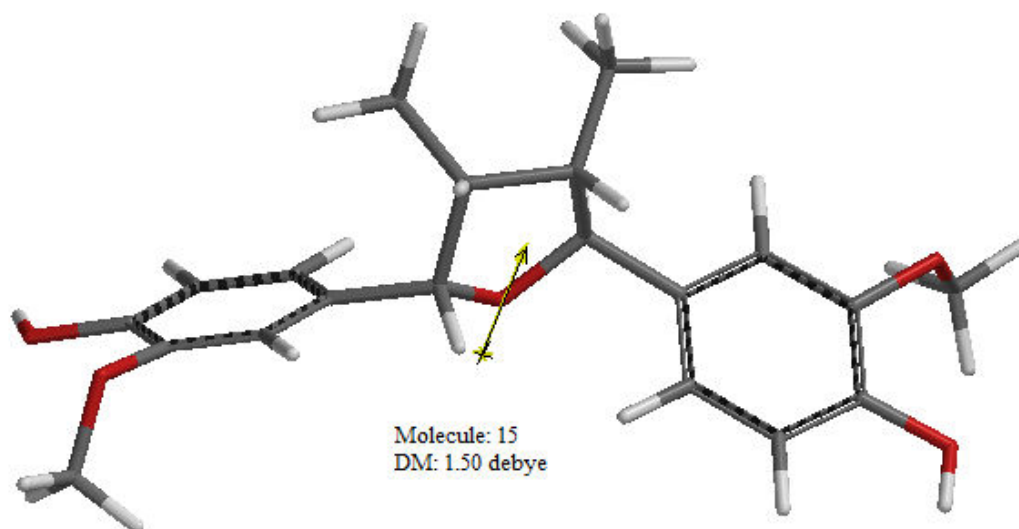




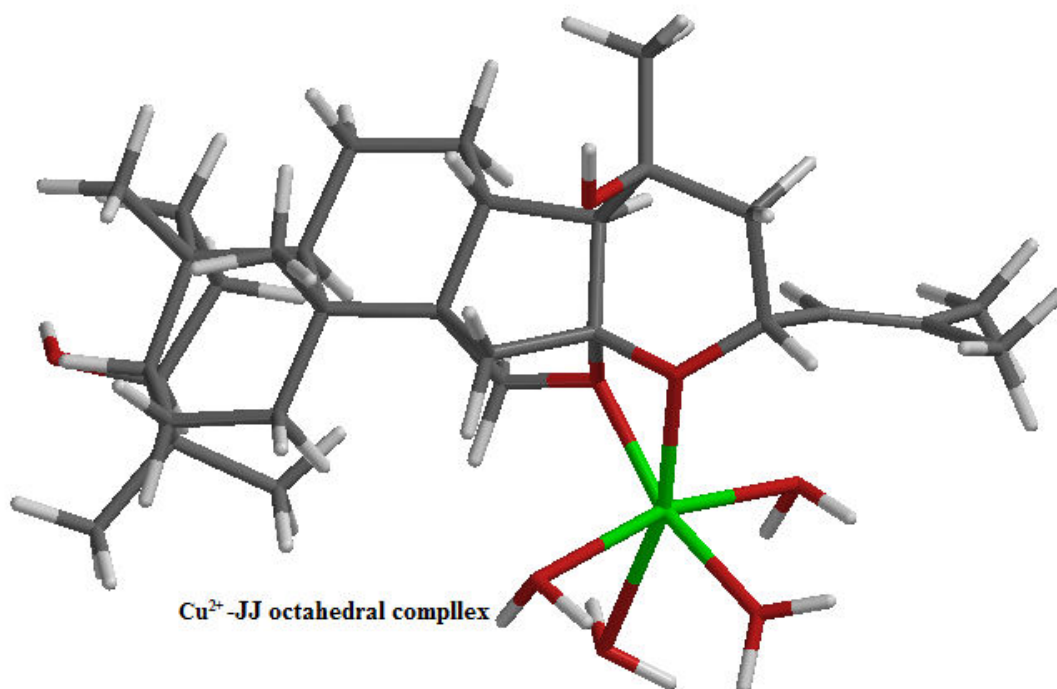
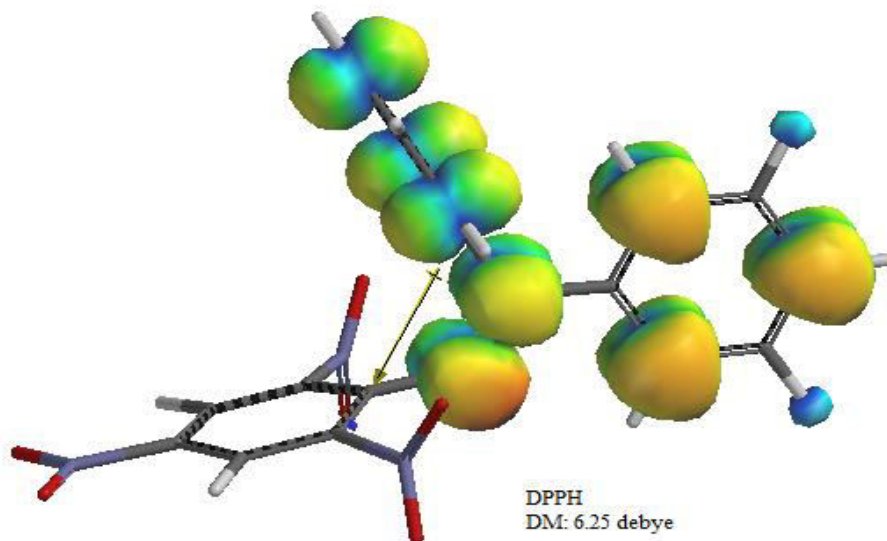


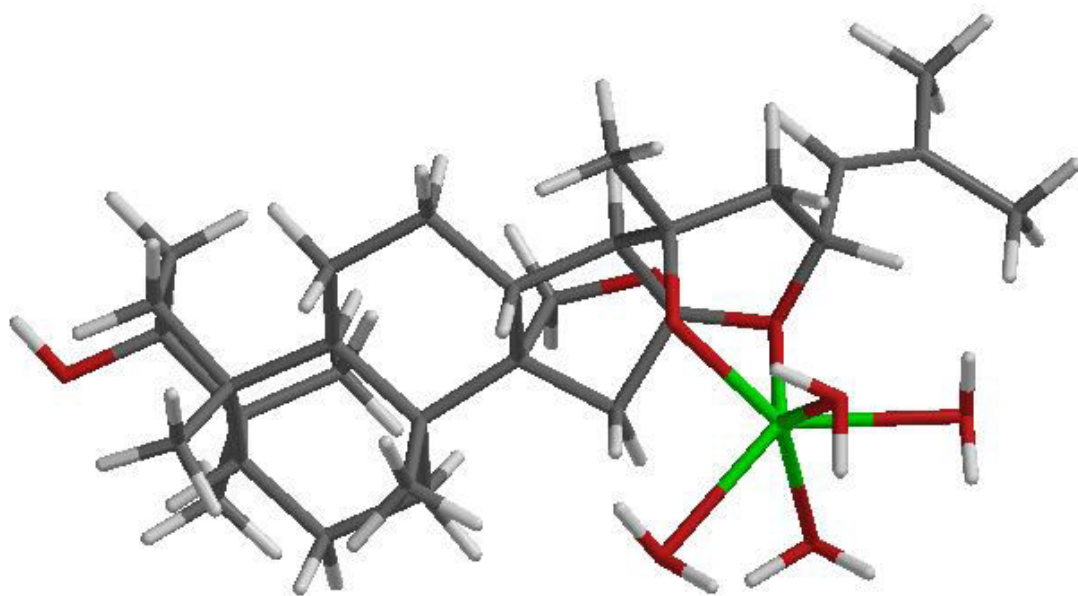




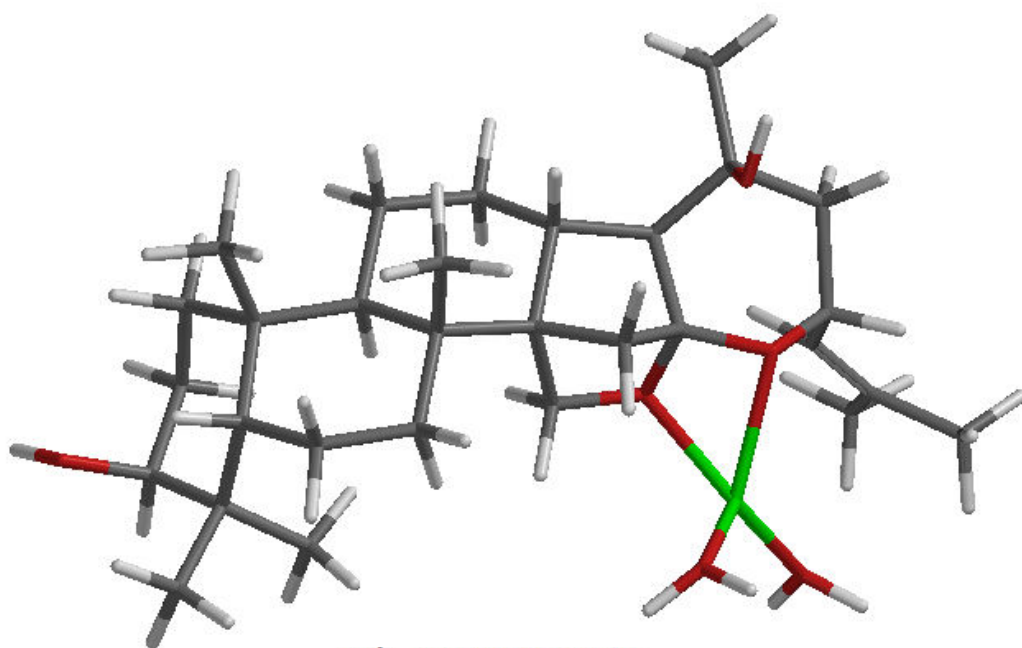


PART B

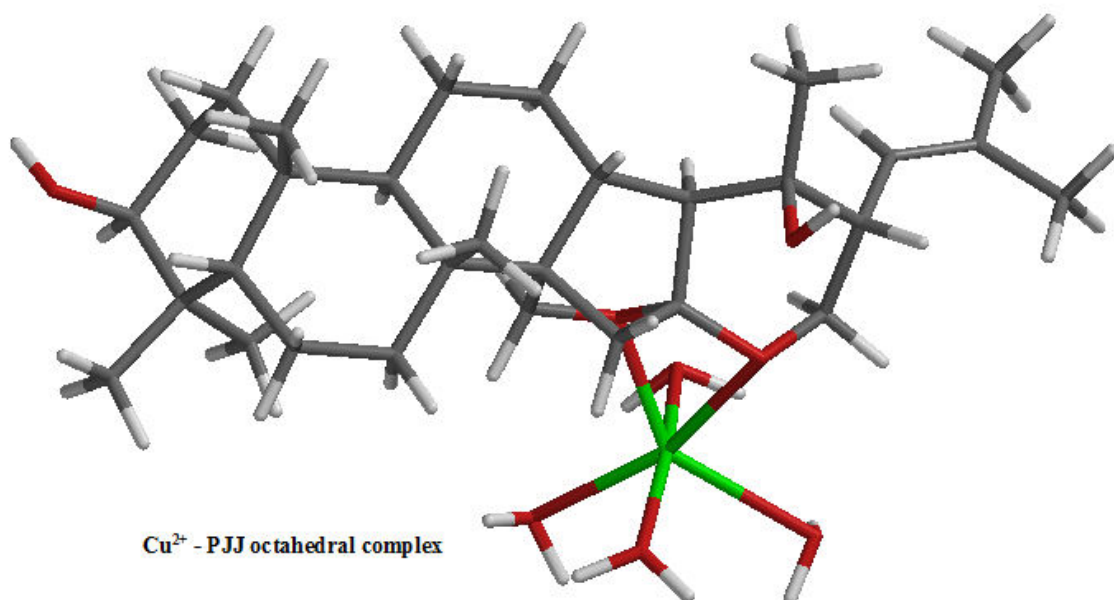
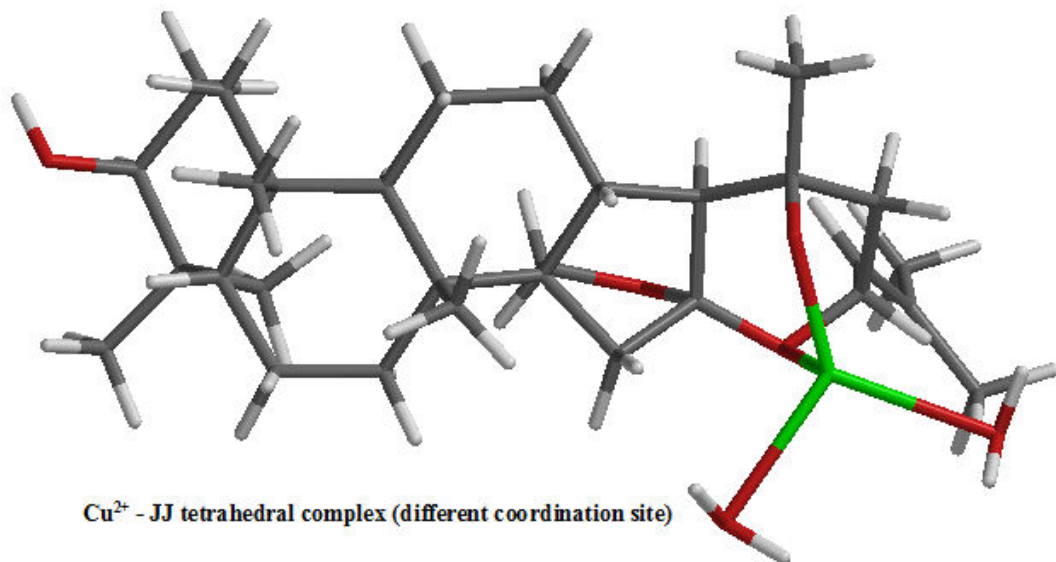


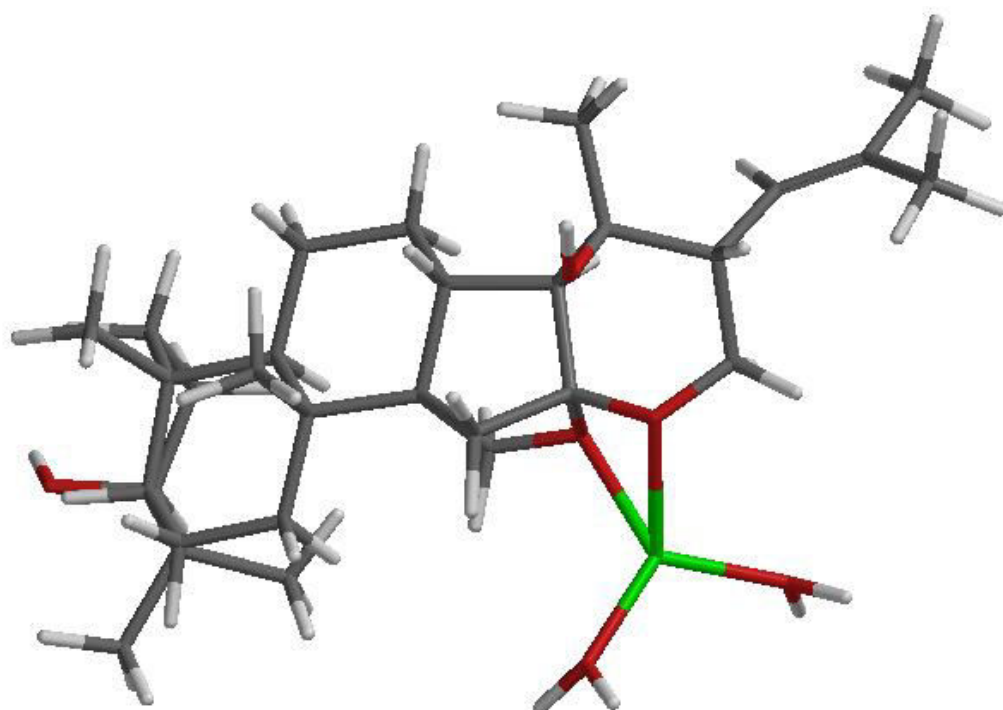
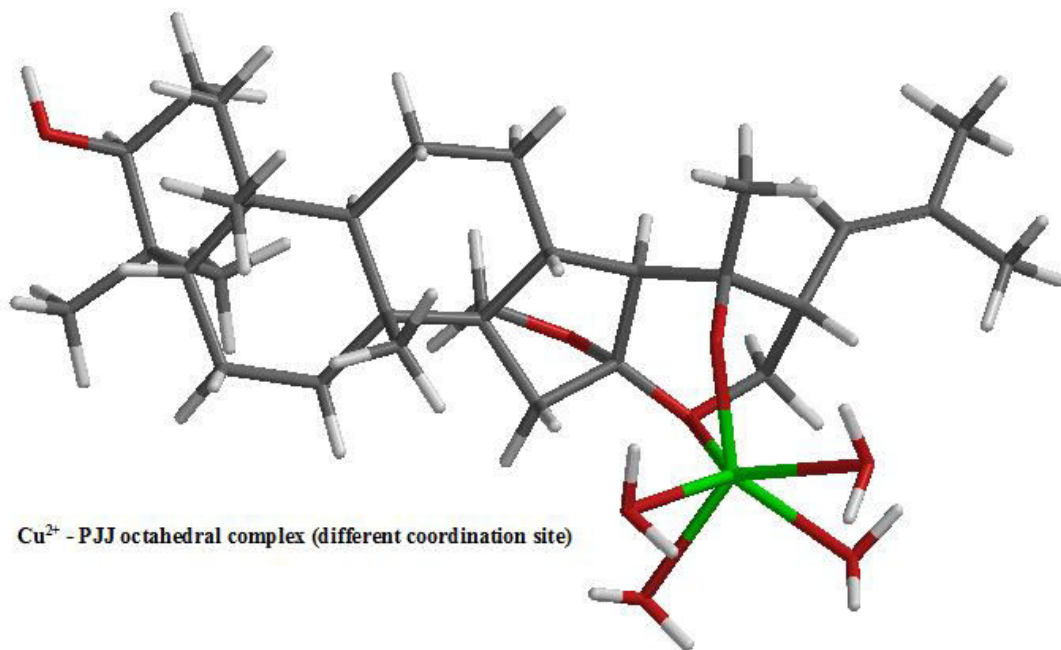


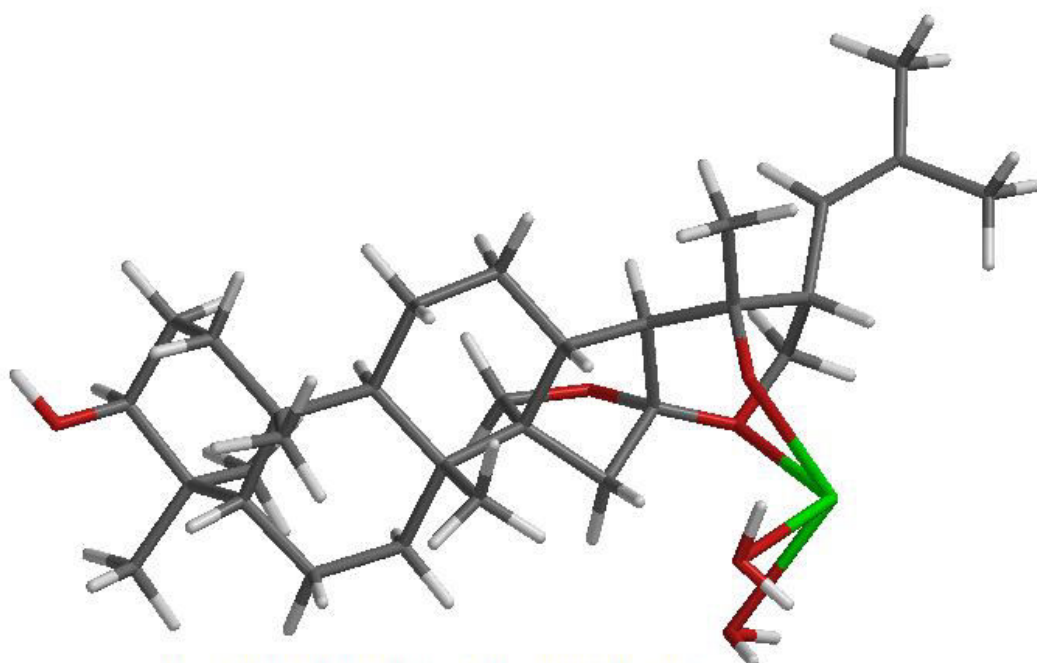
Cu²⁺ - JJ octahedral complex (different coordination site)



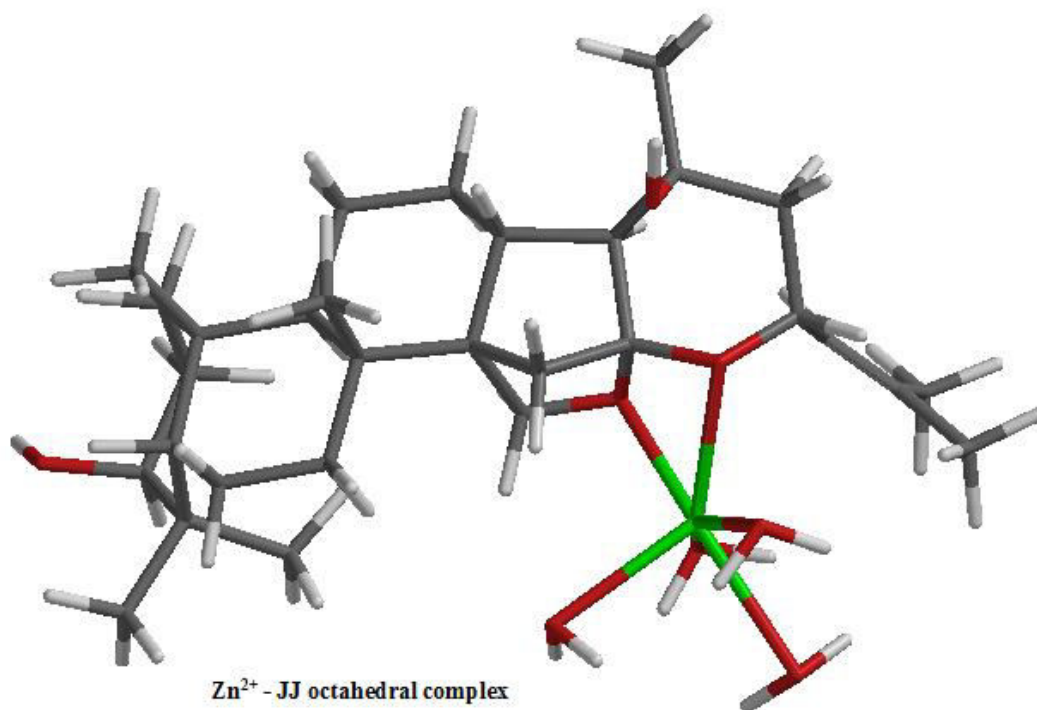
Cu²⁺ - JJ tetrahedral complex



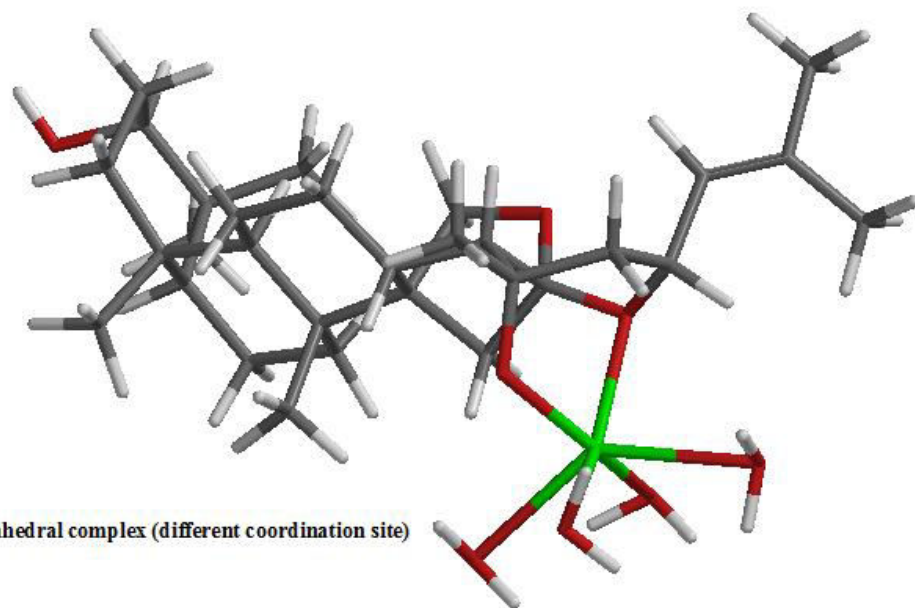




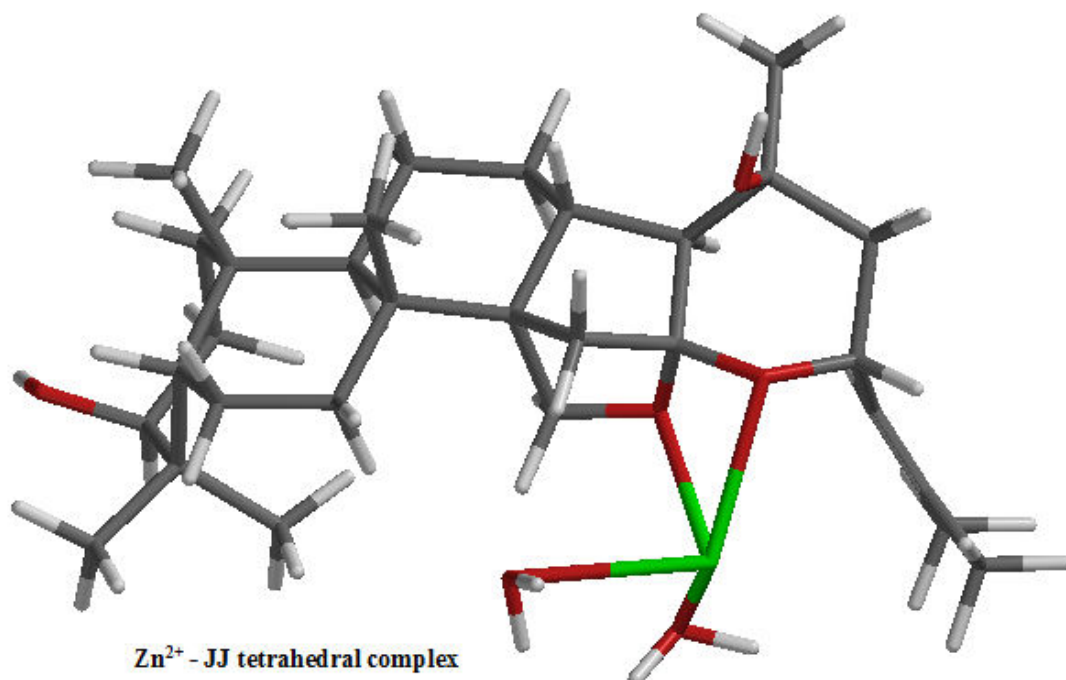
Cu²⁺ - PJJ tetrahedral complex (different coordination site)



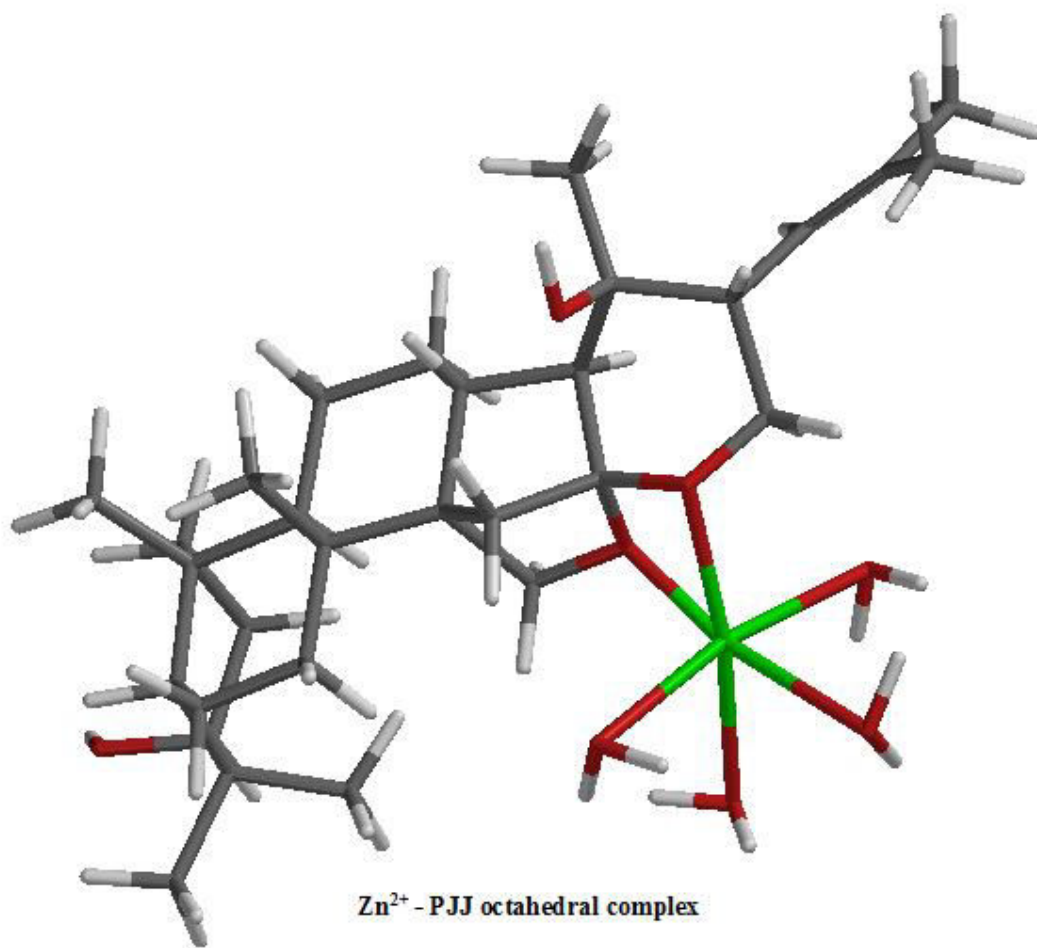
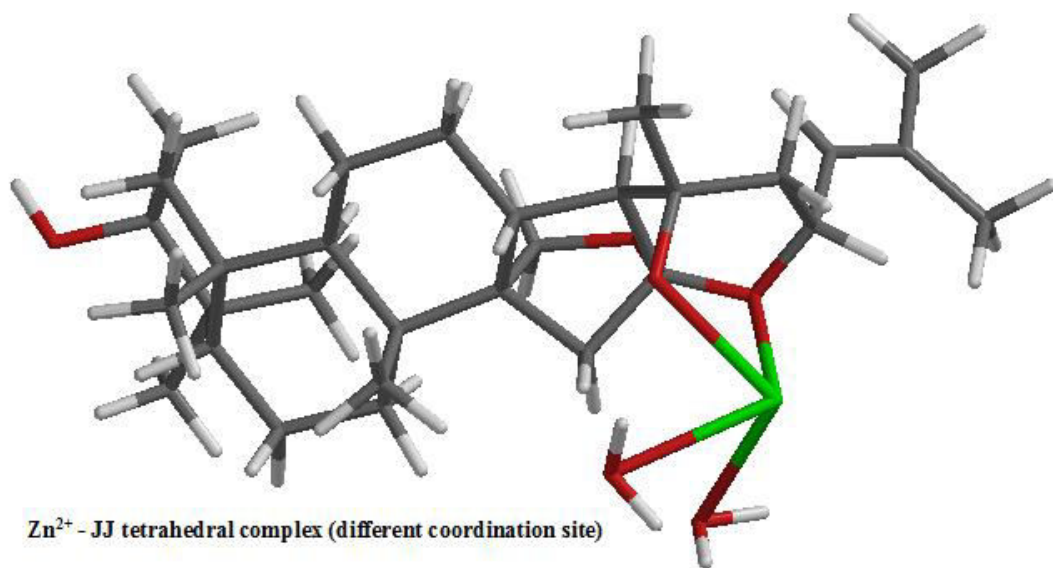
Zn²⁺ - JJ octahedral complex

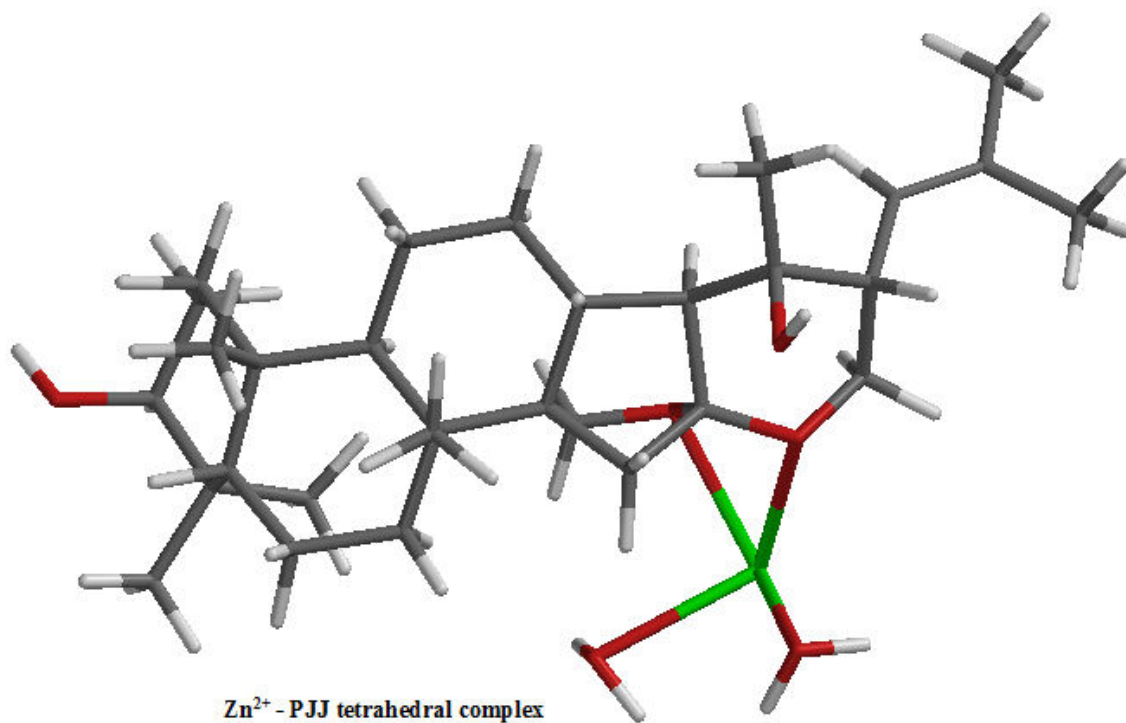
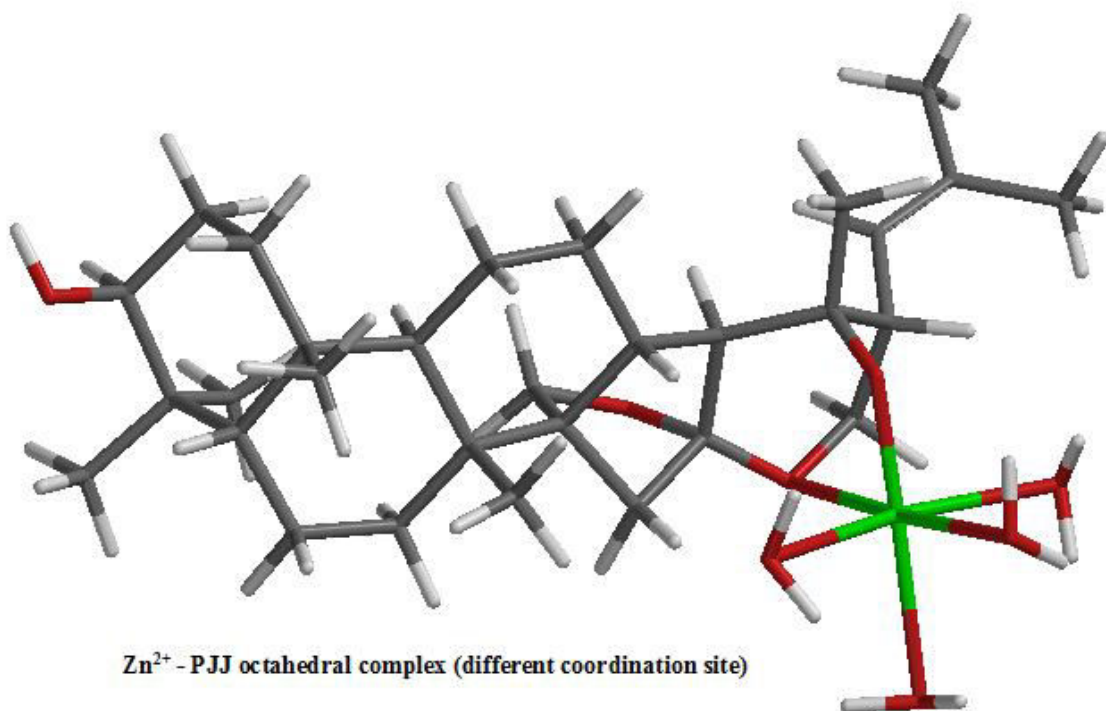


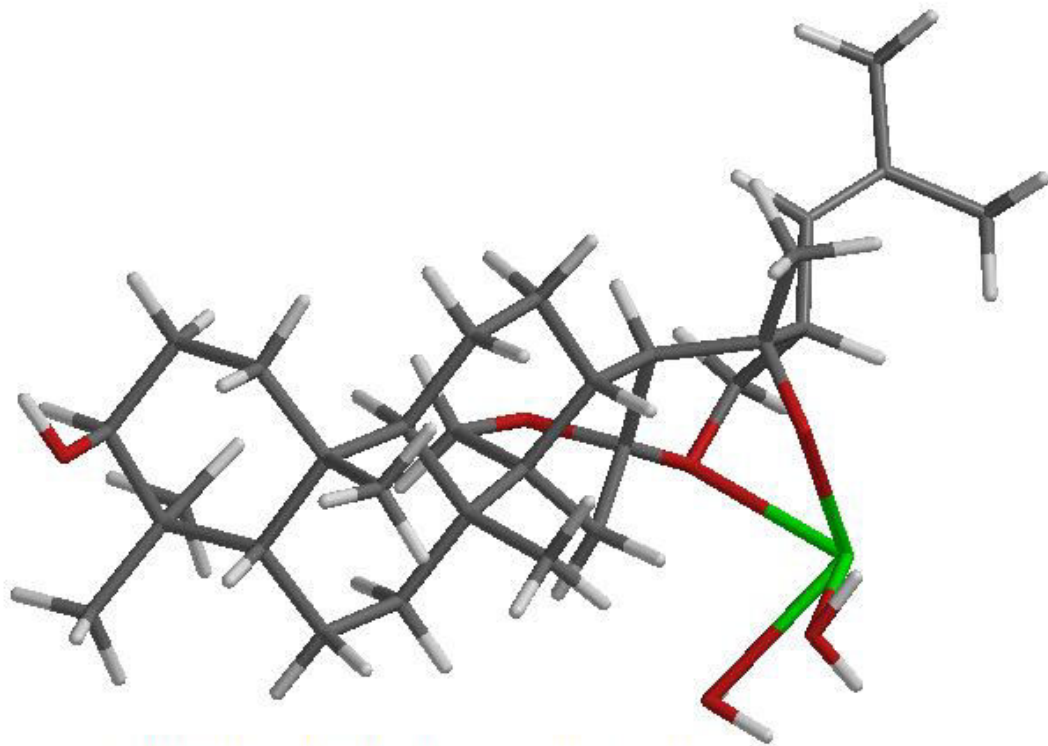
Zn²⁺ - JJ octahedral complex (different coordination site)



Zn²⁺ - JJ tetrahedral complex



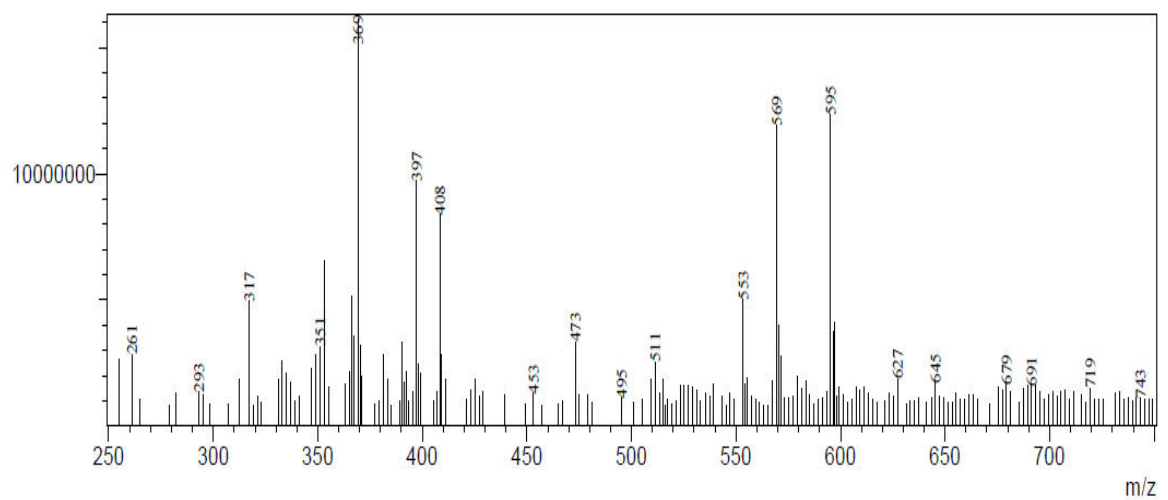




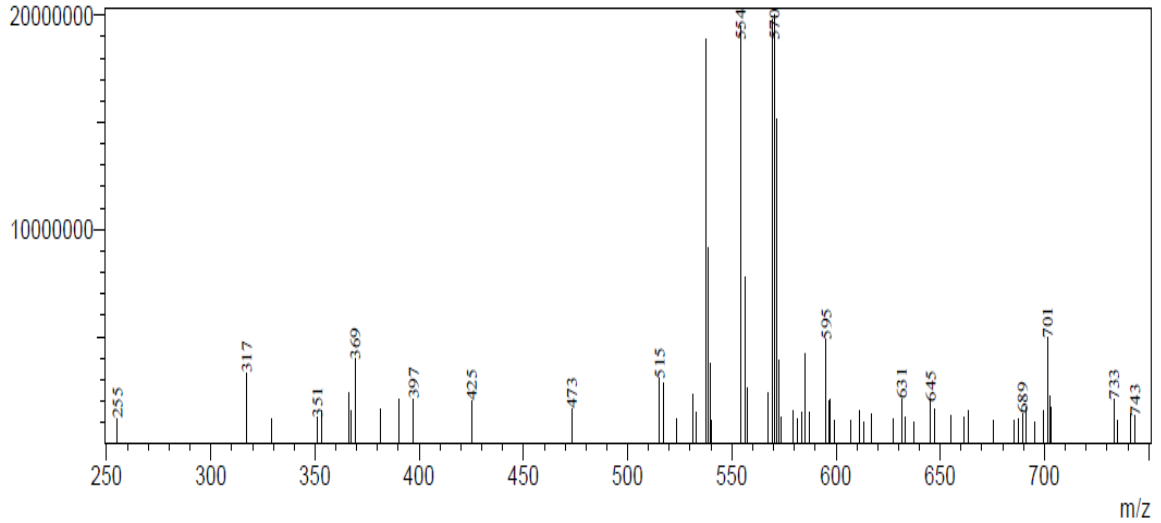
Zn²⁺ - PJJ tetrahedral complex (different coordination site)

ESI-MS (both positive and negative ion mode) of all the fractions of Ethyl acetate extract

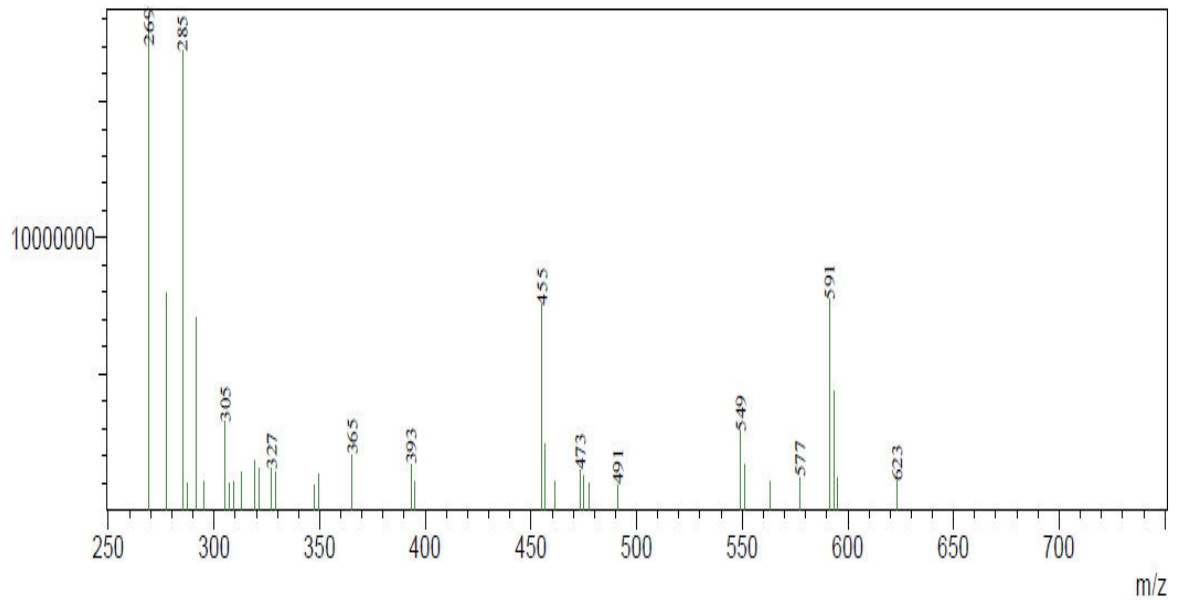
MassPeaks:183 BasePeak:369(16135249)
 Spectrum Mode:Averaged 0.196-0.207(77-81)
 BG Mode:Calc Polarity:Positive Segment 1 - Event 1 Fraction 2



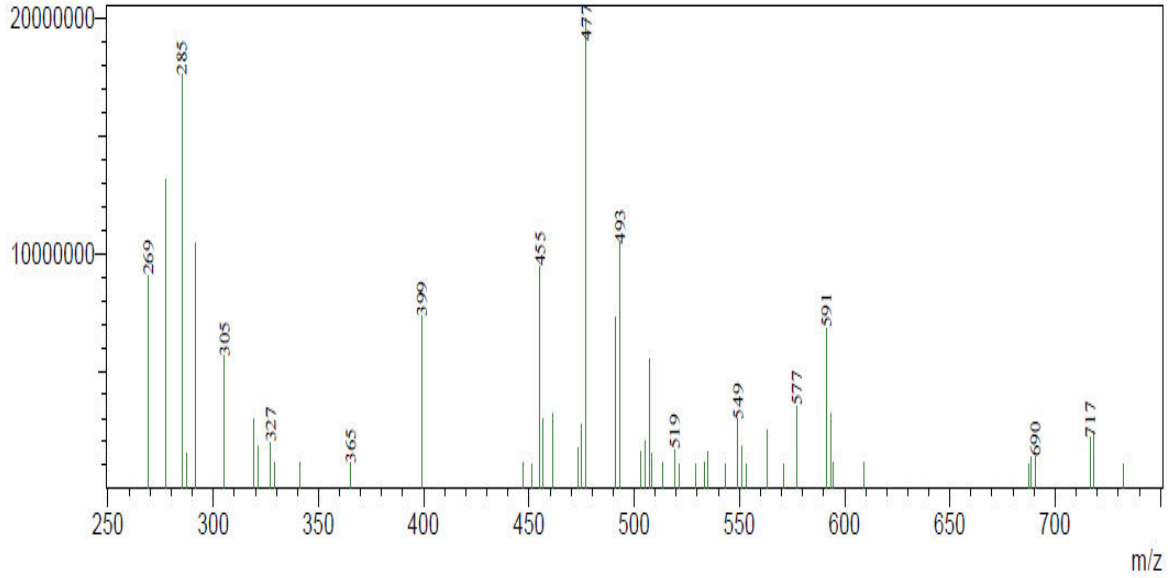
MassPeaks:67 BasePeak:570(20000000)
Spectrum Mode:Averaged 0.124-0.134(49-53)
BG Mode:Calc Polarity:Positive Segment 1 - Event 1 Fraction 3



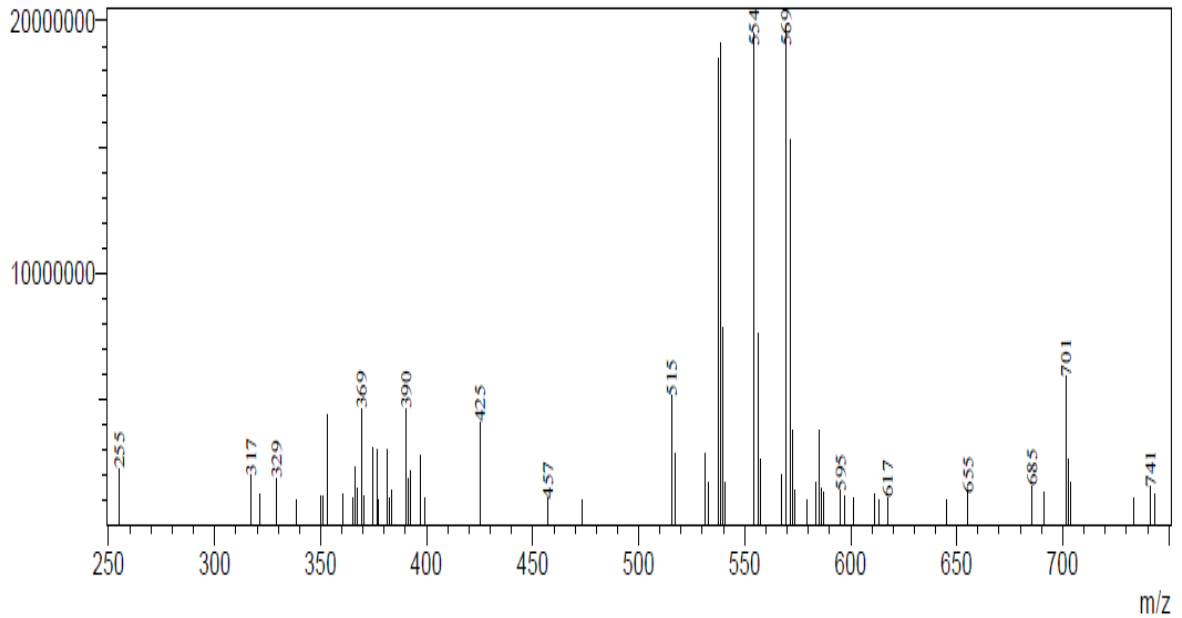
MassPeaks:34 BasePeak:269(18216076)
Spectrum Mode:Averaged 0.199-0.209(78-82)
BG Mode:Calc Polarity:Negative Segment 1 - Event 2 Fraction 2



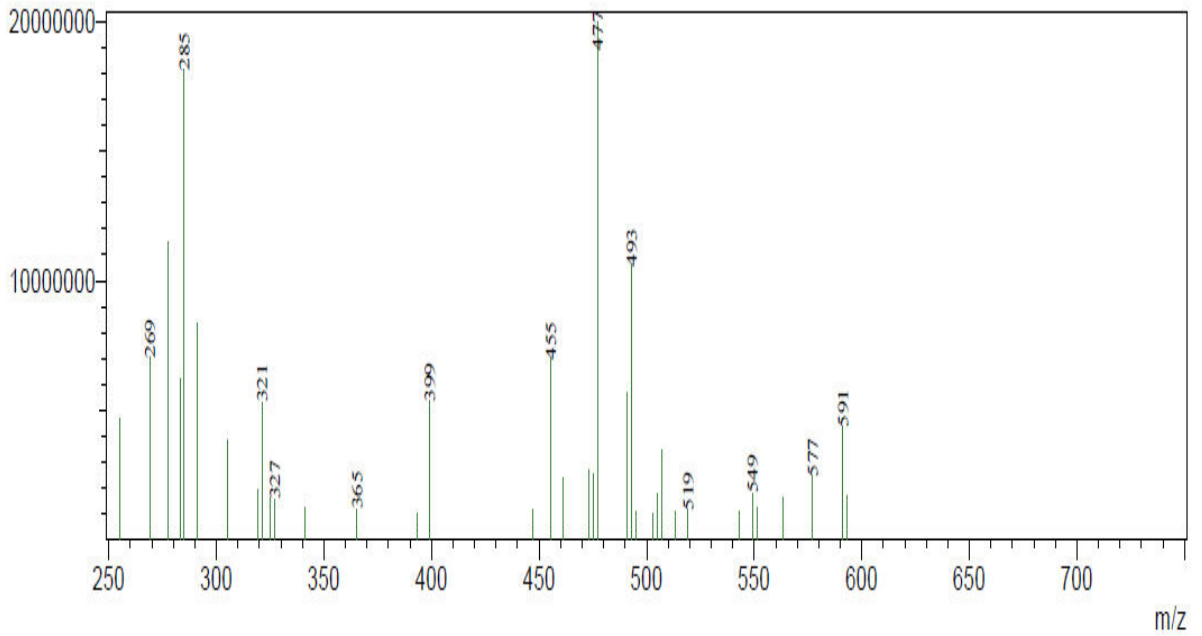
MassPeaks:50 BasePeak:477(20000000)
Spectrum Mode:Averaged 0.127-0.137(50-54)
BG Mode:Calc Polarity:Negative Segment 1 - Event 2 Fraction 3



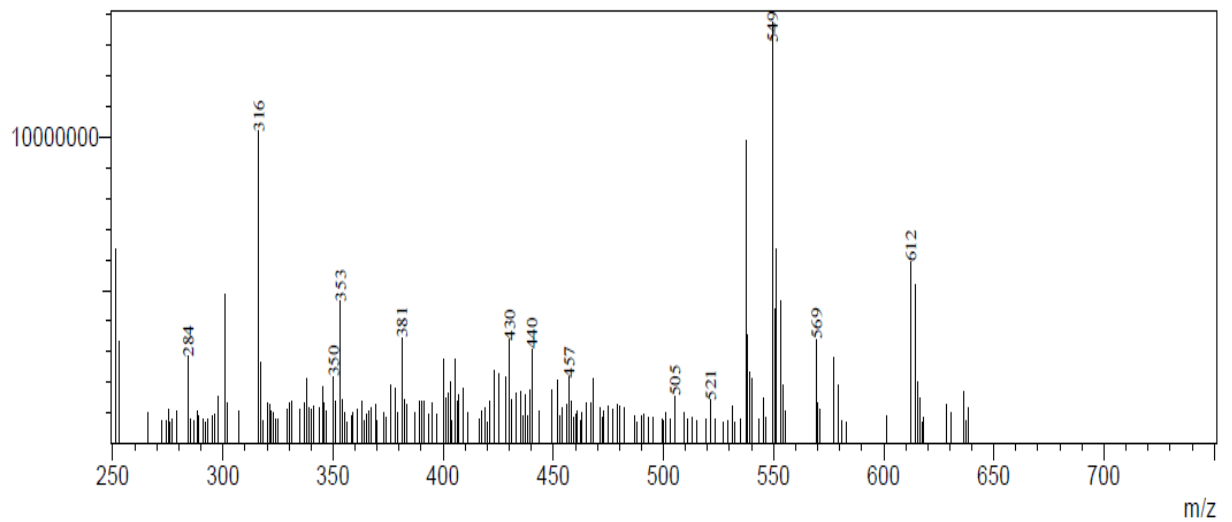
MassPeaks:65 BasePeak:569(19793500)
Spectrum Mode:Averaged 0.129-0.140(51-55)
BG Mode:Calc Polarity:Positive Segment 1 - Event 1 Fraction 4



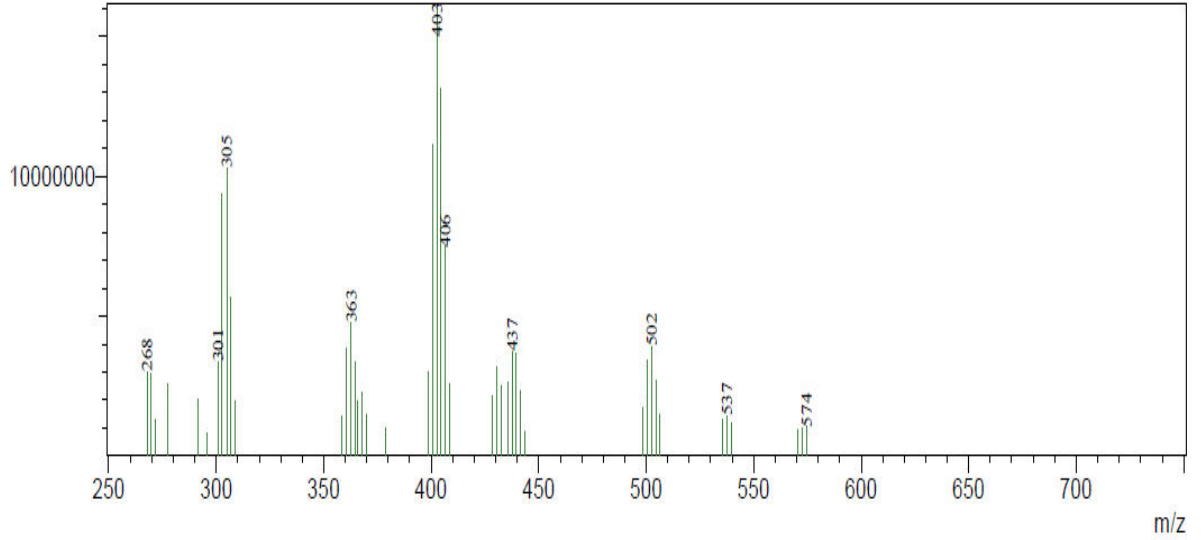
MassPeaks:36 BasePeak:477(20000000)
Spectrum Mode:Averaged 0.132-0.142(52-56)
BG Mode:Calc Polarity:Negative Segment 1 - Event 2 Fraction 4



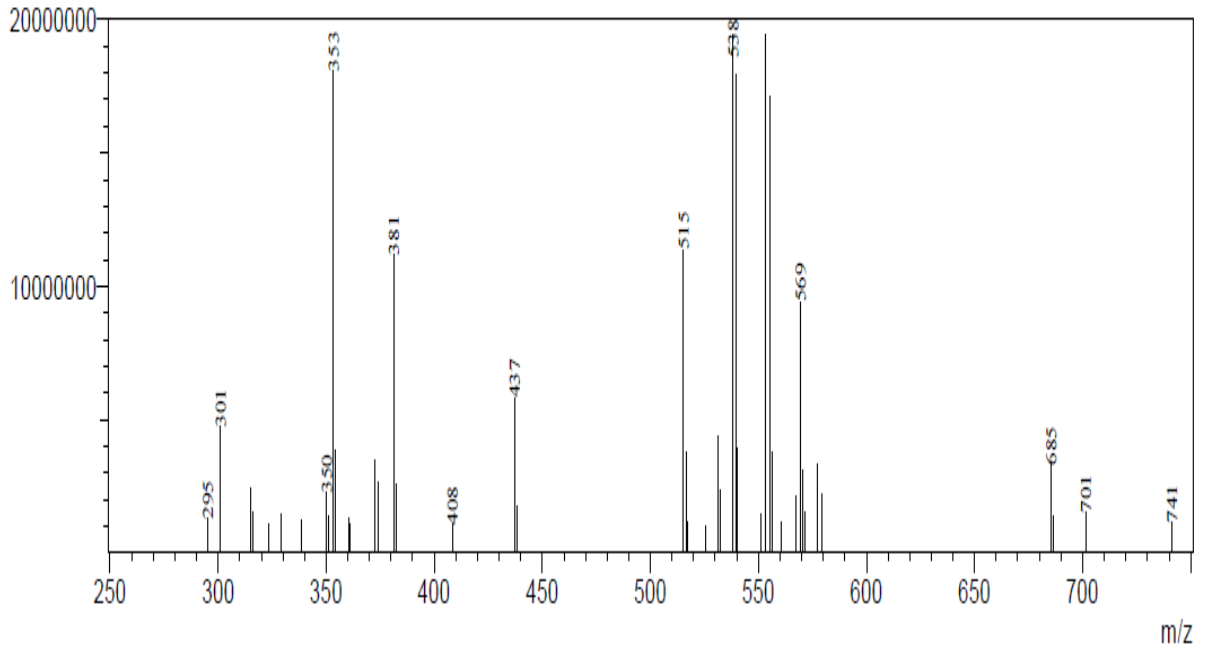
MassPeaks:182 BasePeak:549(13740164)
Spectrum Mode:Averaged 0.140-0.150(55-59)
BG Mode:Calc Polarity:Positive Segment 1 - Event 1 Fraction 6



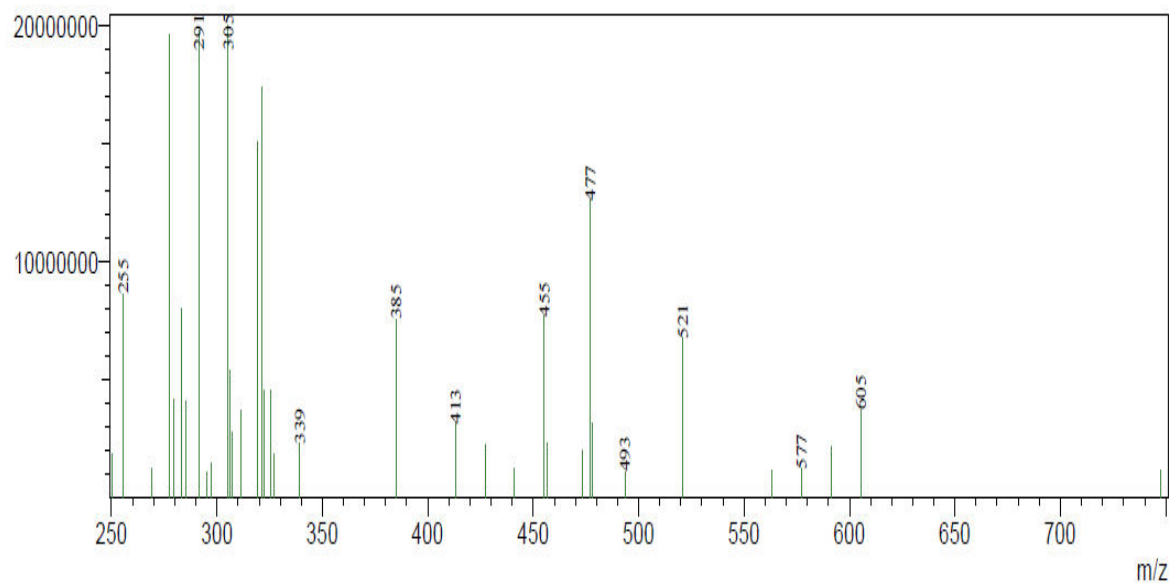
MassPeaks:44 BasePeak:403(16010814)
Spectrum Mode:Averaged 0.142-0.152(56-60)
BG Mode:Calc Polarity:Negative Segment 1 - Event 2 Fraction 6



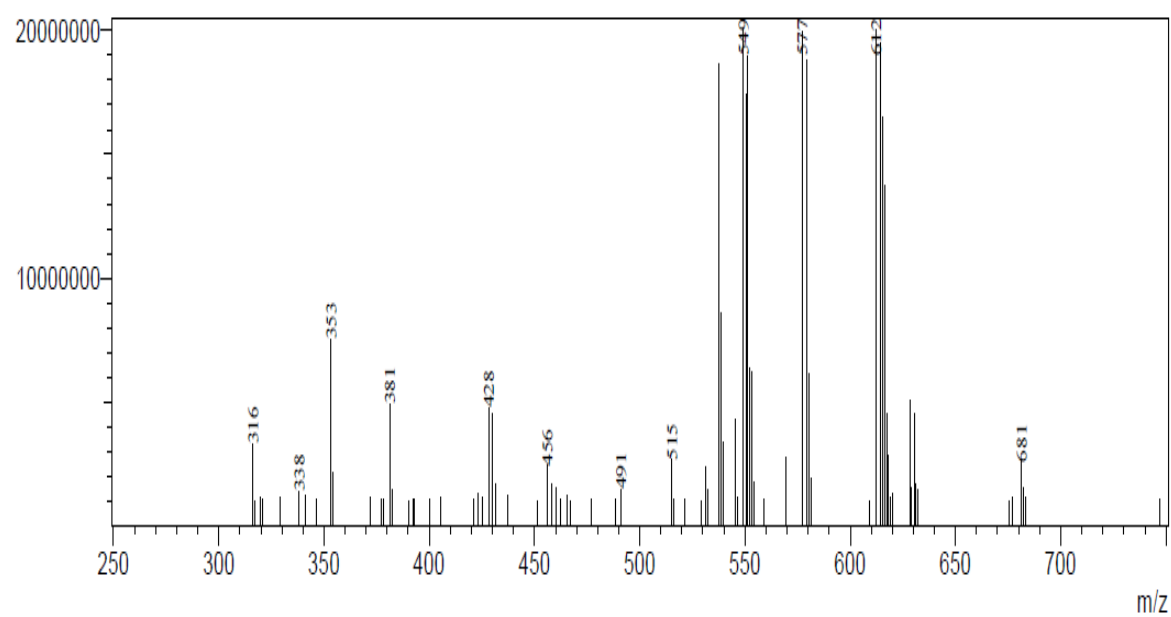
MassPeaks:44 BasePeak:538(19460716)
Spectrum Mode:Averaged 0.129-0.140(51-55)
BG Mode:Calc Polarity:Positive Segment 1 - Event 1 Fraction 7



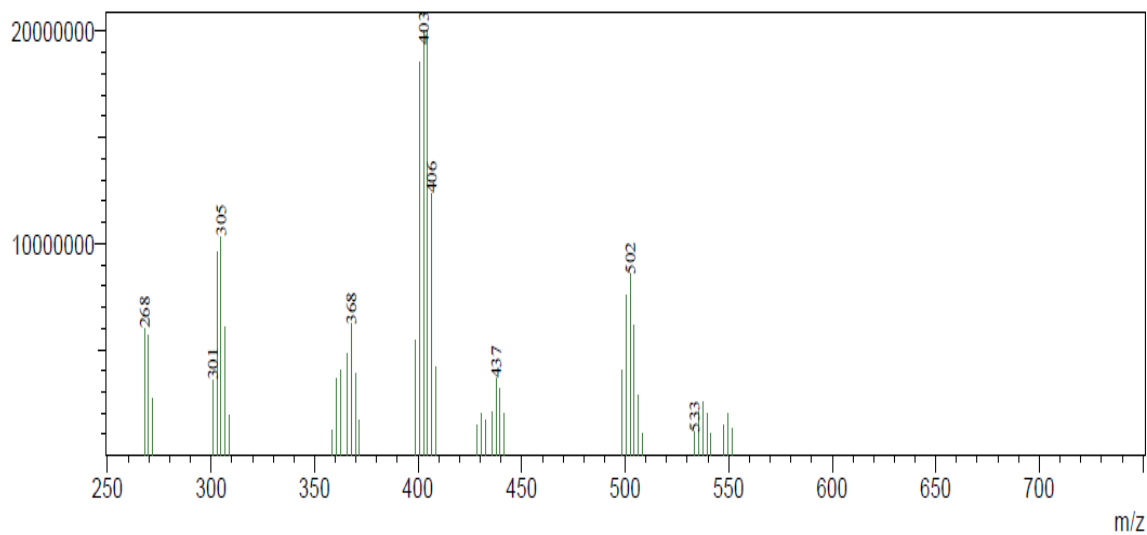
MassPeaks:36 BasePeak:305(20000000)
Spectrum Mode:Averaged 0.132-0.142(52-56)
BG Mode:Calc Polarity:Negative Segment 1 - Event 2 Fraction 7



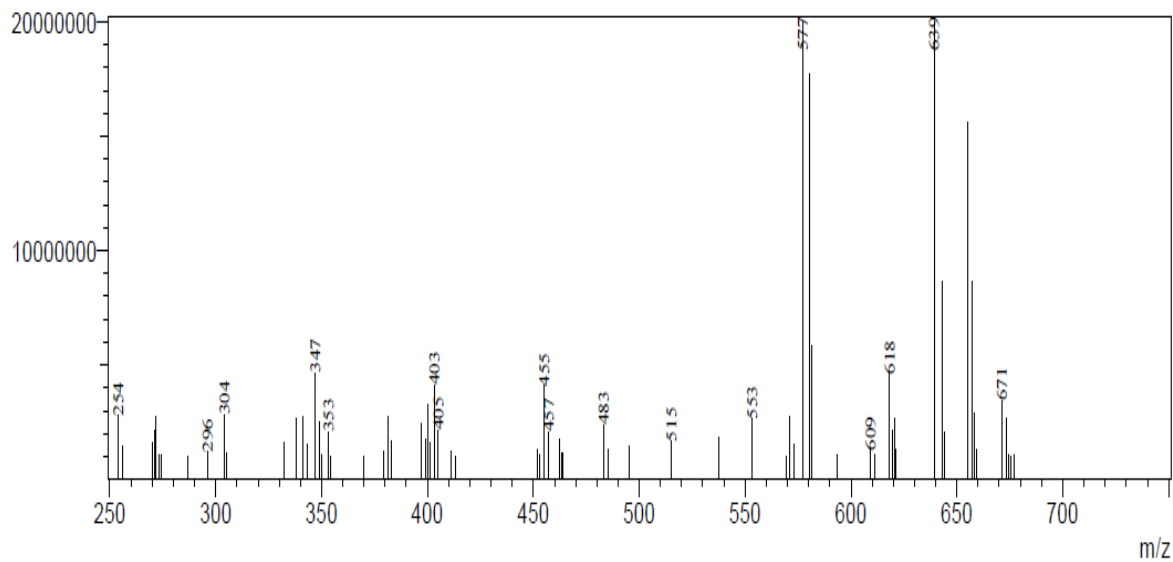
MassPeaks:80 BasePeak:549(20000000)
Spectrum Mode:Averaged 0.134-0.145(53-57)
BG Mode:Calc Polarity:Positive Segment 1 - Event 1 Fraction 8



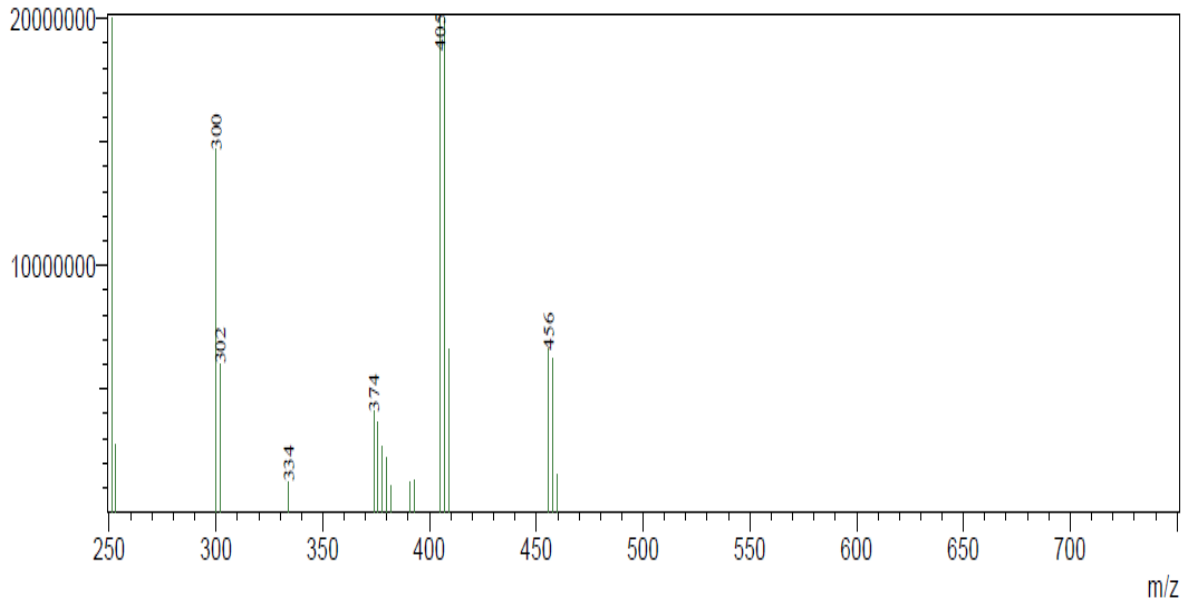
MassPeaks:42 BasePeak:403(20000000)
Spectrum Mode:Averaged 0.137-0.147(54-58)
BG Mode:Calc Polarity:Negative Segment 1 - Event 2 Fraction 8



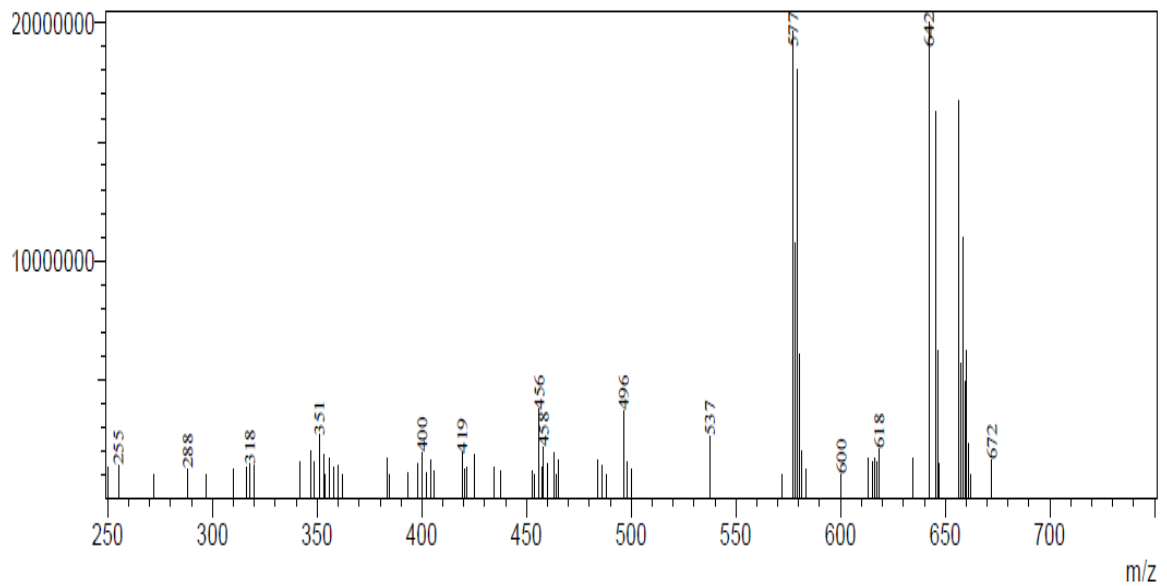
MassPeaks:70 BasePeak:577(20000000)
Spectrum Mode:Single 0.134(53)
BG Mode:None Polarity:Positive Segment 1 - Event 1 Fraction 9



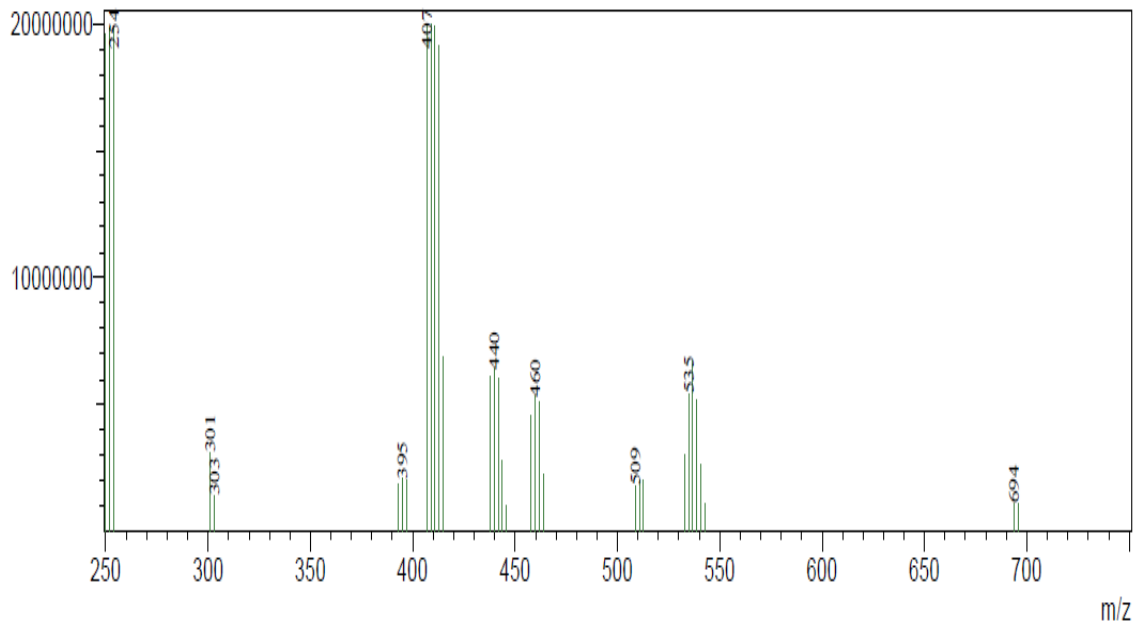
MassPeaks:18 BasePeak:251(20000000)
Spectrum Mode:Single 0.137(54)
BG Mode:None Polarity:Negative Segment 1 - Event 2 Fraction 9



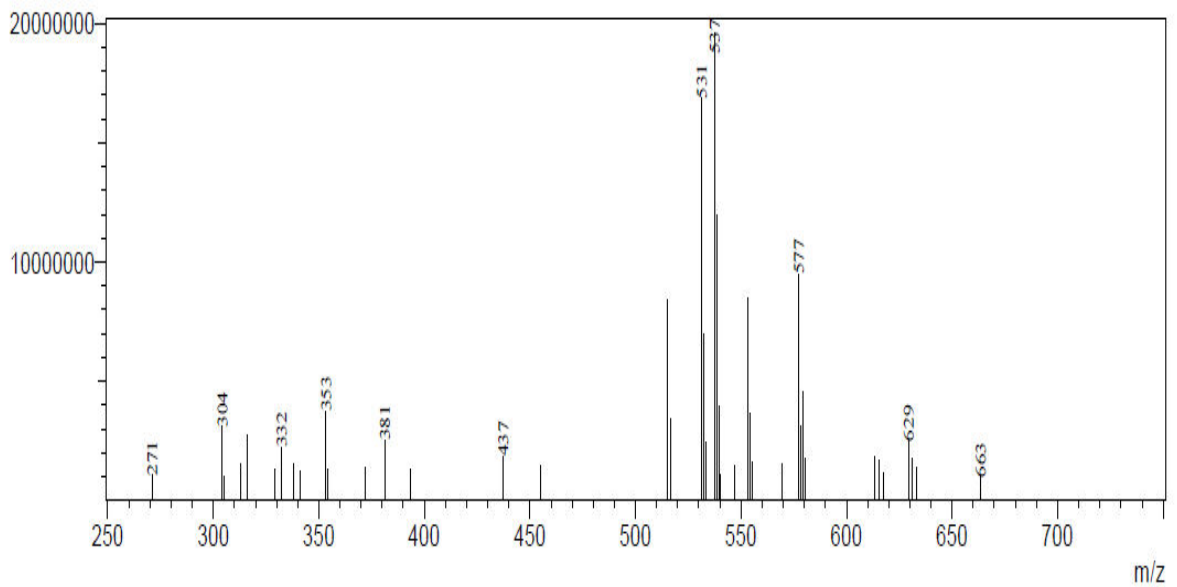
MassPeaks:75 BasePeak:642(20000000)
Spectrum Mode:Averaged 0.119-0.129(47-51)
BG Mode:Calc Polarity:Positive Segment 1 - Event 1 Fraction 10



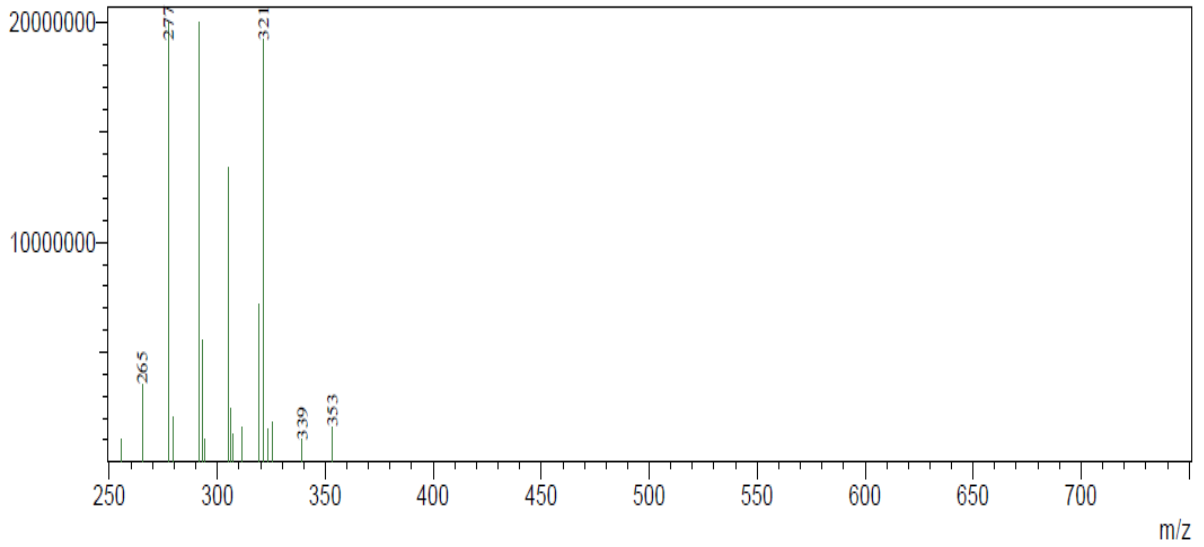
MassPeaks:33 BasePeak:407(20000000)
Spectrum Mode:Averaged 0.121-0.132(48-52)
BG Mode:Calc Polarity:Negative Segment 1 - Event 2 Fraction 10



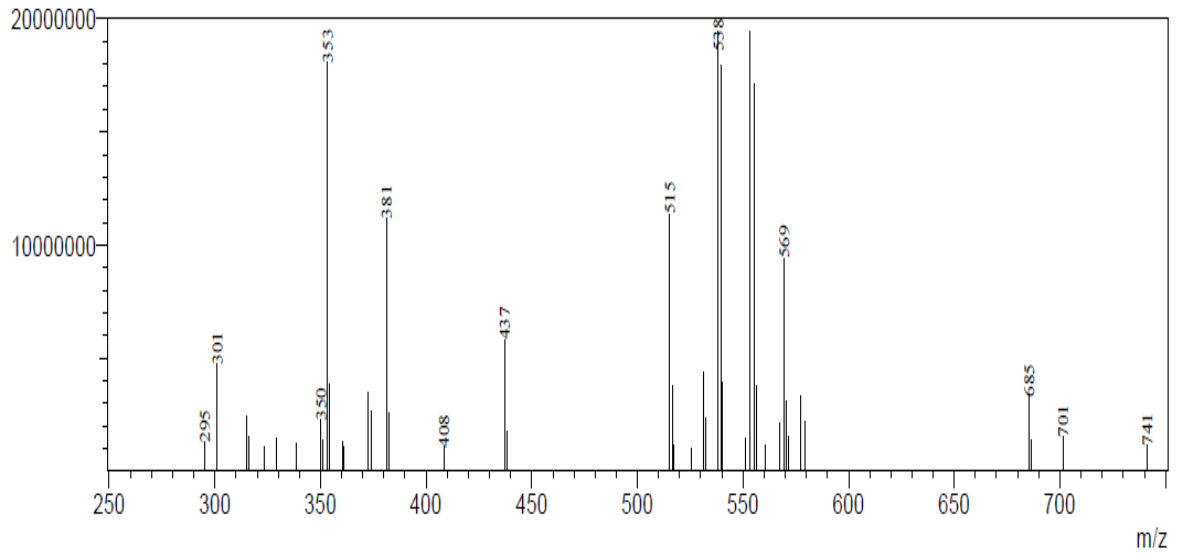
MassPeaks:41 BasePeak:537(19568207)
Spectrum Mode:Single 0.145(57)
BG Mode:None Polarity:Positive Segment 1 - Event 1 Fraction 11



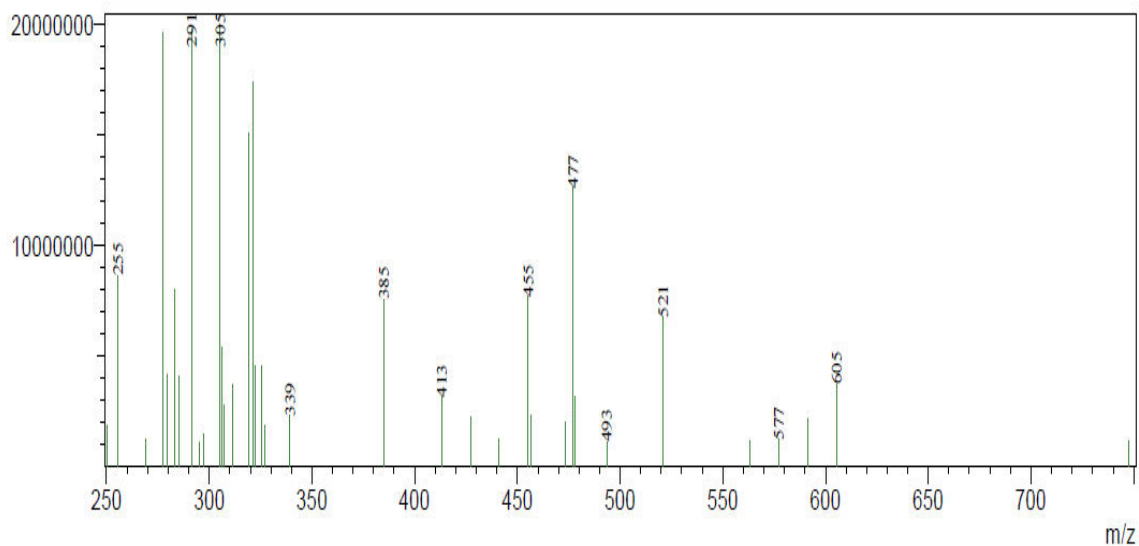
MassPeaks:17 BasePeak:277(20000000)
Spectrum Mode:Single 0.147(58)
BG Mode:None Polarity:Negative Segment 1 - Event 2 Fraction 11



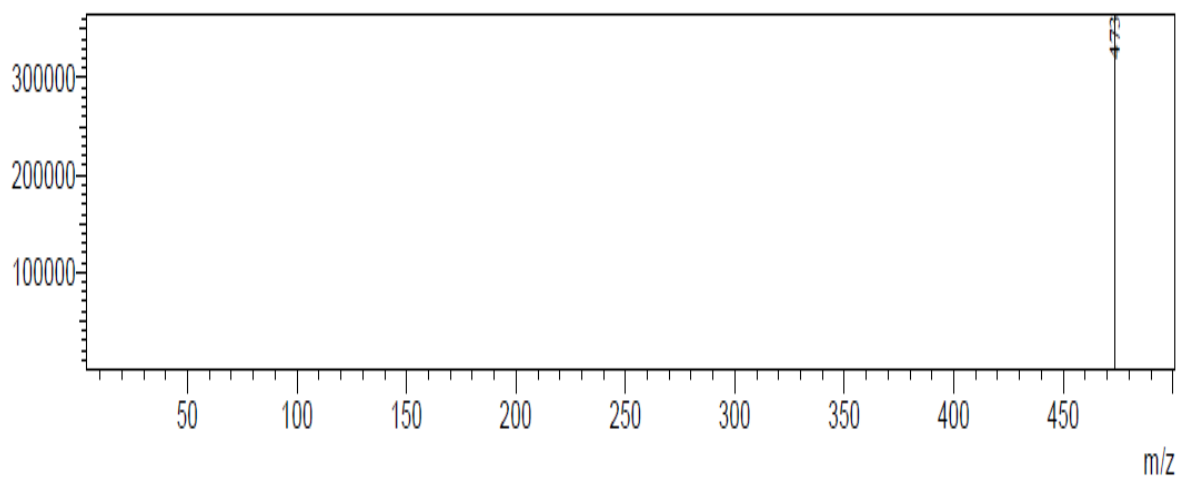
MassPeaks:44 BasePeak:538(19460716)
Spectrum Mode:Averaged 0.129-0.140(51-55)
BG Mode:Calc Polarity:Positive Segment 1 - Event 1 Fraction 12



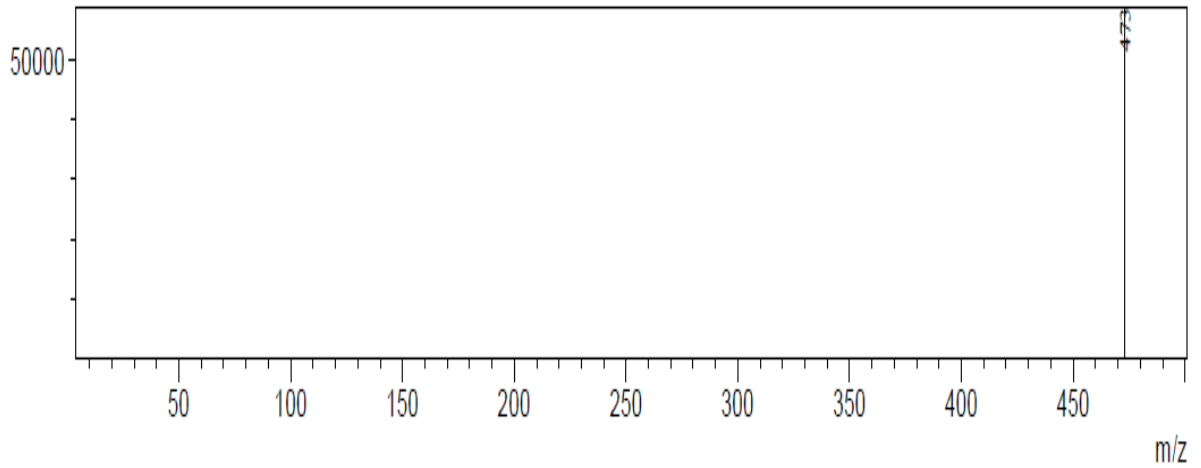
MassPeaks:36 BasePeak:305(20000000)
Spectrum Mode:Averaged 0.132-0.142(52-56)
BG Mode:Calc Polarity:Negative Segment 1 - Event 2 Fraction 12



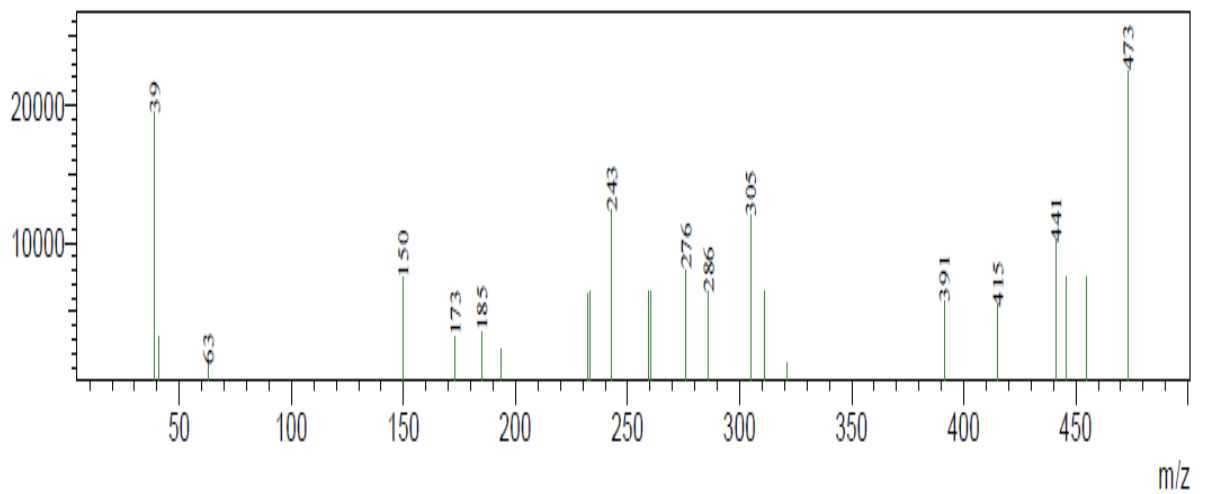
Mass:473.00 CE:-15.0 R.Time:----(Scan#:----)
MassPeaks:1 BasePeak:473(723795)
Spectrum Mode:Averaged 0.330-0.340(199-205)
BG Mode:Calc Polarity:Positive Segment 1 - Event 1 PI of +473



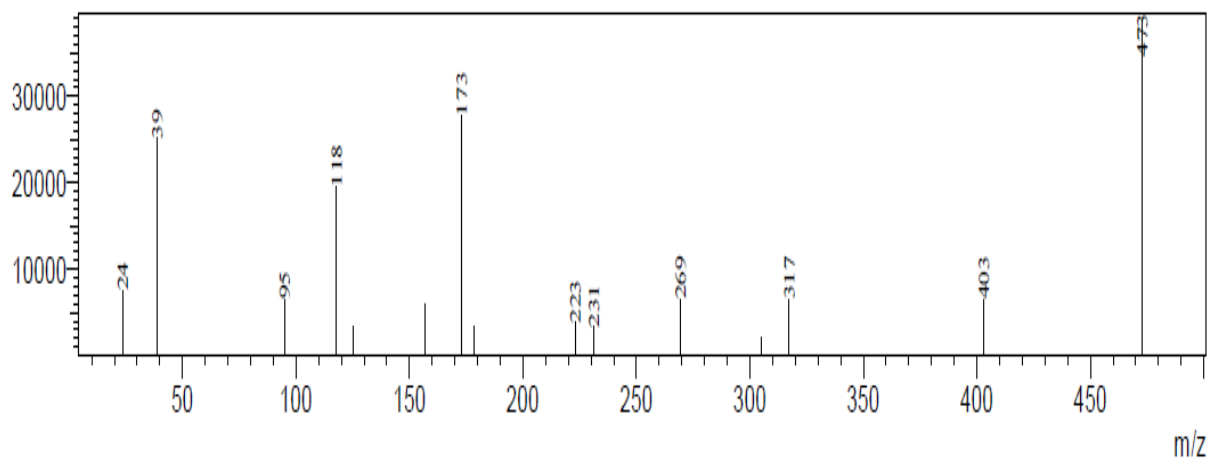
Mass:473.00 CE:-20.0 R.Time:----(Scan#:----)
MassPeaks:1 BasePeak:473(224244)
Spectrum Mode:Averaged 0.295-0.305(178-184)
BG Mode:Calc Polarity:Positive Segment 1 - Event 1 PI of +473



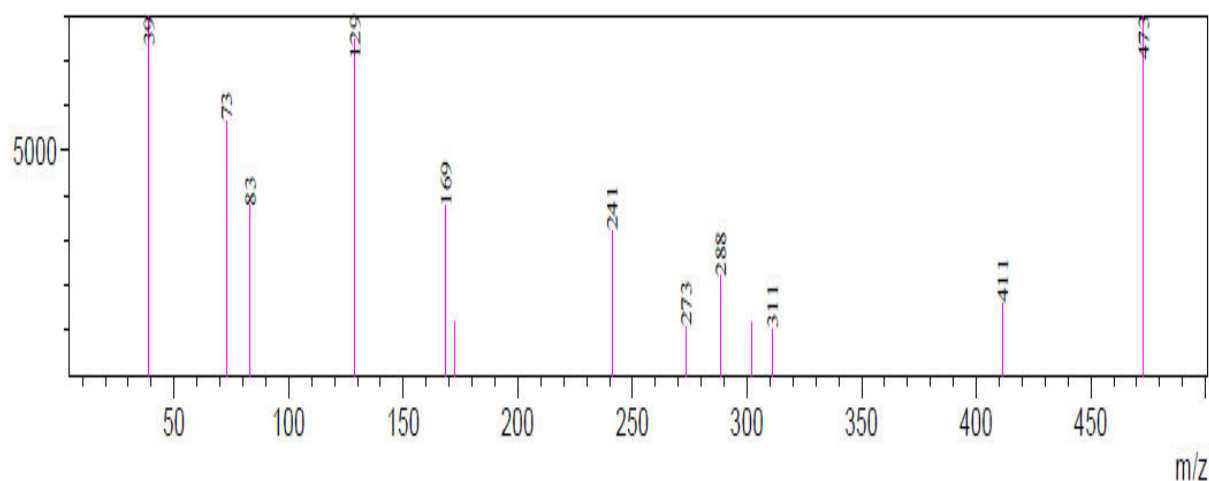
Mass:473.00 CE:-30.0 R.Time:----(Scan#:----)
MassPeaks:23 BasePeak:473(22483)
Spectrum Mode:Averaged 0.362-0.372(218-224)
BG Mode:Calc Polarity:Positive Segment 1 - Event 2 PI of +473



Mass:473.00 CE:-35.0 R.Time:---(Scan#:---)
MassPeaks:15 BasePeak:473(38933)
Spectrum Mode:Averaged 0.360-0.370(217-223)
BG Mode:Calc Polarity:Positive Segment 1 - Event 1 PI of +473



Mass:473.00 CE:-40.0 R.Time:---(Scan#:---)
MassPeaks:13 BasePeak:39(15856)
Spectrum Mode:Averaged 0.363-0.373(219-225)
BG Mode:Calc Polarity:Positive Segment 1 - Event 3 PI of +473



conferenceseries.com

Pharmacognosy 2017
Young Researchers Forum

Prof/Dr/Mr/Ms. Kavitha Sreehari

Victoria University, Australia

for presenting the oral entitled
The search for anti-neurodegenerative drug leads from an Indian traditional
herbal medicinal that is regarded as a "brain tonic"

at the "5th International Conference and Exhibition on
Pharmacognosy, Phytochemistry & Natural Products"
held during July 24-25, 2017 in Melbourne, Australia

The award has been attributed in recognition of research paper quality, novelty and significance.



Dilip Ghosh
Saha Floridis International, Australia

THANK YOU